THE UNIVERSITY
of ADELAIDE

Understanding the interactions between biomass, grain yield and grain protein content in low and high protein wheat cultivars

By

Vahid Rahimi Eichi

Thesis submitted to the University of Adelaide in fulfilment of

the requirements for the degree of

Doctorate of Philosophy

School of Agriculture, Food and Wine

Faculty of Science

The University of Adelaide

July 2020

Understanding the interactions between biomass, grain yield and grain protein content in low and high protein wheat cultivars

By

Vahid Rahimi Eichi

Supervised by:

Professor Peter Langridge

Affiliate Professor

Plant Genomics Centre

The University of Adelaide, AUS

Dr Trevor Garnett

Manager

Research Platforms at GRDC

Grains Research and Development Corporation, AUS

Dr Mamoru Okamoto

Research Scientist

Plant Genomics Centre

The University of Adelaide, AUS

Abstract

Grain protein content (GPC) is a key quality attribute and an important marketing trait in wheat. However, a negative relationship between grain yield and GPC has limited selection for increased GPC, since grain yield is the primary driver of breeding programs. GPC is strongly influenced by nitrogen (N) fertilizer application, but the N-use efficiency (NUE) of high and low GPC genotypes appears to be genetically determined. The aim of this PhD thesis was to investigate the grain yield-GPC relationship under controlled and field conditions, and to suggest selection targets and traits for improving NUE in wheat.

Firstly, the N responsiveness of six wheat genotypes that varied in GPC were examined under controlled condition. This experiment was designed around non-destructive estimation of biomass using a high-throughput image-based phenotyping system. In parallel, field trials were conducted to allow the comparison of results obtained from the controlled condition study using the six selected genotypes. Estimating the rate of biomass accumulation in breeding plots in the field is difficult. Therefore, the growth rate of biomass related traits such as height and ground cover were assessed in these trials. To examine the grain yield-GPC relationship under multi-environmental conditions, the grain yield and GPC data of over 200 wheat genotypes obtained from the Australian National Variety Trials (NVT) across the Australian wheat-belt were analysed.

Results of the controlled environment experiment showed that high GPC genotypes appeared to demand more N to grow their biomass. In both controlled and field environments, high GPC genotypes slowed down the rate of biomass growth under low N supply. Under low yielding conditions, high GPC genotypes seemed able to manage grain N reserves by compromising biomass production. These results indicated the importance of biomass growth analysis to show the differences in the N responsiveness of high and low GPC genotypes.

Differences between high and low GPC genotypes in responding to low N could be due to their history of selection. N effect is strongly associated with the amount of available water in the soil. Controlled and multi-environmental studies showed that the slope of the relationship between grain yield and GPC is steeper in low compared to high yielding environments. Therefore, high GPC genotypes bred under stress conditions sacrifice yield in favour of GPC, possibly to enhance the survival chance by producing fewer grains with sufficient nutrient levels. Conversely, low GPC genotypes bred in high yielding environment are less conservative compared to high GPC genotypes in using N for yield production. The outcomes of this PhD project highlight the importance of considering environmental factors for improving NUE in breeding programs. It recommends that wheat breeders focus on selecting in low yielding environments for high yield and high GPC genotypes.

Thesis Declaration

I certify that this work contains no material which has been accepted for the award of any other degree or diploma in my name, in any university or other tertiary institution and, to the best of my knowledge and belief, contains no material previously published or written by another person, except where due reference has been made in the text. In addition, I certify that no part of this work will, in the future, be used in a submission in my name, for any other degree or diploma in any university or other tertiary institution without the prior approval of the University of Adelaide and where applicable, any partner institution responsible for the joint-award of this degree. I acknowledge that copyright of published works contained within this thesis resides with the copyright holder(s) of those works. I also give permission for the digital version of my thesis to be made available on the web, via the University's digital research repository, the Library Search and also through web search engines, unless permission has been granted by the University to restrict access for a period of time. I acknowledge the support I have received for my research through the provision of an Australian Government Research Training Program Scholarship.

Vahid Rahimi Eichi

July, 2020   29/07/2020

Acknowledgments

thanks to Charity, Benoit, Pooja and Mihiranga for providing a great atmosphere in the office.

I would like to extend my gratitude to my Tasmanian family. Dear Howells, thank you for welcoming me into your home and making me feel at home far away from home. I am grateful for the warmth and love you have always shown me.

I would like to express my deepest gratitude to my family in Iran and afar, Mum, Dad, Habib, Rashid and Maryam. Special thanks to my late father for his never-ending love and support, who was my main encourager to start the PhD in the first place.

And finally, to my wife Alice, who is a great inspiration to me. Hence, great appreciation and enormous thanks are due to her, for without her understanding, I am sure this thesis would have never been completed.

List of Abbreviations

AGR	Absolute Growth Rates (kilo pixels/day)
DAS	Day After Sowing
EC	Plant Establishment Counts
ET	Environment Type
GPC	Grain Protein Content (%)
GPD	Grain Protein Deviation
GS	GreenSeeker
GS NDVI	Ground Cover Measured with GreenSeeker
GY	Grain Yield (t/ha)
HRZ	High Rainfall Zones
Max-AGR	Maximum Absolute Growth Rate (kilo pixels/day)
Max-PSA	Maximum Projected Shoot Area (kilo pixels)
N	Nitrogen
NDVI	Normalized Difference Vegetation Index
NIR	Near Infrared Spectroscopy
NUE	Nitrogen-Use Efficiency
NVT	National Variety Trials
PSA	Projected Shoot Area (kilo pixels)
REML	Restricted Maximum Likelihood Estimation
RGB	Red Green Blue

SWSI	Simulated Water-Stress Index
t-maxAGR	Time of Max-AGR (DAS)
UAV	Unmanned Aerial Vehicle
UAV height	Measured with Unmanned Aerial Vehicle (meter)

Table of Contents

Chapter 1: Introduction

Wheat (*Triticum aestivum* L.) is the most widely cultivated crop in the world and a substantial source of carbohydrate and protein in human diets (Shewry and Hey 2015). Besides high yield, wheat quality has been valued throughout the wheat cultivation history (Wilson 2007). Grain protein content (GPC) is a key quality attribute and an important marketing trait. However, there is a well-documented negative relationship between grain yield and GPC in wheat (McNeal et al. 1972; Kibite and Evans 1984; Simmonds, N. W. 1995). Due to this negative relationship, there is a limitation to increase GPC as grain yield is the primary driver of the current breeding programs of wheat and other crops. In world cropping systems, GPC is strongly influenced by nitrogen (N) fertilizer application (Triboi et al. 2000; Sinclair and Rufty 2012), but the N-use efficiency (NUE) of high and low GPC varieties appears to be genetically different (Beres et al. 2018; Walsh et al. 2018). N translocation into grains for maintaining GPC is more in high compared with low GPC varieties (Rahimi Eichi et al. 2019; Pan et al. 2020).

Only 40%–60% of applied N is taken up by wheat crops (Sylvester-Bradley and Kindred 2009). In addition to the high costs of fertilizer for farmers, the extra N can be lost to the environment, resulting in serious environmental issues (Bouwer 1989; Harrison and Webb 2001). Consequently, there is considerable interest in improving NUE (Birch and Long 1990; Sadras et al. 2016). Understanding the processes that determines N uptake and accumulation in crops is of major importance with respect to both environmental concerns and yield quality (Gastal and Lemaire 2002). Biomass is related to the dynamics of N accumulation in crops in different environments. This suggests that with an adequate soil N supply, N uptake in crops is to a large extent determined by their biomass growth rate (Greenwood et al. 1986; Gastal and Lemaire 2002). Therefore, the above-ground biomass can be a suitable indicator for N response since it is highly N responsive, and corresponds with grain weight, particularly, under controlled conditions (Sharma 1993; Richards 2000;

Sadras et al. 2016; Rahimi Eichi et al. 2019). NUE evaluations are usually simplified by measuring grain weight at given N supply (Araus, J. L. et al. 2002; Cormier et al. 2016) as destructive biomass harvests can be time and labour intensive, especially, for large-scale trials (Royo et al. 2004). Consequently, using image-based phenotyping techniques that allow measurement of biomass non-destructively is attractive as a tool for assessing NUE (Berger et al. 2012; Shi et al. 2013).

The overall aim of this dissertation was to investigate the relationship between grain yield and GPC under controlled, field and multi-environmental conditions in high and low GPC wheat varieties. Measuring biomass through growth analysis was used to examine the differences in N response in high and low GPC wheats. The specific aims of this study were to 1) understand the relationship between biomass, grain yield and GPC in high and low GPC varieties under different N supply in controlled conditions; 2) relate the results in controlled conditions to field environments in South Australia and across the Australian wheat-belt. The main objective of this research was to explore breeding and selection options for breaking the negative association between yield and high GPC.

This thesis consists of six chapters:

Chapter 1 (Introduction) provides a broad overview of the thesis background. Research gaps and specific aims of the thesis are briefly discussed.

Chapter 2 (Literature review) provides a review of the available literature setting the background to the grain yield-GPC relationship, differences between Australian wheat classes based on their GPC, and image-based phenotyping methods. The possible methods to study the N responses in wheat plants under controlled and field conditions is described, highlighting the current research gaps of this field.

Chapter 3 (Understanding the interactions between biomass, grain production and grain protein content in high and low protein wheat genotypes under controlled environments), written in manuscript style and published in the journal A*gronomy*. This chapter provides information about biomass, grain yield and GPC responses to different N treatments in high and low GPC varieties under controlled conditions. This paper also shows the importance of non-destructive methods for biomass growth analysis to show the differences in the N responsiveness of high and low GPC wheat.

Chapter 4 (Understanding the interactions between biomass, grain production and grain protein content in high and low protein wheat genotypes under field environments), written in manuscript style, provides information about the N responsiveness of biomass, yield and GPC in high and low GPC varieties in two field trials conducted in 2018. This manuscript also includes results from a preliminary field trial carried out in 2017. UAV-based imaging platforms were used for the non-destructive estimation of biomass related traits such as height.

Chapter 5 (Strengths and weaknesses of national variety trial data for multi-environment analysis: A case study on grain yield and protein content), written in manuscript style and published in *Agronomy*. This chapter includes an in-depth analysis of the relationship between grain yield and GPC particularly with regard to the results shown in Chapters 3 and 4 in different environments across the Australian wheat-belt. This chapter also provides information about the value of comprehensive multi-environmental analysis for exploring the yield-GPC relationship based on the National Variety Trials dataset.

Chapter 6 (General discussion) provides a discussion on how the findings reported in this dissertation can be used in breeding programs and provide strategies for future research directions.

This thesis also contains two appendices:

Appendix 1

Khan, Z, Rahimi-Eichi, V, Haefele, S, Garnett, T & Miklavcic , SJ 2018, 'Estimation of vegetation indices for high-throughput phenotyping of wheat using aerial imaging', *Plant methods*, vol. 20 p. 14. Doi:10. 950. 10.3390/rs10060950.

Appendix 2

Khan, Z, Chopin, J, Cai, J, Rahimi Eichi, V, Haefele, S & Miklavcic, SJ 2018, 'Quantitative estimation of wheat phenotyping traits using ground and aerial imagery', *Remote Sensing*, vol. 10. Doi:10.1186/s13007-018-0287-6.

The observations, experiences and method developments achieved in both appendices helped in the improvement of the UAV-based imaging in the field.

Chapter 2: Literature review

2.1 Concurrent improvement of yield and grain quality in wheat

2.1.1 Global wheat production

Cereals, the major staple food worldwide, constitute more than 50% of the total daily calories in most human diets (Hawkesford 2014). Wheat alone accounts about 20% of the consumption of carbohydrates and proteins (Hawkesford et al. 2013). The 'green revolution' in the 1960s, which introduced dwarf high yielding new wheat varieties and changed conventional agricultural practices led to large increases in productivity (Farmer 2008). As a result, and despite little or no expansion in the total area sown to wheat, global wheat production has increased substantially over the last fifty years (FAOSTAT 2019; www.fao.org).

Currently, the average rate of increase in wheat production is 1.3% per year. However, this yield increase needs to reach 2.4% per year to meet the demand for the expected 9 billion population by 2050 (Hawkesford et al. 2013; Pardey et al. 2014). Several factors limit yield increase including the depletion of water sources, declining soil fertility and cultivation of varieties poorly adopted to stressful conditions such as drought and heat (Asfaw and Lipper 2012). The impacts of climate change are expected to further limit productivity (Lobell et al. 2011).

2.1.2 Importance of nitrogen and nitrogen-use efficiency

Application of fertilizers, particularly nitrogen (N), at a large-scale has been one of the key elements for the green revolution's success. Plants require large amounts of N for their development and reproduction. Therefore, N is one of the most important macronutrients plants take up from the soil. Accordingly, plant growth and survival highly depend on the maintenance of an optimum equilibrium between N demand and N supply (Marschner et al. 2012). At the end of the 1960s, a newly introduced rice variety in India known as IR8, which

produced around 5 t.ha^{-1} grain yield with no N fertilizer, yielded nearly double after N application (De Datta et al. 1968). It is therefore not surprizing that the worldwide consumption of N fertilizer has increased almost 10-fold since 1961. However, due to a combination of other limitations, such as abiotic and biotic stresses, poor agricultural practices and low yielding germplasm, this fertilizer increase has not been paralleled by the productivity of crops (Figure 2-1) (FAOSTAT 2017; www.fao.org).
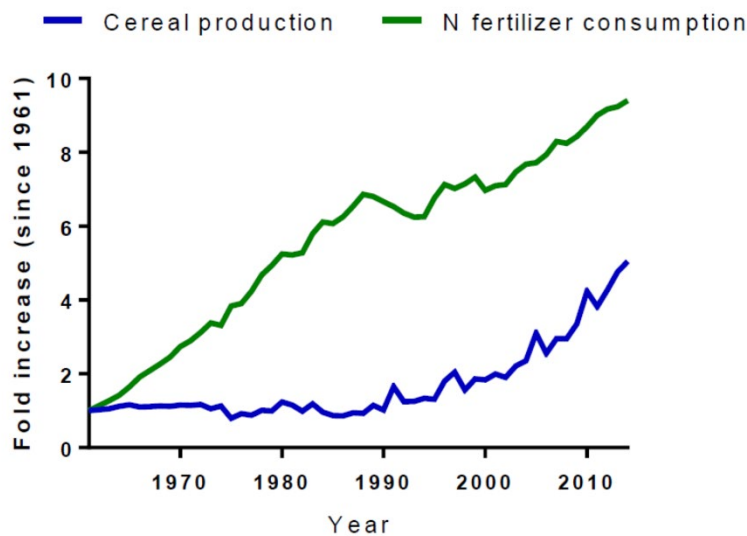
Figure 2-1. The increase (fold increase) in worldwide N fertilizer consumption and cereal production from 1961 to 2014. Data was sourced from FAOSTAT (2017) (www.fao.org).

N fertilizer is industrially produced through the Haber-Bosch process, which demands very high temperature and pressure and, consequently, consumes large amounts of energy. For instance, 3% of the total natural gas produced in USA in 1999 was used in the fertilizer industry (Clark and Kelly 2004). N fertilizer production contributes to both emissions of atmospheric greenhouse gases and depletion of non-renewable energy reserves. Moreover, excess N fertilizer used in agricultural systems can be lost via surface runoff, leaching into groundwater, and denitrification and volatilization in the soil (Ehdaie et al. 2010; Butterbach-Bahl and Dannenmann 2011). This can lead to the pollution and eutrophication of underground and surface water bodies, and release of greenhouse gasses (Matson et al.

1998). However, despite being applied in large amounts in agricultural soils, only a small portion of the available N can be taken up by crops. For instance, wheat crops uptake only 40-60% of the supplied N (Sylvester-Bradley and Kindred 2009). The global cereal N recovery in grains from applied fertilizer in 1996, which was corrected for the amounts obtained from soil and atmosphere, was only 33%, resulting in a $15.9 billion loss (Raun and Johnson 1999). Therefore, to improve the sustainability of agricultural systems, N-use efficiency (NUE) needs to be increased in crops. However, NUE has not often been the target of breeding programmes, as breeders are not inclined to select under low N. In fact, genetic selection is usually conducted with high fertilizer N input in order to reduce N effect as a variable. This can mask the differences in efficiency between genotypes in accumulating and utilizing N for producing grain (Kamprath et al. 1982; Raun and Johnson 1999). Another study in this context showed that high-yielding varieties of corn, wheat and rice released during the Green Revolution were selected to respond to high N inputs (Earl and Ausubel 1983). Nevertheless, NUE has been indirectly increased by selecting for high yielding genotypes (Sadras and Richards 2014). It is well-documented that N uptake is highly associated with water availability (Stoddard and Marshall 1990; Sadras and McDonald 2012). Selection for high yield in water, and consequently N, scarce environments has consistently increased NUE since the early 20th century in Australia (Fischer 2009; Sadras and Richards 2014).

Moll et al. (1982) defined NUE as dry mass of harvested grain per kilogram available N. NUE depends on plant's ability to (i) take-up N from the soil; (ii) use the taken-up N to expand the biomass; and (iii) distribute carbon and N to the grains (Lemaire and Gastal 2009).

2.2 The relationship between N supply, biomass, grain yield and protein

2.2.1 N input and biomass, grain yield and GPC in wheat

Increasing N supply expands crop canopy, and increases radiation-use efficiency and canopy photosynthesis. Previous studies on different crops indicated a linear relationship between N supply and biomass, grain yield and grain protein content (GPC) up to a point where N is not the main factor limiting biomass production (Rodgers and Barneix 1988; An et al. 2006; Lemon 2007; Hawkesford 2014). However, this is not always the case as the availability of water after flowering and temperature can strongly influence GPC (Flohr et al. 2020). Figure 2-2 shows three main areas of N supply in wheat including extreme deficiency (regime 1), moderate (regime 2) and excessive (regime 3) N. Additional N supply in regime 1 increases grain yield but reduces GPC. Consequently, in regime 1 the GPC of wheat may not exceed 7-8%, and the yield potential remains around 50%. Increasing N supply in regime 2 raises the yield potential to 60-80% with the maximum GPC of 10%. In regime 3 with adequate to excessive N, wheat plants nearly reach their yield potential and, therefore, may not respond to extra N. In fact, Figure 2-2 demonstrates that NUE in wheat reduces by increasing N supply. Conversely, GPC in regime 3 increases in response to the additional N applied.
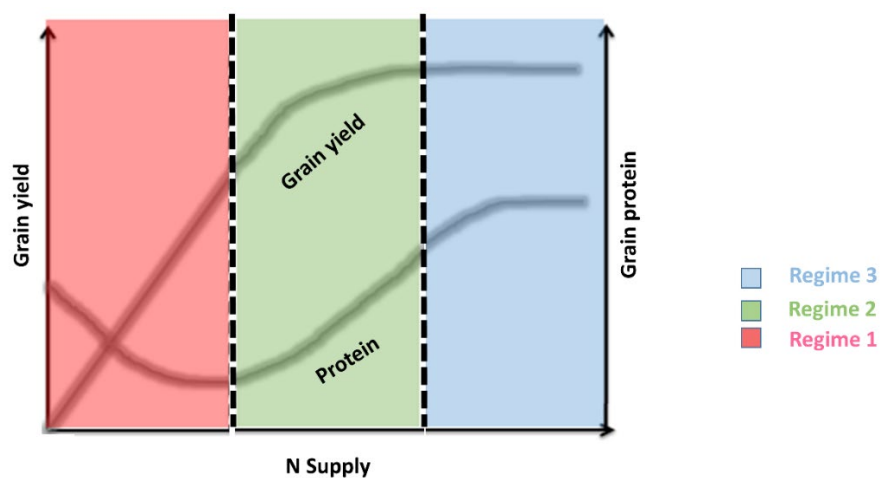
Figure 2-2. The relationship between nitrogen supply, and grain yield and grain protein content in wheat. Adopted and changed from Lemon (2007)

In wheat, high early vigour can improve N uptake efficiency (Pang et al. 2014). Rapid accumulation of shoot biomass is associated with increases in root growth in both length and surface area. This improves the plant's capacity to take-up N before it leaches beyond the root zone (Liao et al. 2004). In high yielding environments, grain yield is positively correlated with the above-ground biomass (Figure 2-3) (Bustos et al. 2013). However, large biomass production can involve yield penalties by increasing susceptibility to lodging (Hawkesford 2014). In low yielding environments with terminal drought and heat stress conditions, "haying-off" is an additional issue, which reduces grain yield and NUE (McDonald, G. K. 1992; van Herwaarden et al. 1998).

There is a negative relationship between grain yield and GPC in wheat (Figure 2-4) (McNeal et al. 1972; Kibite and Evans 1984; Simmonds, N. W. 1995), which limits furthur increase of protein in grain with higher yields.
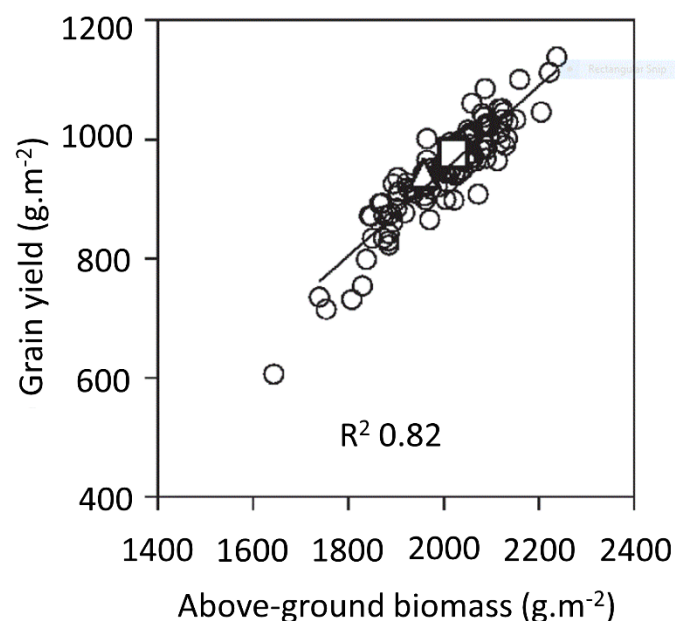
Figure 2-3. Relationship between above-ground dry matter and grain yield in wheat trials grown in the high yielding environments of Mexico, Argentina and Chile. The figure is obtained from Garcia et al. (2013).
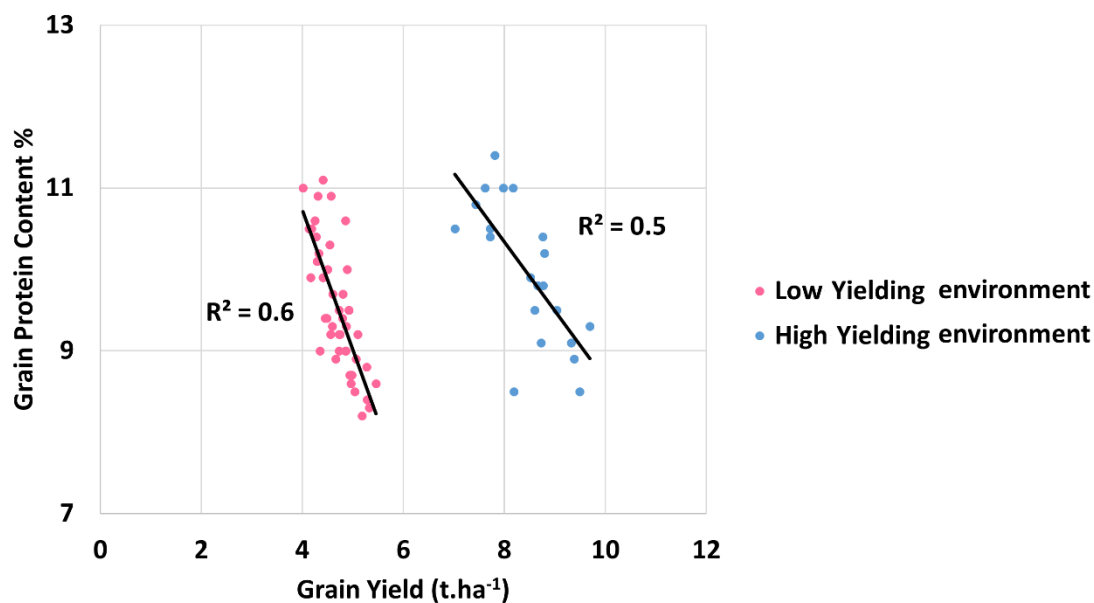
Figure 2-4. Negative relationship between grain yield and grain protein content obtained from the wheat dataset of the National Variety Trials in 2016 in Wagga Wagga (low yielding environment) and Tasmania (high yielding environment).

The inverse relationship between yield and GPC is mainly due to the competition between N and carbon for translocation in to developing grains (Munier-Jolain and Salon 2005), resulting in N dilution by carbon-based components within grains (Acreche and Slafer 2012).

Besides yield production, wheat quality improvement has been valued through thousands of years of cultivation (Wilson 2007). Nowadays, even in regions where food security is an issue, wheat grain quality is important (Husenov et al. 2015). Wheat grain quality can be determined by physical and chemical characteristics. Physical parameters are grain vitreousness, color, weight, shape and hardness, while chemical characteristics include GPC and gluten strength, etc (Gaines et al. 1996; Pasha et al. 2010). In wheat, GPC is a key quality attribute and an important marketing criterion since GPC is a fundamental indicator of wheat classification (Oury and Godin 2007; Husenov et al. 2015). Accordingly, achieving a suitable balance between N-use efficiency and improving the GPC with minimum risk of a yield penalty is desirable in breeding programs.

2.2.2 Wheat grain protein is more influenced by environment than by genetics

GPC in wheat can be affected by a range of factors including genetics, seasonal conditions, agronomic practices, variety and soil type (Figure 2-5) (Stephens et al. 1989; Lemon 2007). However, GPC is more influenced by environmental conditions than by genetics (Blakeney et al. 2009; Rahimi Eichi et al. 2020). High seasonal water availability with prolonged cool moist grain filling period increases the yield and, consequently, dilutes the protein in grains (Larmour 1939; Lemon 2007). Conversely, heat and drought stresses at the end of the season can shorten the maturation period, reduce the grain size by limiting the amount of starch accumulated in the grain, and increase the GPC. Likewise, late sowing in such conditions increases GPC by reducing grain yield through a shortened grain filling stage (Jones and Olson-Rutz 2012). Frost is the other abiotic stress that increases GPC by reducing grain yield (Lemon 2007; Arnott and Richardson 2007).

In the presence of adequate N, the deficiency of other macronutrients and trace elements usually reduces yield and increases GPC in crops (Lemon 2007). The type of soil can also change the GPC by influencing N and moisture reserves in soil. In this context, heavier soils usually store more minerals and water for a given depth, and are less likely to lose mineral N from leaching compared with sandy soils (Munier et al. 2006; Lemon 2007).
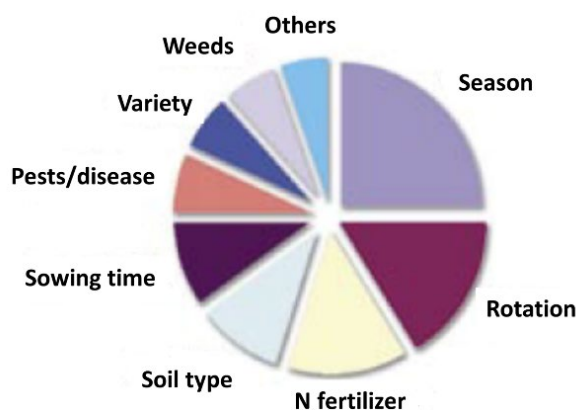
Figure 2-5. Relative influence of factors affecting grain protein content in wheat. Adopted from Lemon (2007)

2.2.3 Australian wheat classes and their end-uses

Among Australian agricultural products, wheat is the most valuable commodity export after beef. Total production of wheat per annum in Australia from 2005 to 2018 is shown in Table 2-1. On average, Australia ranks between 6th and 8th place amongst the major wheat producing nations, while Australia is the 4th main wheat exporting country with 75-80% of the wheat produced in Australia exported (Australian Bureau of Statistics 2018-2019). The value of Australian wheat exports is determined based on the key quality attributes recognized by the importers of Australian wheat (Table 2-2) (Blakeney et al. 2009; Limley et al. 2013). Therefore, improving the capacity and sustainability of production for particular end-use products is important for Australian wheat producers.

Table 2-1. Wheat production statistics for Australia, 2005-2018. Sources: ABARES; Australian Bureau of Statistics; Pulse Australia

Period	Area ('000 ha)	Yield (t.ha^{-1})	Production ('000 tonnes)
2005-06	12443	2.02	25150
2006-07	11798	0.92	10822
2007-08	12578	1.08	13569
2008-09	13530	1.58	21420
2009-10	13881	1.57	21834
2010-11	13502	2.03	27410
2011-12	13902	2.15	29905
2012-13	12979	1.76	22856
2013-14	12613	2.01	25303
2014-15	12384	1.9	23743
2015-16	11282	2.0	22275
2016-17	12191	2.6	31819
2017-18	12237	1.7	21244

Table 2-2. Characteristics and end-use products of different Australian wheat grades (Blakeney et al. 2009).

Class	Attributes	End-uses
Prime Hard	• Minimum GPC of 13% • Hard-grained varieties • Prime hard varieties • High quality of milling • High strength and functionality of dough	High volume pan bread and hearth bread, high quality yellow alkaline and dry white salted noodles
Hard	• Minimum GPC of 11.5% • Hard-grained varieties • Superior quality of milling • Good strength and functionality of dough	High volume pan bread, flatbreads and noodles
Premium White	• Minimum GPC of 10% • Hard-grained varieties • High performance of milling	Noodles, including instant noodles, middle Eastern and Indian-style flatbreads, pan bread and Chinese steamed bread
Standard White	• GPC less than 10% unless Australian Standard White classification	Multipurpose including flatbread, steamed bread, noodles
Noodle	• GPC 9.6-11.5% • Soft grained varieties • Very good noodle quality	Dry white salted noodles and Japanese udon noodles
Durum	• Very hard grained varieties • Good ratio and quality of semolina yield • High levels of yellow pigment	Pasta and couscous
Soft	• Maximum GPC of 9.5% • Soft grained varieties • Weak doughs with low absorption of water	Biscuits, cakes and pastry
General Purpose	• Wheat that fails to meet higher receival standards for milling, or produced to be in Australian General Purpose classification	All purpose flours and blending applications
Feed	• Wheat suitable for animal feed, including all red grained varieties	

In Australia, wheat grades are used as the basis for payment to farmers. Grading is an approach to segregate wheat that exhibits different attributes such as kernel hardness, grain colour, GPC and the suitability of dough strength for various end-products. The differences in hardness modifies many functional properties of the flour and dough including milling,

13

processing, wet gluten, and loaf volume (Morris 2002; Blakeney et al. 2009; Salmanowicz et al. 2012; Baasandorj et al. 2016). Based on kernel hardness wheat can be classified in to soft, medium soft, hard, medium hard and extra hard (Kent and Evers 1994; Hansen, A. and Poll 1997), which is used for differentiating wheat grains in the world market (Pasha et al. 2010). The interaction between starch granules and proteins is an important factor determining kernel hardness and, consequently, flour processing quality (Preston 1998). The endosperm of hard and soft wheats physically differ from each other due to the adhesive strength between the protein matrix and starch granules (Simmonds, D. H. et al. 1973). Such differences between hard and soft grain wheats are genetically determined and result in differences in grain composition (Symes 1965). Variation in the expression of *Pin* genes is the main reason of the different composition between hard and soft wheat grains. The genetic locus controlling this kernel texture is the hardness (*Ha*) locus located on the chromosome 5D (Morris 2002). An additional factor, which affects kernel hardness is the amount of protein in the grain as mentioned earlier. Increasing grain protein up to a certain level is positively correlated with kernel hardness in both hard and soft wheat (Hong et al. 1989; Bettge and Morris 2000). Hard wheat varieties usually have higher GPC compared with soft varieties (Moss 1973; Anderson and Sawkins 1997; Lemon 2007). Australian hard wheat breeders tend to select simultaneously for high grain yield and GPC (Oury and Godin 2007; Mahjourimajd, S., Taylor, et al. 2016). Conversely, for soft wheats, which have different quality targets and end-products compared to hard wheats, lower GPC can be a desirable trait (Huebner et al. 1999).

Until the 1930s, Australian wheat production was dominated by soft and low GPC genotypes. However, since the 1960s the proportion of hard cultivars with high GPC began to increase. Hard and soft wheat cultivars were segregated between the 1950s and 1970s in different Australian regions. This led to the payment of premiums for high GPC hard wheats (Simmonds, D. H. 1989), and soft and feed cultivars that produce low GPC stayed in

irrigated and high rainfall regions (Figure 2-6) (Simmonds, D. H. 1989; Anderson and Sawkins 1997; Spragg 2008). However, the majority of wheat produced in Australia is grown in low yielding regions (Simmonds, D. H. 1989; Anderson and Sawkins 1997; Turner 2004).

Figure 2-6. Cultivation areas for different Australian wheat classes, the production ratio of individual classes to the total Australian wheat, and grain protein content limits for each wheat class. Figure obtained from (AEGIC 2018).

2.3 Phenotyping plant responses to N

2.3.1 Terminology, background and importance of plant phenotyping

Phenomics is mainly based on the examination of a series of traits related with morphology (e.g., plant height, canopy coverage, leaf or tiller number), developmental status (e.g., vegetative and reproductive stages), yield performance (e.g., grain number, grain weight,

protein content or biomass) and physiology (e.g., canopy temperature, water status or photosynthesis rate) (Furbank and Tester 2011).

One of the factors that can affect the probability of identifying superior genotypes is the number of lines phenotyped in breeding programs (White et al. 2012). Today phenotypic capabilities are a bottleneck for the genetic examination of quantitative traits linked with growth, yield and grain quality. The empirical usage of genetic information such as linking the response to selection methods in breeding programs in genomic selection (Jannink et al. 2010) or genome-wide association (Myles et al. 2009) studies require phenotyping of thousands of genetically defined lines. In this context, using image-based high-throughput phenotyping platforms could considerably reduce the time, cost and labour required in comparison with conventional phenotyping techniques (Montes et al. 2007; Furbank 2009).

2.3.2 Image-based biomass measurements can help in NUE studies

Due to the challenges of destructive harvests, NUE evaluations in the field are usually based on measuring grain weight at given N supply (Araus, J. L. et al. 2002; Cormier et al. 2016). However, the above-ground biomass can also be a suitable indicator for N response since it is highly N responsive, and corresponds with grain weight, particularly, under high yielding environments (Sharma 1993; Richards 2000; Sadras et al. 2016). Using conventional destructive methods to measure biomass is time and labour intensive, especially for large-scale trials. For instance, measuring biomass and leaf area index (LAI) with destructive methods in the field requires collecting samples, measuring leaf area, oven-drying and weighting in the laboratory (Royo et al. 2004). Moreover, destructive methods discard a portion of the crop, which limits the use of such techniques in small-sized breeding plots (Prasad et al. 2007). Conversely, image-based phenotyping platforms provide consecutive measurements of biomass during the growing season, and assess plant growth dynamics. Monitoring growth dynamics without the need for periodic destructive harvests, improves

the precision of measurements (Furbank and Tester 2011). Using image-based methods also allows phenotyping of a large number of plots at reasonable costs and good repeatability (Langridge and Fleury 2011; Casadesus and Villegas 2014; Fahlgren et al. 2015).

Plant nutrient status influences the time point of the switch from the vegetative to reproductive stage (Kozłowski 1992; Koelewijn 2004). Extended nutrient starvation can induce an early shift from vegetative to generative growth, and consequently compresses the phenology of plants (Berger et al. 2012; Marschner et al. 2012; Rahimi Eichi et al. 2019). This shifting time point that represents important physiological responses to N can be detected when a plant achieves its maximum growth rate. Accordingly, detecting the maximum growth rate requires using imaging techniques, and cannot be feasibly measured by destructive methods (Berger et al. 2012; Shi et al. 2013).

Imaging techniques provide objective data and exceeds the capabilities of human eyes (Kumar 2015). Nevertheless, post-processing procedures including image adjustment, geometric and radiometric calibrations, atmospheric correction, automatic mosaicking, and algorithms for automatic image segmentation can limit the speed of imaging techniques (Berni et al. 2009; Zarco-Tejada et al. 2013).

2.3.3 Image-based phenotyping under controlled and field conditions

Since the phenome is the result of interactions between the genome and the environment, using controlled conditions can facilitate analysis by reducing environmetal variation (Furbank and Tester 2011). Non-invasive quantitative measurements in controlled environments can be done based on intensive phenotyping using robotics and imaging systems. In intensive methods, a small number of plants are phenotyped individually in high detail and at high resolution in comparison with extensive phenotyping, which includes higher number of plants (Houle et al. 2010). Accordingly, controlled environment experiments allow the examination of traits that may be difficult to measure in the field. For

instance, precise detection of shifts in the time points from vegetative to reproductive stage requires day-to-day imaging, which makes such traits hard to assess in the field conditions (Tardieu and Tuberosa 2010; Hansen, N. J. S. et al. 2018). However, there are also disadvantages with simulation of field conditions in controlled environment (White et al. 2012). Limited root space in pots under greenhouse or growth chamber conditions, and the timing of watering can impact on flowering and seed setting (White et al. 2012; Turner 2019). In the field, plants can be exposed to different stresses that may not be recorded or counted in the analyses (Araus, J. L. and Cairns 2014). In this context, the soil ecosystem in the field cannot be feasibly simulated in nutritiously heterogeneous soils in pots (Araus, J. L. and Cairns 2014). Environmental parameters such as solar radiation, wind speed and evaporation rates can be more severe in field than in controlled conditions. Accordingly, water deficit provokes higher soil penetration resistance in field compared to the soil in pots (Cairns et al. 2011; Araus, J. L. and Cairns 2014).

Field-based high-throughput phenotyping (FBHTP) provides high-throughput information from actual cropping systems (White et al. 2012; Qiu et al. 2019). Precise FBHTP requires identifying and controlling possible site variation, selecting suitable measurement parameters, and using effective methods for data analysis and modelling (Araus, J. L. and Cairns 2014). The most challenging question in FBHTP is finding suitable indices for particular traits in the field (Ghanem et al. 2015). In FBHTP methods, it is important to use inexpensive and easy-to-handle tools, otherwise high costs, labor and time may limit the number of measurements (Araus, Jose L. et al. 2012; Araus, J. L. and Cairns 2014).

2.3.3.1 Conventional visible imaging

Imaging in the visible light range reproduces human perception by obtaining phenotypic information from digital images. Visible images are mainly obtained with silicon sensors, which are sensitive to visible light bands (400-750 nm), and are capable of imaging in two and three dimensions (2D & 3D). RGB (red, green and blue) cameras can be used in

controlled and field conditions for monitoring canopy structure and growth dynamics. Such traits indicate the plant status in response to biotic and abiotic stresses (Casadesús et al. 2007; Berger et al. 2012; Kumar 2015). Due to the low price, portability, high resolution and convenient usage, conventional digital photography with RGB cameras can help for high-throughput phenotyping of crops under controlled and field conditions (Mullan and Reynolds 2010; Khan, Rahimi-Eichi, et al. 2018; Rahimi Eichi et al. 2019).

2.3.3.2 Multispectral imaging

Plant tissues interact with electromagnetic radiation through absorbance, reflectance and transmittance. The fraction of irradiated light that is reflected by leaves is described as leaf reflectance (Li, L. et al. 2014; Kumar 2015). Each constituent of plant cells and tissues absorbs, reflects and transmits an individual wavelength pattern. Accordingly, imaging at various wavelengths can present a wide range of information about the plant tissue's composition and status (Li, L. et al. 2014). Plants can be characterized by electromagnetic waves reflected from visible (VIS) and near infrared (NIR) spectral regions (Berni et al. 2009; Zarco-Tejada et al. 2013). Due to the high absorption of visible wavelengths (400-750 nm) by photoactive pigments (chlorophylls, anthocyanins and carotenoids), vigorous canopies show lower reflectance compared to unhealthy plants. Conversely, healthy canopies show strong reflectance in near-infrared bands (750-1200 nm). The possible reason might be the multiple scattering of light from intercellular areas of mesophyll in leaves (Li, L. et al. 2014; Kumar 2015).

Vegetation indices indicate multiple biophysical variables such as leaf area index (LAI), canopy chlorophyll content, vegetation fraction, absorbed photosynthetically active radiation (PAR), biomass and gross primary production (Hatfield et al. 2008; Delegido et al. 2013). Vegetation indices are mostly obtained from reflectance in PAR range (400-700 nm), near-infrared (NIR) (700-1000 nm) and mid-infrared (MIR) (>4000 nm) bands.

The most common index for estimating vegetation conditions is the normalized difference vegetation index (NDVI), which is calculated from the visible and near-infrared light reflected by vegetation (Rouse et al. 1974; Jensen 2007; Shen et al. 2013):

$$NDVI = \frac{NIR - VIS}{NIR + VIS}$$

It has been reported that NDVI can indicate chlorophyll concentration, N content, biomass, PAR absorption and LAI (Tucker 1979; Sellers 1985; Aparicio et al. 2000; Magney et al. 2016). The multispectral camera used in this dissertation included blue, green, red, red-edge and near-infrared bands.

2.3.4 Effectiveness of unmanned aerial vehicles (UAVs) compared to other phenotyping platforms

Phenotyping data can be obtained by deploying various platforms, e.g., ground-based booms, aircraft, satellites or UAVs (Table 2-3). In comparison with other platforms, UAVs have recently been particularly popular for applications in field phenotyping (De Castro et al. 2018; Khan, Chopin, et al. 2018). Table 2-3 shows the effectiveness of UAVs in FBHTP in comparison with other platforms.

UAVs can be classified into very small, small, medium and large sizes. Using small UAVs, is an economical solution for providing high-quality aerial images. UAVs can carry a wide range of payloads including different kinds of cameras (Radoglou-Grammatikis et al. 2020). Based on their aerodynamic features, UAVs can be categorized into fixed-wing, rotary-wing and hybrid-wing types (Sylvester 2018; Radoglou-Grammatikis et al. 2020). Fixed-wing UAVs have longer endurance and can cover larger areas due to their fast flight speed. However, fixed-wing UAVs need an area for landing and take-off and are harder to manoeuvre. Fixed-wing UAVs can be suitable for aerial survey, high-resolution aerial photos, mapping and land surveying. In comparison with fixed-wing UAVs, rotary-wing

UAVs have lower speed, shorter flight duration and limited payload. Nevertheless, they have a good manoeuvrability, ability to hover around a particular area, and ability to operate in confined areas. Accordingly, rotary-wing UAVs are ideal for surveillance and for monitoring crop health in field (Sylvester 2018). Rotary-wing UAVs are the easiest to manufacture, the cheapest and the most common type among different UAV types (Gonzalez et al. 2018). Hybrid-wing type UAVs are the combination of fixed-wing and rotary-wing types (Sylvester 2018).

Canopy height, biomass and ground cover are often targeted with UAVs in breeding plots (Watanabe et al. 2017; Chen et al. 2018; Makanza et al. 2018). Canopy height, an important indicator of crop development, defined as the distance between canopy base and the highest line of photosynthetic tissues. Using a ruler has long been the traditional way of measuring plant height. However, besides being labour intensive, measuring by ruler does not precisely indicate the average height of the canopy (Holman et al. 2016; Watanabe et al. 2017).

In this dissertation, a set of six wheat varieties differing in GPC were selected based on available data from National Variety Trials (NVT) (Supplementary Figure S2 in Rahimi Eichi et al. (2019)). Among these varieties, Spitfire, Mace and Gregory were hard, and Impala, QAL2000 and Gazelle were soft wheats. In our field trial, RGB and multi-spectral cameras installed on rotary-wing UAVs were used on wheat trials to measure plot-wise characteristics, such as canopy height and NDVI.

Table 2-3. The limitations and application of different phenotyping platforms (West et al. 2003; Jacobi and Kuhbauch 2005; Ollero et al. 2006; Niethammer et al. 2012; Deery et al. 2014; Li, L. et al. 2014; Whitehead and Hugenholtz 2014).

Platform Type	Advantages	Disadvantages
Immobile platforms	• Unmanned frequent monitoring. • Capable of operating throughout day and night. • Capable of recording with high repetition.	• High cost • Monitor limited numbers of plots
Phenomobile platforms	• Easy to use in the field. • Suitable for geo-tagging. • High spatial resolution.	• Generally slow-moving, which makes it time consuming for covering large trials, therefore susceptible to environmental variations.
Blimps & balloons	• Lower costs in comparison with other aerial systems. • Higher payload compared to UAVs (several kilograms). • Simultaneous operation of sensors.	• Highly vulnerable to wind speed. • Low versatility. • Requires high labour work for control. • Requires large storage space after inflation.
Satellite	• Capable of covering large areas, sometimes the size of countries. • Higher payload compared to other airborne platforms.	• High cost. • Lack of spatial resolution. • Limitations in revisit time. • Vulnerable to cloud coverage.
Aircraft	• Capable of carrying a wide range of cameras and sensors regardless of their size and weight. • Higher spatial and spectral resolutions in comparison with satellites. • Rapid monitoring of large-scale trials.	• High operating costs. • Operational complexity. • Less availability and repeatability compared to UAVs. • Low temporal resolution.
UAVs	• Lower prices with lower operational costs in comparison with manned airborne platforms. • Can be operated by one person, so reduces the risks to pilots. • Flexible deployment and high versatility improves temporal and spatial resolution. • Easy to transport. • Capable of imaging large trials in minutes. • Advanced UAVs are commercially available and affordable.	• Limitation in the size and weight of the attached cameras. • Limited flying height. • Limitation in the total time of flight, which limits the whole coverage. • Influenced by wind, albeit less than blimps. • Regulatory rules

2.4 Thesis scope and outline

The objective of this study was to investigate the relationships between grain yield and protein under controlled, field and multi-environmental conditions in high and low GPC wheat varieties. The work described in this dissertation also evaluates the importance of non-destructive methods for biomass measurements to show the differences in the N responsiveness of high and low GPC wheat.

The specific aims of this project were:

a) To understand the relationship between biomass, grain yield and GPC in high and low GPC varieties under different N supply in controlled conditions;

b) To relate the results in controlled conditions to field environments in South Australia;

c) To relate the results, regarding the grain yield-GPC relationship, in controlled and field conditions to different environments across the Australian wheat-belt.

Chapter 3: Understanding the Interactions between Biomass, Grain Production and Grain Protein Content in High and Low Protein Wheat Genotypes under Controlled Environments

Vahid Rahimi Eichi [1,2], Mamoru Okamoto [1,2], Stephan M. Haefele [3],

Nathaniel Jewell [1,4], Chris Brien [1,4], Trevor Garnett [1,2,4] and Peter Langridge [1,5],*

[1]School of Agriculture Food and Wine, University of Adelaide, Glen Osmond 5064, South Australia;

vahid.rahimi-eichi@adelaide.edu.au (V.R.E.); mamoru.okamoto@adelaide.edu.au (M.O.);

nathaniel.jewell@adelaide.edu.au (N.J.); chris.brien@adelaide.edu.au (C.B.);

Trevor.Garnett@grdc.com.au (T.G.)

[2]ARC Industrial Transformation Research Hub for Wheat in a Hot and Dry Climate, Waite Research Institute,

University of Adelaide, Glen Osmond SA 5064, Australia

[3]Rothamsted Research, Harpenden, Hertfordshire AL5 2JQ, UK;

stephan.haefele@rothamsted.ac.uk

[4]The Plant Accelerator, Australian Plant Phenomics Facility, Waite Research Institute,

University of Adelaide,

Adelaide SA 5064, Australia

[5]Wheat Initiative, Julius-Kühn-Insititute, 14195 Berlin-Dahlem, Germany

***** Correspondence: peter.langridge@adelaide.edu.au; Tel.: +61-83137368

Statement of Authorship

Title of Paper	Understanding the interactions between biomass, grain production and grain protein content in high and low protein wheat genotypes under controlled environments
Publication Status	☑ Published ☐ Accepted for Publication ☐ Submitted for Publication ☐ Unpublished and Unsubmitted work written in manuscript style
Publication Details	Manuscript prepared in accordance with the guidelines for *agronomy*

Principal Author

Name of Principal Author (Candidate)	Vahid Rahimi Eichi
Contribution to the Paper	Conceptualization, methodology, formal analysis, investigation, writing (original draft preparation), writing (review and editing)
Overall percentage (%)	80%
Certification	This paper reports on original research I conducted during the period of my Higher Degree by Research candidature and is not subject to any obligations or contractual agreements with a third party that would constrain its inclusion in this thesis. I am the primary author of this paper.
Signature	Date 14.07.2020

Co-Author Contributions

By signing the Statement of Authorship, each author certifies that:

i. the candidate's stated contribution to the publication is accurate (as detailed above);

ii. permission is granted for the candidate in include the publication in the thesis; and

iii. the sum of all co-author contributions is equal to 100% less the candidate's stated contribution.

Name of Co-Author	Prof. Peter Langridge
Contribution to the Paper	Conceptualization, methodology, writing (original draft preparation), writing (review and editing), supervision
Signature	Date 16/7/2020

Name of Co-Author	Dr. Trevor Garnett
Contribution to the Paper	Conceptualization, methodology, writing (original draft preparation), writing (review and editing), supervision
Signature	Date 16/7/2020

Name of Co-Author	Dr. Mamoru Okamoto
Contribution to the Paper	Methodology, writing (original draft preparation), writing (review and editing), supervision
Signature	Date 16/07/2020

Name of Co-Author	Dr. Stephan M. Haefele		
Contribution to the Paper	Conceptualization, methodology, supervision		
Signature		Date	16.07.2020

Name of Co-Author	Dr. Chris Brien		
Contribution to the Paper	Methodology, formal analysis, statistical supervision		
Signature		Date	16/07/2020

Name of Co-Author	Dr. Nathaniel Jewell		
Contribution to the Paper	Formal analysis		
Signature		Date	17/7/20

Please cut and paste additional co-author panels here as required.

Understanding the Interactions between Biomass, Grain Production and Grain Protein Content in High and Low Protein Wheat Genotypes under Controlled Environments

Vahid Rahimi Eichi [1,2], Mamoru Okamato [1,2], Stephan M. Haefele [3], Nathaniel Jewell [1,4], Chris Brien [1,4], Trevor Garnett [1,2,4] and Peter Langridge [1,5,*]

1   School of Agriculture Food and Wine, University of Adelaide, Glen Osmond 5064, South Australia;
     vahid.rahimi-eichi@adelaide.edu.au (V.R.E.); mamoru.okamoto@adelaide.edu.au (M.O.);
     nathaniel.jewell@adelaide.edu.au (N.J.); chris.brien@adelaide.edu.au (C.B.);
     Trevor.Garnett@grdc.com.au (T.G.)
2   ARC Industrial Transformation Research Hub for Wheat in a Hot and Dry Climate, Waite Research Institute,
     University of Adelaide, Glen Osmond SA 5064, Australia
3   Rothamsted Research, Harpenden, Hertfordshire AL5 2JQ, UK; stephan.haefele@rothamsted.ac.uk
4   The Plant Accelerator, Australian Plant Phenomics Facility, Waite Research Institute, University of Adelaide,
     Adelaide SA 5064, Australia
5   Wheat Initiative, Julius-Kühn-Insititute, 14195 Berlin-Dahlem, Germany
*   Correspondence: peter.langridge@adelaide.edu.au; Tel.: +61-83137368

Abstract: Grain protein content (GPC) is a key quality attribute and an important marketing trait in wheat. In the current cropping systems worldwide, GPC is mostly determined by nitrogen (N) fertilizer application. The objectives of this study were to understand the differences in N response between high and low GPC wheat genotypes, and to assess the value of biomass growth analysis to assess the differences in N response. Six wheat genotypes from a range of high to low GPC were grown in low, medium and high N, under glasshouse conditions. This experiment was designed around non-destructive estimation of biomass using a high throughput image-based phenotyping system. Results showed that Spitfire and Mace had higher grain N% than Gazelle and QAL2000, and appeared to demand more N to grow their biomass. Moreover, at low N, Spitfire grew faster and achieved the maximum absolute growth rate earlier than high N-treated plants. High grain N% genotypes seem able to manage grain N reserves by compromising biomass production at low N. This study also indicated the importance of biomass growth analysis to show the differences in the N responsiveness of high and low GPC wheat.

Keywords: grain protein content; grain nitrogen concentration; biomass; growth rate; time to maximum growth rate; nitrogen response; imaging; hard and soft wheat

1. Introduction

Wheat is the most widely cultivated crop in the world and a substantial source of carbohydrate and protein in human diets [1]. Increasing grain weight and grain quality are the two main goals in improving wheat production. In this context, grain protein content (GPC) is a key quality attribute and an important marketing trait [2]. Increasing GPC is positively correlated with grain hardness in both hard and soft wheats [3–5]. Changes in kernel hardness can affect milling, downstream processing and consequently end products [6]. Due to the negative correlation between grain weight and GPC [7–9], grain weight increase may reduce the end-use quality of hard wheats [1,10]. However, lower GPC

for soft wheats, which have different quality targets and end products compared to hard wheats, can be a desirable trait [11]. Soft wheat lines produce substantially lower GPC compared with hard wheats [12,13]. In the current world cropping systems, GPC is mostly determined by nitrogen (N) fertilizer application [14,15]. Therefore the nitrogen use efficiency (NUE) of soft genotypes may be genetically defined.

Only 40%–60% of the applied N is taken up by wheat plants [16], which inflates production costs and environmental impacts [17,18]. Consequently, there is considerable interest in improving NUE [19,20]. NUE, which can be defined as the ratio of grain weight to N supplied, has been mostly improved by indirect selections for high grain weight [21,22]. In fact, efforts to improve NUE in wheat has focused on increasing grain weight response to higher N inputs [23]. In this context, comparing the N responses of high and low GPC wheats may reveal the mechanisms used by the contrasting genotypes in their N use at high and low N input [24,25].

Due to the challenges of destructive harvests, NUE evaluations in the field are usually based on measuring grain weight at given N supply [22,26]. Controlled environment phenotyping platforms can help to dissect complex traits into simple components under reduced environmental variation. Therefore, controlled environment experiments allow the examination of traits that may be difficult to measure in the field [27–29]. In this respect, the above-ground biomass can be a suitable indicator for N response since it is highly N responsive, and corresponds with grain weight under glasshouse conditions [19,30–33].

Growth curves of single plants resemble consecutive measurements of biomass during the season, and give a view of plant growth dynamics. Monitoring growth dynamics without the need for periodic destructive harvests improves the precision of measurements [34]. Destructive methods, on the other hand, require frequent harvests at specific time points and do not allow continuous growth measurement from individual plants [35]. Therefore, deploying imaging platforms, which allow for consecutive measurements, reduces the number of required plants and improves the precision of growth analysis. Phenotyping based on imaging can also help to analyze plant nutrient status. Plant nutrient status influences the time point of the switch from the vegetative to reproductive stage [36,37]. Extended nutrient starvation can induce the early shift from vegetative to generative growth, and consequently compresses the phenology of plants [35,38,39]. Maximum absolute growth rate (max-AGR) indicates the transition point from vegetative to generative growth [40]. Accordingly, the interval of the plant life cycle required to reach the max-AGR, which is known as the time of max-AGR (t-maxAGR), can be studied as a trait for N response. These traits, max-AGR and t-maxAGR, can be measured with imaging techniques and represent important physiological responses to N that cannot be feasibly measured by destructive methods [35,41]. Also the requirement of day-to-day imaging, for precise measurement of t-maxAGR makes this trait hard to assess in the field conditions.

Here, we report on a study based on growth measurement of single wheat plants under controlled conditions with different N supply. The objectives of this study were: (1) to understand the differences in N response between high and low GPC wheats; (2) to assess the value of biomass growth analysis for the examination of differences in N response in high and low GPC wheats. To address these objectives, a set of six genotypes differing in GPC were selected based on available data from National Variety Trials (NVT) (Supplementary Figure S2).

2. Materials and Methods

2.1. Plant Material, Growth Conditions and N Treatment

Based on the NVT data from 11 years (Supplementary Figure S2), six wheat (*Triticum aestivum* L.) genotypes were selected to cover a range of high to low GPC. The six genotypes, Spitfire, Mace, Gregory, Impala, Gazelle and QAL2000, were grown at three N levels under greenhouse conditions. The experiment was carried out in The Plant Accelerator (Australian Plant Phenomics Facility, University of Adelaide, Australia; Latitude: −34.97113, Longitude: 138.63989) during spring and

summer (June–November 2016). Temperature in the greenhouse was regulated based on a sinusoidal cycle with 22 °C day/15 °C night.

Three seeds were sown in 150 mm pots (2.5 litre) with drainage holes, in 50:50 (*v/v*) coco-peat mix: UC Davis potting soil with adequate fertilizers except nitrogen. The three levels of nitrogen comprised of 25 (low), 75 (medium) and 150 (high) mg N per kg soil and were applied in the form of urea during soil mixing. Soil surface was covered with blue poly-vinyl chloride mats to reduce soil moisture evaporation while providing a favourable background colour for image analysis. A blue carnation frame was placed in the pot to support the plant. Five days after emergence, seedlings were thinned to one uniformly sized plant per pot.

2.2. Experimental Design

A spilt-plot design was used to assign the genotypes and N treatments to 108 plant carts (that is pots) on a conveyor belt system. Each cart held one pot with a single plant, arranged in 6 lanes by 18 plant carts (Supplementary Figure S1). Automatic imaging started on 29 days after sowing (DAS) (before stem elongation) by transferring the pots to the conveyor system, where the plants remained until 61 DAS. Water levels were monitored and adjusted daily to field capacity through an automated weighing and watering system (LemnaTec GmbH, Aachen, Germany). After 61 DAS, plants were returned to the greenhouse and grown to maturity. When mature, the plants were destructively harvested for biomass measurements and N analysis of grain and non-grain tissues.

2.3. Red, Green, Blue (RGB) Image Capture and Image Analysis

Shoot images were taken using the LemnaTec 3D Scanalyzer system. Plants were imaged daily with two 5-megapixel visible/RGB cameras (Basler Pilot piA2400-17gm). One image from the top and two from the side at a 90 degrees rotation were prepared at each imaging session. All captured images were analysed using the LemnaTec Grid software package (LemnaTec GmbH, Aachen, Germany).

The projected shoot area (PSA) was extracted from all three RGB images, and the sum of PSA from the three images was used to estimate shoot biomass. Absolute growth rates (AGRs) were calculated from the estimated PSA between two time points of t_k and t_j, [42]:

$$\text{AGR}\left(t_j, t_k\right) = \frac{\text{PSA}tk - \text{PSA}tj}{tk - tj} \tag{1}$$

Projected shoot area values were smoothed by fitting a cubic smoothing spline to the data for each plant. Smoothed absolute growth rates were calculated from the smoothed PSA [42].

2.4. N Measurements

Nitrogen content in grain (grain N%) and non-grain (non-grain N%) tissues were determined by using a nitrogen analyser (Rapid N exceed®, Elementar, Germany). Accordingly, grain and non-grain tissues were ground to a fine powder using ball mills after being dried at 60 °C. Non-grain tissues, including vegetative tissues and the non-grain parts of spikes, were shredded before grinding.

2.5. Statistical Analysis

The design of the plots was generated using DAE [43], a package for the R [44] statistical computing environment. The need for unequal residual variance for the imaging was tested through restricted maximum likelihood estimation (REML) ratio tests using ASReml-R [45] and ASRemlPlus [46], packages for the R statistical computing environment. If non-significant, then equal residual variances were assumed. The phenotypic means were obtained using the resulting model. Significant differences were accepted at $p \leq 0.05$.

3. Results

NVT data analysis showed that Spitfire produced the highest GPC, with Gazelle and QAL2000 showing the lowest compared to the other genotypes (Supplementary Figure S2). Mace was also selected as it was reported to be highly N responsive [47,48].

As mentioned above, plants were imaged daily from 29 to 61 DAS. Over the course of imaging, differences in PSA between the three N treatments increased over time. Maximum projected shoot area (max-PSA), which was the curve vertex, was reduced for all genotypes as N supply decreased (Figure 1A and Supplementary Figure S4A).
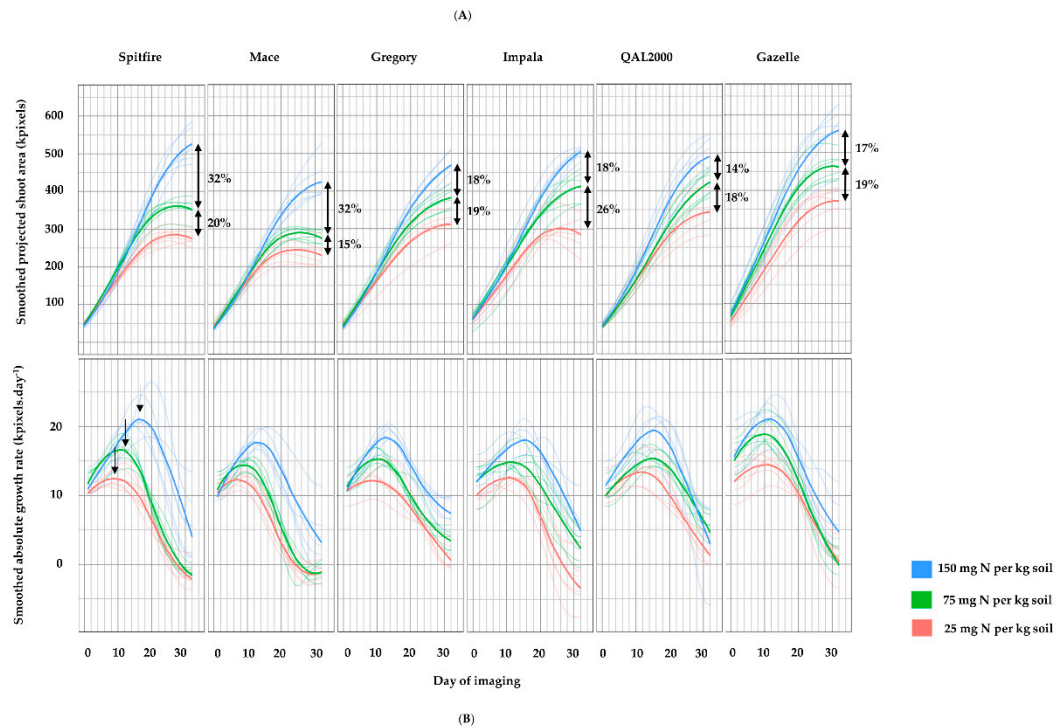
Figure 1. Smoothed projected shoot area (PSA) (**A**) and smoothed absolute growth rate (AGR) (**B**). 6 wheat genotypes were grown in low (red), medium (green) and high (blue) nitrogen supply. Each line represents the average of 6 replicates. Numbers with % show the reduce rates from high to medium and from medium to low. Black arrows in Figure B indicate the maximum absolute growth rate. The unit of projected shoot area is kilo pixels, and the unit of absolute growth rate is kilo pixels per day.

However, the biggest reduction in max-PSA from high to low N was in Spitfire and Mace with 46% and 43% decrease, respectively. In this context, maximum projected shoot area from high to medium nitrogen was more reduced in Spitfire and Mace with 32% compared to other genotypes. Conversely, less PSA reductions from high to low N were found in Gazelle and QAL2000 (Figures 1A and 2, and Table 1).
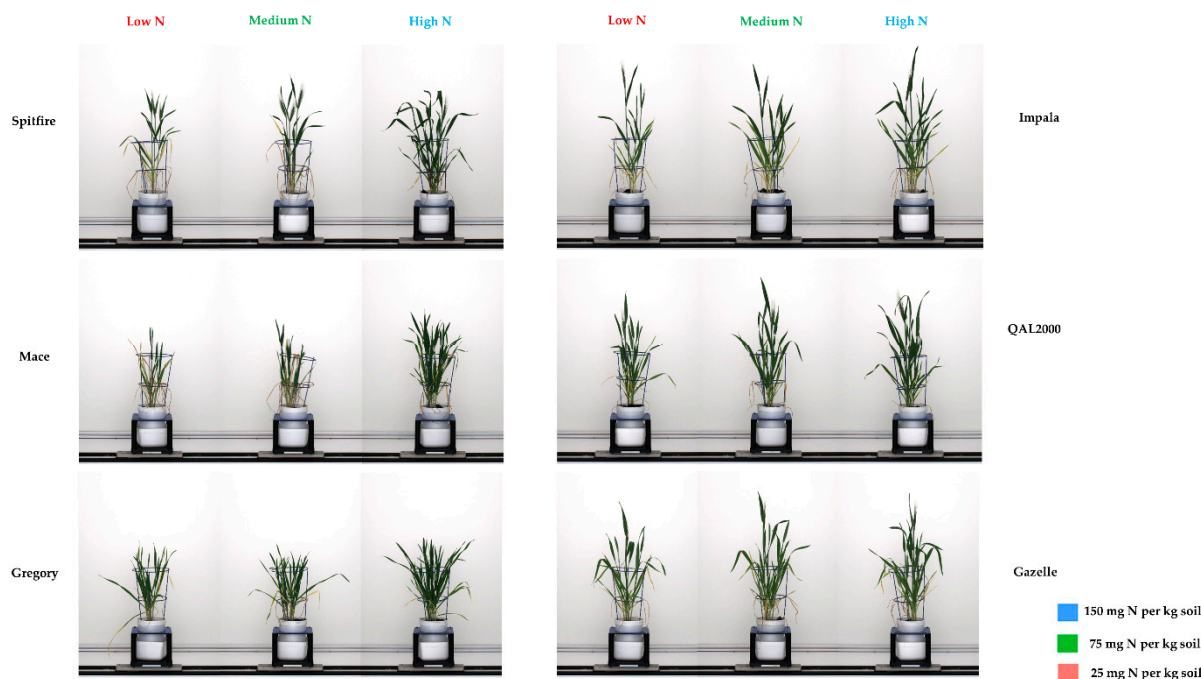
Figure 2. Red, green, blue (RGB) camera images from side views showing phenotypic changes of the 6 wheat genotypes in response to high, medium and low N treatments 61 days after sowing. Samples are selected from low and high nitrogen treatments.

Table 1. Table of grain protein content (GPC) from National Variety Trials (NVT) trials, grain and non-grain nitrogen concentration measured in this study, total reduction of maximum projected shoot area (max-PSA), maximum absolute growth rate (max-AGR) and the time of max-AGR (t-maxAGR) in 6 wheat genotypes. GPC is the average of all NVT trials across the Australian wheat belt between 2008 to 2018. Total reduction rate in max-PSA, max-AGR and t-maxAGR were calculated as: ((high N-lowN)/(high N)) × 100.

	Spitfire	Mace	Gregory	Impala	QAL2000	Gazelle
Average of GPC from 11 years of NVT data	13.4	11.3	12	11.6	10.9	10.9
Average of grain N% in all N treatments	1.7	1.7	1.6	1.5	1.3	1.4
Average of non-grain N% in all N treatments	0.3	0.4	0.3	0.2	0.2	0.2
% total reduction of max-PSA from high to low N	46	43	34	39	30	33
% total reduction of tmax from high to low N	44	35	25	32	19	8
% total reduction of max-AGR from high to low N	43	33	33	31	32	32

After Spitfire and Mace, max-PSA declined more in Impala compared to other genotypes. However, PSA in Spitfire and Mace were mostly reduced from high to medium N, while PSA in Impala was highly restricted by reducing N inputs from medium to low (Figure 1A, and Table 1).

Max-AGR was also reduced as N level decreased in all genotypes (Figure 1B and Supplementary Figure S4B). Spitfire showed the highest decrease in maximum absolute growth rate from high to low N (Figure 1B and Table 1). Accordingly, the time to max-AGR (t-maxAGR) declined with reducing N supply in most of the genotypes, except Gazelle where t-maxAGR was not significantly reduced (Figure 3).

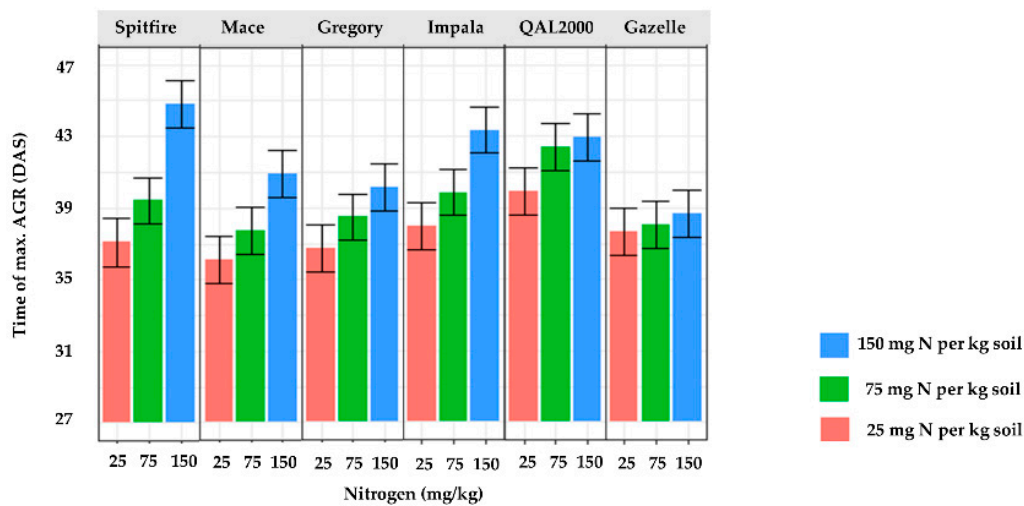**Figure 3.** Predictions from full interaction model of the time of maximum absolute growth rate (t-maxAGR) of 6 wheat genotypes grown in low (red), medium (green) and high (blue) nitrogen supply. The unit of t-maxAGR is day after sowing (DAS). Each columns represents 6 replicate plants. The error bars are half of the least significant differences ($p = 0.05$) so that non-overlapping bars indicate significant differences.

All genotypes, other than Gazelle, grew faster and achieved maximum absolute growth rate earlier at low N compared to high N-treatment. Under low N condition, QAL2000 showed the lowest reduction in the time of max-AGR after Gazelle, whereas the highest t-maxAGR decline was in Spitfire and Mace.

The post-harvest analysis showed that the above-ground biomass and grain weight were enhanced by increasing N inputs (Figure 4G–I and Supplementary Figure S3).
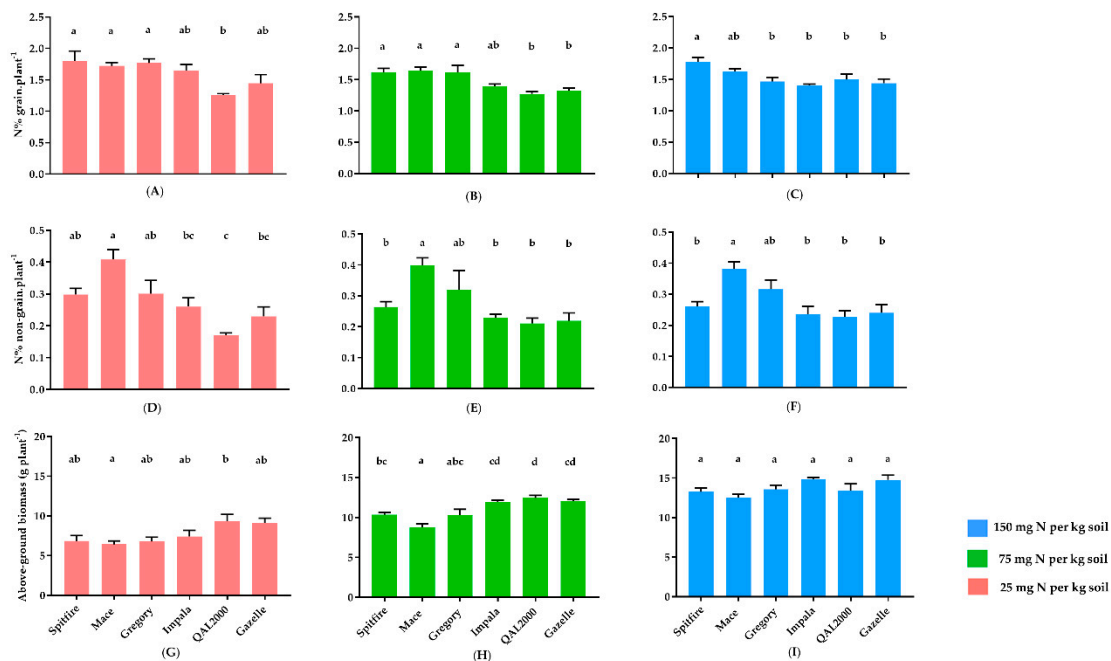
Figure 4. Grain (**A**, **B** and **C**) and non-grain (**D**, **E** and **F**) nitrogen concentration (N%), and the dry weight of above-ground biomass (**G**, **H** and **I**) measured at maturity in 6 wheat genotypes grown in low (red), medium (green) and high (blue) nitrogen supply. Columns represent the average of 6 replicates and the error bars are the sample standard errors. Each column represents 6 replicate plants. Different letters indicate significant differences between genotypes according to the Tukey's test ($p < 0.05$).

At low and medium N, Gazelle and QAL2000 produced relatively higher above-ground biomass and grain weight compared with other genotypes. However, at high N there was no difference in above-ground biomass and grain weight production between genotypes (Figure 4G–I and Supplementary Figure S3A–C). There was a positive correlation between above-ground biomass and grain weight in all N treatments and genotypes (Figure 5A).
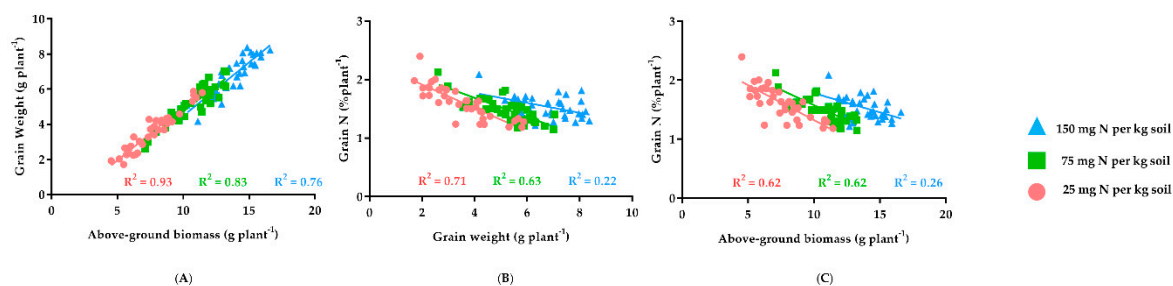

Figure 5. Relationships between above-ground biomass weight and grain weight (**A**), grain weight and the percentage of nitrogen in grains (**B**), and above-ground biomass weight and the percentage of nitrogen in grains (**C**) in low (red), medium (green) and high (blue) nitrogen supply. Each shape represents a single plant. Plants were the 6 wheat genotypes used in this study.

Grain N% was negatively correlated with above-ground biomass and grain weight particularly at low N (Figure 5B,C). This negative relationship was stronger at low and medium compared to high N treatments. In other words, there was a tendency for decreased GPC with increased grain weight at high N for all genotypes.

In this study, the grain N% of all genotypes were not increased from low to high N. Consistent with NVT data (Supplementary Figure S2), N analysis showed that Spitfire tended to produce higher grain N% at low, medium and high N relative to the low GPC genotypes Gazelle and QAL2000 (Figure 4A–C, and Table 1). Interestingly, the N% in the non-grain tissues of Mace was higher than for Spitfire (Figure 4D–F).

There were no differences between the grain N% of Impala, Gazelle and QAL2000 in this study. However, results from 11 years of NVT data in different environments (Supplementary Figure S2A) showed that Impala and Gregory produced higher GPC compared to Gazelle and QAL2000, and lower GPC relative to Spitfire. Grain N% constituted most of the N reserves in all genotypes (Figure 4A–C). Based on the average of grain N% in all nitrogen supplies, genotypes in this study were categorized into three groups; high (Spitfire and Mace), medium (Impala and Gregory), and low (QAL2000 and Gazelle) grain N% genotypes. Genotypes were grouped solely based on the grain N% results obtained in this study. However, NVT data showed that the average GPC of Mace was not higher than Gregory and Impala (Table 1). The lower average GPC of Mace in NVT data might be due to its higher yield at some of the sites compared with Gregory and Impala. Mace is adapted to the low-yielding environments of southern Australia [49] and its GPC tends to drop at high yielding sites [50]. In this context, the grain protein deviation of Mace, after Spitfire, was higher than the other four genotypes (Supplementary Figure S2B).

Overall, the influence of N treatments on t-maxAGR was related to the difference from high to low grain N concentration genotypes (Table 1 and Figure 6A–C).
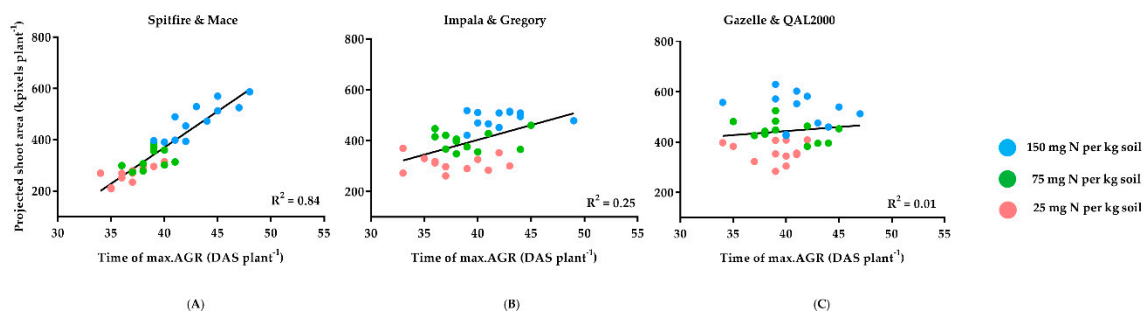
Figure 6. Relationships between the day of maximum absolute growth rate (t-maxAGR) and projected shoot area (PSA) in high (**A**), medium (**B**) and low (**C**) grain N concentration genotypes. The unit of t-maxAGR is day after sowing (DAS). Different colours indicate the nitrogen treatments. Each shape represents a single plant.

In Spitfire and Mace, which are considered as high grain N concentration genotypes, the time to maximum absolute growth rate was strongly correlated with projected shoot area. However, the strength of the relationship between t-maxAGR and PSA diminished in Gregory and Impala (medium grain N concentration) and was entirely lost in Gazelle and QAL2000 (low grain N concentration). The absence of a linear relationship between t-maxAGR and grain N% in Spitfire and Mace is shown in Figure 7A,B. Despite the high influence of the time to maximum absolute growth rate on biomass production in Spitfire and Mace, grain N% were unaffected at different N inputs.
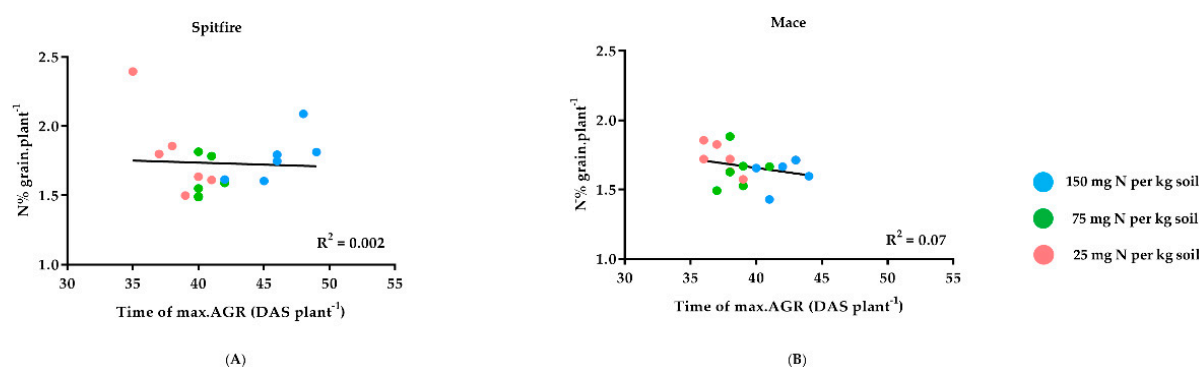
Figure 7. Relationships between the day of maximum absolute growth rate (t-maxAGR) and grain nitrogen concentration per plant in Spitfire (**A**) and Mace (**B**). Different colours indicate the nitrogen treatments. The unit of t-maxAGR is days after sowing (DAS). Each shape represents a single plant.

4. Discussion

4.1. Biomass Can Indicate the Impact of Nitrogen on Grain Weight

As noted in previous studies [30,31,33], the strong correlation between above-ground biomass and grain weight (Figure 5A) showed that biomass can be used as an indicator of grain weight responses to N in the six wheat genotypes evaluated in this experiment. The relationship between above-ground biomass and grain weight is likely to be due to the positive correlation between leaf surface area and total photosynthesis per unit ground area [33,51]. Previous studies using destructive methods also showed a strong relationship between biomass and grain weight in both hard and soft wheat genotypes [25,52,53].

The high positive correlation between above-ground biomass and grain weight (Figure 5A) is counteracted by the negative correlation between biomass and grain N% (Figure 5B,C). Consequently, increasing grain weight appears to result in a grain N% penalty, particularly at low N. The reduction in grain N% with increasing grain weight may reflect the high priority placed on elevating grain weight by wheat breeders rather than grain N% accumulation under low N conditions. The results

suggest that once the maximum level of grain weight has been achieved, the additional N is invested in increasing grain N%, particularly, for high GPC genotypes [54,55]. The relatively low grain N% seen for all varieties in this study (Figure 4A–C) may be due to the favourable growth conditions in the greenhouse and, consequent, increase in biomass. It appears that the high N requirements of plants seen in this experiment, meant that the applied N at low and medium N was mostly used for grain weight production rather than to increase grain N%.

4.2. Differences in Nitrogen Responsiveness between High and Low GPC Genotypes

Spitfire and Mace produced less biomass at low N than the other genotypes and were more responsive at high N compared with the low grain N% genotypes (Figures 1A and 4G–I). Related studies on wheat and oilseed spring rape indicate that genotypes, which show reduced yield at low N may show greater responses to higher N levels compared to other genotypes [48,56,57]. It is shown that high compared to low GPC wheat genotypes require higher N rates to show favourable yield responses [58].

In accordance with previous studies [39,59–61], reducing N supply diminished the total biomass and growth rate. However, by reducing N inputs, biomass and growth rate declined more in high than in low grain N concentration genotypes. In fact, the biomass of genotypes that were selected for high GPC was more vulnerable to low N in comparison with the biomass of low GPC genotypes (Figure 1A, Figure 2, and Figure 4G–I). The high reduction of biomass growth in high GPC genotypes at low N was previously observed in wheat [62,63]. In high GPC genotypes, biomass growth under limited N may be reduced in favour of root growth to support N uptake after anthesis [62].

This study showed that shortening t-maxAGR was the key limiting factor for PSA production for high grain N genotypes (Figure 6A). In other words, high N genotypes appear to reach the peak of growth and terminate the vegetative stage earlier in low N than high N-treated plants (Figure 1B, Figure 3 and Table 1). Compressing phenology at low N, which decreases N requirement, has been previously observed in different species [39,60,64–66]. However, the low impact of N shortage on the t-maxAGR and biomass growth of Gazelle and QAL2000 was a new finding in this study.

Our results indicated that the rate of t-maxAGR reduction from high to low N was related to the grain N concentration (Table 1 and Figure 6A–C). Spitfire and Mace had higher grain N than Gazelle and QAL2000, and appeared to demand more N to grow their biomass. It might be that high grain N% genotypes sense the low N status early in development and shorten their vegetative growth phase to maintain sufficient N for grain development and filling. Hence, Spitfire responded to low N by reducing growth rate, possibly to conserve N for grains (Figure 1B and Table 1). In this context, the grain N% of Spitfire and Mace were not influenced by t-maxAGR at different N treatments (Figure 7A,B). Therefore, high grain N% genotypes in this study were able to prevent grain N loss at low N conditions regardless of the variations in the time to maximum absolute growth rate.

Accelerating the life cycle is a typical response of plants to low N [39]. N translocation corresponds with senescence since senescing leaf and stem tissues are an important N source for grains [67–69]. Therefore, the increase of shoot biomass and carbon assimilation after flowering can compete with grain demand for N [70]. In Gazelle and QAL2000, which are genotypes used for low GPC purposes [11], low N supply did not trigger accelerated development and a decrease in the time to maxAGR (Figure 6C). This suggests that Gazelle and QAL2000 use the available N primarily for biomass production and do not show the conservative strategy used by Spitfire and Mace.

Increases of max-AGR and t-maxAGR from low to high N in Mace were not as high as in Spitfire (Figure 1B and Table 1). Spitfire is known to produce higher GPC compared to Mace and many other genotypes (Supplementary Figure S2A) [71,72]. Therefore, Mace may be less sensitive to low N in comparison with Spitfire. The modest max-AGR increase in Mace from low to high N could be due to mechanisms that help the plants adapt to unfavourable conditions late in the season. In contrast to Spitfire, Mace is mostly grown in regions where late-season drought is common [19,48,73]. In such regions, characterized by terminal drought, compressing phenology may be a beneficial trait [65].

Extending the time to maxAGR and increasing max-AGR at high N in summer for Mace could raise the risk of drought and haying-off at late season. Increasing t-maxAGR under high N supply conditions may be an effective trait for building biomass provided that the available time for full development is not limited.

Differences in N responsiveness between genotypes may be due to their history of selection Dhugga and Waines [74] suggested that selection of new wheat genotypes in high N soils would improve the breeding efficiency for high GPC. Over 20 years, N fertiliser application was steadily increased [75] and wheat breeders have tended to select for high yielding genotypes under high N supply. Applying N beyond the demand for maximum yield can raise the GPC (Figure 5B), which would be undesirable for low GPC soft genotypes [76–79]. Soft wheats can be downgraded if they have more than 9.5% GPC in Australia [13]. Thus, the rate of applied N for producing low-protein soft wheats is less than for high GPC hard wheats [80,81]. Consequently, soft wheats are bred primarily for high yield and GPC is a low priority since this can be managed by maintaining low N supply [82]. Selection under high N may have resulted in the higher sensitivity of Spitfire and Mace to low N in comparison with Gazelle and QAL2000. Therefore, it is possible that Australian hard wheat breeders have unintentionally selected for increased N demand in modern hard genotypes.

Gazelle and QAL2000 are grown mostly in east coast regions with high rainfall or irrigation [83–85]. Frequent rainfall or watering can lead to N leaching into deeper soil layers that reduces the amount of available N in the soil [86]. Therefore, plants grown on such soils with poor available N, may respond strongly to even low amounts of N [19,87]. In addition, several Australian soft wheat genotypes originate from Western Australian regions characterized by light and sandy soils [88,89]. Sandy soils have low water retention capacity, which reduces the amount of available N compared with finer textured soils [19,87,88]. Consequently, Western Australian soils are potentially N-deficient [88,90].

Although Impala is a biscuit soft wheat, it is known to produce slightly higher GPC compared to QAL2000 and Gazelle (Supplementary Figure S2A) [83]. Therefore, the higher decline in the biomass and t-maxAGR of Impala from high to low N, compared to QAL2000 and Gazelle, may be due to the higher N demand of Impala (Table 1). However, due to different selection purposes, less N% was required in the grain of Impala compared to Spitfire and Mace. Consequently, PSA in Impala was mostly reduced from medium to low N, whereas in Spitfire and Mace it was from high to medium N (Figure 1A).

5. Conclusions

Accelerated development appeared to reduce the effect of low N supply on the grain N concentration of genotypes with high GPC. High grain N% genotypes seem able to manage grain N reserves by reducing biomass production at low N. This mechanism may sacrifice biomass and, consequently, yield but helps to ensure the required amounts of N are available for grains to maintain high GPC. Breeders appear to have selected for this trait through selection for high GPC in low yielding environments. Conversely, for the low grain N% genotypes, Gazelle and QAL2000, low N has little impact on the biomass production, and the yield of these genotypes shows greater tolerance to N deficiency [91,92]. Consistent with the previous NUE studies on wheat and maize [25,63,93], the current results suggest that there is value in including screening and selection at low N supply rather than focusing only on high N environments in breeding programs. This can be beneficial for identifying N-use efficient genotypes and novel NUE traits in wheat. This study also confirms the importance of non-destructive method for biomass growth analysis to show the differences in the N responsiveness of high and low GPC wheat.

Abbreviations

AGR	Absolute growth rate
DAS	Days after sowing
GPC	Grain protein content
N	Nitrogen
NUE	Nitrogen use efficiency
NVT	National variety trials
PSA	Projected shoot area
t-maxAGR	Time to maximum growth rate

References

1. Shewry, P.R.; Hey, S.J. The contribution of wheat to human diet and health. *Food Energy Secur.* **2015**, *4*, 178–202. [CrossRef] [PubMed]

2. Husenov, B.; Makhkamov, M.; Garkava-Gustavsson, L.; Muminjanov, H.; Johansson, E. Breeding for wheat quality to assure food security of a staple crop: The case study of tajikistan. *Agric. Food Secur.* **2015**, *4*, 9. [CrossRef]

3. Kuhn, J.C.; Stubbs, T.L.; Carter, A.H. Effect of the gpc-b1 allele in hard red winter wheat in the us pacific northwest. *Crop Sci.* **2016**, *56*, 1009–1017. [CrossRef]

4. Hong, B.H.; Rubenthaler, G.L.; Allan, R.E. Wheat pentosans. 1. Cultivar variation and relationship to kernel hardness. *Cereal Chem.* **1989**, *66*, 369–373.

5. Bettge, A.D.; Morris, C.F. Relationships among grain hardness, pentosan fractions, and end-use quality of wheat. *Cereal Chem.* **2000**, *77*, 241–247. [CrossRef]

6. Saint Pierre, C.; Peterson, C.J.; Ross, A.S.; Ohm, J.B.; Verhoeven, M.C.; Larson, M.; Hoefer, B. White wheat grain quality changes with genotype, nitrogen fertilization, and water stress. *Agron. J.* **2008**, *100*, 414–420. [CrossRef]

7. Kibite, S.; Evans, L. Causes of negative correlations between grain yield and grain protein concentration in common wheat. *Int. J. Plant. Breed.* **1984**, *33*, 801–810. [CrossRef]

8. Simmonds, N.W. The relation between yield and protein in cereal grain. *J. Sci. Food Agric.* **1995**, *67*, 309–315. [CrossRef]

9. Bogard, M.; Allard, V.; Brancourt-Hulmel, M.; Heumez, E.; Machet, J.-M.; Jeuffroy, M.-H.; Gate, P.; Martre, P.; Le Gouis, J. Deviation from the grain protein concentration–grain yield negative relationship is highly correlated to post-anthesis n uptake in winter wheat. *J. Exp. Bot.* **2010**, *61*, 4303–4312. [CrossRef]

10. Ortiz-Monasterio, R.J.I.; Sayre, K.D.; Rajaram, S.; McMahon, M. Genetic progress in wheat yield and nitrogen use efficiency under four nitrogen rates. *Crop Sci.* **1997**, *37*, 898. [CrossRef]

11. Huebner, F.R.; Bietz, J.A.; Nelsen, T.; Bains, G.S.; Finney, P.L. Soft wheat quality as related to protein composition. *Cereal Chem.* **1999**, *76*, 650–655. [CrossRef]

12. Moss, H.J. Quality standards for wheat varieties. *J. Aust. Inst. Agric. Sci.* **1973**, *39*, 109–115.

13. Anderson, W.K.; Sawkins, D. Production practices for improved grain yield and quality of soft wheats in western australia. *Aust. J. Exp. Agric.* **1997**, *37*, 173–180. [CrossRef]

14. Triboi, E.; Abad, A.; Michelena, A.; Lloveras, J.; Ollier, J.L.; Daniel, C. Environmental effects on the quality of two wheat genotypes: 1. Quantitative and qualitative variation of storage proteins. *Eur. J. Agron.* **2000**, *13*, 47–64. [CrossRef]

15. Sinclair, T.R.; Rufty, T.W. Nitrogen and water resources commonly limit crop yield increases, not necessarily plant genetics. *Glob. Food Secur.* **2012**, *1*, 94–98. [CrossRef]

16. Sylvester-Bradley, R.; Kindred, D.R. Analysing nitrogen responses of cereals to prioritize routes to the improvement of nitrogen use efficiency. *J. Exp. Bot.* **2009**, *60*, 1939–1951. [CrossRef] [PubMed]

17. Harrison, R.; Webb, J. A review of the effect of n fertilizer type on gaseous emissions. *Adv. Agron.* **2001**, *73*, 65–108.

18. Bouwer, H. Agricultural contaminants: Problems and solutions. *J. Water Environ. Technol.* **1989**, *1*, 292–297.

19. Sadras, V.O.; Hayman, P.T.; Rodriguez, D.; Monjardino, M.; Bielich, M.; Unkovich, M.; Mudge, B.; Wang, E. Interactions between water and nitrogen in australian cropping systems: Physiological, agronomic, economic, breeding and modelling perspectives. *Crop Pasture Sci.* **2016**, *67*, 1019–1053. [CrossRef]

20. Birch, C.J.; Long, K.E. Effect of nitrogen on the growth, yield and grain protein-content of barley (*Hordeum vulgare*). *Aust. J. Exp. Agric.* **1990**, *30*, 237–242. [CrossRef]

21. Sadras, V.O.; Richards, R.A. Improvement of crop yield in dry environments: Benchmarks, levels of organisation and the role of nitrogen. *J. Exp. Bot.* **2014**, *65*, 1981–1995. [CrossRef] [PubMed]

22. Cormier, F.; Foulkes, J.; Hirel, B.; Gouache, D.; Moenne-Loccoz, Y.; Le Gouis, J. Breeding for increased nitrogen-use efficiency: A review for wheat (*T. aestivum* L.). *Plant Breed.* **2016**, *135*, 255–278. [CrossRef]

23. Sanford, D.; MacKown, C. Variation in nitrogen use efficiency among soft red winter wheat genotypes. *Int. J. Plant. Breed. Res.* **1986**, *72*, 158–163. [CrossRef] [PubMed]

24. Bogard, M.; Jourdan, M.; Allard, V.; Martre, P.; Perretant, M.R.; Ravel, C.; Heumez, E.; Orford, S.; Snape, J.; Griffiths, S.; et al. Anthesis date mainly explained correlations between post-anthesis leaf senescence, grain yield, and grain protein concentration in a winter wheat population segregating for flowering time QTLS. *J. Exp. Bot.* **2011**, *62*, 3621–3636. [CrossRef] [PubMed]

25. Hitz, K.; Clark, A.J.; Van Sanford, D.A. Identifying nitrogen-use efficient soft red winter wheat lines in high and low nitrogen environments. *Field Crops Res.* **2017**, *200*, 1–9. [CrossRef]

26. Araus, J.L.; Slafer, G.A.; Reynolds, M.P.; Royo, C. Plant breeding and drought in c$_3$ cereals: What should we breed for? *Ann. Bot.* **2002**, *89*, 925–940. [CrossRef]

27. Tardieu, F.; Tuberosa, R. Dissection and modelling of abiotic stress tolerance in plants. *Curr. Opin. Plant Biol.* **2010**, *13*, 206–212. [CrossRef]

28. Dunbabin, V. Simulating the role of rooting traits in crop-weed competition. *Field Crops Res.* **2007**, *104*, 44–51. [CrossRef]

29. Hansen, N.J.S.; Plett, D.; Berger, B.; Garnett, T. Tackling nitrogen use efficiency in cereal crops using high-throughput phenotyping. In *Engineering Nitrogen Utilization in Crop Plants*; Shrawat, A., Zayed, A., Lightfoot, D.A., Eds.; Springer International Publishing: Cham, Switzerland, 2018; pp. 121–139.

30. Sharma, R. Selection for biomass yield in wheat. *Int. J. Plant Breed.* **1993**, *70*, 35–42. [CrossRef]

31. Oscarson, P. The strategy of the wheat plant in acclimating growth and grain production to nitrogen availability. *J. Exp. Bot.* **2000**, *51*, 1921–1929. [CrossRef]

32. Alzueta, I.; Abeledo, L.G.; Mignone, C.M.; Miralles, D.J. Differences between wheat and barley in leaf and tillering coordination under contrasting nitrogen and sulfur conditions. *Eur. J. Agron.* **2012**, *41*, 92–102. [CrossRef]

33. Richards, R.A. Selectable traits to increase crop photosynthesis and yield of grain crops. *J. Exp. Bot.* **2000**, *51*, 447–458. [CrossRef] [PubMed]

34. Furbank, R.T.; Tester, M. Phenomics—Technologies to relieve the phenotyping bottleneck. *Trends Plant Sci.* **2011**, *16*, 635–644. [CrossRef] [PubMed]

35. Berger, B.; De Regt, B.; Tester, M. High-throughput phenotyping of plant shoots. In *High-throughput Phenotyping in Plants*; Normanly, J., Ed.; Humana Press: Totowa, NJ, USA, 2012; Volume 918.

36. Koelewijn, H.P. Rapid change in relative growth rate between the vegetative and reproductive stage of the life cycle in plantago coronopus. *New Phytol.* **2004**, *163*, 67–76. [CrossRef]

37. Kozłowski, J. Optimal allocation of resources to growth and reproduction: Implications for age and size at maturity. *Trends Ecol. Evol.* **1992**, *7*, 15–19. [CrossRef]

38. Hawkesford, M.J.; Kopriva, S.; De Kok, L.J. *Nutrient Use Efficiency in Plants: Concepts and Approaches*; Springer International Publishing: Cham, Switzerland, 2014; Volume 10.

39. Marschner, H.; Marschner, P.; Marschner, H. *Marschner's Mineral Nutrition of Higher Plants*, 3rd ed.; Elsevier Academic Press: London, UK, 2012.

40. Neilson, E.H.; Edwards, A.M.; Blomstedt, C.K.; Berger, B.; Moller, B.L.; Gleadow, R.M. Utilization of a high-throughput shoot imaging system to examine the dynamic phenotypic responses of a c-4 cereal crop plant to nitrogen and water deficiency over time. *J. Exp. Bot.* **2015**, *66*, 1817–1832. [CrossRef]

41. Shi, P.-J.; Men, X.-Y.; Sandhu, H.S.; Chakraborty, A.; Li, B.-L.; Ou-Yang, F.; Sun, Y.-C.; Ge, F. The "general" ontogenetic growth model is inapplicable to crop growth. *Ecol. Model.* **2013**, *266*, 1–9. [CrossRef]

42. Al-Tamimi, N.; Brien, C.; Oakey, H.; Berger, B.; Saade, S.; Ho, Y.S.; Schmöckel, S.M.; Tester, M.; Negrão, S. Salinity tolerance loci revealed in rice using high-throughput non-invasive phenotyping. *Nat. Commun.* **2016**, *7*, 13342. [CrossRef]

43. Brien, C.J. Dae: Functions Useful in the Design and Anova of Experiments. R Package Version 3.0-32. Available online: https://cran.at.r-project.org/package=dae (accessed on 17 June 2019).

44. *R: A Language and Environment for Statistical Computing*; R Foundation for Statistical Computing, R Development Core Team: Vienna, Austria, 2009.

45. Butler, D.G.; Cullis, B.R.; Gilmour, A.R.; Gogel, B.J.; Thompson, R. Asreml-R Reference Manual. Version 4. Available online: http://asreml.org (accessed on 2 February 2018).

46. Brien, C.J. Asremlplus: Augments Asreml-R in Fitting Mixed Models and Packages Generally in Exploring Prediction Differences. R Package Version 4.1-28. Available online: https://cran.at.r-project.org/package=asremlPlus (accessed on 17 June 2019).

47. Davis, L.; Ware, A.; Cook, A. *Port. Kenny, Franklin Harbour, Elliston and Wharminda Wheat and Barley Variety Trials in 2015*; PIRSA: Adelaide, SA, Australia, 2016.

48. Mahjourimajd, S.; Kuchel, H.; Langridge, P.; Okamoto, M. Evaluation of australian wheat genotypes for response to variable nitrogen application. *Int. J. Plant Soil Relatsh.* **2016**, *399*, 247–255. [CrossRef]

49. Eagles, H.A.; McLean, R.; Eastwood, R.F.; Appelbee, M.J.; Cane, K.; Martin, P.J.; Wallwork, H. High-yielding lines of wheat carrying Gpc-B1 adapted to mediterranean-type environments of the south and west of australia. *Crop Pasture Sci.* **2014**, *65*, 854–861. [CrossRef]

50. Mosleth, E.F.; Wan, Y.; Lysenko, A.; Chope, G.A.; Penson, S.P.; Shewry, P.R.; Hawkesford, M.J. A novel approach to identify genes that determine grain protein deviation in cereals. *Plant Biotechnol. J.* **2015**, *13*, 625–635. [CrossRef] [PubMed]

51. Cowling, S.A.; Field, C.B. Environmental control of leaf area production: Implications for vegetation and land-surface modeling. *Glob. Biogeochem. Cycles* **2003**, *17*, 1–14. [CrossRef]

52. White, E.M.; Wilson, F.E.A. Responses of grain yield, biomass and harvest index and their rates of genetic progress to nitrogen availability in ten winter wheat varieties. *Ir. J. Agric. Food Res.* **2006**, *45*, 85–101.

53. Kato, Y. Grain nitrogen concentration in wheat grown under intensive organic manure application on andosols in central japan. *Plant Prod. Sci.* **2012**, *15*, 40–47. [CrossRef]

54. Jones, C.; Olson-Rutz, K. *Practices to Increase Wheat Grain Protein*; Extension; Montana State University: Bozeman, MT, USA, 2012.

55. McKenzie, R.H.; Bremer, E.; Grant, C.A.; Johnston, A.M.; DeMulder, J.; Middleton, A.B. In-crop application effect of nitrogen fertilizer on grain protein concentration of spring wheat in the canadian prairies. *Crop Appl. Eff. Nitrogen Fertil. Grain Protein Conc. Spring Wheat Can. Prairies* **2006**, *86*, 565–572. [CrossRef]

56. Yau, S.K.; Thurling, N. Variation in nitrogen response among spring rape (brassica napus) cultivars and its relationship to nitrogen uptake and utilization. *Field Crops Res.* **1987**, *16*, 139–155. [CrossRef]

57. Ulas, A.; Behrens, T.; Wiesler, F.; Horst, W.J.; Erley, G.S.A. Does genotypic variation in nitrogen remobilisation efficiency contribute to nitrogen efficiency of winter oilseed-rape cultivars (*Brassica napus* L.)? *Plant Soil* **2013**, *371*, 463–471. [CrossRef]

58. Johnson, V.A.; Dreier, A.F.; Grabousk, P. Yield and protein responses to nitrogen fertilizer of two winter wheat varieties differing in inherent protein content of their grain. *Agron. J.* **1973**, *65*, 259–263. [CrossRef]

59. Poorter, H.; Niklas, K.J.; Reich, P.B.; Oleksyn, J.; Poot, P.; Mommer, L. Biomass allocation to leaves, stems and roots: Meta-analyses of interspecific variation and environmental control. *New Phytol.* **2012**, *193*, 30–50. [CrossRef]

60. Broadley, M.R.; Escobar-Gutiérrez, A.J.; Burns, A.; Burns, I.G. What are the effects of nitrogen deficiency on growth components of lettuce? *New Phytol.* **2000**, *147*, 519–526. [CrossRef]

61. Xiao, J.; Yin, X.; Ren, J.; Zhang, M.; Tang, L.; Zheng, Y. Complementation drives higher growth rate and yield of wheat and saves nitrogen fertilizer in wheat and faba bean intercropping. *Field Crops Res.* **2018**, *221*, 119–129. [CrossRef]

62. Cox, M.C.; Qualset, C.O.; Rains, D.W. Genetic variation for nitrogen assimilation and translocation in wheat. I. Dry matter and nitrogen accumulation. *Genet. Var. Nitrogen Assim. Translocat. Wheat. I. Dry Matter Nitrogen Accumul.* **1985**, *25*, 430–435.

63. Brancourt-Hulmel, M.; Heumez, E.; Pluchard, P.; Beghin, D.; Le Gouis, C.; Depatureaux, A.; Giraud, J. Indirect versus direct selection of winter wheat for low-input or high-input levels. *Crop Sci.* **2005**, *45*, 1427–1431. [CrossRef]

64. Shepherd, K.D.; Cooper, P.J.M.; Allan, A.Y.; Drennan, D.S.H.; Keatinge, J.D.H. Growth, water-use and yield of barley in mediterranean-type environments. *J. Agric. Sci.* **1987**, *108*, 365–378. [CrossRef]

65. Nord, E.A.; Lynch, J.P. Plant phenology: A critical controller of soil resource acquisition. *J. Exp. Bot.* **2009**, *60*, 1927–1937. [CrossRef]

66. Thies, J.E.; Singleton, P.W.; Bohlool, B.B. Phenology, growth, and yield of field-grown soybean and bush bean as a function of varying modes of n-nutrition. *Soil Biol. Biochem.* **1995**, *27*, 575–583. [CrossRef]

67. Aerts, R. Nutrient resorption from senescing leaves of perennials: Are there general patterns? *J. Ecol.* **1996**, *84*, 597–608. [CrossRef]

68. Gobert, S.; Lejeune, P.; Lepoint, G.; Bouquegneau, J.M. C, n, p concentrations and requirements of flowering posidonia oceanica shoots. *Hydrobiologia* **2005**, *533*, 253–259. [CrossRef]

69. Milla, R.; Castro-Diez, P.; Maestro-Martinez, M.; Montserrat-Marti, G. Relationships between phenology and the remobilization of nitrogen, phosphorus and potassium in branches of eight mediterranean evergreens. *New Phytol.* **2005**, *168*, 167–178. [CrossRef]

70. Lynch, J.; White, J.W. Shoot nitrogen dynamics in tropical common bean. *Crop Sci.* **1992**, *32*, 392–397. [CrossRef]

71. Dechorgnat, J.; Kaiser, B.N. Grain nitrogen filling in two contrasting australian wheat cultivars. In *COMBIO Symposium*; Adelaide, 2 October 2017.

72. Fettell, N.; Brill, R.; Gardner, M.; McMullen, G. *Yield and Protein Relationships in Wheat*; Grains Research & Development Corporation: Canberra, Australia, 2012.

73. Savin, R.; Slafer, G.A.; Cossani, C.M.; Abeledo, L.G.; Sadras, V.O. Cereal yield in mediterranean-type environments: Challenging the paradigms on terminal drought, the adaptability of barley vs. wheat and the role of nitrogen fertilization. In *Crop Physiology*, 2nd ed.; Sadras, V.O., Calderini, D.F., Eds.; Elsevier: Amsterdam, The Netherlands, 2014; pp. 141–158.

74. Dhugga, K.S.; Waines, J.G. Analysis of nitrogen accumulation and use in bread and durum wheat. *Crop Sci.* **1989**, *29*, 1232–1239. [CrossRef]

75. Anderson, W.K.; Hamza, M.A.; Sharma, D.L.; D'Antuono, M.F.; Hoyle, F.C.; Hill, N.; Shackley, B.J.; Amjad, M.; Zaicou-Kunesch, C. The role of management in yield improvement of the wheat crop—A review with special emphasis on western australia. *Aust. J. Agric. Res.* **2005**, *56*, 1137–1149. [CrossRef]

76. Rao, A.C.S.; Smith, J.L.; Jandhyala, V.K.; Papendick, R.I.; Parr, J.F. Cultivar and climatic effects on the protein content of soft white winter wheat. *Agron. J.* **1993**, *85*, 1023–1028. [CrossRef]

77. Sullivan, D.M.; Bary, A.I.; Cogger, C.G.; Shearin, T.E. Predicting biosolids application rates for dryland wheat across a range of northwest climate zones. *Commun. Soil Sci. Plant Anal.* **2009**, *40*, 1770–1789. [CrossRef]

78. Cogger, C.G.; Bary, D.M.; Sullivan, A.I.; Kropf, J.A. Matching plant-available nitrogen from biosolids with dryland wheat needs. *J. Prod. Agric.* **1998**, *11*, 41–47. [CrossRef]

79. Hunter, A.; Gerard, C.; Waddoups, H.; Hall, W.; Cushman, H.; Alban, L. The effect of nitrogen fertilizers on the relationship between increases in yields and protein content of pastry-type wheats. *Agron. J.* **1958**, *50*, 311. [CrossRef]

80. Mahler, R.L.; Guy, S.O. Soft wheat spring wheat. In *Northern Idaho Fertilizer Guide*; University of Idaho: Moscow, ID, USA, 2007.

81. Stewart, W.M. Fertilizer for better bread. *Better Crops* **2003**, *87*, 15–17.

82. Swanston, J.S.; Newton, A.C.; Brosnan, J.M.; Fotheringham, A.; Glasgow, E. Determining the spirit yield of wheat varieties and variety mixtures. *J. Cereal Sci.* **2005**, *42*, 127–134. [CrossRef]

83. Matthews, P.; McCaffery, D.; Jenkins, L. *Winter Crop Variety Sowing Guide 2017*; Department of Primary Industries: Orange, NSW, Australia, 2017.

84. Fuller, P. New wheat varieties meet the quality challenge. In *Grain Business*; Glencore Grain Pty Ltd.: Melbourne, VIC, Australia, 2013.

85. Lush, D.; Forknall, C.; Neate, S.; Sheedy, J. *Queensland Wheat Varieties 2017*; GRDC: Canberra, Australia; DAF: Brisbane, QLD, Australia, 2017.

86. Wang, Q.; Li, F.R.; Zhao, L.; Zhang, E.H.; Shi, S.L.; Zhao, W.Z.; Song, W.X.; Vance, M.M. Effects of irrigation and nitrogen application rates on nitrate nitrogen distribution and fertilizer nitrogen loss, wheat yield and nitrogen uptake on a recently reclaimed sandy farmland. *Plant Soil* **2010**, *337*, 325–339. [CrossRef]

87. Oliver, Y.M.; Robertson, M.J. Quantifying the benefits of accounting for yield potential in spatially and seasonally responsive nutrient management in a mediterranean climate. *Aust. J. Soil Res.* **2009**, *47*, 114. [CrossRef]

88. Chen, W.; Bell, R.W.; Brennan, R.F.; Bowden, J.W.; Dobermann, A.; Rengel, Z.; Porter, W. Key crop nutrient management issues in the western australia grains industry: A review. *Aust. J. Soil Res.* **2009**, *47*, 1–18. [CrossRef]

89. Simmonds, D.H. *Wheat and Wheat Quality in Australia*; CSIRO Publishing: Clayton, Australia, 1989.

90. Mason, M.G. Nitrogen. In *Soil Guide: A Handbook for Understanding and Managing Agricultural Soils*; Moore, G., Ed.; Department of Agriculture and Food Western Australia: Kensington, Australia, 1998; Volume 4343, pp. 164–167.

91. Girondé, A.; Poret, M.; Etienne, P.; Trouverie, J.; Bouchereau, A.; Le Cahérec, F.; Leport, L.; Orsel, M.; Niogret, M.-F.; Deleu, C.; et al. A profiling approach of the natural variability of foliar n remobilization at the rosette stage gives clues to understand the limiting processes involved in the low n use efficiency of winter oilseed rape. *J. Exp. Bot.* **2015**, *66*, 2461–2473. [CrossRef] [PubMed]

92. Sorin, C.; Leport, L.; Cambert, M.; Bouchereau, A.; Mariette, F.; Musse, M. Nitrogen deficiency impacts on leaf cell and tissue structure with consequences for senescence associated processes in *Brassica napus*. *Bot. Stud.* **2016**, *57*, 11. [CrossRef] [PubMed]

93. Presterl, T.; Seitz, G.; Landbeck, M.; Thiemt, E.M.; Schmidt, W.; Geiger, H.H. Improving nitrogen-use efficiency in european maize: Estimation of quantitative genetic parameters. *Crop Sci.* **2003**, *43*, 1259. [CrossRef]

Chapter 3: Supplementary material

The following are available online at http://www.mdpi.com/2073-4395/9/11/706/s1.
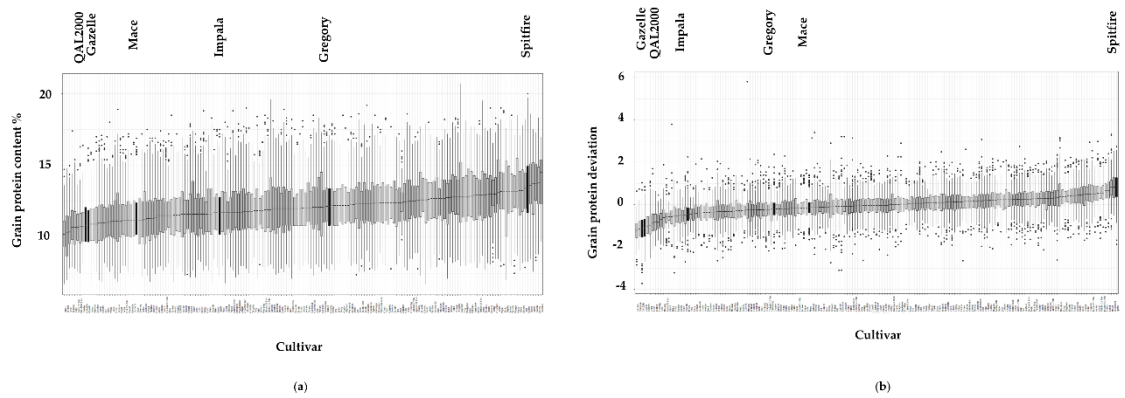
Figure S1: Grain protein content (**a**) and grain protein deviation (**b**) of 179 genotypes in 206 NVT sites from 2008 to 2018. Grain protein deviation of each cultivar was calculated separately in each individual site, season and year. Total number of site*year*season for each genotype was between 50 – 896. Total number of site*year*season for 6 genotypes were as: Spitfire: 476, Mace: 850, Gregory: 897, Impala: 522, QAL2000: 346 and Gazelle: 445. Based on GPC, 6 genotypes were selected in this study.
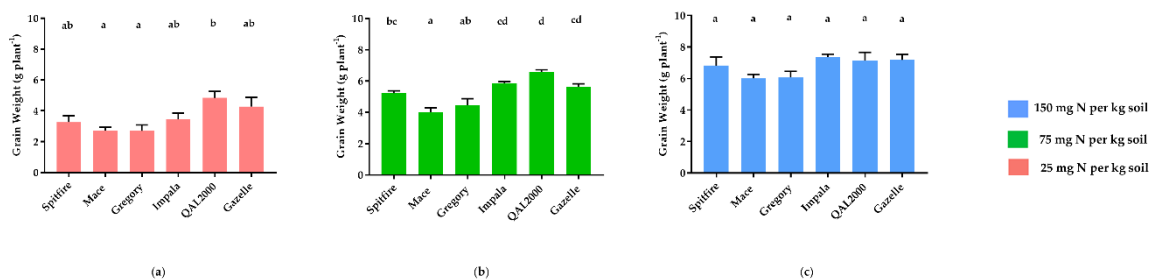
Figure S2: Grain weight of 6 wheat genotypes grown in low (**a**), medium (**b**) and high (**c**) nitrogen supply. Grain weights were measured for each individual plant. Each column represents the average of 6 replicates. Different letters demonstrate significant differences between genotypes according to the Tukey's test ($P < 0.05$).
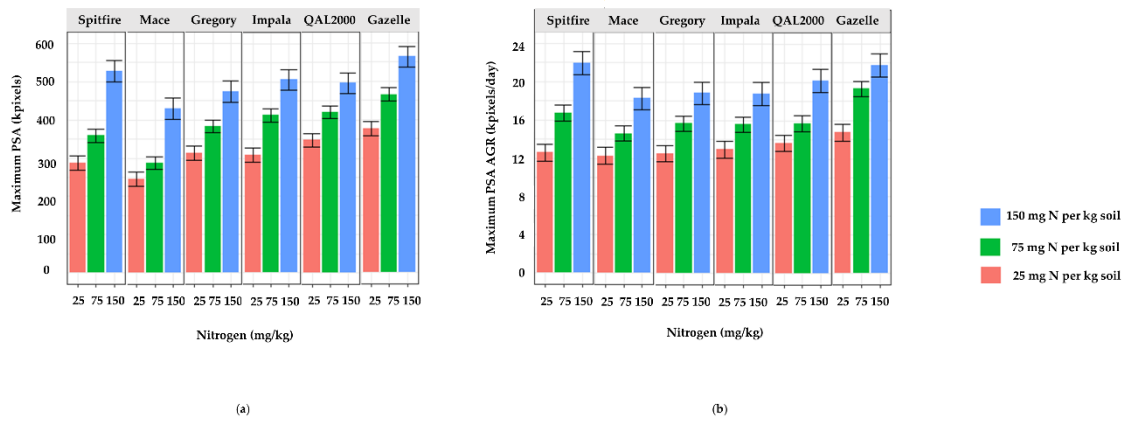
Figure S3: Predictions from full interaction models of maximum projected shoot area (Maximum PSA) (**a**) and maximum absolute growth rate calculated from projected shoot area (maximum PSA AGR) (**b**) of 6 wheat genotypes grown in low (red), medium (green) and high (blue) nitrogen supply. The unit of projected shoot area is kilo pixels, and the unit of maximum absolute growth rate is kilo pixels per day. Each columns represents 6 replicates. The error bars are half of the least significant differences.

Understanding the Interactions between Biomass, Grain Production and Grain Protein Content in High and Low Protein Wheat Genotypes under Controlled Environments

Chapter 4: Understanding the Interactions between Biomass, Grain Production and Grain Protein Content in High and Low Protein Wheat Genotypes under Field Environments

Vahid Rahimi Eichi [1,2], Mamoru Okamoto [1,2], Trevor Garnett [1,2], Paul Eckermann [1,2], Sanjiv Satija [1,2], Ramesh Raja Segaran [2,3], Dillon Ross Campbell [3], Peter Langridge [1,4*]

[1]School of Agriculture Food and Wine, University of Adelaide, Glen Osmond, 5064, South Australia

[2]ARC Industrial Transformation Research Hub for Wheat in a Hot and Dry Climate, Waite Research Institute, University of Adelaide, Glen Osmond, SA 5064, Australia

[3]School of Biological Sciences, University of Adelaide, Adelaide, 5000, South Australia

[4] Wheat Initiative, Julius-Kühn-Institute, Berlin-Dahlem, Germany

*Correspondence: peter.langridge@adelaide.edu.au; Tel.: +61- 83137368

Statement of Authorship

Title of Paper	Understanding the interactions between biomass, grain production and grain protein content in high and low protein wheat genotypes under field environments
Publication Status	☐ Published ☐ Accepted for Publication ☐ Submitted for Publication ☑ Unpublished and Unsubmitted work written in manuscript style
Publication Details	Manuscript prepared in accordance with the guidelines for *agronomy*

Principal Author

Name of Principal Author (Candidate)	Vahid Rahimi Eichi		
Contribution to the Paper	Conceptualization, methodology, formal analysis, investigation, writing (original draft preparation), writing (review and editing)		
Overall percentage (%)	80%		
Certification:	This paper reports on original research I conducted during the period of my Higher Degree by Research candidature and is not subject to any obligations or contractual agreements with a third party that would constrain its inclusion in this thesis. I am the primary author of this paper.		
Signature		Date	14.07.2020

Co-Author Contributions

By signing the Statement of Authorship, each author certifies that:

    i.   the candidate's stated contribution to the publication is accurate (as detailed above);

    ii.   permission is granted for the candidate in include the publication in the thesis; and

    iii.   the sum of all co-author contributions is equal to 100% less the candidate's stated contribution.

Name of Co-Author	Prof. Peter Langridge		
Contribution to the Paper	Conceptualization, methodology, writing (original draft preparation), writing (review and editing), supervision		
Signature		Date	16/7/2020

Name of Co-Author	Dr. Trevor Garnett		
Contribution to the Paper	Conceptualization, methodology, writing (original draft preparation), writing (review and editing), supervision		
Signature		Date	16/7/2020

Name of Co-Author	Dr. Mamoru Okamoto		
Contribution to the Paper	Conceptualization, methodology, writing (original draft preparation), writing (review and editing), supervision		
Signature		Date	16/07/2020

Name of Co-Author	Paul Eckermann		
Contribution to the Paper	Methodology		
Signature		Date	

Name of Co-Author	Sanjiv Satija			
Contribution to the Paper	Methodology			
Signature			Date	20/7/2020

Name of Co-Author	Dr. Ramesh Raja Segaran			
Contribution to the Paper	Methodology			
Signature			Date	17/7/20

Name of Co-Author	Dillon Ross Campbell			
Contribution to the Paper	Methodology			
Signature			Date	17/7/20

Please cut and paste additional co-author panels here as required.

48

Abstract: Grain protein content (GPC) is a key quality attribute and an important marketing trait in wheat. In the current cropping systems worldwide, GPC is mostly determined by nitrogen (N) fertilizer application. The objectives of this study were to assess the value of height and ground cover growth analysis for the examination of differences in N response in high and low GPC wheats, and to propose some approaches for increasing N responses in the nitrogen use efficiency wheat trials of low yielding environments in South Australia. Six wheat genotypes from a range of high to low GPC were grown under different N treatments at three field trials located in South Australia in 2017 and 2018 seasons. Differences between N treatments were not significant in 2017. Therefore, in 2018 some changes were made to enhance the N treatment effects. This experiment was designed around non-destructive measurement of the increase in height and ground cover measured with unmanned aerial vehicle (UAV height) and GreenSeeker (GS NDVI), respectively. Results showed that high GPC genotypes, such as Spitfire and Impala, slowed down the rate of increase in UAV height and GS NDVI under low N supply.

Keywords: Grain protein content; multi-environment; grain yield; National Variety Trials; high and low protein wheat; environment type; grain protein deviation

1. Introduction

Wheat is the most widely cultivated crop in the world and a substantial source of carbohydrate and protein in human diets (Shewry and Hey 2015). Increasing grain yield and grain quality are the two main goals in improving wheat production. In this context, grain protein content (GPC) is a key quality attribute and an important marketing trait (Husenov et al. 2015).

In the current world cropping systems, GPC is mostly determined by nitrogen (N) fertilizer application (Triboi et al. 2000; Sinclair and Rufty 2012). N is an essential nutrient for plant

growth, development and reproduction. However, only 40-60% of the applied N is taken up by wheat plants (Sylvester-Bradley and Kindred 2009), which inflates production costs and environmental impacts (Bouwer 1989; Harrison and Webb 2001). Consequently, there is considerable interest in improving nitrogen use efficiency (NUE) (Birch and Long 1990; Sadras et al. 2016). NUE, which can be defined as the ratio of grain yield to N supplied, has been mostly improved by indirect selections for high grain yield (Sadras and Richards 2014; Cormier et al. 2016). In fact, efforts to improve NUE in wheat has focused on increasing grain yield response to higher N inputs (Sanford and MacKown 1986). Comparing the N responses of high and low GPC wheats may reveal the mechanisms used by the contrasting genotypes in their N use at high and low N input (Bogard et al. 2011; Hitz et al. 2017).

Previous studies showed that the above-ground biomass is highly responsive to N, and therefore can be a suitable indicator for NUE studies in grain crops (Sharma 1993; Richards 2000; Sadras et al. 2016; Rahimi Eichi et al. 2019). However, due to the challenges of destructive harvests, NUE evaluations in the field are usually based on measuring grain yield at a given N supply (Araus, J. L. et al. 2002; Cormier et al. 2016). Using conventional destructive methods to measure biomass is time and labour intensive, especially, for large-scale trials. For instance, measuring biomass in field requires collecting, oven-drying and weighting samples in the laboratory (Royo et al. 2004). Moreover, destructive methods discard a portion of the crop, which limits the use of such techniques in small sized breeding plots (Prasad et al. 2007). Conversely, image-based phenotyping platforms provide consecutive measurements of biomass during the growing season, and assess plant growth dynamics. Monitoring growth dynamics without the need for periodic destructive harvests improves the precision of measurements (Furbank and Tester 2011). Using image-based methods also allows phenotyping of a large number of plots at reasonable costs and good repeatability (Langridge and Fleury 2011; Casadesus and Villegas 2014; Fahlgren et al. 2015).

Phenotyping based on imaging can also help to analyse plant nutrient status (Berger et al. 2012). Previous study in controlled conditions (Rahimi Eichi et al. 2019) showed that reducing N inputs decreases the growth rate more in high than in low GPC genotypes. However, in the previous study, biomass was estimated based on a comprehensive set of image data obtained daily from the top and both sides of single plants (Rahimi Eichi et al. 2019). Obviously, measuring the total biomass in the same way on breeding plots under field conditions is not feasible. Therefore, measuring biomass related traits may help to assess the growth rate in the field.

Ground cover is one of the parameters related with plant growth in the field (Rebetzke et al. 2012). Normalized difference vegetation index (NDVI) can indicate the ground cover in crops. GreenSeeker NDVI (GS NDVI), which can be measured conveniently in the field, is correlated with biomass up to the point of canopy closure (Hill et al. 2004; Rebetzke et al. 2012; Adeel Hassan et al. 2019).

Plant height and its response to environmental variables such as water, nutrition, temperature, light, is another important factor for quantifying the wheat growth dynamics particularly during stem elongation (Kronenberg et al. 2017). Traditional methods for measuring height using a yardstick reduces the throughput and accuracy of the measurements. Recently, some effective techniques to measure height became available using a broad range of sensors (Walter et al. 2015; Jimenez-Berni et al. 2018). In the current study, the rate of height increase of wheat plants was measured with conventional Red Green Blue (RGB) cameras.

Here, we report on a study based on biomass assessed through height and NDVI measurement of wheat breeding plots with different N supply. The objectives of this study were: (1) to assess the value of height and ground cover-based growth analysis for the examination of differences in N response in high and low GPC wheats; (2) to propose some approaches for increasing N responses in the NUE wheat trials of low yielding environments

in South Australia. To address these objectives, a set of six genotypes differing in GPC were selected based on available data from National Variety trials (NVT) (Supplementary Figure S2 of Rahimi Eichi et al. (2019)).

2. Material and Methods

2.1 Experimental site

Three field experiments were conducted in 2017 and 2018 seasons on breeding trials in Pinery (34°20'21.0"S 138°28'28.4"E) and Freeling (34°26'43.5"S 138°47'44.0"E) located in South Australia. In 2017, the trial was a preliminary experiment and was conducted only in Pinery on the same farm with Pinery 2018. There were 144 mini-plot trials including 3 rows in 2018. The climate type of the experimental sites are semi-arid Mediterranean with a mean long-term rainfall of 429.8 and 490.1 mm in Pinery and Freeling, respectively (Table 1 and Supplementary Figure S1).

2.2 Experimental design and crop management

Based on the NVT data (Supplementary Figure S2 of Rahimi Eichi et al. (2019)) six wheat (*Triticum aestivum* L.) genotypes, Spitfire, Mace, Gregory, Impala, Gazelle and QAL2000, were selected to cover a range of high to low GPC. These experiments investigate six genotype of wheat, *T.aestivum*, and different levels of nitrogen on an 8 × 12 grid in 2017 (Figure 1A and D) and 12 × 12 grid in 2018 (Figure 1B, C, E and F) indexed by rows and ranges.

Table 1. Plot and environmental characteristics of the experimental sites during the two growing seasons (2017 and 2018). Inter plot gap represents the distance between rows. The long-term data were recorded between 1925-2017 for Pinery and 1963-2017 for Freeling at less than 10km ditance from the experimental sites. Data are available at: *http://www.bom.gov.au/climate/data/*

Plot characteristics	Pinery 2017	Pinery 2018	Freeling 2018
Latitude	-34°33'9431"S	-34°33'6281"S	-34°26'50.9"S
Longitude	138°472217"E	138°475720"E	138°47'36.1"E
Mean long-term cumulative annual rainfall (mm)	429.8	429.8	490.1
Annual cumulative rainfall (mm)	387.0	270.8	355.7
Annual mean maximum temperature (°C)	24.1	24.6	24.0
Annual mean minimum temperature (°C)	9.7	9.9	10.0
Number of ranges	12	12	12
Number of rows	8	12	12
Seeded rows/plot	6	3	3
Range length (m)	6	6	6
Seeding length (m)	5	5.8	5.8
Harvest length (m)	4	4	4
Plot width (m)	1.33	0.8	0.8
Row Spacing (m)	0.19	0.225	0.225
Inter plot gap (between rows) (m)	0.38	0.35	0.35
Gap between ranges (m)	2	2	2
Residual nitrate N in 0-10 cm depth soil (mg/kg)	41.8	31	23
Residual nitrate N in 10-30 cm depth soil (mg/kg)	11.6	8	6
Sowing date	May 25th	May 17th	May 17th
Biomass crop cuts at harvest	Nov. 28th	Dec. 5th	Dec. 5th
Grain Yield measurement	Dec.	Dec.	Dec.
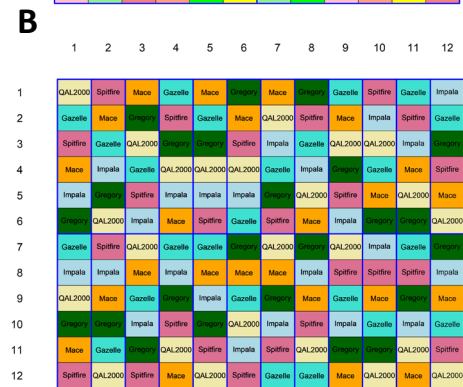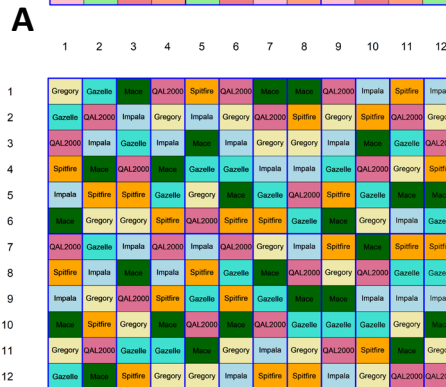
Figure 1. Treatments (**A**, **B** and **C**) and genotypes (**D**, **E** and **F**) layouts in 3 field trials. Biomass cuts for validation in Pinery 2018 (**B** and **E**) were harvested from rows 7-12 of ranges 1-4 including 48 plots in total. In three top Figures, the codes for each N supply were 1) 50+30, 2) 50+0, 3) 0+30 and 4) 0+0 kgN/ha in Figure **A**, 1) 60+0, 2) 0+60, 3) 30+30 and 4) 0+0 kgN/ha in Figure **B**, 1) 60+60, 2) 60+0, 3) 0+60, 4) 30+30, 5) 30+0 and 6) 0+0 kgN/ha in Figure **C**. In three bottom Figures, the colour codes for each genotype were:

Colour code						
Figure **D**	Mace	Gregory	Gazelle	Impala	QAL2000	Spitfire
Figure **E**	Mace	Gazelle	Impala	Gregory	Spitfire	QAL2000
Figure **F**	Gregory	Gazelle	Impala	QAL2000	Mace	Spitfire
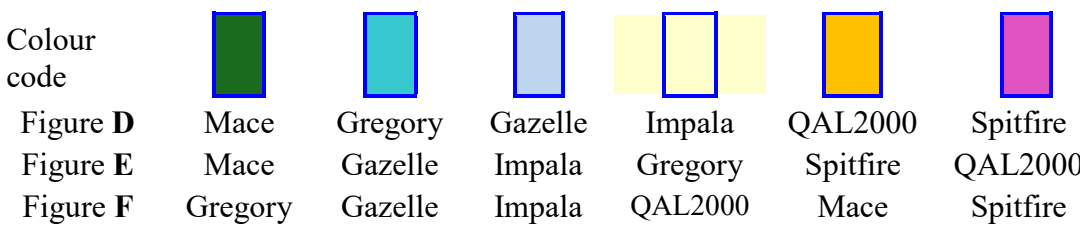
The designs used were split-plot design in which rows in 2017 and ranges in 2018 formed the main plots and N was assigned to these using a randomized complete block design. The design in 2017 included 3 blocks of 4 main plots, whereas in 2018 it was 2 blocks of 6 main plots, each main-plot being a range. Then the subplot was a plot and lines were assigned to these using a resolved, spatially-optimized, row-column design. The 6 plots were within a row in 2017 and within a range in 2018. The subplot design was generated using DiGGer

(Coombes 2009), a package for the *R* statistical computing environment (*R* Development Core Team 2017).

As will be discussed later, differences between N treatments were not significant in Pinery 2017. Therefore, in 2018 some changes were made to enhance the N treatment effects. One of the differences between 2017 and 2018 trials was the direction of N treatments from alongside the rows in 2017 (Figure 1A), to alongside the ranges in 2018 (Figure 1B and C). Due to the higher pre-sowing residual N in the soil of Pinery 2018 compared with Freeling 2018 (Table 1), a high residual N design with 4 N treatments (Table 2) and 6 replicates was used for Pinery 2018.

Table 2. Nitrogen treatment patterns applied in 2017 and 2018 on Pinery and Freeling sites. N treatments were in the form of urea being top-dressed on wet soil in rainy days.

Trial location and year	Nitrogen rate (kgN/ha) applied at early germination	Nitrogen rate (kgN/ha) applied at stem elongation	Nitrogen rate (kgN/ha) applied at anthesis	The name used in this study	The numbers used in Figure 1A, B and C
Pinery 2017	-	50	30	50+30	1
	-	50	0	50+0	2
	-	0	30	0+30	3
	-	0	0	0+0 or Null	4
Pinery 2018	60	0	-	60+0	1
	0	60	-	0+60	2
	30	30	-	30+30	3
	0	0	-	0+0 or Null	4
Freeling 2018	60	60	-	60+60	1
	60	0	-	60+0	2
	0	60	-	0+60	3
	30	30	-	30+30	4
	30	0	-	30+0	5
	0	0	-	0+0 or Null	6

However, for validating the non-destructive measurements, 2 replicates were harvested at two different time points during the 2018 season in Pinery (Khan, Chopin, et al. 2018; Khan, Rahimi-Eichi, et al. 2018). Accordingly, replicate numbers in Pinery 2018 reduced to 4 by

the end of the season. In Freeling, on the other hand, a wider range of N treatments compared to Pinery 2018 was deployed, which included 6 treatments and 4 replicates (Table 2). The aim of adding the 4 extra N treatments was to examine the possible biological differences between N treatments in the low N residual soil of Freeling 2018.

Another difference between 2017 and 2018 was that in 2017, N treatments were applied at early stem elongation and anthesis, whereas in 2018 they were applied at early germination and early stem elongation stages (Table 2). Washed N into the soil is less susceptible to volatilization than the N left on the soil surface (McDonald, G. and Hooper 2013). Therefore, the urea granules were top-dressed on wet soils on rainy days that were followed by a minimum of 7mm rain over the next few days.

2.3 Data collection and calculations

Prior to sowing, soil samples were collected from 5 spots across the trails from the depth ranges of 0-10 and 10-30 cm, and were analysed for soil mineral nutrients (CSBP soil and plant laboratory, Bibra Lake, WA, Australia).

Plant establishment data in 2018 were collected between 2nd and 3rd leaf stage (Rebetzke et al. 2012). Two establishment counts per plot from the middle row were measured with a 50 cm piece of white dowel. Measurements from 2017 and 2018 trials are listed in Table 3.

In 2017, NDVI was measured only at two time points using a multi-spectral sensor based on an unmanned aerial vehicle (UAV). However, NDVI in 2018 was measured with a GreenSeeker (GS) chlorophyll sensor® from early stages until the full canopy cover. The UAV height was measured using a drone-based RGB camera. The 99th percentile of height values, which gives a good representation of the canopy top, was used to calculate the distance between ground level and the top of the canopy (Castrignano et al. 2020). A previous study by Jimenez-Berni et al. (2018) indicated the relationship between point cloud

volume and biomass. Although, their results were obtained from a LiDAR unit, the theory

could also be applied for UAV point clouds.

Table 3. List of measurements and measurement dates based on days after sowing (DAS) from Pinery 2017, Pinery 2018 and Freeling 2018 sites. UAV: Unmanned aerial vehicle. GS: GreenSeeker. NIR: Near infrared spectroscopy.

Measure		Pinery 2017 (DAS)	Pinery 2018 (DAS)	Freeling 2018 (DAS)
Plant Establishment	Plants were counted in 1 meter scale	NA	37	45
Ground cover	GreenSeeker NDVI (GS NDVI)	43, 120	62, 84, 95, 104, 120	62, 84, 95, 104, 120
	Multi-spectral camera on UAV platform (UAV NDVI)	43, 120	NA	NA
Crop development	Zadoks stage	120, 132	86, 124, 137	93, 102, 118
Height measurement	RGB camera on UAV platform (UAV height)	NA	35, 47, 120, 154	35, 47, 120, 154
	Manual height measurement from rows 1-6 and ranges 1-4	NA	120	NA
	Manual height measurement from rows 7-12 and ranges 1-4	NA	154	NA
Biomass Validation	1st sampling from rows 1-6 and ranges 1-4	NA	120	NA
	2nd sampling from rows 7-12 and ranges 1-4	NA	154	NA
	Final biomass cut from all plots	187	194	194
Grain yield	Grain harvested from all plots	203	204	204
Grain protein	Grain protein% with NIR	> 210	NA	NA
	Grain nitrogen% with N analyser	NA	> 210	> 210

The actual height was measured in 48 plots by a ruler at 120 and 154 DAS in Pinery 2018

(Table 3). On the same day, 3×0.5 meter biomass cuts were harvested from 3 seeded rows

of the mentioned plots. After drying the samples at 70° for 48 hours, the total biomass was measured.

The GPC in 2017 was measured using a portable near infrared spectrometer (NIR). In 2018, however, the total N in grains was measured using a nitrogen analyser (Rapid N exceed®, Elementar, Germany). Afterwards, the GPC was calculated by multiplying the total N% by 5.7.

The rate of increase of UAV height and GS NDVI was calculated by dividing the differences between two consecutive measurements by the number of days. For instance, the increase rate of GS NDVI from first to second measurement date in Freeling 2018 was calculated as:

$$1^{st} \textit{ GS NDVI increase rate} = \frac{\text{GS NDVI } (84-62)}{84-62}$$

2.4 Statistical analysis

The differences in biomass, grain yield, GPC, and the rate of increase in UAV height and GS NDVI was measured using a two-way ANOVA analysis with interaction followed by Tukey's multiple comparison test. The average of grain yield and GPC from Freeling site in 2018 were compared between genotypes (one-way ANOVA, Tukey's test, p<0.05). Statistical analysis were performed using GraphPad Prism version 7.00 for Windows. Finally a Pearson correlation analysis was performed to highlight the relationships between non-destructive (UAV height and GS NDVI) and destructive (manually measured height, in-season and harvest biomass and harvest grain yield) measurements (GraphPad Software, La Jolla California USA, www.graphpad.com).

3. Results

3.1 Weather and trial conditions

The cumulative rainfall in Pinery 2017 was only 10% below the long-term average. In 2018, however, the total rainfall in 2018-2019 was 37% and 27% less than the long-term average for Pinery and Freeling, respectively (Table 1). The relatively higher cumulative rainfall in Freeling 2018 compared to Pinery 2018 was in accordance with their long-term average cumulative rainfall (Table 1 and Supplementary Figure S1). Due to the severe drought in 2018, Zadoks stages were not consistent across trials and slight differences in soil moisture could vary the growth stage within and between plots. Accordingly, the time points in this study were identified by day after sowing (DAS). The establishment counts, indicating the density of germinated seeds (Rebetzke et al. 2012), were uniform across the trials (Supplementary Figure S2).

3.2 Growth rate measurements

In order to validate the relationship between UAV height and the actual height of plots, the average height of 48 plots (Figure 1B and E) were measured at 120 and 154 DAS in Pinery 2018 (Table 3). On the same day, biomass cuts were harvested from the mentioned plots to validate the relationship between GS NDVI and total biomass. However, in the second validation (154 DAS), the maturity stage had already started and, therefore, the GS NDVI was not recorded at this date (Table 4). Due to the severe drought conditions in 2018 (Table 1), plants started to mature earlier than in a normal season.

There were significant differences in the rates of increase in UAV height and GS NDVI between N treatments in Freeling (Figure 2A, D and J) but not in Pinery (data not shown).
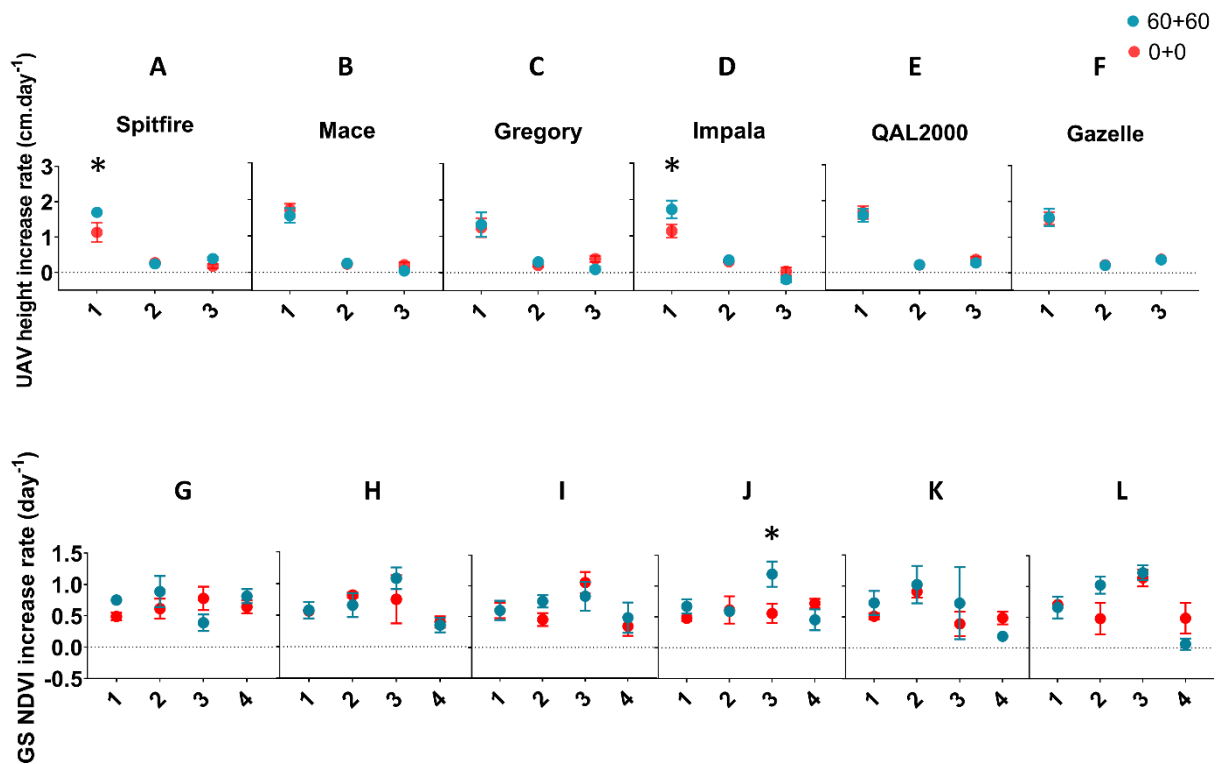
Figure 2. The rate of increase in UAV height (**A-F**) and GS NDVI (**G-L**) per day in Freeling 2018. Only the highest (60+60) and lowest (0+0) N treatments were analyzed. The numbers on the X axes for UAV height (**A-F**) refer to **1**: 35-47, **2**: 47-120, **3**: 120-154 days after sowing, and for the GS NDVI (**G-L**) **1**: 62-84, **2**: 84-95, **3**: 95-104, **4**: 104-120 days after sowing. Stars (*) indicate significant differences within genotypes between N treatments by two-way ANOVA with Tukey's test ($p < 0.05$); the vertical error bars represent the standard errors.

Rainfall in Freeling 2018 was 27% below the average, which imposed a severe drought (Table 1). Therefore, due to the severe drought, 4 N treatments in Freeling 2018 (i.e. 30+0, 30+30, 0+60, and 60+0) were not effective in discriminating between treatments but created noise in the analysis. Accordingly, only the growth rates of the two extreme N treatments (60+60 and 0+0) were analysed. In Spitfire and Impala, the rate of increase in UAV height was higher in 60+60 compared with the null (0+0) N treatments from 35 to 47 DAS (Figure 2A and D). Furthermore, in Impala the GS NDVI growth rate was higher in 60+60 than the null N treatment between 95 and 104 DAS (Figure 2J). In fact, differences in the rates of increase in height and NDVI between high and low N treatments were found only in Spitfire and Impala.

3.3 Post-harvest measurements

The average biomass and grain yield in Pinery 2018 were 78% and 68% lower, respectively, in comparison with Pinery 2017 (Figure 3).
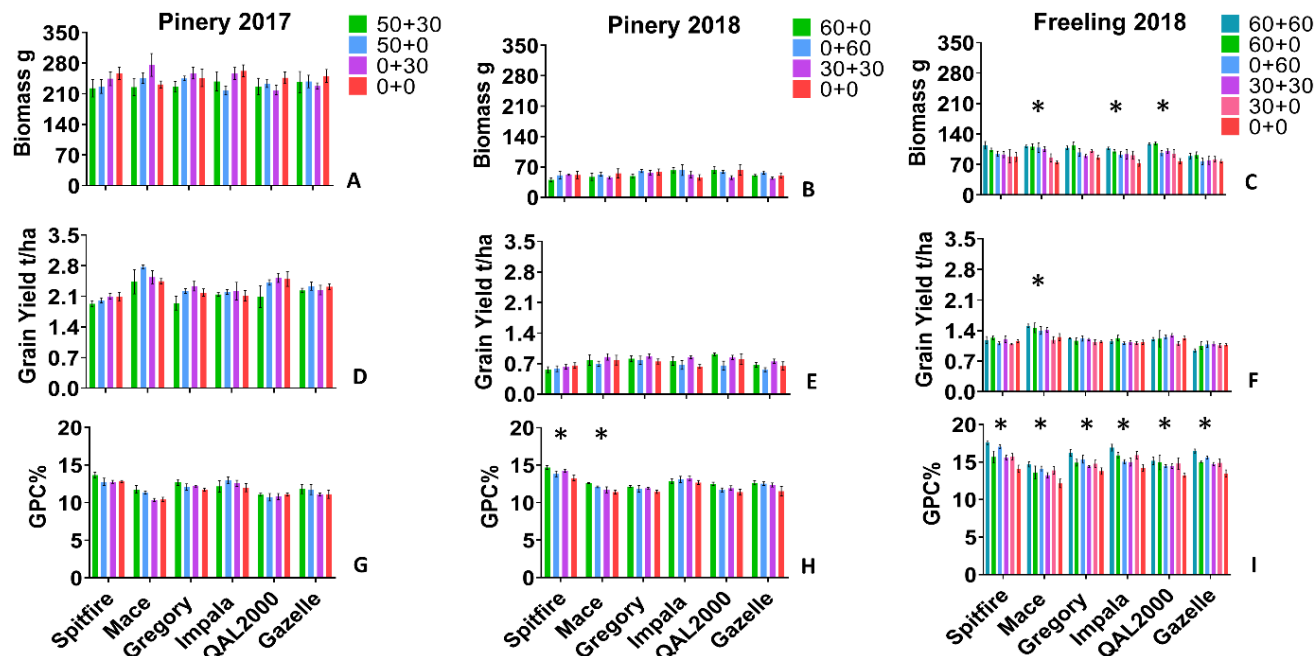
Figure 3. Biomass per 0.5 meter row (**A**, **B** and **C**), grain yield (**D**, **E** and **F**) and grain protein content% (GPC%) (**G**, **H** and **I**) from Pinery 2017 (**A**, **D** and **G**), Pinery 2018 (**B**, **E** and **H**) and Freeling 2018 (**C**, **F** and **I**). The grain protein content % in 2018 trials was calculated based on the total grain N% multiplied by 5.7. Stars (*) indicate significant differences within genotypes between N treatments by two-way ANOVA with Tukey's test (p<0.05); the vertical error bars represent the standard errors.

The average yield in Freeling 2018 was 1.2 t/ha, while the average yield of NVT trials in Turretfield, which is only 10km from Freeling, from 2014 to 2017 was 4.3 t/h ('National Variety Trial' 2019). The Turretfield NVT site produced only 1.5 t/ha in 2018, which was consistent with the results from Freeling 2018. The relatively higher grain yield in the NVT trial (1.5 t/ha) compared to the Freeling trial (1.2 t/ha) in 2018 could be due to the optimal fertiliser rates and other differences in agronomic practices at the NVT trials (Giles et al. 2012).

In Pinery 2017, biomass, grain yield and GPC were not different between N treatments (Figure 3A, D and G). In Pinery 2018, however, differences were observed in the GPC of

Spitfire and Mace between 60+0 and 0+0 N treatments (Figure 3H). In Freeling 2018, on the other hand, N treatment effects were found in biomass, grain yield and GPC% (Figure 3C, F and I). Biomass was different between N treatments for Mace, Impala and QAL2000 (Figure 3C). For these three genotypes, 60+60 or 60+0 produced higher biomass compared with the null N treatment. Mace produced higher biomass in 60+60, 60+0, 0+60 and 30+30 compared to the null N treatment. Grain yield was influenced by N treatments only in Mace, being at its highest level in 60+60 and 60+0 treatments (Figure 3F). The GPC of all six genotypes in Freeling 2018 were higher in 60+60 or 0+60 compared with the null N treatment.

The highest average GPC between genotypes in Freeling 2018 was in Spitfire and Impala with the GPC of 15.2 and 14.5%, respectively (Figure 4B). Mace produced the highest average grain yield between genotypes (Figure 4A).
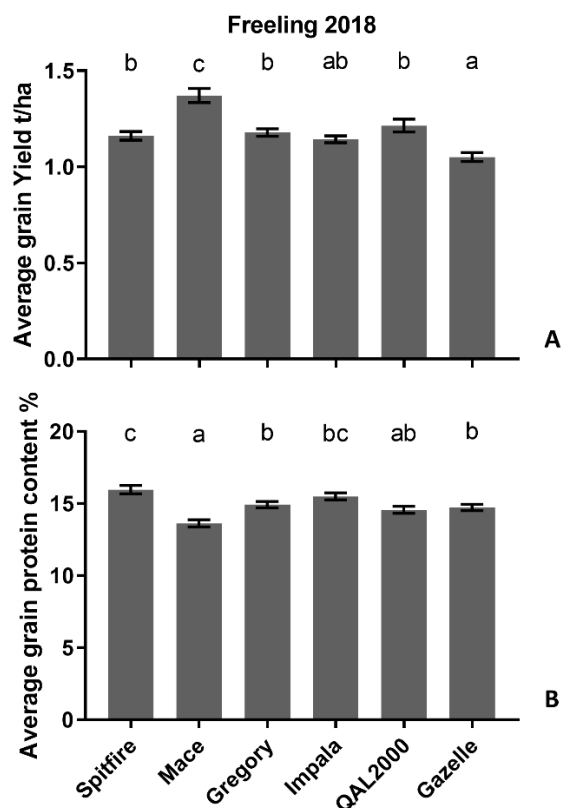

Figure 4. The average grain yield (**A**) and protein content % (**B**) of six wheat genotypes in Freeling site in 2018. Grain protein content in these trials is calculated based on the total grain N% multiplied by 5.7. Letters indicate significant different between genotypes by one-way ANOVA with Tuckey's correction (p<0.05).

3.4 Correlations between non-destructive and destructive or manual measurements

In 2018 there were relatively high correlations between non-destructive and destructive or manual measurements (Table 4).

Table 4. The correlation coefficient of the relationships between non-destructive and destructive or manual measurements in Freeling and Pinery 2018. Biomass and grain yield in Y axis are measured at harvest, which was at 204 DAS. GS NDVI: GreenSeeker NDVI, UAV height: height measured by drone-based RGB camera, r^2: Pearson's correlation coefficient.

X axis	DAS	Y axis	r^2
UAV height	35	Biomass (harvest)	0.0005
	47		0.63
	120		0.70
	154		0.68
	35	Grain yield (harvest)	0.01
	47		0.68
	120		0.74
	154		0.70
GS NDVI	62	Biomass (harvest)	0.04
	84		0.51
	95		0.58
	104		0.58
	120		0.63
	62	Grain yield (harvest)	0.03
	84		0.54
	95		0.55
	104		0.58
	120		0.63
Manually measured plot height	120	UAV height	0.60
	154		0.67
Manually measured biomass	120	GS NDVI	0.58
	204	Grain yield (harvest)	0.63

The Pearson's correlation coefficient of the relationship between UAV height and GS NDVI during the season, and biomass and grain yield at harvest was best at 120 DAS (Table 4). Such relationships with final biomass and grain yield remarkably increased after 47 and 84 DAS for UAV height and GS NDVI, respectively. Manual height and biomass

measurements during the season in Pinery 2018 indicated relatively good correlations with UAV height and GS NDVI (Table 4).

4. Discussion

4.1 UAV height and GS NDVI can indicate the impact of nitrogen on biomass and grain yield

Ground-based measurements showed relatively good correlations between manually measured plant height and biomass, and UAV height and GS NDVI (Table 4). Therefore, UAV height and GS NDVI can be used as indicators of biomass response to N in the six genotypes evaluated in this experiment. The reason that the Pearson's correlation coefficient of the relationship between manual and UAV height was not more than 0.67 (Table 4) could be due to differences in measuring individual plants as opposed to an entire plot. Manual height was defined based on one or two height measurements with a ruler for each plot. However, UAV height was measured based on the differences between the averages of all point clouds at the top of the canopy and the ground. Therefore, the UAV height data can be more precise compared to the manual height measurement.

The correlation of UAV height and GS NDVI with final biomass or grain yield was low at early growth stages and increased towards 120 DAS (Table 4). Previous studies on wheat showed that biomass development in early growth stages, until 60 DAS, has little correlation with the final biomass or grain yield (Freeman et al. 2003; Kovalchuk et al. 2016). The highest correlation between canopy coverage and final biomass or yield can be achieved at heading and flowering stage or two months before harvest (Mahey et al. 1991; Raun et al. 2001; Kovalchuk et al. 2016; Magney et al. 2016). Accordingly, in Spitfire the differences between N treatments for the increase rate of UAV height (Figure 2A) at early stages (35-

47 DAS) were not transferred to the harvest biomass (Figure 3C). In Impala, the GS NDVI differences between N treatments were at later stages (95-104 DAS), and the final biomass was different between high and low N treatments (Figure 3C). In addition to Impala, the differences between N treatments in the harvest biomass were also found in Mace and QAL2000 (Figure 3C). However, the UAV height and GS NDVI during 2018 season were not different between N treatments in these two genotypes (Figure 2). It is important to note that in this study, UAV height and GS NDVI indicated height and ground coverage, and therefore may not represent the total biomass.

In this study, the r^2 value of the relationship between biomass and grain yield was 0.63 (Table 4), whereas it was up to 0.93 in the previous results obtained in controlled environments (Rahimi Eichi et al. 2019). This confirms the lower correlation between biomass and grain yield in low yielding environments compared to favourable conditions (van Herwaarden et al. 1998).

4.2. Differences in the nitrogen responsiveness of biomass between high and low GPC genotypes

In Freeling 2018, the differences between N treatments for grain yield were found only in Mace (Figure 3F), which is known as a high N responsive wheat genotype (Davis et al. 2016; Mahjourimajd, Saba, Kuchel, et al. 2016). Biomass analysis, however, showed such differences between N treatments in two additional genotypes. Interestingly, the biomass of Mace was statistically different across a wider range of N treatments compared to other genotypes (Figure 3C). These results indicate the higher N responsiveness of biomass compared with grain yield.

The biomass growth analysis in Freeling 2018 (Figure 2) revealed some differences between high and low GPC genotypes in responding to N treatments. Spitfire and Impala produced higher GPC compared to other genotypes in Freeling 2018 (Figure 4B). The rates of increase

in UAV height and GS NDVI in low N treatments was reduced more in Spitfire and Impala than in other genotypes (Figure 2A, D and J). The higher restriction in the growth rate of high compared to low GPC wheat genotypes at low N was previously shown under controlled conditions (Rahimi Eichi et al. 2019). It was suggested that high GPC genotypes may use a conservative strategy by slowing down their rate biomass accumulation under low N to conserve available N for their grains. It is also possible that in high GPC genotypes, biomass growth under limited N may be reduced in favour of root growth to support N uptake after anthesis (Cox et al. 1985).

The period between 35 and 47 DAS is around the beginning of stem elongation. The height increase before stem elongation is mostly determined by the length of leaf sheath (Sylvester-Bradley et al. 2008). Southern Australian wheat crops sown in May could take up 20-30% of the total N by the start of stem elongation (McDonald, G. and Hooper 2013). However, the highest N demand is during stem elongation when crop growth and leaf area expansion are most rapid. Accordingly, increasing the frequency of imaging sessions between 47-120 DAS could enhance the identifications of differences in the rate of increase in UAV height between N treatments. In this experiment, unfavourable weather conditions such as wind and clouds limited the feasibility of UAV imaging during this period.

Contrary to the previous study in controlled conditions (Rahimi Eichi et al. 2019), the GPC of Mace was not high in the current experiment. This might be due to the higher grain yield of Mace compared to other genotypes in the low yielding environment (Eagles et al. 2014; Mahjourimajd, Saba, Kuchel, et al. 2016). Such results confirm a previous multi-environmental study (Rahimi Eichi et al. 2020) that GPC in wheat is highly influenced by environmental conditions and agronomic management practices.

4.3. Methods to increase the effect of nitrogen treatment in field trials

Despite the severe drought condition in 2018, N treatments were more distinctive in the trials of 2018 compared with 2017 (Figure 3). It seems that the adopted strategies in 2018 increased the effectiveness of N treatments. For instance, applying N treatments at earlier growth stages in 2018 than in 2017 (Table 2) could lead to clearer N responses. Grain yield and biomass in the 60+60 and 60+0 treatments were higher compared to other N treatments in Freeling 2018 (Figure 3C and F). McDonald, G. and Hooper (2013) showed that the highest yield response to N could be achieved when N was applied near the sowing date in low yielding environments of Southern Australia (McDonald, G. and Hooper 2013). The number of spikes per unit area in wheat is set before stem elongation (Li, C. et al. 2001), and applying N fertilizer at germination increases vegetative growth, tiller number, grain per ear and, consequently, grain yield. Therefore, delaying N application at this time may reduce the chance of achieving maximum yield response.

Applying N later than the onset of stem elongation, however, leads to the translocation of the extra N into the grains (Quinlan and Wherrett 2013). The highest GPC in Freeling 2018 was achieved for the 60+60 and 0+60 treatments (Figure 3I), when 60 kgN/ha was applied at stem elongation. In Pinery 2018, on the other hand, applying 60 kgN/ha at germination stage (60+0) produced the highest GPC (Figure 3H). In the drought season of 2018, Pinery trial received even less rainfall than Freeling (Table 1). Therefore, due to the severity of drought in Pinery 2018, the early-applied N may not have been used for producing biomass but were reserved for the grains. Reducing biomass and yield in favour of GPC increase is a strategy in plants to maintain sufficient nutrient levels under stress to support germination and plant establishment (Stone and Nicolas 1995; Daniel and Triboi 2002; Zorb et al. 2017). However, the overall higher influence of N treatments on biomass, grain yield and GPC in Freeling 2018 (Figure 3C, F and I) compared with Pinery 2018 (Figure 3B, E and H) could

be due to the higher rainfall in Freeling (Table 1). Previous studies showed that the N treatment effect is strongly associated with the amount of available water in the soil (Stoddard and Marshall 1990; Angus 2001; Sadras and McDonald 2012; Mahjourimajd, Saba, Kuchel, et al. 2016).

The other possible reason for the more extensive N treatment effect in Freeling 2018 compared to Pinery 2017 and 2018, could be the lower rates of pre-sowing residual N in soil in Freeling 2018 (Table 1). The crop histories of Pinery 2017 and 2018 were lentils, whereas it was canola for Freeling 2018. The amount of residual N in paddocks with the crop history of legume family such as lentils can be relatively high (Evans et al. 2003). Usually in Southern Australian regions, the residual N stays in soil due to the low rain over summer and autumn (Fillery 2001). After the early winter rainfalls in South Australia, the residual N can be leached below the plants rooting depth (Asseng et al. 1998). However, this residual N is still present in the soil at the time of sowing, when N effect is at its highest level for wheat plants in the low yielding environment (McDonald, G. and Hooper 2013). Accordingly, more replicates in Pinery 2018 (Figure 1B and E) compared to Freeling 2018 (Figure 1C and F) could be helpful to overcome the heterogeneity of soil N.

The other approach that may have improved the N treatment effects in 2018 could be increasing the distance between treatment plots from 0.2m in 2017 to 2m in 2018 (Table 1 and Figure 1). Contamination from neighbouring plots due to the short distance (i.e. 0.2m) between rows (Figure 1A and D) could have counteracted the N treatments in 2017. In 2018, however, the 2m gap between ranges (Table 1 and Figure 1B, C, E and F) could reduce the possibility of N contaminations between different treatment plots. In 2017, a heavy rain could have washed away the top-dressed urea granules to neighbouring plots. The roots of field-grown wheat can occupy a volume of soil extending around 0.3 meters on all sides (Weaver 1926; Yamaguchi and Tanaka 1990). Therefore, 0.2 m distance between different

N treatments in 2017 may have been insufficient to prevent N leakage to the root zone of neighbouring plots.

5. Conclusion

Consistent with the previous results under controlled conditions (Rahimi Eichi et al. 2019), the current study confirms the advantage of the non-destructive methods of biomass growth analysis for NUE studies of wheat in the field. High GPC genotypes, such as Spitfire and Impala, slowed down the rate of increase in UAV height and GS NDVI under low N supply. Deploying UAV in the field, however, can be limited by weather conditions.

Conflicts of Interest: The authors declare no conflict of interest

6. References (Chapter 4)

Adeel Hassan, M, Yanga, M, Rasheeda, A, Yang, G, Reynolds, M, Xia, X, Xiao, Y & He, Z 2019, 'A rapid monitoring of NDVI across the wheat growth cycle for grain yield prediction using a multi-spectral UAV platform', *Plant Science*, vol. 282, pp. 95-103.

Angus, JF 2001, 'Nitrogen supply and demand in Australian agriculture', *Australian Journal of Experimental Agriculture*, vol. 41, no. 3, pp. 277-288.

Asseng, S, Fillery, IR, Anderson, GC, Dolling, PJ, Dunin, FX & Keating, BA 1998, 'Use of the APSIM wheat model to predict yield, drainage and nitrate leaching for a deep sand', *Australian Journal of Agricultural Research*, vol. 49, no. 3, pp. 363-377.

Berger, B, De Regt, B & Tester, M 2012, 'High-Throughput Phenotyping of Plant Shoots', in N J. (ed.), *High-Throughput Phenotyping in Plants*, vol. 918, Humana Press, Totowa, NJ.

Birch, CJ & Long, KE 1990, 'Effect of nitrogen on the growth, yield and grain protein-content of barley (*hordeum vulgare*)', *Australian Journal of Experimental Agriculture*, vol. 30, no. 2, pp. 237-242.

Bogard, M, Jourdan, M, Allard, V, Martre, P, Perretant, MR, Ravel, C, Heumez, E, Orford, S, Snape, J, Griffiths, S, Gaju, O, Foulkes, J & Le Gouis, J 2011, 'Anthesis date mainly explained correlations between post-anthesis leaf senescence, grain yield, and grain protein concentration in a winter wheat population segregating for flowering time QTLs', *Journal of Experimental Botany*, vol. 62, no. 10, pp. 3621-3636.

Bouwer, H 1989, 'Agricultural contaminants: Problems and solutions', *Journal of Water and Environment Technology*, pp. 292-297.

Casadesus, J & Villegas, D 2014, 'Conventional digital cameras as a tool for assessing leaf area index and biomass for cereal breeding', *Journal of Integrative Plant Biology*, vol. 56, no. 1, Jan, pp. 7-14.

Castrignano, A, Buttafuoco, G, Khosla, R, Mouazen, A, Moshou, D & Naud, O 2020, *Agricultural internet of things and decision support for precision smart farming*, Business & Economics, Academic Press.

Coombes, NE, 2009, *Digger design search tool in R*,

Cormier, F, Foulkes, J, Hirel, B, Gouache, D, Moenne-Loccoz, Y & Le Gouis, J 2016, 'Breeding for increased nitrogen-use efficiency: a review for wheat (*T.aestivum* L.)', *Plant Breeding*, vol. 135, no. 3, Jun, pp. 255-278.

Cox, MC, Qualset, CO & Rains, DW 1985, 'Genetic variation for nitrogen assimilation and translocation in wheat. I. Dry matter and nitrogen accumulation', *Genetic variation for nitrogen assimilation and translocation in wheat. I. Dry matter and nitrogen accumulation*, vol. 25, no. 3, pp. 430-435.

Daniel, C & Triboi, E 2002, 'Changes in wheat protein aggregation during grain development: effects of temperatures and water stress', *European Journal of Agronomy*, vol. 16, no. 1, Jan, pp. 1-12.

Davis, L, Ware, A & Cook, A 2016, *Port Kenny, Franklin Harbour, Elliston and Wharminda wheat and barley variety trials in 2015*, Crop and Pasture Report, PIRSA, South Australia.

Eagles, HA, McLean, R, Eastwood, RF, Appelbee, MJ, Cane, K, Martin, PJ & Wallwork, H 2014, 'High-yielding lines of wheat carrying Gpc-B1 adapted to Mediterranean-type environments of the south and west of Australia', *Crop & Pasture Science*, vol. 65, no. 9, pp. 854-861.

Evans, J, Scott, G, Lemerle, D, Kaiser, A, Orchard, BA, Murray, GM & Armstrong, EL 2003, 'Impact of legume 'break' crops on the residual amount and distribution of soil mineral nitrogen', *Crop and Pasture Science*, vol. 54, no. 8, pp. 763-776.

Fahlgren, N, Gehan, MA & Baxter, I 2015, 'Lights, camera, action: high-throughput plant phenotyping is ready for a close-up', *Current Opinion in Plant Biology*, vol. 24, Apr, pp. 93-99.

Fillery, I 2001, 'The fate of biologically fixed nitrogen in legume-based dryland farming systems: a review', *Aust. J. Exp. Agric.*, vol. 41, pp. 361-381.

Freeman, K, Raun, W, Johnson, G, Mullen, RW, Stone, M & Solie, J 2003, 'Late-season prediction of wheat grain yield and grain protein', *Commun. Soil Sci. Plant Anal.*, vol. 34, no. 13-14, pp. 1837-1852.

Furbank, RT & Tester, M 2011, 'Phenomics - technologies to relieve the phenotyping bottleneck', *Trends in Plant Science*, vol. 16, no. 12, Dec, pp. 635-644.

Giles, T, Bedggood, A & Kelly, A 2012, 'Trials with maximum value', in E Leonard (ed.), *National variety trials supplement*, GRDC.

Harrison, R & Webb, J 2001, 'A review of the effect of N fertilizer type on gaseous emissions', *Advances in Agronomy*, vol. 73, pp. 65-108.

Hill, MJ, Donald, GE, Hyder, MW & Smith, RCG 2004, 'Estimation of pasture growth rate in the south west of Western Australia from AVHRR NDVI and climate data', *Remote Sensing of Environment*, vol. 93, pp. 28-45.

Hitz, K, Clark, AJ & Van Sanford, DA 2017, 'Identifying nitrogen-use efficient soft red winter wheat lines in high and low nitrogen environments', *Field Crops Research*, vol. 200, pp. 1-9.

Husenov, B, Makhkamov, M, Garkava-Gustavsson, L, Muminjanov, H & Johansson, E 2015, 'Breeding for wheat quality to assure food security of a staple crop: the case study of Tajikistan.', *Agriculture and Food Security*, vol. 4, p. 9.

Jimenez-Berni, JA, Deery, DM, Rozas-Larraondo, P, Condon, AG, Rebetzke, GJ, James, RA, Bovill, WD, Furbank, RT & Sirault, XRR 2018, 'High throughput determination of plant height, ground cover, and above-ground biomass in wheat with LiDAR', *Frontiers in Plant Science*, vol. 9.

Kovalchuk, N, Laga, H, Cai, J, Kumar, P, Parent, B, Lu, Z, Miklavcic, SJ & Haefele, SM 2016, 'Phenotyping of plants in competitive but controlled environments: a study of drought response in transgenic wheat', *Functional Plant Biology*, vol. 44, no. 3, pp. 290-301.

Kronenberg, L, Yu, K, Walter, A & Hund, A 2017, 'Monitoring the dynamics of wheat stem elongation: genotypes differ at critical stages', *Euphytica*, vol. 213, no. 157

Langridge, P & Fleury, D 2011, 'Making the most of 'omics' for crop breeding', *Trends in Biotechnology*, vol. 29, no. 1, pp. 33-40.

Li, C, Cao, W & Dai, T 2001, 'Dynamic characteristics of floret primordium development in wheat', *Field Crops Research*, vol. 71, pp. 71–76.

Magney, TS, Eitel, JUH, Huggins, DR & Vierling, LA 2016, 'Proximal NDVI derived phenology improves in-season predictions of wheat quantity and quality', *Agricultural and Forest Meteorology*, vol. 217, pp. 46-60.

Mahey, RK, Singh, R, Sidhu, SS & Narang, RS 1991, 'The use of remote sensing to assess the effects of water stress on wheat', *Ex. Agric.*, vol. 27, no. 4, pp. 423-429.

Mahjourimajd, S, Kuchel, H, Langridge, P & Okamoto, M 2016, 'Evaluation of Australian wheat genotypes for response to variable nitrogen application', *An International Journal on Plant-Soil Relationships*, vol. 399, no. 1, pp. 247-255.

McDonald, G & Hooper, P 2013, 'Nitrogen decision - Guidelines and rules of thumb', in Uo Adelaide (ed.), *GRDC update papers*, GRDC, Australia.

'National Variety Trial' 2019, Grains Research and Development Corporation Australia.

Prasad, B, Carver, BF, Stone, ML, Babar, MA, Raun, WR & Klatt, AR 2007, 'Potential Use of Spectral Reflectance Indices as a Selection Tool for Grain Yield in Winter Wheat under Great Plains Conditions', *Potential Use of Spectral Reflectance Indices as a Selection Tool for Grain Yield in Winter Wheat under Great Plains Conditions*, vol. 47, no. 4, pp. 1426-1440.

Quinlan, R & Wherrett, A 2013, *Fact Sheets: Nitrogen-New South Wales*, The New South Wales Department of Primary Industries, New South Wales, <http://www.soilquality.org.au/factsheets/nitrogen-nsw>.

R Development Core Team, 2017, *R: A language and environment for statistical computing*, Vienna, Austria.

Rahimi Eichi, V, Okamato, M, Haefele, SM, Jewell, N, Brien, C, Garnett, T & Langridge, P 2019, 'Understanding the interactions between biomass, grain production and grain protein content in high and low protein wheat genotypes under controlled environments ', *Agronomy*, vol. 9, p. 706.

Rahimi Eichi, V, Okamoto, M, Garnett, T, Eckermann, P, Darrier, B, Riboni, M & Langridge, P 2020, 'Strengths and weaknesses of national variety trial data for multi-environment analysis: A case study on grain yield and protein content', *Agronomy*, vol. 10, no. 753.

Raun, WR, Solie, JB, Johnson, GV, Stone, ML, Lukina, EV, Thomason, WE & Schepers, JS 2001, 'In-season prediction of potential grain yield in winter wheat using canopy reflectance', vol. 93, pp. 131-138.

Rebetzke, GJ, Van Herwaarden, A, Biddulph, B, Moeller, C & Rattey, A 2012, 'Protocols for experimental plot sampling, handling and processing of cereal experiments - Standardised methods for use in field studies', in PrometheusWiki (ed.)CSIRO, <http://prometheuswiki.publish.csiro.au/tiki-index.php>.

Richards, RA 2000, 'Selectable traits to increase crop photosynthesis and yield of grain crops', *Journal of Experimental Botany*, vol. 51, pp. 447-458.

Royo, C, Aparicio, N, Blanco, R & Villegas, D 2004, 'Leaf and green area development of durum wheat genotypes grown under Mediterranean conditions', *Leaf and green area development of durum wheat genotypes grown under Mediterranean conditions*, vol. 20, no. 4, pp. 419-430.

Sadras, VO, Hayman, PT, Rodriguez, D, Monjardino, M, Bielich, M, Unkovich, M, Mudge, B & Wang, E 2016, 'Interactions between water and nitrogen in Australian cropping systems: physiological, agronomic, economic, breeding and modelling perspectives', *Crop and Pasture Science*, vol. 67, no. 10, pp. 1019-1053.

Sadras, VO & McDonald, G 2012, *Benchmarking wheat water use efficiency: accounting for climate and nitrogen*, Water use efficiency of grain crops in Australia: principles, benchmarks and managemen, GRDC, Adelaide, Australia.

Sadras, VO & Richards, RA 2014, 'Improvement of crop yield in dry environments: benchmarks, levels of organisation and the role of nitrogen', *Journal of Experimental Botany*, vol. 65, no. 8, May, pp. 1981-1995.

Sanford, D & MacKown, C 1986, 'Variation in nitrogen use efficiency among soft red winter wheat genotypes', *International Journal of Plant Breeding Research*, vol. 72, no. 2, pp. 158-163.

Sharma, R 1993, 'Selection for biomass yield in wheat', *International Journal of Plant Breeding*, vol. 70, no. 1, pp. 35-42.

Shewry, PR & Hey, SJ 2015, 'The contribution of wheat to human diet and health', *Food and Energy Security*, vol. 4, no. 3, Oct, pp. 178-202.

Sinclair, TR & Rufty, TW 2012, 'Nitrogen and water resources commonly limit crop yield increases, not necessarily plant genetics', *Global Food Security*, vol. 1, no. 2, Dec, pp. 94-98.

Stoddard, FL & Marshall, DR 1990, 'Variability in grain protein in australian hexaploid wheats', *Australian Journal of Agricultural Research*, vol. 41, no. 2, pp. 277-288.

Stone, PJ & Nicolas, ME 1995, 'A survey of the effects of high-temperature during grain filling on yield and quality of 75 wheat cultivars', *Australian Journal of Agricultural Research*, vol. 46, no. 3, pp. 475-492.

Sylvester-Bradley, R, Berry, P, Blake, J, Kindred, D, Spink, J, Bingham, I, McVittie, J & Foulkes, J 2008, *The wheat growth guide*, Second edn, eds C Edwards & G Dodgson, London.

Sylvester-Bradley, R & Kindred, DR 2009, 'Analysing nitrogen responses of cereals to prioritize routes to the improvement of nitrogen use efficiency', *Journal of Experimental Botany*, vol. 60, no. 7, May, pp. 1939-1951.

Triboi, E, Abad, A, Michelena, A, Lloveras, J, Ollier, JL & Daniel, C 2000, 'Environmental effects on the quality of two wheat genotypes: 1. quantitative and qualitative variation of storage proteins', *European Journal of Agronomy*, vol. 13, no. 1, Jul, pp. 47-64.

van Herwaarden, AF, Farquhar, GD, Angus, JF, Richards, RA & Howe, GN 1998, ''Haying-off', the negative grain yield response of dryland wheat to nitrogen fertiliser - I. Biomass, grain yield, and water use', *Australian Journal of Agricultural Research*, vol. 49, no. 7, pp. 1067-1081.

Walter, A, Liebisch, F & Hund, A 2015, 'Plant phenotyping: from bean weighing to image analysis', *Plant methods*, vol. 11, no. 14

Weaver, JE 1926, *Root development of field crops*, McGraw-HillBook Company, New York.

Yamaguchi, J & Tanaka, A 1990, 'Quantitative observation on the root system of various crops growing in the field', *Soil Science and Plant Nutrition*, vol. 36, no. 3, pp. 483-493.

Zorb, C, Becker, E, Merkt, N, Kafka, S, Schmidt, S & Schmidhalter, U 2017, 'Shift of grain protein composition in bread wheat under summer drought events', *Journal of Plant Nutrition and Soil Science*, vol. 180, no. 1, Feb, pp. 49-55.

Chapter 4: Supplementary material

Long-term monthly rainfall
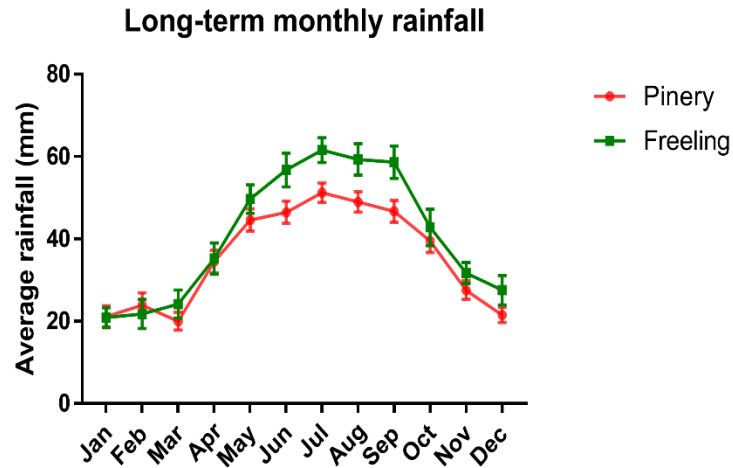
Figure S1. Long-term monthly rainfall at Freeling and Pinery experimental sites. The long-term data were recorded between 1925-2017 for Pinery and 1963-2017 for Freeling in less than 10km distance from the experimental sites. Data are available at: *http://www.bom.gov.au/climate/data/*.
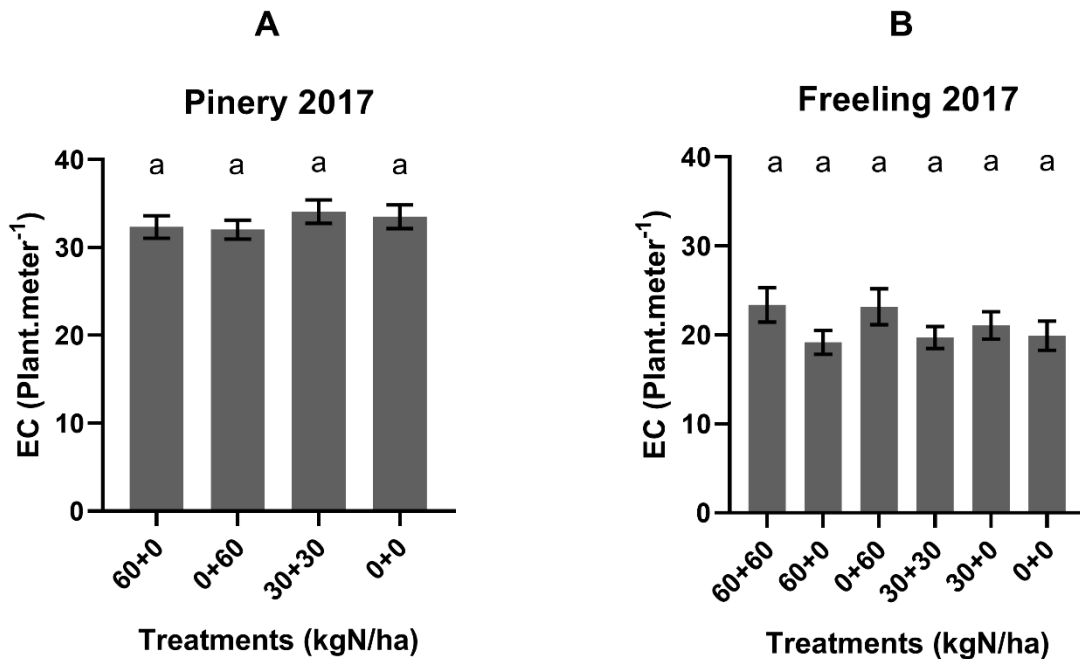
Figure S2. Plant establishment counts (EC) per plot from 1 meter of the middle row in Pinery (**A**) and Freeling (**B**) in 2018. Letters indicate significant different between genotypes by one-way ANOVA with Tuckey's correction (p<0.05).

Chapter 5: Strengths and Weaknesses of National Variety Trial Data for Multi-Environment Analysis: A Case Study on Grain Yield and Protein Content

Vahid Rahimi Eichi [1,2], Mamoru Okamoto [1,2], Trevor Garnett [1,2,3], Paul Eckermann [1,2], Benoit Darrier [1], Matteo Riboni [1] and Peter Langridge [1,4,*]

[1]School of Agriculture Food and Wine, University of Adelaide, Glen Osmond 5064, Australia;

vahid.rahimi-eichi@adelaide.edu.au (V.R.E.); mamoru.okamoto@adelaide.edu.au (M.O.); trevor.garnett@grdc.com.au (T.G.); paul.eckermann@adelaide.edu.au (P.E.); benoit.darrier@adelaide.edu.au (B.D.); matteoriboni@hotmail.it (M.R.)

[2]ARC Industrial Transformation Research Hub for Wheat in a Hot and Dry Climate, Waite Research Institute,

University of Adelaide, Glen Osmond 5064, Australia

[3]Australian Plant Phenomics Facility, The University of Adelaide, PMB1, Glen Osmond, South Australia 5064, Australia

[4]Wheat Initiative, Julius-Kühn-Institute, 14195 Berlin, Germany

* Correspondence: peter.langridge@adelaide.edu.au; Tel.: +61-8-83137368

Statement of Authorship

Title of Paper	Strengths and weaknesses of National Variety Trial data for multi-environment analysis: a case study on grain yield and protein content
Publication Status	☑ Published ☐ Accepted for Publication ☐ Submitted for Publication ☐ Unpublished and Unsubmitted work written in manuscript style
Publication Details	Manuscript prepared in accordance with the guidelines for *agronomy*

Principal Author

Name of Principal Author (Candidate)	Vahid Rahimi Eichi		
Contribution to the Paper	Conceptualization, methodology, formal analysis, investigation, writing (original draft preparation), writing (review and editing)		
Overall percentage (%)	80%		
Certification:	This paper reports on original research I conducted during the period of my Higher Degree by Research candidature and is not subject to any obligations or contractual agreements with a third party that would constrain its inclusion in this thesis. I am the primary author of this paper.		
Signature		Date	14.07.2020

Co-Author Contributions

By signing the Statement of Authorship, each author certifies that:

     i.   the candidate's stated contribution to the publication is accurate (as detailed above);

     ii.   permission is granted for the candidate in include the publication in the thesis; and

     iii.   the sum of all co-author contributions is equal to 100% less the candidate's stated contribution.

Name of Co-Author	Prof. Peter Langridge		
Contribution to the Paper	Conceptualization, methodology, writing (original draft preparation), writing (review and editing), supervision		
Signature		Date	16/7/2020

Name of Co-Author	Dr. Trevor Garnett		
Contribution to the Paper	Conceptualization, methodology, writing (original draft preparation), writing (review and editing), supervision		
Signature		Date	16/7/2020

Name of Co-Author	Dr. Mamoru Okamoto		
Contribution to the Paper	Conceptualization, methodology, writing (original draft preparation), writing (review and editing), supervision		
Signature		Date	16/07/2020

Name of Co-Author	Paul Eckermann		
Contribution to the Paper	Methodology		
Signature		Date	20/7/2020

Name of Co-Author	Dr. Matteo Riboni			
Contribution to the Paper	Methodology			
Signature			Date	21/07/2020

Name of Co-Author	Dr. Benoit Darrier			
Contribution to the Paper	Formal analysis			
Signature			Date	16/07/2020

Please cut and paste additional co-author panels here as required

78

Strengths and Weaknesses of National Variety Trial Data for Multi-Environment Analysis: A Case Study on Grain Yield and Protein Content

Vahid Rahimi Eichi [1,2], **Mamoru Okamoto** [1,2] , **Trevor Garnett** [1,2,3] , **Paul Eckermann** [1,2],
Benoit Darrier [1], **Matteo Riboni** [1] and **Peter Langridge** [1,4,*]

1 School of Agriculture Food and Wine, University of Adelaide, Glen Osmond 5064, Australia;
  vahid.rahimi-eichi@adelaide.edu.au (V.R.E.); mamoru.okamoto@adelaide.edu.au (M.O.);
  trevor.garnett@grdc.com.au (T.G.); paul.eckermann@adelaide.edu.au (P.E.);
  benoit.darrier@adelaide.edu.au (B.D.); matteoriboni@hotmail.it (M.R.)
2 ARC Industrial Transformation Research Hub for Wheat in a Hot and Dry Climate, Waite Research Institute,
  University of Adelaide, Glen Osmond 5064, Australia
3 Australian Plant Phenomics Facility, The University of Adelaide, PMB1, Glen Osmond,
  South Australia 5064, Australia
4 Wheat Initiative, Julius-Kühn-Institute, 14195 Berlin, Germany
* Correspondence: peter.langridge@adelaide.edu.au; Tel.: +61-8-83137368

Abstract: Multi-environment trial studies provide an opportunity for the detailed analysis of complex traits. However, conducting trials across a large number of regions can be costly and labor intensive. The Australian National Variety Trials (NVT) provide grain yield and protein content (GPC) data of over 200 wheat varieties in many and varied environments across the Australian wheat-belt and is representative of similar trials conducted in other countries. Through our analysis of the NVT dataset, we highlight the advantages and limitations in using these data to explore the relationship between grain yield and GPC in the low yielding environments of Australia. Eight environment types (ETs), categorized in a previous study based on the time and intensity of drought stress, were used to analyze the impact of drought on the relationship between grain yield and protein content. The study illustrates the value of comprehensive multi-environment analysis to explore the complex relationship between yield and GPC, and to identify the most appropriate environments to select for a favorable relationship. However, the NVT trial design does not follow the rigor associated with a normal genotype × environment study and this limits the accuracy of the interpretation.

Keywords: National Variety Trials; grain protein content; multi-environment; grain yield; high and low protein wheat; environment type; grain protein deviation

1. Introduction

Wheat is a major source of protein in the human diet and, along with rice, the most important crop product for carbohydrate [1,2]. Meeting the food demands of an estimated 9 billion people in 2050 [3,4] requires about 70% increased production over the next 30 years [5,6]. Through advances in agronomic practices and breeding, wheat yields have increased spectacularly over the past few decades [2,4,5]. Many of the major traits, such as yield and GPC, targeted for improvement in breeding programs and of prime importance to farmers, are under complex genetic control and strongly influenced by the production environment. For both wheat breeders and farmers, the relationship between yield and GPC is important. Consequently, many countries run extensive varietal trials to provide information for farmers on performance of varieties under their likely production conditions and for

breeders to assess the advances they have achieved through breeding and selection. The variety trials also provide a potentially valuable resource for researchers to understand the basis of genotype × environment relationships.

Concurrently, grain protein content (GPC), a key attribute for end use quality with high nutritional value and an important marketing factor for wheat, will also have to be maintained [7–9]. For example, in Australia, GPC is used in determining the value of the wheat crop to farmers [10]. However, there is an unfavorable relationship between grain yield and GPC with increased yield frequently associated with a decline in GPC and this presents a significant challenge to breeders [9,11,12]. A study on winter wheat in Germany showed that good progress in raising grain yield was associated with a considerable loss in GPC over the last 32 years [9]. Consequently, wheat germplasm is often divided into high yielding or high quality varieties, as defined by high GPC% [13]. To simultaneously improve both grain yield and GPC, grain protein deviation (GPD) has been suggested as a useful selection target [14,15]. Grain protein deviation measures the grain yield/GPC trade-off by compensating for GPC dilution when selecting for higher yield potential [16]. Grain yield and GPC in wheat have low heritability since they are highly sensitive to environmental variations and under complex genetic control [9,17]. Therefore, despite evidence for the genetic origin of the negative relationship between grain yield and GPC in wheat [9,18], its expression can be highly influenced by the environment [11,19]. A previous study using six Southern and Western Australian sites showed that the inverse relationship between grain yield and GPC varied across different regions [20]. Therefore, multi-environment trial studies can provide an opportunity for the simultaneous selection of both grain yield and GPC [11,19,20]. However, conducting trials across a large number of regions can be costly and labor intensive. In this context, Australian National Variety Trials (NVT) funded by Australian Grains Research and Development Corporation (GRDC) provide a useful source of multi-environment data. The NVT system provides information to growers through the NVT website (https://www.nvtonline.com.au/) to assist with decisions about suitable varieties for particular regions in Australia. NVT data has been used in previous studies to examine the relationship between grain yield and GPC in some hard wheats [21,22]. The NVT system in Australia is similar to varietal trials conducted in many other countries and regions, such as the UK (https://ahdb.org.uk), Germany (https://www.bundessortenamt.de), and Kentucky, USA (http://www.uky.edu/Ag/wheatvarietytest/).

NVT are designed to provide unbiased information on the performance of varieties across different Australian regions [23]. Deploying small plots in NVT trials minimizes the large-scale field variation effects. Accordingly, a combination of the small plot trials with modern statistical methods have provided an accurate way to evaluate the performance of varieties [24]. The rationale for all NVT trials is to achieve the best performance of varieties within the constraints of water-limited yield potential under management regimes suited to the trial region. In NVT trials, optimal fertilizer rates are usually applied to prevent the nutrition limitation [24] along with other appropriate agronomic practices. Environmental categorization of NVT sites adds the option of characterization of genotype and environment interactions [25] and comparison of biotic and abiotic stresses [26,27]. The majority of the Australian wheat-belt area suffers from drought conditions [28]. Drought stress may reduce the production of wheat up to 50% depending on its severity and duration [29]. It has been shown that grain yield reductions due to drought can increase the GPC in wheat [30–32]. Based on the time and intensity of drought stress, Chenu and Deihimfard [28] categorized different drought patterns across the Australian wheat-belt into four major environment types (ETs). Accordingly, ET1 represents a stress-free or short-term water deficit. ET2 shows a mild water shortage mainly during grain filling that terminates by maturity. In ET3 water stress is severe at the vegetative stage but is usually over by mid-grain filling. In ET4, water deficit begins from the early stage onwards, and becomes severe during grain-set and grain filling [28]. All of the four ETs can be seen across most the Australian wheat-belt. However, the frequency of occurrence for each ET varies between different regions. In this study, 11 years of NVT dataset were categorized based on their most frequent ETs. Through the use of the NVT data, we have sought to highlight the advantages and limitations of using a large multi-environment

datasets. We present a case study of applying the NVT data to explore the negative grain yield–GPC relationship across diverse environments. If there is variation associated with the environmental conditions, and under what conditions should breeders screen high yielding germplasms for high GPC? Our previous study in a controlled environment indicated a stronger inverse relationship between grain yield and GPC under low nitrogen (N) treatment in selected wheat varieties [33]. Since N deficiency can be associated with water availability [34,35], it is worthwhile to search the effect of ETs on the grain yield–GPC relationship. The goals of this study were: (1) assess the potential of using NVT data for large-scale multi-environment analysis and (2) to see if GPC is a stable trait across different environments. The lessons learned here, should be applicable to other varietal evaluation datasets and could be used to address some of the limitations in the current design of varietal trials.

2. Materials and Methods

2.1. General NVT Protocols

Trials analyzed in this study were organized and managed under the GRDC NVT program between 2008 and 2018 for 215 wheat (*Triticum aestivum* L.) varieties in 206 sites across the Australian wheat-belt and Tasmania (Supplementary Figure S1). At some sites, a year could include up to three seasons described as early, main or late seasons. However, only 2% of the entire data set are obtained from long seasons. There is 79% and 18% of the data from main and early seasons, respectively. Based on the popularity of varieties with growers in each region, newly released varieties could remain for up to 5 years in an NVT system. Subsequently, varieties that represent less than 3% of the annual yield are withdrawn from the NVT list. NVT breeding materials comprise varieties prior to their commercial release and released varieties. Commercial varieties that are widely grown in a region, e.g., Mace in South and Western Australia, are used as benchmark varieties [23].

Selection and management of NVT sites are determined by standard, outcome-based protocols. However, additional fertilizer and pesticides are applied when required [23]. In this context, fertilizer rates applied for NVT trials are often higher than the commercial rates in the region [24]. All NVT trials are designed with three replicates but only grain yield is obtained from the individual plot. Due to its high cost, GPC is assessed by using composite samples. In this method, equal weight grain samples collected from each replicate are physically mixed to form a homogenous composite unit. GPC measurements are made on the subsample, with an appropriate size, of each of these composite units [36].

2.2. Multi-Environmental Analysis and Graph Depiction

Chenu, Deihimfard [28] characterized 60 sites by simulated water-stress index obtained from their climate and the typical soil of their region (Supplementary Table S1). Simulated water-stress index corresponds to the ratio of soil water supply to crop water demand, and reflects how the crops experience the stress [28,37,38]. In the mentioned study, they performed a set of simulations for a medium maturing variety, Hartog, based on 123 years of historical climate data obtained from 22 regions across the Australian wheat-belt (Supplementary Figures S2 and S3). The 22 regions represent the major production areas in the Australian wheat cropping system. Data shown in Supplementary Table S1 are mostly obtained from Ababaei and Chenu [39] simulations on Janz variety.

Among the 206 NVT sites examined in this research, 46 sites were identical with the locations in Chenu, Deihimfard [28] study. The location of other NVT sites were individually checked to determine their regions and ETs. Except for Tasmania, all mainland NVT sites were located in the recognized 22 regions [39].

Categorizing NVT data based on ETs requires additional information, such as cumulative rainfall and soil type, for all 206 individual sites over 11 years. Furthermore, some sites could cover multiple seasons in one year due to differences in sowing date. Consequently, in this study, individual sites were categorized based on the most frequent ETs in their regions (Supplementary Information). This can

be an efficient and quick method to provide an overview of the long-term drought stress conditions across the Australian wheat-belt. NVT datasets are available for a range of consecutive years in similar locations. Therefore, the average long-term results for yield and GPC could be more influenced by the dominant ETs compared to other ETs in each region. Accordingly, NVT sites, except for Tasmanian sites, were categorized based on their dominant ETs in each region. In this research, the number of sites for each of 22 regions ranged from 4 to 32, while they were between 1 and 8 in Chenu, Deihimfard [28] study. The map of frequencies of each ET across the Australian wheat-belt [28] were used to categorize different regions (Supplementary Figure S4).

Grain yield and GPC between different ETs were compared based on their average and median values. *p*-Values and statistical tests were not conducted due to potential limitations with the analysis of NVT dataset. These limitations are explained in the discussion section. Correlations between grain yield and GPC were assessed using Pearson's correlation coefficient. The slope of grain yield–GPC relationship was measured for each ET by averaging the grain yield–GPC slope from individual sites in each year. GPD was calculated for individual sites in each year as the residual from the regression line of grain yield–GPC relationship [14]. All the analyses and the graphics were performed using R v3.5.1 [40].

3. Results

Based on the map of the frequencies of each ET across the Australian wheat-belt [28], there were two dominant ETs in some areas (Supplementary Figure S4). Such regions were categorized as separate ETs since they lie in between of the two ETs. For instance, regions with dominant ET1 and ET2 were named with ET1/2. Accordingly, there were eight ETs for NVT data in this study: ET0, ET1, ET1/2, ET2, ET2/3, ET3, ET3/4, and ET4. In this context, ET1/2, ET2, and ET2/3 covered respectively, 20%, 26%, and 24% of the entire NVT data set (Table 1).

Chenu and Deihimfard [28] did not include Tasmania in their study. However, there were NVT sites near Launceston where the average rainfall was ~600 mm per year [41]. Accordingly, the datasets of these sites located in the high rainfall zones (HRZ) of Tasmania were categorized as ET0 in this study. Average grain yield for the different environments ranged from 9.2 t/ha for ET0 down to 1.6 t/ha for ET4 (Figure 1A).

Table 1. General information about National Variety Trials (NVT) dataset. The average number of varieties per site, number of years, total number of sites during consecutive years, and total number of data in individual environment types (ETs).

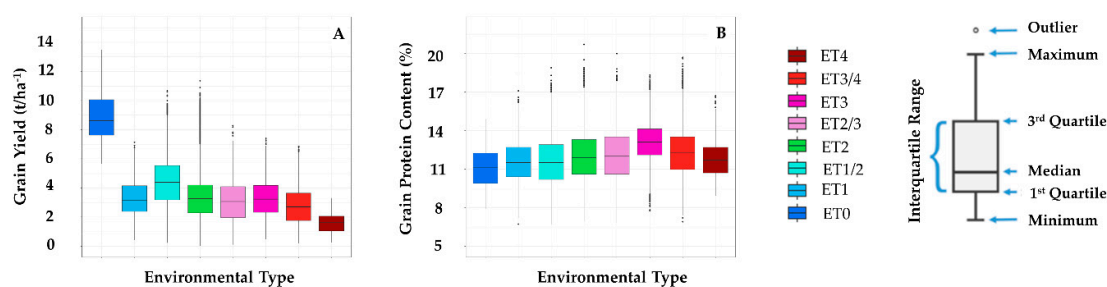| Environment Type	ET0	ET1	ET1/2	ET2	ET2/3	ET3	ET3/4	ET4
Average no. of varieties per site	20	32	41	43	40	43	38	28
No. of years	7	11	11	11	11	11	11	11
No. of sites × year	7	132	254	321	317	85	193	29
Total no. of variety × site × year × season	140	4263	10,347	13,766	12,597	3666	7237	805

Figure 1. Grain yield (**A**) and grain protein content (**B**) of all 215 varieties in the NVT dataset. Total numbers of variety × site × year × season were 52,822 collected from 206 sites. Name of varieties is listed in Supplementary Data S1. Boxes refer to the 25th (first quartile), 50th (median), and 75th (third quartile) percentile of data.

The decline in in-season rainfall from ET0 to ET4 corresponds to the declining average yield (Figure 1A and Supplementary Table S1) with ET1 being an exception, most probably associated with the low soil fertility and short season in the ET1 environments of Western Australia [42–44]. After the HRZ of Tasmania (ET0), areas with dominant ET1/2 produced the highest grain yield compared to other ETs (Figure 1A). ET1/2 dominant regions are located in the HRZ of South Australia, Victoria and New South Wales, whereas ET1 areas are in the HRZ of Western Australia. ET1/2 and ET1 regions produced 4.4 and 3.3 t/ha, respectively. There were data available for most ETs during all 11 years except for ET0 where only 7 years of NVT trials were available.

GPC average appeared to increase from ET0 to ET3, and then decline towards ET4 (Figure 1B). The GPC mean of ET0, ET3 and ET4 were 11.1%, 13.1%, and 11.8%, respectively. This variation may not be entirely due to environmental effects since the variety lists did vary between different ETs. There were inverse relationships between grain yield and GPC when the entire NVT dataset was plotted (Figure 2A) and this trend could also be seen for the individual ETs (Figure 2B–I).

The negative relationship between grain yield and GPC is apparent but there is a very wide spread of results, indicating the complexity of the relationship and the influence of diverse environmental factors on the yield and GPC (Figure 2A). By plotting the data for each environment type separately, more clarity in the trends emerged (Figure 2B–I). The regression line for the grain yield–GPC relationship of each ET was steepest in ET4 (Figure 2B), but close to horizontal in ET0 (Figure 2I). However, the high variation within ETs counteracted this clarity of trends, particularly, for the ETs between ET0 and ET4 (Figure 2C–H). Therefore, the slope values of the grain yield–GPC relationship were calculated for individual sites in each year to reduce the variation between sites within ETs (Table 2). This slope increased from −0.45 in ET0 to −1.63 in ET4 (Table 2) indicating that the strength of the negative yield and GPC relationship is associated with the severity of drought stress.

Table 2. Average grain yield (GY), grain protein content (GPC), and the slope of the GY–GPC relationship in individual environment types (ETs). Slope, average GY and average GPC were obtained from individual sites in each year and have been averaged. SE: standard errors.

Environment Type	ET0	ET1	ET1/2	ET2	ET2/3	ET3	ET3/4	ET4
Average GPC (%)	11.2	11.6	11.6	11.9	12.1	13.1	12.2	11.8
Average GY (t/ha)	9.2	3.3	4.3	3.1	2.9	3.2	2.6	1.6
Average slope of GY-GPC relationship	−0.45	−1.19	−0.93	−1.27	−1.43	−1.35	−1.44	−1.63
SE of GPC	0.5	0.1	0.1	0.1	0.1	0.2	0.1	0.2
SE of GY	0.6	0.1	0.1	0.1	0.1	0.1	0.1	0.1
Range of Average GPC (%)	7	10.37	12.2	13.8	13.2	10.56	12.8	7.8
Range of Average GY (t/ha)	7.85	6.71	10.46	11.34	8.17	6.93	6.67	3.05

An even clearer relationship can be seen between the steepness of the grain yield–GPC slope and the average yield in each ET (Table 2 and Figure 3).

The variation in GPC across the range of different yielding environments was high. For example, GPC varied from 8.9% to 18.3% at sites where the average grain yield was around 2 t/ha (Figure 2A). This high GPC variation was also observed in individual ETs (Figure 2B–I).

The nature of variation in GPC was explored by examining the performance of individual varieties within the large NVT dataset. For this purpose, six varieties were selected based on their average GPC and their inclusion is a large number of trials at diverse sites (Figure 4).

Despite the large variation in the GPC of individual varieties (Figure 4), the median GPC of Spitfire was high, particularly, compared to QAL2000 and Gazelle (Figure 4A). Under similar dominant ETs (Figure 4C), the first and third quartile of the GPC varied between 11.5% and 14.8% in Spitfire, and 9.7% and 12% in QAL2000. Differences between low and high GPC varieties were even more evident with GPD values. Accordingly, the first and third quartiles of GPD was 0.3 and 1.2 in Spitfire, and −1.6 and −0.7 in QAL2000 (Figure 4D). In the entire NVT dataset from all ETs, Gazelle showed the lowest median GPD among the selected varieties (Figure 4B).
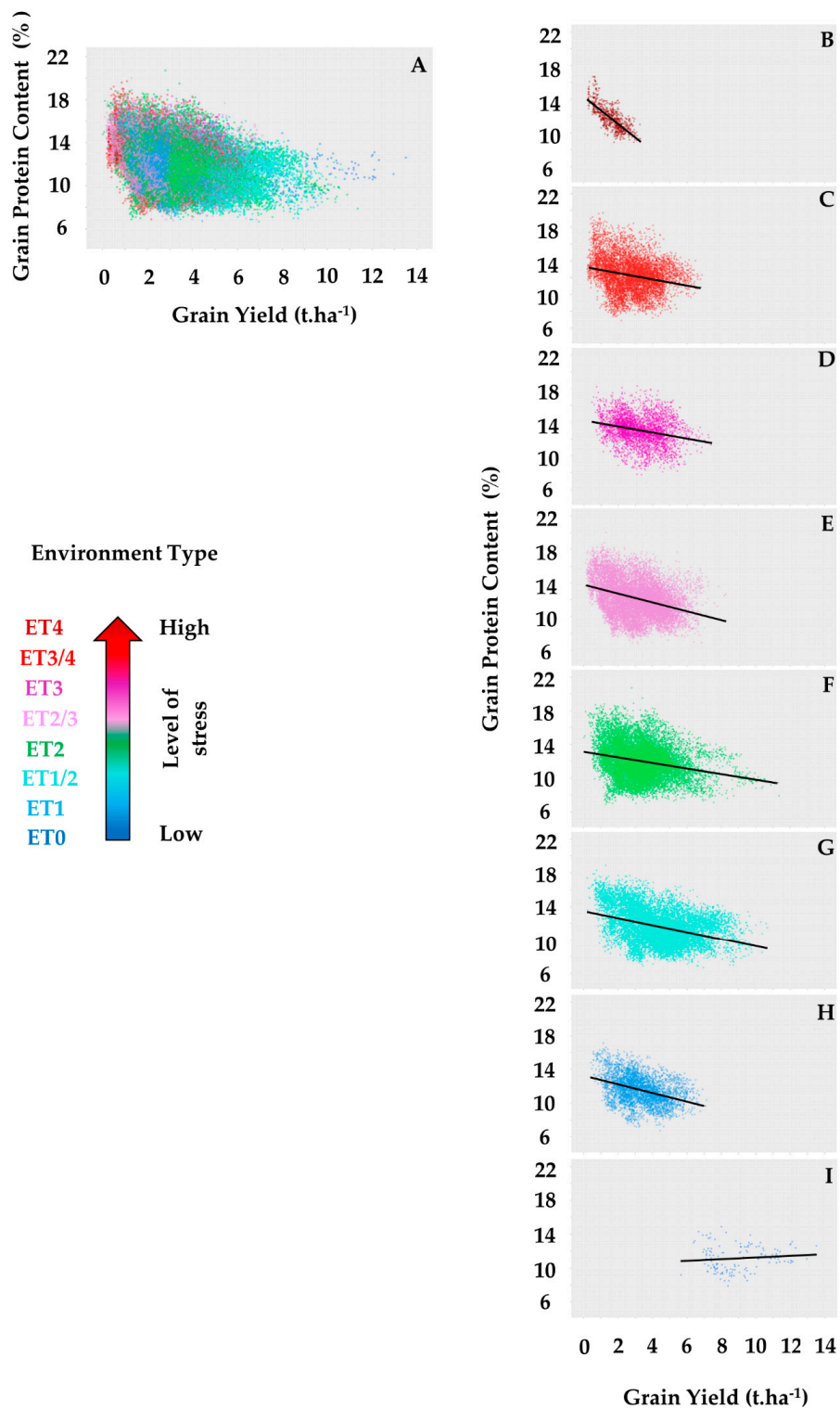
Figure 2. Relationship between grain yield and grain protein content across all (**A**) and in the individual environment types (ETs) (**B–I**). For the entire dataset (**A**), 215 wheat varieties were grown in 206 NVT sites across the Australian wheat-belt and Tasmania. The total number of varieties × site × year × season data in (**A**) were 52,822. The number of varieties, years and sites for the individual ETs in (**B–I**) are shown in Table 1. The lines in (**B–I**) show the best linear fit to the data. The negative relationships in all figures, except (I), are significant. The highest and lowest R^2 values are 0.57 and 0.01 for (B) and (I), respectively.
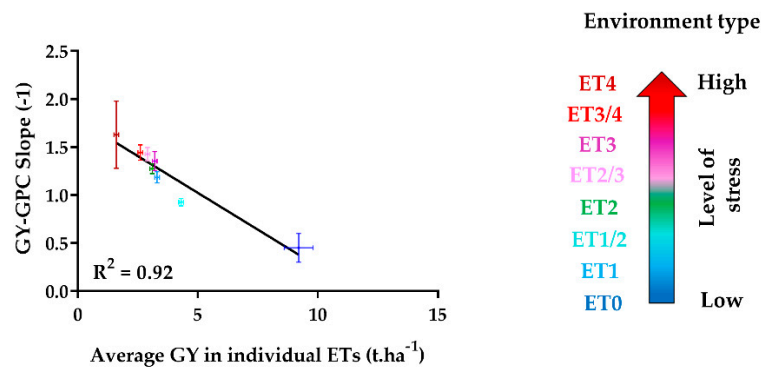
Figure 3. Relationship between the average grain yield (GY) in different environmental types (ETs), and the slope of the relationship between grain yield and grain protein content. Slope, average grain yield and average grain protein content were obtained from individual sites in each year and have been averaged. Error bars indicate the standard errors. R^2 represents the correlation coefficient.
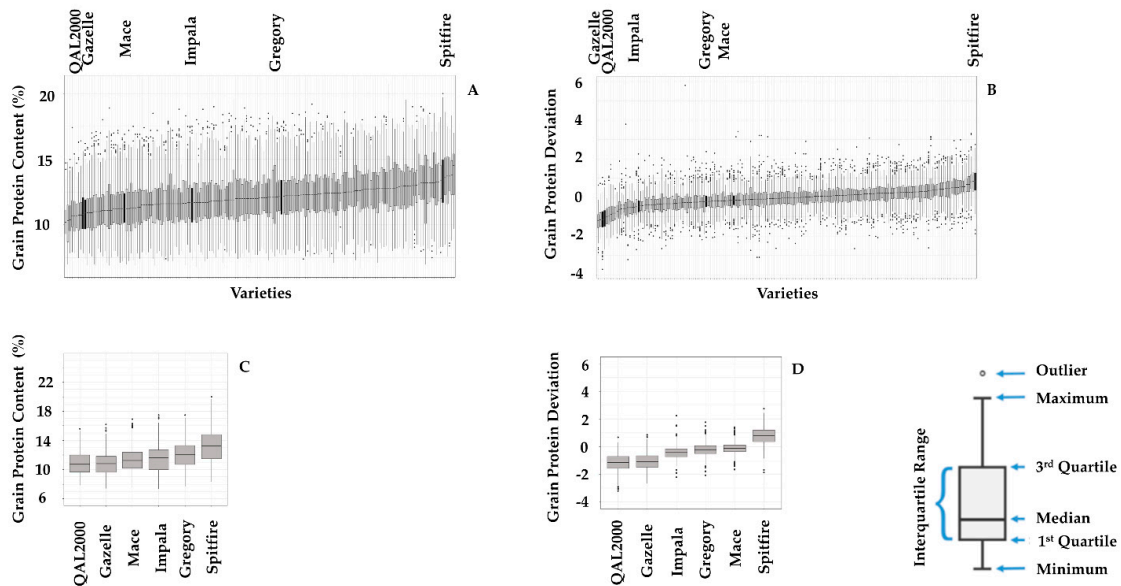

Figure 4. Grain protein content (**A**,**C**) and grain protein deviation (**B**,**D**) of 179 varieties in 206 sites, and 6 varieties in 168 sites from 2008 to 2018. ETs common between 6 varieties in (**C**,**D**) are ET1/2, ET2, ET2/3, and ET3/4. Grain protein deviation of each variety is calculated separately for each site, season, and year. The number of available trial data for each variety in (**A**,**C**) ranged from 50 to 896. The data available for the six selected varieties in (**C**,**D**) were: Spitfire: 366, Mace: 823, Gregory: 680, Impala: 429, QAL2000: 305 and Gazelle: 371. Boxes refer to the 25th (first quartile), 50th (median), and 75th (third quartile) percentile of data. (**A**,**B**) are obtained and modified from the Supplementary Figure S2 of Rahimi Eichi et al., 2019.

For the six selected varieties, the relationship between grain yield and GPC was plotted (Figure 5). All varieties showed a similar negative correlation between grain yield and GPC although they showed a large variation in GPC. There is also large variation in GPC across the yield spectrum which reflects the complexity of the influences of wheat production environments on GPC (Figure 5A–F and Supplementary Data S2).
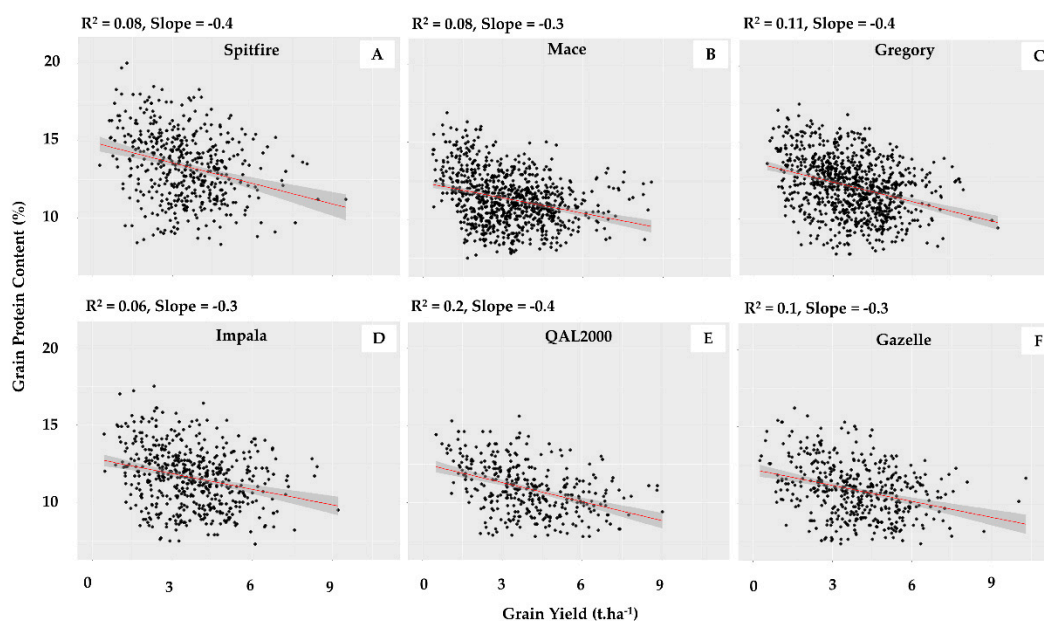
Figure 5. Relationship between grain yield and grain protein content of six selected wheat varieties obtained from NVT sites across Australia between 2008 and 2018. The number of available data for each variety was 476 (Spitfire), 850 (Mace), 897 (Gregory), 522 (Impala), 346 (QAL2000), and 445 (Gazelle). R^2 represents the correlation coefficient, and slope refers to the slope of the regression line. The negative relationship in all figures is significant.

4. Discussion

In this study, we have made use of a large, publicly available field trial dataset, to explore the relationship between stress, yield and grain protein content for wheat production in Australia. The NVT trial scheme in Australia is similar to varietal evaluation schemes operating in many countries and regions. These trials provide a potentially valuable resource for researchers since they cover a large number of trials and production environments. However, the trials are primarily designed to allow growers and agricultural agencies to compare the performance of different varieties in their regions. Consequently, the trial design does not necessarily reflect the rigor normally deployed in a scientific experiment and this can present issues with the analysis of trial data. Through our analysis of the NVT dataset, we have sought to highlight the advantages and problems in using large varietal trials.

In order to undertake this analysis, we needed to associate the 206 field sites for the NVT trials with environments. Previous studies from Chenu and Deihimfard [28], and Ababaei and Chenu [39] provided a good framework to categorize Australian wheat-belt regions based on their environmental characteristics. Yield and environment information studies indicated clear differences between environment types. Cumulative precipitation and simulated water-stress index reduced from ET1 to ET4. Based on Chenu, Deihimfard [28] work, we were able to group the trials into seven ETs. We then added the eighth environment to cover the high rainfall and high yielding sites in Tasmania. In comparison with the high rainfall zones (HRZ) of mainland Australia, Tasmania has higher rainfall and a milder climate with fewer extreme hot and cold temperatures [45]. These conditions allow average wheat yields of almost 9 t/ha in the ET0 of the NVT dataset. Accordingly, potential average yield of wheat in HRZ of Tasmania (ET0) is ~10 t/ha [45].

Some explanation is also needed for ET1, which does not follow the expected trend for yield (Figure 1A and light blue points in Figure 2A). Despite the higher rainfall and simulated water-stress index in ET1 (Supplementary Table S1), its average grain yield was less than of ET1/2 (Figure 1A). In this context, Ababaei and Chenu [39] showed lower simulated biomass and yield in ET1 compared to ET2 (Supplementary Table S1). The lower yield of Western Australia's high rainfall zone (ET1) compared to South–Eastern (ET1/2) and Tasmanian (ET0) high rainfall regions was shown in previous

studies [43,45]. Chenu, Deihimfard [28] categorized all ETs mainly based on the time and severity of drought stress regardless of their yield potential. The low yield in ET1, 50% of yield potential, might be due to the poor fertility of their cropping soils [42–44]. The shorter growing season of ET1 compared to other HRZ may also result in reduced yield [43]. A previous study on grain yield–GPC relationship suggested the separate assessment of Western Australian sites from other regions for GPC improvement in breeding programs [20]. The average yield of ET1 in this study was 3.3 t/ha, while the yield in Western HRZ was 2.7 t/ha [43,44]. The slightly higher average yield of NVT compared to the actual yield in Western HRZ can be due to the agronomic practices in NVT sites.

The higher average of GPC in ET3 compared to other environments (Figure 1B) might be due to differences in the drought pattern. It has been previously shown that drought stress before the end of grain filling increases GPC in wheat [46]. N uptake after anthesis, which increases N accumulation into grains, depends on the availability of water and nitrogen [35,47,48]. NVT sites receive adequate N fertilizer, therefore water availability may be the limiting factor of N uptake [24]. Relief from drought stress during grain filling in ET3 may permit post-anthesis N uptake. In ET4, however, water stress begins early in the season and intensifies towards the end of grain filling [28]. Consequently, pre and post-anthesis N uptake may not be sufficient to maintain yield and GPC in ET4. The high trade-off between yield and GPC (Figure 2B,D and Table 2) can be another reason for the lower GPC in ET4 compared to ET3. In ET0, on the other hand, the dilution effect of high grain yield might reduce GPC in comparison with ET3.

There is the potential for a range of variables to affect yield and GPC data from the NVT trials, including varieties, seasonal factors, level of replication, edaphic and disease pressures, and agronomic practices. In order to assess the reliability of the ET effects on yield and GPC, six varieties were examined and compared to the full dataset (Figures 4 and 5). The same varieties were used previously to examine their responses to N application in a controlled environment where plant growth rates were assessed [33]. In the previous study, it was found that the severity of stress, in that case the stress was induced through N starvation, intensified the negative relationship between yield and GPC. Grain protein content in wheat is strongly influenced by environment, and environmental factors have a greater impact than genetics effect [49,50].

The agronomic management of the NVT system aims to reflect the optimum practices for all sites and varies between sites. Consequently, N fertilizer may be applied at different rates between ETs. This may add to the variability of yield and GPC both between and within ETs. Moreover, in this study sites with similar first dominant ET were categorized together regardless of their second, third, or fourth dominant ETs. Therefore, the high yield and GPC variation of individual ETs (Figures 1 and 2) might come from inconsistencies in the ETs classification or different agronomic practices. For instance, the second dominant ET of two ET2 sites, Birchip and Cummins, were ET4 and ET1/2, respectively. Therefore, the average yield at Birchip was 3 t/ha, whereas, it was 4.9 t/ha for Cummins. However, these comparisons are based on averages and only indicate trends.

The inverse relationship between yield and GPC was stronger in low than in high yielding ETs (Figure 2A–I and Table 2). The NVT data show that a 1 t/ha increase in yield leads to an average GPC loss of 0.45% and 1.63% in ET0 and ET4, respectively. Previous studies on wheat also found a stronger negative relationship between yield and GPC under low N compared to high N supply [20,33,51]. The strong GPC-yield trade off under low N conditions can be due to a higher priority for the plants to maintain grain number and weight than for grain protein accumulation. A study on wheat [33] showed that under low N, high GPC varieties bred for low yielding environments sacrificed biomass and, consequently, yield in order to reserve N for grain protein. Conversely, low GPC varieties selected for high yielding regions used the available N primarily for biomass and yield regardless of grain N concentration. Reducing biomass and yield in favor of GPC increase can be considered as a strategy for plants to maintain GPC under stress. Under the stressed scenarios, fewer grains are produced but with sufficient nutrient levels to support germination and plant establishment [52–54]. The steep slope

of the yield–GPC relationship under stress suggests that simultaneous selection for high yield and GPC will be more effective in low than in high yielding regions.

Until the 1930s, Australian wheat production was dominated by soft and low GPC genotypes. However, since the 1960s the proportion of hard varieties with high GPC began to increase. Hard and soft wheat varieties were segregated between the 1950s and 1970s in different Australian regions. This led to the payment of premiums for high GPC hard wheats [50], and soft and feed varieties that were high yielding but with low GPC stayed in irrigated and high rainfall regions [50,55,56]. Higher GPC varieties, tended to be grown in dryer regions with lower yield potentials and the majority of wheat produced in Australia is grown in low yielding regions [50,55,57]. Over the last decade, there has been a significant increase in the premium price for high GPC wheat grains. Consequently, growers and breeders have targeted high GPC varieties even though this results in a small yield penalty [21,22].

Corresponding to the work of Bogart et al., [15], this study also showed the relative robustness of GPD across different environments. GPD corrects for the environmental effects on GPC and reveals the genotypic differences more clearly. The large variation in GPC due to environmental effects were reduced using GPD (Figure 4). The varieties Gazelle and QAL2000, which are considered as low GPC soft varieties had the lowest GPD, while, Spitfire, Mace, and Impala, high GPC varieties, showed higher average GPD. Therefore, GPD can be used as a potential target for selection in wheat breeding.

Our results (Figure 5 and Supplementary Data S2) confirmed a previous study on NVT data [21], indicating the inverse relationship between yield and GPC in individual varieties. However, this negative relationship was as small as a 1 t/ha increase in yield corresponded to the average GPC loss of ~0.4%. Indeed, the negative relationship between yield and GPC could be managed by applying suitable agronomic practices [9,51,58]. As mentioned above, the agronomic practices in NVT sites are based on the optimum for that region. For instance, delaying the final fertilizer application to around heading has been shown to increase GPC without yield penalty [15,59]. However, the success of this approach depends on climate conditions, particularly, water availability after anthesis. In the absence of sufficient water, the additional N is not beneficial and leads to multiple environmental consequences such as underground water pollution and eutrophication.

In the NVT system, varieties are selected to suit the production environments. Therefore, varieties, agronomic practices, and the number of sites and entries can vary between years, sites, and ETs. This variability means that statistical tests need to be applied with caution. The unbalanced nature of these trials can affect the validity of statistical tests, which often assume that varieties have been allocated at random to trials. However, in the NVT system the variables such as varieties and agronomical treatments (e.g., sowing date, fertilizer rate, chemical application, etc.) are not random but systematically decided in each field site. For example, the variety list of each NVT site is selected based on their suitability to the region [23]. If a variety does not produce acceptable yield or GPC in a site, it will usually be eliminated from the list at that site. Such limitations lead to the sampling process bias and, consequently, reduce the value of statistical assumptions. Accordingly, in this study, comparisons between varieties and ETs were based on averages or medians and only indicate trends. Showing the trends of values for different ETs and varieties indicates the potential of using such large numbers of data for multi-environmental studies. However, these are unbalanced datasets and this limits there value for detailed statistical analysis. A possible approach to analyze such unbalanced data can be the method developed by Smith and Cullis [60]. In other words, this study presented a useful dataset that others can examine further in more statistically rigorous ways to answer questions about the relationship between yield and GPC. Applying one standard agronomic practice in all sites could also improve the comprehensive multi-environmental analysis of NVT dataset in future.

5. Conclusions

While grain yield is of critical importance to wheat farmers, the protein content will influence the value of the grain. The relationship between grain yield and protein content is complex and highly dependent on the production environment but breeders have targeted both traits for selection in their

breeding programs. Achieving significant genetic gain for both yield and protein is difficult, given the large environmental and relatively small genetic component. Controlled environment studies have been helpful in understanding the impact of stress on the yield/protein relationship [11,20,33] but these results require validation through actual field trials. Here we have explored the option of exploiting the extensive field trial data used to evaluate germplasm across a large number of environments. Many countries run extensive variety evaluation trials, and these usually cover a large number of sites and environments. However, the trials are not designed with a view for the detailed statistical analysis required to explore the genotype × environment interactions that strongly influence the yield/protein relationship. In this study, we have attempted this analysis by using the ETs, categorized in Chenu and Deihimfard [28] and based on the time and intensity of drought stress, identified the potential for robust analysis of the impact of drought on yield–GPC relationship. However, further improvements in statistical approaches and NVT trials management may enhance the precision of the analysis.

The negative relationship between yield and GPC is more significant in low than in high yielding environments. This conclusion is consistent with controlled environment studies [11,20,33] and supports the view that GPC needs to be interpreted with a consideration of environmental factors that may limit yield. Selecting wheat varieties in low yielding regions might be more effective for the simultaneous increase of yield and GPC, and transferring varieties bred in low yielding environments to high yielding regions might provide results better than the reverse.

GPD revealed the genetic differences across different ETs, and therefore can be considered as a worthwhile potential target for breeders to improve both yield and GPC in wheat. Despite the genetic differences between varieties, selecting suitable sites and agronomic practices can help wheat farmers to achieve their targeted GPC [55,61,62]. For farmers, GPC loss with yield increase is best compensated using suitable region and agronomic management. Breeders, on the other hand, can select for varieties in environments where the impact of stress on GPC loss can be assessed.

ET3 regions might be suitable to grow high GPC varieties with reasonable yield while the high rainfall regions of Tasmania and the South–East Australian mainland should remain focused on soft or feed varieties with high yield but low GPC.

References

1. Shewry, P.R.; Hey, S.J. The contribution of wheat to human diet and health. *Food Energy Secur.* **2015**, *4*, 178–202. [CrossRef]

2. Curtis, T.; Halford, N.G. Food security: The challenge of increasing wheat yield and the importance of not compromising food safety. *Ann. Appl. Boil.* **2014**, *164*, 354–372. [CrossRef]

3. Godfray, H.C.J.; Beddington, J.R.; Crute, I.R.; Haddad, L.; Lawrence, D.; Muir, J.F.; Pretty, J.; Robinson, S.; Thomas, S.M.; Toulmin, C. Food security: The challenge of feeding 9 billion people. *Science* **2010**, *327*, 812–818. [CrossRef]

4. FAOSTAT. Available online: http://faostat.fao.org/default.aspx (accessed on 20 February 2020).

5. FAO. *How to Feed the World 2050*; Food and Agriculture Organization of the United Nations: Rome, Italy, 2009.

6. Pardey, P.; Beddow, J.; Hurley, T.; Beatty, T.; Eidman, V. A bounds analysis of world food futures: Global agriculture through to 2050. *Aust. J. Agric. Resour. Econ.* **2014**, *58*, 571–589. [CrossRef]

7. Husenov, B.; Makhkamov, M.; Garkava-Gustavsson, L.; Muminjanov, H.; Johansson, E. Breeding for wheat quality to assure food security of a staple crop: The case study of Tajikistan. *Agric. Food Secur.* **2015**, *4*, 9. [CrossRef]

8. Kuhn, J.C.; Stubbs, T.L.; Carter, A.H. Effect of the gpc-b1 allele in hard red winter wheat in the US pacific northwest. *Crop. Sci.* **2016**, *56*, 1009–1017. [CrossRef]

9. Laidig, F.; Piepho, H.P.; Rentel, D.; Drobek, T.; Meyer, U.; Huesken, A. Breeding progress, environmental variation and correlation of winter wheat yield and quality traits in german official variety trials and on-farm during 1983–2014. *Theor. Appl. Genet.* **2017**, *130*, 223–245. [CrossRef]

10. Blakeney, A.B.; Cracknell, R.L.; Crosbie, G.B.; Jefferies, S.P.; Miskelly, D.M.; O'Brien, L.; Panozzo, J.F.; Suter, D.A.I.; Solah, V.; Watts, T.; et al. *Understanding Australian Wheat Quality: A Basic Introduction to Australian Wheat Quality*; GRDC: Canberra, Australia, 2009.

11. Oury, F.X.; Bérard, P.; Brancourt-Hulmel, M.; Depatureaux, C.; Doussinault, G.; Galic, N.; Giraud, A.; Heumez, E.; Lecomte, C.; Pluchard, P.; et al. Yield and grain protein concentration in bread wheat: A review and a study of multi-annual data from a french breeding program. *J. Genet. Breed.* **2003**, *57*, 59–68.

12. Cooper, M.; Woodruff, D.R.; Philips, I.G.; Basford, K.E.; Gilmour, A.R. Genotype-by-management interactions for grain yield and grain protein concentration of wheat. *Field Crop. Res.* **2001**, *70*, 87–88. [CrossRef]

13. Zörb, C.; Ludewig, U.; Hawkesford, M.J. Perspective on wheat yield and quality with reduced nitrogen supply. *Trends Plant Sci.* **2018**, *23*, 1029–1037. [CrossRef]

14. Monaghan, J.; Snape, J.; Chojecki, A.; Kettlewell, P. The use of grain protein deviation for identifying wheat cultivars with high grain protein concentration and yield. *Int. J. Plant Breed.* **2001**, *122*, 309–317.

15. Bogard, M.; Allard, V.; Brancourt-Hulmel, M.; Heumez, E.; Machet, J.-M.; Jeuffroy, M.-H.; Gate, P.; Martre, P.; Le Gouis, J. Deviation from the grain protein concentration–grain yield negative relationship is highly correlated to post-anthesis n uptake in winter wheat. *J. Exp. Bot.* **2010**, *61*, 4303–4312. [CrossRef] [PubMed]

16. Michel, S.; Loschenberger, F.; Ametz, C.; Pachler, B.; Sparry, E.; Burstmayr, H. Simultaneous selection for grain yield and protein content in genomics-assisted wheat breeding. *Theor. Appl. Genet.* **2019**, *132*, 1745–1760. [CrossRef] [PubMed]

17. Bilgin, O.; Guzman, C.; Baser, I.; Crossa, J.; Korkut, K.Z. Evaluation of grain yield and quality traits of bread wheat genotypes cultivated in northwest turkey. *Crop Sci.* **2016**, *56*, 73–84. [CrossRef]

18. Thorwarth, P.; Piepho, H.P.; Zhao, Y.; Ebmeyer, E.; Schacht, J.; Schachschneider, R.; Kazman, E.; Reif, J.C.; Würschum, T.; Longin, C.F.H. Higher grain yield and higher grain protein deviation underline the potential of hybrid wheat for a sustainable agriculture. *Plant Breed.* **2018**, *137*, 326–337. [CrossRef]

19. Oury, F.X.; Godin, C. Yield and grain protein concentration in bread wheat: How to use the negative relationship between the two characters to identify favourable genotypes? *Euphytica* **2007**, *157*, 45–57. [CrossRef]

20. Mahjourimajd, S.; Taylor, J.; Rengel, Z.; Khabaz-Saberi, H.; Kuchel, H.; Okamoto, M.; Langridge, P. The genetic control of grain protein content under variable nitrogen supply in an australian wheat mapping population. *PLoS ONE* **2016**, *11*, e0159371. [CrossRef]

21. Brill, R.; Gardner, M.; Fettell, N.; Martin, P.; Haskins, B.; McMullen, G. Grain Protein Concentration of Several Commercial Wheat Varieties. In Proceedings of the 16th ASA Conference: Capturing Opportunities and Overcoming Obstacles in Australian Agronomy, Armidale, Australia, 14–18 October 2012.

22. Fettell, N.; Brill, R.; Gardner, M.; McMullen, G. *Yield and Protein Relationships in Wheat*; GRDC: Canberra, Australia, 2012.

23. Giles, T. How nvt works. In *National Variety Trials Supplement*; Leonard, E., Ed.; GRDC: Canberra, Australia, 2012; p. 3.

24. Giles, T.; Bedggood, A.; Kelly, A. Trials with maximum value. In *National Variety Trials Supplement*; Leonard, E., Ed.; GRDC: Canberra, Australia, 2012.

25. Hochman, Z. Pushing the yield frontier. In *National Variety Trials Supplement*; Leonard, E., Ed.; GRDC: Canberra, Australia, 2012; p. 13.

26. Braun, H.J.; Rajaram, S.; vanGinkel, M. Cimmyt's approach to breeding for wide adaptation. *Euphytica* **1996**, *92*, 175–183. [CrossRef]

27. Hodson, D.P.; White, J.W. Use of spatial analyses for global characterization of wheat-based production systems. *J. Agric. Sci.* **2007**, *145*, 115–125. [CrossRef]

28. Chenu, K.; Deihimfard, R.; Chapman, S.C. Large-scale characterization of drought pattern: A continent-wide modelling approach applied to the australian wheatbelt spatial and temporal trends. *New Phytol.* **2013**, *198*, 801–820. [CrossRef]

29. Reynolds, M.; Dreccer, F.; Trethowan, R. Drought-adaptive traits derived from wheat wild relatives and landraces. *J. Exp. Bot.* **2007**, *58*, 177–186. [CrossRef] [PubMed]

30. Dupont, F.M.; Hurkman, W.J.; Vensel, W.H.; Tanaka, C.; Kothari, K.M.; Chung, O.K.; Altenbach, S.B. Protein accumulation and composition in wheat grains: Effects of mineral nutrients and high temperature. *Eur. J. Agron.* **2006**, *25*, 96–107. [CrossRef]

31. Flagella, Z.; Giuliani, M.M.; Giuzio, L.; Volpi, C.; Masci, S. Influence of water deficit on durum wheat storage protein composition and technological quality. *Eur. J. Agron.* **2010**, *33*, 197–207. [CrossRef]

32. Rharrabti, Y.; Villegas, D.; Royo, C.; Martos-Nunez, V.; del Moral, L.F.G. Durum wheat quality in mediterranean environments ii. Influence of climatic variables and relationships between quality parameters. *Field Crop. Res.* **2003**, *80*, 133–140. [CrossRef]

33. Rahimi Eichi, V.; Okamato, M.; Haefele, S.M.; Jewell, N.; Brien, C.; Garnett, T.; Langridge, P. Understanding the interactions between biomass, grain production and grain protein content in high and low protein wheat genotypes under controlled environments. *Agronomy* **2019**, *9*, 706. [CrossRef]

34. Sadras, V.O.; McDonald, G. *Benchmarking Wheat Water Use Efficiency: Accounting for Climate and Nitrogen*; GRDC: Adelaide, Australia, 2012.

35. Stoddard, F.L.; Marshall, D.R. Variability in grain protein in australian hexaploid wheats. *Aust. J. Agric. Res.* **1990**, *41*, 277–288. [CrossRef]

36. Smith, A.B.; Thompson, R.; Butler, D.G.; Cullis, B.R. The design and analysis of variety trials using mixtures of composite and individual plot samples. *J. R. Stat. Soc. Ser. C (Appl. Stat.)* **2011**, *60*, 437–455. [CrossRef]

37. Chapman, S.C.; Hammer, G.L.; Meinke, H. A sunflower simulation model: I. *Model development. Agron. J.* **1993**, *85*, 725–735. [CrossRef]

38. Chenu, K.; Cooper, M.; Hammer, G.L.; Mathews, K.L.; Dreccer, M.F.; Chapman, S.C. Environment characterization as an aid to wheat improvement: Interpreting genotype–environment interactions by modelling water-deficit patterns in north-eastern australia. *J. Exp. Bot.* **2011**, *62*, 1743–1755. [CrossRef]

39. Ababaei, B.; Chenu, K. Heat shocks increasingly impede grain filling but have little effect on grain setting across the Australian wheatbelt. *Agric. For. Meteorol.* **2020**, *284*, 107889. [CrossRef]

40. R Foundation for Statistical Computing. *R: A Language and Environment for Statistical Computing*; R Development Core Team: Vienna, Austria, 2009.

41. Bureau of Meteorology. *Climate Statistics for Australian Locations, Monthly Climate Statistics, Summary Statistics*, 29th ed.; Australian Government: Launceston, Ti Tree Bend, Australia, 2019.

42. Acuna, T.B.; Dean, G.; Riffkin, P. Constraints to achieving high potential yield of wheat in a temperate, high-rainfall environment in south-eastern Australia. *Crop Pasture Sci.* **2011**, *62*, 125–136. [CrossRef]

43. Zhang, H.; Turner, N.C.; Poole, M.L.; Simpson, N. Crop production in the high rainfall zones of Southern Australia—Potential, constraints and opportunities. *Aust. J. Exp. Agric.* **2006**, *46*, 1035–1049. [CrossRef]

44. Chen, W.; Bell, R.W.; Brennan, R.F.; Bowden, J.W.; Dobermann, A.; Rengel, Z.; Porter, W. Key crop nutrient management issues in the western australia grains industry: A review. *Aust. J. Soil Res.* **2009**, *47*, 1–18. [CrossRef]

45. Hill, N.; Zhang, H.; Trezise, T.; Young, J.; Moyes, N.; Carslake, L.; Turner, N.C.; Anderson, W.; Poole, M. *Successful Cropping in the High Rainfall Zone of Western Australia: Crop Research and Extension in the Zone*; Department of Agriculture and Food: Perth, Western Australia, 2005.

46. Gooding, M.J.; Ellis, R.H.; Shewry, P.R.; Schofield, J.D. Effects of restricted water availability and increasedtemperature on the grain filling, dryingand quality of winter wheat. *J. Cereal Sci.* **2003**, *37*, 295–309. [CrossRef]

47. Barbottin, A.; Lecomte, C.; Bouchard, C.; Jeuffroy, M.H. Nitrogen remobilization during grain filling in wheat: Genotypic and environmental effects. *Crop Sci.* **2005**, *45*, 1141–1150. [CrossRef]

48. Triboi, E.; Martre, P.; Triboi-Blondel, A.M. Environmentally-induced changes in protein composition in developing grains of wheat are related to changes in total protein content. *J. Exp. Bot.* **2003**, *54*, 1731–1742. [CrossRef]

49. Crosbie, G.B.; Fisher, H. Variation in wheat protein content: The effect of environment. *J. Agric. West. Aust.* **1987**, *28*, 124–127.

50. Simmonds, D.H. *Wheat and Wheat Quality in Australia*; CSIRO Publishing: Clayton, Australia, 1989.

51. Torrion, J.A.; Walsh, O.S.; Liang, X.; Bicego, B.; Sapkota, A. Managing 'egan' wheat with a gene for high grain protein. *Agrosystems Geosci. Environ.* **2019**, *2*, 1–8. [CrossRef]

52. Zorb, C.; Becker, E.; Merkt, N.; Kafka, S.; Schmidt, S.; Schmidhalter, U. Shift of grain protein composition in bread wheat under summer drought events. *J. Plant Nutr. Soil Sci.* **2017**, *180*, 49–55. [CrossRef]

53. Stone, P.J.; Nicolas, M.E. A survey of the effects of high-temperature during grain filling on yield and quality of 75 wheat cultivars. *Aust. J. Agric. Res.* **1995**, *46*, 475–492. [CrossRef]

54. Daniel, C.; Triboi, E. Changes in wheat protein aggregation during grain development: Effects of temperatures and water stress. *Eur. J. Agron.* **2002**, *16*, 1–12. [CrossRef]

55. Anderson, W.K.; Sawkins, D. Production practices for improved grain yield and quality of soft wheats in western australia. *Aust. J. Exp. Agric.* **1997**, *37*, 173–180. [CrossRef]

56. Spragg, J. *Benefit to Australian Grain Growers in the Feed Grain Market*; Grains Research and Development Corporation: Victoria, Australia, 2008.

57. Turner, N.C. Agronomic options for improving rainfall-use efficiency of crops in dryland farming systems. *J. Exp. Bot.* **2004**, *55*, 2413–2425. [CrossRef] [PubMed]

58. Rozbicki, J.; Ceglinska, A.; Gozdowski, D.; Jakubczak, M.; Cacak-Pietrzak, G.; Madry, W.; Golba, J.; Piechocinski, M.; Sobczynski, G.; Studnicki, M.; et al. Influence of the cultivar, environment and management on the grain yield and bread-making quality in winter wheat. *J. Cereal Sci.* **2015**, *61*, 126–132. [CrossRef]

59. Fischer, R.A.; Howe, G.N.; Ibrahim, Z. Irrigated spring wheat and timing and amount of nitrogen-fertilizer. 1. Grain-yield and protein-content. *Field Crop. Res.* **1993**, *33*, 37–56.

60. Smith, A.B.; Cullis, B.R. Plant breeding selection tools built on factor analytic mixed models for multi-environment trial data. *Euphytica* **2018**, *214*, 143. [CrossRef]

61. Anderson, W.K.; Hamza, M.A.; Sharma, D.L.; D'Antuono, M.F.; Hoyle, F.C.; Hill, N.; Shackley, B.J.; Amjad, M.; Zaicou-Kunesch, C. The role of management in yield improvement of the wheat crop—A review with special emphasis on western australia. *Aust. J. Agric. Res.* **2005**, *56*, 1137–1149. [CrossRef]

62. Anderson, W.K.; Impiglia, A. Management of dryland wheat. In *Bread Wheat Improvement and Production*; Curtis, B.C., Rajaram, S., Gomez Macpherson, H., Eds.; FAO: Rome, Italy, 2002; pp. 407–432.

Chapter 5: Supplementary material

The following are available online at http://www.mdpi.com/2073-4395/10/5/753/s1

Table S1. Simulated biomass and yield, cumulative precipitation (Cum-Rain), simulated water-stress index (Mean-SWSI) and duration of each phase for four environment types (ETs). Cumulative precipitation, simulated water-stress index and the number of days for each phase are shown from sowing (0) to anthesis (6) and maturity (9). Simulated water-stress index is shown for Janz over the same periods (Ababaei and Chenu 2020) and for Hartog at anthesis (Chenu et al. 2013). Historical records of 60 sites from 1889 to 2011 (Hartog) and from 1981 to 2018 (Janz) were used to simulate the drought impact. Standard errors for mean-SWSI and duration of ETs were ~ zero. SE: standard errors.

Environment type	ET1	ET2	ET3	ET4
Simulated biomass (t/ha)	5.80	6.40	5.53	4.06
Simulated yield (t/ha)	2.07	2.38	1.64	0.97
Cum-Rain-0-6 (mm)	192.1	171.8	149.0	107.6
Cum-Rain-0-9 (mm)	265.1	212.9	196.5	130.2
Cum-Rain-6-9 (mm)	73.1	41.1	47.5	22.6
Mean-SWSI-0-6 for Janz variety	0.95	0.95	0.88	0.81
Mean-SWSI-0-9 for Janz variety	0.95	0.90	0.85	0.71
Mean-SWSI-6-9 for Janz variety	0.97	0.75	0.78	0.41
Mean-SWSI at anthesis for Hartog variety	0.95	0.77	0.56	0.38
Duration-0-6 (days)	116	124	123	121
Duration-0-9 (days)	165	170	166	163
Duration-6-9 (days)	49	47	43	42
SE of simulated biomass (t/ha)	0.03	0.04	0.03	0.03
SE of simulated yield (t/ha)	0.01	0.02	0.01	0.01
SE of Cum-Rain-0-6 (mm)	0.9	1.4	1	0.9
SE of Cum-Rain-0-9 (mm)	1	1.5	1.1	1.2
SE of Cum-Rain-6-9 (mm)	0.4	0.5	0.5	0.5

Figure S1. The site location map of all wheat NVT trials in a single year (2015). Green rectangles indicate single wheat trials, and blue and purple circles show the clusters of <15 and _15 multi trials, respectively.

Supplementary explanations for "Materials and methods"

Chenu et al. (2013) ran the simulations for the 60 sites (Supplementary Figure S2) using the Agricultural Production Systems Simulator (APSIM) crop model (Wang et al. 2002; Keating et al. 2003) based on the local practices of farmers, soil characteristics and preceding rainfall.
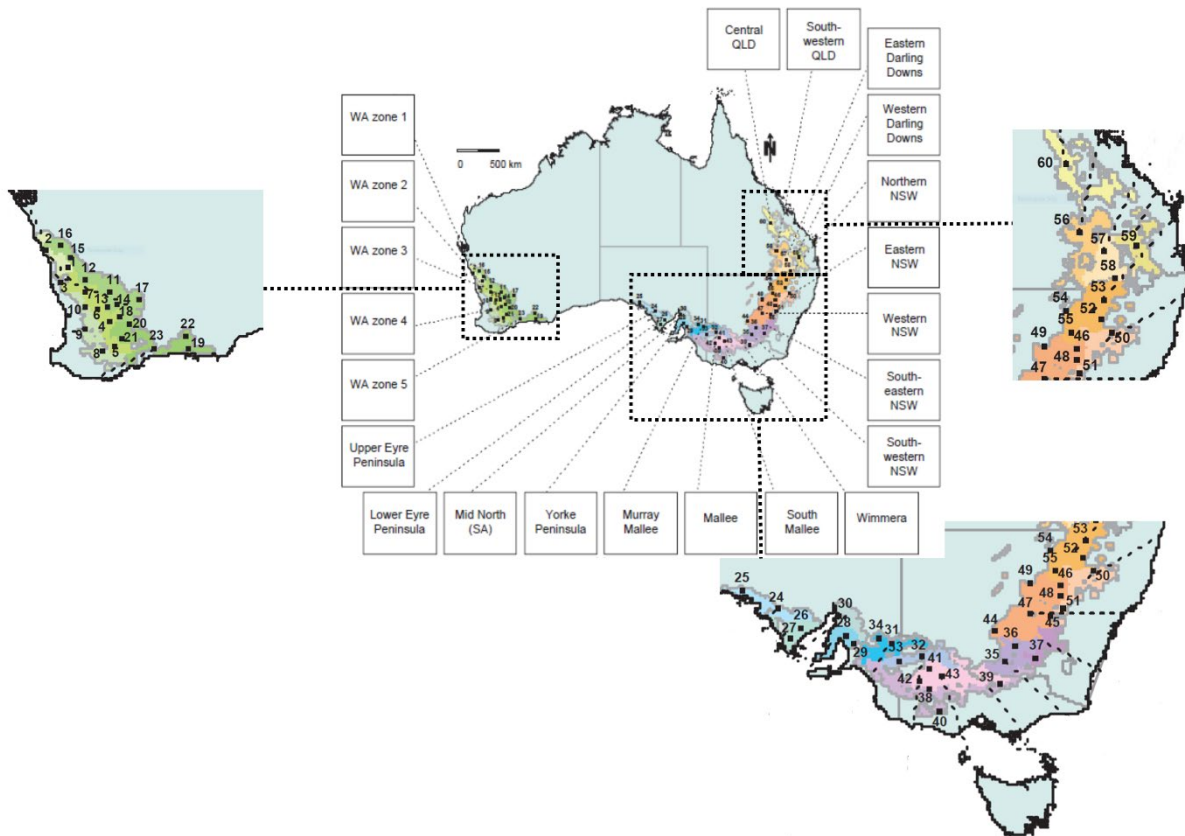
Figure S2. The 22 regions (coloured and named in each box) and 60 sites used in Chenu et al. (2013) study across the Australian wheatbelt: the 'West' area (green colours); 'South' (blue); 'South-east' (purple); 'East' (orange). State abbreviations: QLD, Queensland; NSW, New South Wales; SA, South Australia; WA, Western Australia. Figure obtained from New Phytologist (2013) 198: 801–820

After performing a cluster analysis at national level, Chenu et al. (2013) identified four main

Environment types (ETs) as representative of drought patterns that wheat crops experience

in the wheat-belt of Australia (Supplementary Figure S3).
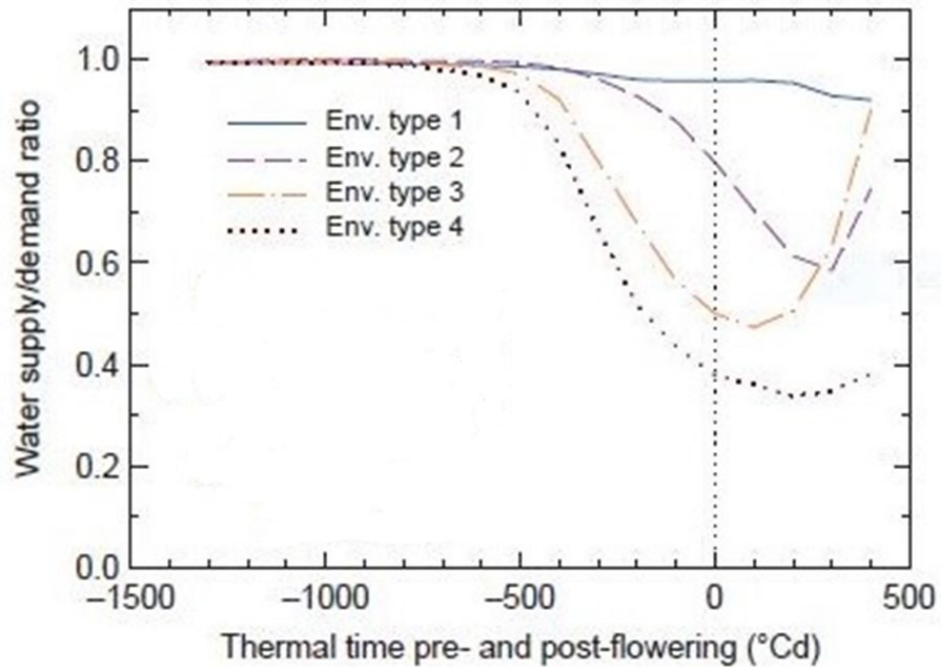
Figure S3. Simulated water-stress index for four environment types (ETs) identified in all regions combined across the Australian wheat-belt in Chenu et al. (2013) study. The stress index corresponds to the ratio of soil water supply to crop water demand and is shown as a function of cumulative thermal time relative to flowering, from the emergence of crop to 450 degree days (°Cd), which is after flowering. Figure obtained from New Phytologist (2013) 198: 801–820

In our study, sites were categorized with their 1st dominant ETs based on the map of the frequencies of each ET shown in Supplementary Figure S4.
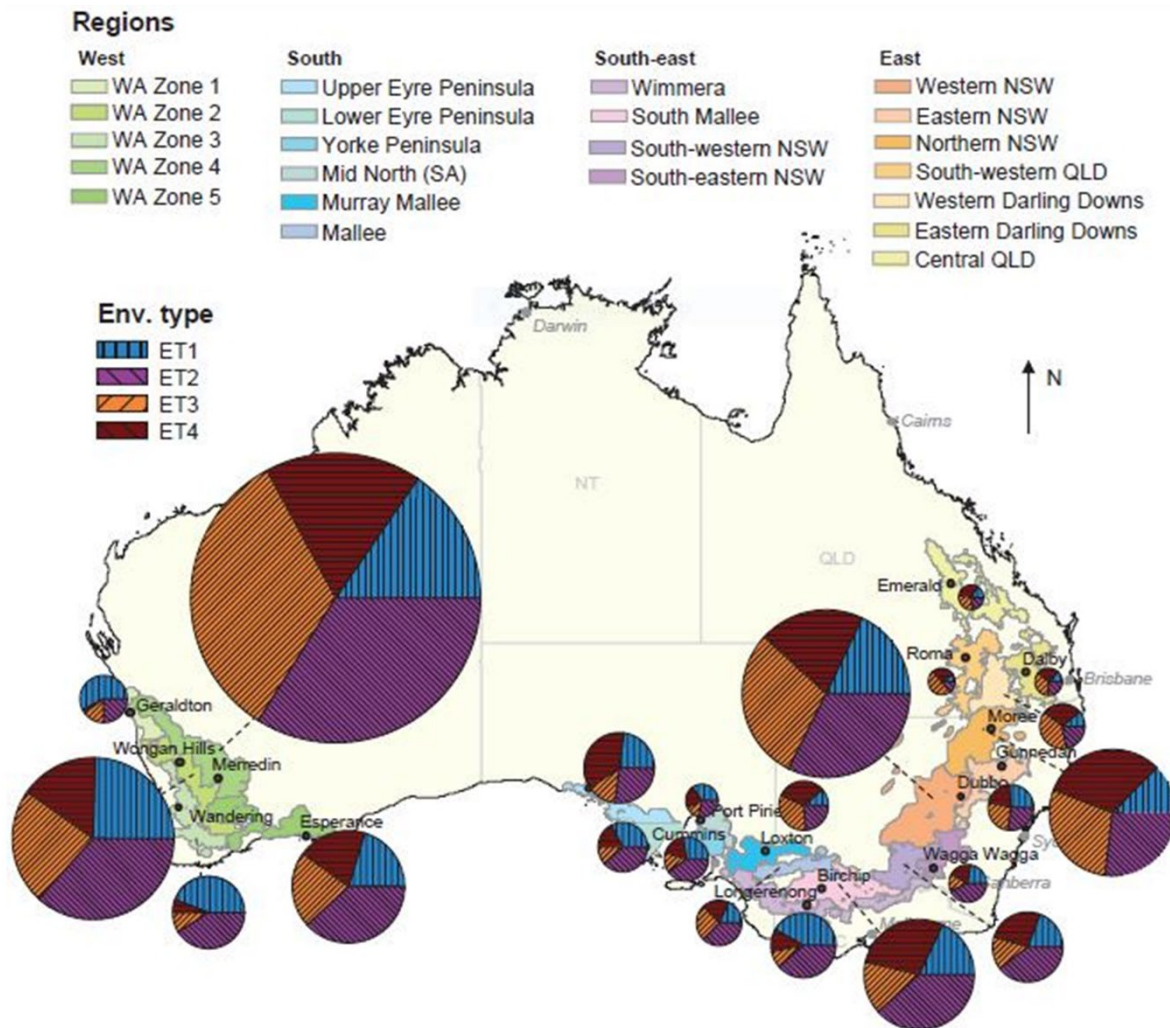
Figure S4. The pie chart map of the frequencies of each environment type (ET) across the Australian wheat-belt. Chenu et al. (2013) simulated the data for the check variety 'Hartog' over 123 years of historical data for the 22 regions of the wheat-belt (shown in Figure S2). The size of the pie charts is proportional to the wheat-planted area in the associated region. The ETs are shown in Supplementary Figure S3. State abbreviations: QLD, Queensland; NSW, New South Wales; SA, South Australia; WA, Western Australia. Figure obtained from New Phytologist (2013) 198: 801–820

Some regions had more than one dominant ET. Therefore, ET1/2, ET2/3 and ET 3/4 were added to the list of ETs based on the map in Supplementary Figure S4.

One of the aims of this study was to examine the stability of GPC in low and high yielding environments. Most of the Australian wheat is produced in mainland regions frequently

subjected to severe stress (Chenu et al. 2013). Accordingly, Tasmania, which produces higher grain yield compared with mainland Australia, was selected as a high yielding region in our study. However, Tasmania was not between the 22 regions of Chenu et al. (2013) study. Characterization of drought patterns in Tasmania was beyond the scope of this study. However, the average grain yield of 9.2 t/ha and the 600 mm average annual participation ('Bureau of Meteorology, Climate statistics for Australian locations, Monthly climate statistics, Summary statistics ' 2019) implied the different weather conditions of the Tasmanian site from mainland Australia. Therefore, Tasmania was categorized with a different name (ET0) in this study.

References (Supplementary material of Chapter 5)

'Bureau of Meteorology, Climate statistics for Australian locations, Monthly climate statistics, Summary statistics ' 2019, 29 August edn, Australian Government, Launceston, Ti Tree Bend, <http://www.bom.gov.au/climate/averages/tables/cw_091237.shtml>.

Chenu, K, Deihimfard, R & Chapman, SC 2013, 'Large-scale characterization of drought pattern: a continent-wide modelling approach applied to the Australian wheatbelt spatial and temporal trends', *New Phytologist*, vol. 198, no. 3, May, pp. 801-820.

Keating, BA, Carberry, PS, Hammer, GL, Probert, ME, Robertson, MJ, Holzworth, D, Huth, NI, Hargreaves, JNG, Meinke, H, Hochman, Z, McLean, G, Verburg, K, Snow, V, Dimes, JP, Silburn, M, Wang, E, Brown, S, Bristow, KL, Asseng, S, Chapman, S, McCown, RL, Freebairn, DM & Smith, CJ 2003, 'An overview of APSIM, a model designed for farming systems simulation', *European Journal of Agronomy*, vol. 18, no. 3-4, Jan, pp. 267-288.

Wang, E, Robertson, MJ, Hammer, GL, Carberry, PS, Holzworth, D, Meinke, H, Chapman, SC, Hargreaves, JNG, Huth, NI & McLean, G 2002, 'Development of a generic crop model template in the cropping system model APSIM', *European Journal of Agronomy*, vol. 18, no. 1-2, Dec, pp. 121-140.

Chapter 6: General Discussion

Increasing grain yield and quality are two major goals of wheat breeding programs. Grain protein content (GPC) is a key quality attribute and an important marketing trait (Husenov et al. 2015; Gabriel et al. 2017; Michel et al. 2019). However, the simultaneous selection for both grain yield and GPC poses a major challenge for wheat breeders due the trade-off between grain yield and GPC (Simmonds, N. W. 1995). Accordingly, wheat breeders who seek high protein aim to break this undesirable correlation by increasing grain yield while maintaining the GPC (Simmonds, N. W. 1995; DePauw et al. 2007).

Another challenge for improving grain yield and protein content in wheat is the low heritability of these traits. The large genotype-by-environment interaction and a complex quantitative inheritance governed by many genes of small-to-medium effect, complicate the genetic improvement of grain yield and GPC in wheat (Tanksley and McCouch 1997; Hoffstetter et al. 2016; Mahjourimajd, S., Taylor, et al. 2016; Schulthess et al. 2017). In other words, despite the strong influence of genetics on the negative correlation between grain yield and GPC (Laidig et al. 2017; Thorwarth et al. 2018), environmental effects can change the magnitude of this relationship (Oury and Godin 2007). Since the genetic variation in grain yield and GPC between different genotypes are masked by the interactions with environment, testing genotypes in different environments helps to identify heritable variation in grain yield and GPC (Oury et al. 2003; Semenov and Halford 2009).

The purpose of this project was to explore the relationship between grain yield and GPC under different production conditions, with a view to providing advice to breeders on how they might select for high yield and high GPC. This study involved identifying the appropriate target environments for selecting high yield and high GPC genotypes.

In the current world cropping systems, GPC is strongly influenced by nitrogen (N) fertilizer application (Triboi et al. 2000; Sinclair and Rufty 2012). Comparing the N responses between high and low GPC wheats may reveal the mechanisms used by contrasting genotypes in their N use at high and low N input (Bogard et al. 2011; Hitz et al. 2017). Therefore, germplasm used in this study had been selected over a long period for either high or low GPC based on their end-use. Grain yield and GPC can be assessed precisely only at harvest and, consequently, may not demonstrate how high and low GPC genotypes use their N reserves during the growing season. Therefore, biomass growth traits were examined in this study since these could reflect the N response of plants throughout the season.

Due to the high influence of environment on the grain yield-GPC relationship, the first approach was to fix the environment and try to determine the biomass growth responses to different N treatments. This experiment was conducted in controlled environment phenotyping platforms which allowed dissection of complex growth traits into simple components such as growth rate and the time to maximum growth rate under reduced environmental variation (Chapter 3). Results showed that under low N condition, biomass production was limited more in high than in low GPC genotypes. Moreover, high GPC genotypes grew faster and achieved the maximum growth rate earlier at low compared to high N-treated plants. Consequently, in low N treatments the grain yield was reduced more in high than in low GPC genotypes.

Field trials were used to validate the controlled environment findings under conditions that emulate breeders' trials in terms of plot size, trial location and agronomic practices (Chapter 4). However, N effects were not clearly detected in the first field trial in 2017. This could have been due to the high pre-sowing residual N in the soil, late N treatment application when the plant's response to N was low, and/or N leakage between different plots. Accordingly, two field trials, with revised N treatments, were conducted in 2018

(Chapter 4). The main strategies to increase N treatment effects in the 2018 trials were locating the trials based on their pre-sowing residual N level in the soil, applying N treatments at early growth stages, and increasing the distance between treatment plots.

Measuring total biomass in wheat breeding plots is not simple for either destructive or non-destructive methods. Non-destructive methods rely on the measurement of biomass related traits such as height and ground cover to examine the N response of wheat plants in the field experiment. The main outcome of this study, which confirmed the controlled environment results, was that under low N treatments the rate of increase in biomass related traits were more restricted in high than in low GPC genotypes. Based on the non-destructive measurements of biomass related traits, this experiment also confirmed the value of using biomass growth for NUE studies in field.

After assessing wheat responses to N under controlled and field conditions, the last stage was to use a large number of different environments and try to determine the environmental relationship between grain yield and GPC. This study was based on National Variety Trial (NVT) data and included an assessment of the potentials and limitations of the NVT dataset for multi-environmental analysis across the Australian wheat-belt (Chapter 5). Results showed that the negative relationship between grain yield and GPC was most extreme under stressed (low yielding) conditions. The low N treatment in the controlled environment experiment and the high water stressed regions in the multi-environment analysis, demonstrated the strongest grain yield-GPC relationship. The significance of stress was emphasised by the observation that the slope of this relationship decreased in more favourable or high-yielding environments.

The controlled and field experiments indicated that the way in which high GPC lines manage biomass was critical and, biomass and yield were reduced at low N to conserve N for grain. Therefore, under stress conditions varieties bred in low yielding regions are

able to restrict their growth in favour of GPC to produce fewer grains with sufficient nutrient levels. In addition to the environmental conditions, intensive selection by breeders can also influence the grain yield-GPC relationship. In other words, wheat breeders have selected for lines that are able to balance biomass production to allow for high GPC.

The results reported here highlight the importance of considering environmental factors in breeding programs. In order to break the grain yield-GPC relationship, wheat breeders should select under stressed (low yielding) rather than high yielding conditions for high yield and high GPC genotypes. However, breeders should also be aware that by applying such methods they, inadvertently, select for germplasm that limit biomass and, consequently yield production to help conserve N for grain. Furthermore, breeders are often inclined to select under high N input in order to minimise the impact of N as a variable, and this may mask N-use efficiency (NUE) differences between genotypes (Kamprath et al. 1982). Selection in low yielding environments of Australia with low rainfall can improve the NUE due to the strong link between N uptake and water availability (Stoddard and Marshall 1990; Sadras and McDonald 2012).

Conversely, lines selected in high yielding conditions tend to expend N for biomass and yield production regardless of the grain N reserves. The negative relationship between grain yield and GPC has an advantage for those end-products that favour low GPC (DePauw et al. 2007). Therefore, low GPC genotypes can be best selected in high yielding environments that result in low GPC but increasing grain yield. The large variation of GPC across the yield spectrum in this study reflected the high influence of wheat production environments on GPC. Accordingly, GPC loss with yield increase for farmers can be compensated in some environments through agronomic management such as N fertilizer.

In summary, the research conducted and presented in this dissertation is the first examination of the relationship between grain yield and protein in high and low GPC wheat genotypes under controlled, field and multi-environmetal conditions. Due to the strong influence of the environment on the yield-GPC relationship, multi-environment trials are recommended for future studies. However, conducting multiple trials in diverse range of environments can be cost and labour intensive. NVT data can provide a valuable resource for further research to explore the grain yield-GPC relationship in Australian environments. Improvements in statistical approaches together with applying one standard agronomic practice in all NVT sites in future could improve the multi-environmental analysis of these datasets. Moreover, developing non-destructive phenotyping techniques that allow for frequent biomass measurements, regardless of weather condition, can be useful to detect biomass responses to N in field.

.

References (Chapters 1, 2 and 6)

Ababaei, B & Chenu, K 2020, 'Heat shocks increasingly impede grain filling but have little effect on grain setting across the Australian wheatbelt', *Agricultural and Forest Meteorology*, vol. 284.

Acreche, MM & Slafer, GA 2012, 'Variation of grain nitrogen content in relation with grain yield in old and modern Spanish wheats grown under a wide range of agronomic conditions in a Mediterranean region'.

AEGIC 2018, 'Australian grain note wheat', *Australian wheat*, Australian Export Grains Innovation Centre, pp. Australian wheat classes and their end-uses

An, D, Su, J, Liu, Q, Zhu, Y, Tong, Y, Li, J, Jing, R, Li, B & Li, Z 2006, 'Mapping QTLs for nitrogen uptake in relation to the early growth of wheat (*Triticum aestivum* L.)', *An International Journal on Plant-Soil Relationships*, vol. 284, no. 1, pp. 73-84.

Anderson, WK & Sawkins, D 1997, 'Production practices for improved grain yield and quality of soft wheats in Western Australia', *Australian Journal of Experimental Agriculture*, vol. 37, no. 2, pp. 173-180.

Aparicio, N, Villegas, D, Casadesus, J, Araus, JL & Royo, C 2000, 'Spectral vegetation indices as nondestructive tools for determining durum wheat yield', *Agronomy Journal*, vol. 92, no. 1, Jan-Feb, pp. 83-91.

Araus, JL & Cairns, JE 2014, 'Field high-throughput phenotyping: the new crop breeding frontier', *Trends in Plant Science*, vol. 19, no. 1, pp. 52-61.

Araus, JL, Serret, MD & Edmeades, GO 2012, 'Phenotyping maize for adaptation to drought', *Frontiers in Physiology*, vol. 3, 2012.

Araus, JL, Slafer, GA, Reynolds, MP & Royo, C 2002, 'Plant breeding and drought in C_3 cereals: what should we breed for?', *Annals of Botany*, vol. 89 no. 7, pp. 925-940.

Arnott, R & Richardson, E 2007 'Feeding frosted cereal grain to ruminants', *Primefact*, vol. 373, September.

Asfaw, S & Lipper, L 2012, 'Economics of plant genetic resource management for adaptation to climate change', *Agricultural Development Economics Working paper*, vol. 12, Food and Agriculture Organization of the United Nations, Rome, Italy.

Baasandorj, T, Ohm, JB & Simsek, S 2016, 'Effects of kernel vitreousness and protein level on protein molecular weight distribution, milling quality, and breadmaking quality in hard red spring wheat', *Cereal Chemistry*, vol. 93, no. 4, pp. 426-434.

Beres, BL, Graf, RJ, Irvine, RB, O'Donovan, JT, Harker, KN, Johnson, EN, Brandt, S, Hao, X, Thomas, BW, Turkington, TK & Stevenson, FC 2018, 'Enhanced nitrogen management strategies for winter wheat production in the Canadian prairies (vol 98, pg 683, 2018)', *Canadian Journal of Plant Science*, vol. 98, no. 5, Oct, pp. 989-989.

Berger, B, de Regt, B & Tester, M 2012, 'High-throughput phenotyping of plant shoots', *Methods in Molecular Biology*, vol. 918, pp. 9-20.

Berni, JAJ, Zarco-Tejada, PJ, Suarez, L & Fereres, E 2009, 'Thermal and Narrowband Multispectral Remote Sensing for Vegetation Monitoring From an Unmanned Aerial Vehicle', *Ieee Transactions on Geoscience and Remote Sensing*, vol. 47, no. 3, Mar, pp. 722-738.

Bettge, AD & Morris, CF 2000, 'Relationships among grain hardness, pentosan fractions, and end-use quality of wheat', *Cereal Chemistry*, vol. 77, no. 2, Mar-Apr, pp. 241-247.

Birch, CJ & Long, KE 1990, 'Effect of nitrogen on the growth, yield and grain protein-content of barley (*hordeum vulgare*)', *Australian Journal of Experimental Agriculture*, vol. 30, no. 2, pp. 237-242.

Blakeney, AB, Cracknell, RL, Crosbie, GB, Jefferies, SP, Miskelly, DM, O'Brien, L, Panozzo, JF, Suter, DAI, Solah, V, Watts, T, Westcott, T & Williams, RM 2009, *Understanding Australian Wheat Quality: A basic introduction to Australian wheat quality* GRDC, Australia.

Bogard, M, Jourdan, M, Allard, V, Martre, P, Perretant, MR, Ravel, C, Heumez, E, Orford, S, Snape, J, Griffiths, S, Gaju, O, Foulkes, J & Le Gouis, J 2011, 'Anthesis date mainly explained correlations between post-anthesis leaf senescence, grain yield, and grain protein concentration in a winter wheat population segregating for flowering time QTLs', *Journal of Experimental Botany*, vol. 62, no. 10, pp. 3621-3636.

Bouwer, H 1989, 'Agricultural contaminants: Problems and solutions', *Journal of Water and Environment Technology*, pp. 292-297.

'Bureau of Meteorology, Climate statistics for Australian locations, Monthly climate statistics, Summary statistics ' 2019, 29 August edn, Australian Government, Launceston, Ti Tree Bend, <http://www.bom.gov.au/climate/averages/tables/cw_091237.shtml>.

Bustos, DV, Hasan, AK, Reynolds, MP & Calderini, DF 2013, 'Combining high grain number and weight through a DH-population to improve grain yield potential of wheat in high-yielding environments', *Field Crops Research*, vol. 145, pp. 106–115.

Butterbach-Bahl, K & Dannenmann, M 2011, 'Denitrification and associated soil N_2O emissions due to agricultural activities in a changing climate', *Current Opinion in Environmental Sustainability*, vol. 3, pp. 389-395.

Cairns, JE, Impa, SM, O'Toole, JC, Jagadish, SVK & Price, AH 2011, 'Influence of the soil physical environment on rice (Oryza sativa L.) response to drought stress and its implications for drought research', *Field Crops Research*, vol. 121, no. 3, Apr 3, pp. 303-310.

Casadesús, J, Kaya, Y, Bort, J, Nachit, MM, Araus, JL, Amor, S, Ferrazzano, G, Maalouf, F, Maccaferri, M, Martos, V, Ouabbou, H & Villegas, D 2007, 'Using vegetation indices derived from conventional digital cameras as selection criteria for wheat breeding in water-limited environments', *Annals of Applied Biology*, vol. 150, no. 2, pp. 227-236.

Casadesus, J & Villegas, D 2014, 'Conventional digital cameras as a tool for assessing leaf area index and biomass for cereal breeding', *Journal of Integrative Plant Biology*, vol. 56, no. 1, Jan, pp. 7-14.

Chen, DJ, Shi, RL, Pape, JM, Neumann, K, Arend, D, Graner, A, Chen, M & Klukas, C 2018, 'Predicting plant biomass accumulation from image-derived parameters', *Gigascience*, vol. 7, no. 2, Jan.

Chenu, K, Deihimfard, R & Chapman, SC 2013, 'Large-scale characterization of drought pattern: a continent-wide modelling approach applied to the Australian wheatbelt spatial and temporal trends', *New Phytologist*, vol. 198, no. 3, May, pp. 801-820.

Clark, W & Kelly, E 2004, 'Energy efficiency in fertilizer production and use', in W Clark & B Kornelis (eds), *Efficient use and conservation of energy*, Eolss, Oxford, UK.

Cobb, JN, DeClerck, G, Greenberg, A, Clark, R & McCouch, S 2013, 'Next-generation phenotyping: requirements and strategies for enhancing our understanding of genotype-phenotype relationships and its relevance to crop improvement', *Theoretical and Applied Genetics*, vol. 126, no. 4, Apr, pp. 867-887.

Cormier, F, Foulkes, J, Hirel, B, Gouache, D, Moenne-Loccoz, Y & Le Gouis, J 2016, 'Breeding for increased nitrogen-use efficiency: a review for wheat (*T.aestivum* L.)', *Plant Breeding*, vol. 135, no. 3, Jun, pp. 255-278.

De Castro, AI, Torres-Sánchez, J, Peña, JM, Jiménez-Brenes, FM, Csillik, O & López-Granados, F 2018, 'An automatic Random Forest-OBIA algorithm for early weed mapping between and within crop rows using UAV imagery', *Remote Sensing*, vol. 10, p. 285.

De Datta, S, Tauro, A & Balaoing, S 1968, 'Effect of plant type and nitrogen level on the growth characteristics and grain yield of Indica rice in the tropics', *Agronomy Journal*, vol. 60, p. 643.

Deery, D, Jimenez-Berni, J, Jones, H, Sirault, X & Furbank, R 2014, 'Proximal remote sensing buggies and potential applications for field-based phenotyping', *Agronomy*, vol. 4, pp. 349-379.

Delegido, J, Verrelst, J, Meza, CM, Rivera, JP, Alonso, L & Moreno, J 2013, 'A red-edge spectral index for remote sensing estimation of green LAI over agroecosystems', *European Journal of Agronomy*, vol. 46, Apr, pp. 42-52.

DePauw, RM, Knox, RE, Clarke, FR, Wang, H, Fernandez, MR, Clarke, JM & McCaig, TN 2007, 'Shifting undesirable correlations', *Euphytica*, vol. 157, no. 3, Oct, pp. 409-415.

Earl, CD & Ausubel, FM 1983, 'The genetic engineering of nitrogen fixation', *Nutrition Reviews*, vol. 41, pp. 1-6.

Ehdaie, B, Merhaut, DJ, Ahmadian, S, Hoops, AC, Khuong, T, Layne, AP & Waines, JG 2010, 'Root system size influences water-nutrient uptake and nitrate leaching potential in wheat', *Journal of Agronomy and Crop Science*, vol. 196, pp. 455-466.

Fahlgren, N, Gehan, MA & Baxter, I 2015, 'Lights, camera, action: high-throughput plant phenotyping is ready for a close-up', *Current Opinion in Plant Biology*, vol. 24, Apr, pp. 93-99.

Farmer, BH 2008, 'Perspectives on the 'Green Revolution' in South Asia', *Modern Asian Studies*, vol. 20, pp. 175-199.

Fischer, RA 2009, *Farming Systems of Australia-Chapter 2:Exploiting the Synergy between Genetic Improvement and Agronomy*, Elsevier Inc.

Furbank, RT 2009, 'Plant phenomics: from gene to form and function', *Functional Plant Biology*, vol. 36, no. 10-11, 2009, pp. V-VI.

Furbank, RT & Tester, M 2011, 'Phenomics - technologies to relieve the phenotyping bottleneck', *Trends in Plant Science*, vol. 16, no. 12, Dec, pp. 635-644.

Gabriel, D, Pfitzner, C, Haase, NU, Husken, A, Prufer, H, Greef, JM & Ruhl, G 2017, 'New strategies for a reliable assessment of baking quality of wheat - Rethinking the current indicator protein content', *Journal of Cereal Science*, vol. 77, Sep, pp. 126-134.

Gaines, CS, Finney, PF, Fleege, LM & Andrews, LC 1996, 'Predicting a hardness measurement using the single-kernel characterization system', *Cereal Chemistry*, vol. 73, pp. 278-283.

Garcia, GA, Hasan, AK, Puhl, LE, Reynolds, MP, Calderini, DF & Miralles, DJ 2013, 'Grain yield potential strategies in an elite wheat double-haploid population grown in contrasting environments.', *Crop Science*, vol. 53, no. 6, p. 2577.

Gastal, F & Lemaire, G 2002, 'N uptake and distribution in crops: an agronomical and ecophysiological perspective', *Journal of Experimental Botany*, vol. 53, no. 370, pp. 789-799.

Ghanem, ME, Marrou, H & Sinclair, TR 2015, 'Physiological phenotyping of plants for crop improvement', *Trends in Plant Science*, vol. 20, no. 3, March pp. 139–144.

Gonzalez, F, Mcfadyen, A & Puig, E 2018, 'Advances in unmanned aerial systems and payload technologies for precision agriculture ', in G Chen (ed.), *Advances in agricultural machinery and technologies*, Boca Raton, Florida, US.

Greenwood, DJ, Neeteson, JJ & Draycott, A 1986, 'Quantitative relationships for the dependence of growth rate of arable crops on their nitrogen content, dry weight and aerial environment', *Plant and Soil*, vol. 91, pp. 281-301.

Hansen, A & Poll, L 1997, *Raavarekvalitet: Frugt, Groensager, Kartofler og Korn*, DSR Forlag, Copenhagen.

Hansen, NJS, Plett, D, Berger, B & Garnett, T 2018, 'Tackling nitrogen use efficiency in cereal crops using high-throughput phenotyping', in A Shrawat, A Zayed & DA Lightfoot (eds), *Engineering nitrogen utilization in crop plants*, Springer International Publishing, Cham, pp. 121-139.

Harrison, R & Webb, J 2001, 'A review of the effect of N fertilizer type on gaseous emissions', *Advances in Agronomy*, vol. 73, pp. 65-108.

Hatfield, J, Gitelson, AA, Schepers, J & Walthall, C 2008, 'Application of spectral remote sensing for agronomic decisions', *Agron. J.*, vol. 100, pp. S117-S131.

Hawkesford, MJ 2014, 'Reducing the reliance on nitrogen fertilizer for wheat production', *Journal of Cereal Science*, vol. 59, no. 3, May, pp. 276-283.

Hawkesford, MJ, Araus, JL, Park, RF, Calderini, DF, Miralles, DJ, Shen, T, Zhang, J & Parry, MAJ 2013, 'Prospects of doubling global wheat yields', *Food and Energy Security*, vol. 2, pp. 34-48.

Hill, MJ, Donald, GE, Hyder, MW & Smith, RCG 2004, 'Estimation of pasture growth rate in the south west of Western Australia from AVHRR NDVI and climate data', *Remote Sensing of Environment*, vol. 93, pp. 28-45.

Hitz, K, Clark, AJ & Van Sanford, DA 2017, 'Identifying nitrogen-use efficient soft red winter wheat lines in high and low nitrogen environments', *Field Crops Research*, vol. 200, pp. 1-9.

Hoffstetter, A, Cabrera, A & Sneller, C 2016, 'Identifying quantitative trait loci for economic traits in an elite soft red winter wheat population', *Crop Science*, vol. 56, p. 547.

Holman, FH, Riche, AB, Michalski, A, Castle, M, Wooster, MJ & Hawkesford, MJ 2016, 'High Throughput Field Phenotyping of Wheat Plant Height and Growth Rate in Field Plot Trials Using UAV Based Remote Sensing', *Remote Sensing*, vol. 8, no. 12, Dec.

Hong, BH, Rubenthaler, GL & Allan, RE 1989, 'Wheat pentosans .1. Cultivar variation and relationship to kernel hardness', *Cereal Chemistry*, vol. 66, no. 5, Sep-Oct, pp. 369-373.

Houle, D, Govindaraju, DR & Omholt, S 2010, 'Phenomics: the next challenge', *Nature Reviews Genetics*, vol. 11, no. 12, Dec, pp. 855-866.

Huebner, FR, Bietz, JA, Nelsen, T, Bains, GS & Finney, PL 1999, 'Soft Wheat Quality as Related to Protein Composition', *Cereal Chemistry*, vol. 76, no. 5, pp. 650-655.

Husenov, B, Makhkamov, M, Garkava-Gustavsson, L, Muminjanov, H & Johansson, E 2015, 'Breeding for wheat quality to assure food security of a staple crop: the case study of Tajikistan.', *Agriculture and Food Security*, vol. 4, p. 9.

Jacobi, J & Kuhbauch, W 2005, *Site-specific identification of fungal infection and nitrogen deficiency in wheat crop using remote sensing*, Precision Agriculture 05, ed. JV Stafford.

Jannink, J-L, Lorenz, AJ & Iwata, H 2010, 'Genomic selection in plant breeding: from theory to practice', *Briefings in Functional Genomics*, vol. 9, no. 2, Mar, pp. 166-177.

Jensen, JR 2007, 'Vegetation indices', in KC Klark (ed.), *Remote Sensing of the Environment: An Earth Resource Perspective*, Pearson Prentice Hall, Upper Saddle River, NJ pp. 382-392.

Jones, C & Olson-Rutz, K 2012, 'Practices to Increase Wheat Grain Protein', in MSU Extension (ed.)Montana.

Kamprath, E, Moll, R & Rodriguez, N 1982, 'Effects of Nitrogen Fertilization and Recurrent Selection on Performance of Hybrid Populations of Corn', *Agronomy Journal*, vol. 74, no. 6, p. 955.

Keating, BA, Carberry, PS, Hammer, GL, Probert, ME, Robertson, MJ, Holzworth, D, Huth, NI, Hargreaves, JNG, Meinke, H, Hochman, Z, McLean, G, Verburg, K, Snow, V, Dimes, JP, Silburn, M, Wang, E, Brown, S, Bristow, KL, Asseng, S, Chapman, S, McCown, RL, Freebairn, DM & Smith, CJ 2003, 'An overview of APSIM, a model designed for farming systems simulation', *European Journal of Agronomy*, vol. 18, no. 3-4, Jan, pp. 267-288.

Kent, NL & Evers, AD 1994, *Technology of Cereals*, 4th edn, Pergamon Press, Oxford.

Khan, Z, Chopin, J, Cai, J, Rahimi Eichi, V, Haefele, S & Miklavcic, SJ 2018, 'Quantitative estimation of wheat phenotyping traits using ground and aerial imagery', *Remote Sensing*, vol. 10.

Khan, Z, Rahimi-Eichi, V, Haefele, S, Garnett, T & Miklavcic , SJ 2018, 'Estimation of vegetation indices for high-throughput phenotyping of wheat using aerial imaging', *Plant methods*, vol. 20 p. 14.

Kibite, S & Evans, L 1984, 'Causes of negative correlations between grain yield and grain protein concentration in common wheat', *International Journal of Plant Breeding*, vol. 33, no. 3, pp. 801-810.

Koelewijn, HP 2004, 'Rapid change in relative growth rate between the vegetative and reproductive stage of the life cycle in Plantago coronopus', *New Phytologist*, vol. 163, no. 1, pp. 67-76.

Kozłowski, J 1992, 'Optimal allocation of resources to growth and reproduction: Implications for age and size at maturity', *Trends in Ecology & Evolution*, vol. 7, no. 1, pp. 15-19.

Kumar, J 2015, *Phenomics in Crop Plants Trends, Options and Limitations*, Phenomics in Crop Plants, eds A Pratap & S Kumar, Springer, New Delhi.

Laidig, F, Piepho, HP, Rentel, D, Drobek, T, Meyer, U & Huesken, A 2017, 'Breeding progress, environmental variation and correlation of winter wheat yield and quality traits in German official variety trials and on-farm during 1983-2014', *Theoretical and Applied Genetics*, vol. 130, no. 1, Jan, pp. 223-245.

Langridge, P & Fleury, D 2011, 'Making the most of 'omics' for crop breeding', *Trends in Biotechnology*, vol. 29, no. 1, pp. 33-40.

Larmour, RK 1939, 'The Effect of Environment on Wheat Quality: A Resume', *Transactions of the Kansas Academy of Science*, vol. 42, pp. 81-89.

Lemaire, G & Gastal, F 2009, *Quantifying Crop Responses to Nitrogen Deficiency and Avenues to Improve Nitrogen Use Efficiency-Chapter 8*, Elsevier Inc.

Lemon, J 2007, *Nitrogen management for wheat protein and yield in the Esperance port zone*, Bulletin Department of Agriculture and Food, Western Australia, Perth.

Li, C, Cao, W & Dai, T 2001, 'Dynamic characteristics of floret primordium development in wheat', *Field Crops Research*, vol. 71, pp. 71–76.

Li, L, Zhang, Q & Huang, D 2014, 'A Review of Imaging Techniques for Plant Phenotyping', *Sensors*, vol. 14, pp. 20078-20111.

Liao, M, Fillery, IRP & Palta, JA 2004, 'Early vigorous growth is a major factor influencing nitrogen uptake in wheat', *Functional Plant Biology*, vol. 31, pp. 121-129.

Limley, HA, Crosbie, GB, Lim, KK, Williams, HG, Diepeveen, DA & Solah, VA 2013, 'Wheat Quality Requirements for Char Siew Bao Made from Australian Soft Wheat', *Cereal Chemistry*, vol. 90, no. 3, May-Jun, pp. 231-239.

Lobell, DB, Schlenker, W & Costa, RJ 2011, 'Climate trends and global crop production since 1980', *Science*, vol. 333, p. 616.

Magney, TS, Eitel, JUH, Huggins, DR & Vierling, LA 2016, 'Proximal NDVI derived phenology improves in-season predictions of wheat quantity and quality', *Agricultural and Forest Meteorology*, vol. 217, pp. 46-60.

Mahjourimajd, S, Kuchel, H, Langridge, P & Okamoto, M 2016, 'Evaluation of Australian wheat genotypes for response to variable nitrogen application', *An International Journal on Plant-Soil Relationships*, vol. 399, no. 1, pp. 247-255.

Mahjourimajd, S, Taylor, J, Rengel, Z, Khabaz-Saberi, H, Kuchel, H, Okamoto, M & Langridge, P 2016, 'The genetic control of grain protein content under variable nitrogen supply in an australian wheat mapping population', *PLoS ONE*, vol. 11, no. 7, Jul.

Makanza, R, Zaman-Allah, M, Cairns, JE, Magorokosho, C, Tarekegne, A, Olsen, M & Prasanna, BM 2018, 'High-Throughput Phenotyping of Canopy Cover and Senescence in Maize Field Trials Using Aerial Digital Canopy Imaging', *Remote Sensing*, vol. 10, no. 2, Feb.

Marschner, H, Marschner, P & Marschner, H 2012, *Marschner's mineral nutrition of higher plants*, 3rd edn, ed. P Marschner, Elsevier Academic Press, London

Matson, PA, Naylor, R & Ortiz-Monasterio, I 1998, 'Integration of environmental, agronomic, and economic aspects of fertilizer management', *Science*, vol. 280, pp. 112-115.

McDonald, G & Hooper, P 2013, 'Nitrogen decision - Guidelines and rules of thumb', in Uo Adelaide (ed.), *GRDC update papers*, GRDC, Australia.

McDonald, GK 1992, 'Effects of Nitrogenous fertilizer on the growth, grain-yield and grain protein-concentration of wheat ', *Australian Journal of Agricultural Research*, vol. 43, no. 5, pp. 949-967.

McNeal, FH, Berg, MA, McGuire, CF, Stewart, VR & Baldridge, DE 1972, 'Grain and plant nitrogen relationships in eight spring wheat crosses, *Triticum aestivum L.*', *Crop Science*, vol. 12 no. 5, pp. 599-602.

Michel, S, Loschenberger, F, Ametz, C, Pachler, B, Sparry, E & Burstmayr, H 2019, 'Combining grain yield, protein content and protein quality by multi-trait genomic selection in bread wheat', *Theoretical and Applied Genetics*, vol. 132, no. 10, Oct, pp. 2767-2780.

Moll, RH, Kamprath, EJ & Jackson, WA 1982, 'Analysis and interpretation of factors which contribute to efficiency of nitrogen-utilization', *Agronomy Journal*, vol. 74, pp. 562–564.

Montes, JM, Melchinger, AE & Reif, JC 2007, 'Novel throughput phenotyping platforms in plant genetic studies', *Trends in Plant Science*, vol. 12, no. 10, Oct, pp. 433-436.

Morris, CF 2002, 'Puroindolines: the molecular genetic basis of wheat grain hardness', *Plant Molecular Biology*, vol. 48, no. 5, Mar, pp. 633-647.

Moss, HJ 1973, 'Quality standards for wheat varieties', *Journal of the Australian Institute of Agricultural Science*, vol. 39, no. 2, pp. 109-115.

Mullan, DJ & Reynolds, MP 2010, 'Quantifying genetic effects of ground cover on soil water evaporation using digital imaging', *Functional Plant Biology*, vol. 37, no. 8, pp. 703-712.

Munier-Jolain, NG & Salon, C 2005, 'Are the carbon costs of seed production related to the quantitative and qualitative performance? An appraisal for legumes and other crops', *Plant, Cell & Environment*, vol. 28, no. 11, pp. 1388-1395.

Munier, D, Kearney, T, Pettygrove, GS, Britt, K, Mathews, M & Jackson, L 2006, 'Fertilization of Small Grains', *Small grain production manual* vol. 4, University of California, California.

Myles, S, Peiffer, J, Brown, PJ, Ersoz, ES, Zhang, Z, Costich, DE & Buckler, ES 2009, 'Association Mapping: Critical Considerations Shift from Genotyping to Experimental Design', *Plant Cell*, vol. 21, no. 8, Aug, pp. 2194-2202.

'National Variety Trial' 2019, Grains Research and Development Corporation Australia.

Niethammer, U, James, MR, Rothmund, S, Travelletti, J & Joswig, M 2012, 'UAV-based remote sensing of the Super-Sauze landslide: Evaluation and results', *Engineering Geology*, vol. 128, Mar 9, pp. 2-11.

Ollero, A, Martínez-de-Dios, JR & Merino, L 2006, 'Unmanned aerial vehicles as tools for forest-fire fighting', *Forest Ecology And Management*, vol. 234, pp. S263-S263.

Oury, Bérard, P, Brancourt-Hulmel, M, Depatureaux, C, Doussinault, G, Galic, N, Giraud, A, Heumez, E, Lecomte, C, Pluchard, P, Rolland, B, Rousset, M & Trottet, M 2003, 'Yield and grain protein concentration in bread wheat: a review and a study of multi-annual data from a French breeding program', *Journal of Genetics and Breeding*, vol. 57, no. 1, pp. 59-68.

Oury & Godin, C 2007, 'Yield and grain protein concentration in bread wheat: how to use the negative relationship between the two characters to identify favourable genotypes?', *Euphytica*, vol. 157, no. 1-2, Sep, pp. 45-57.

Pan, WL, Kidwell, KK, McCracken, VA, Bolton, RP & Allen, M 2020, 'Economically optimal wheat yield, protein and nitrogen use component responses to varying N supply and genotype', *Frontiers in Plant Science*, vol. 10.

Pardey, P, Beddow, J, Hurley, T, Beatty, T & Eidman, V 2014, 'A bounds analysis of world food futures: Global agriculture through to 2050', *Australian Journal of Agricultural and Resource Economics*, vol. 58, no. 4, pp. 571-589.

Pasha, I, Anjum, FM & Morris, CF 2010, 'Grain Hardness: A Major Determinant of Wheat Quality', *Food Science and Technology International*, vol. 16, no. 6, Dec, pp. 511-522.

Prasad, B, Carver, BF, Stone, ML, Babar, MA, Raun, WR & Klatt, AR 2007, 'Potential Use of Spectral Reflectance Indices as a Selection Tool for Grain Yield in Winter Wheat under Great Plains Conditions', *Potential Use of Spectral Reflectance Indices as a Selection Tool for Grain Yield in Winter Wheat under Great Plains Conditions*, vol. 47, no. 4, pp. 1426-1440.

Preston, KR 1998, 'Protein-carbohydrate interactions', in RJ Hamer & RC Hoseney (eds), *Interactions: The Keys to Cereal Quality*, St. Paul, pp. 83-91.

Qiu, Q, Sun, N, Bai, H, Wang, N, Fan, ZQ, Wang, YJ, Meng, ZJ, Li, B & Cong, Y 2019, 'Field-Based High-Throughput Phenotyping for Maize Plant Using 3D LiDAR Point Cloud Generated With a "Phenomobile"', *Frontiers in Plant Science*, vol. 10, May.

Radoglou-Grammatikis, P, Sarigiannidis, P, Lagkas, T & Moscholios, I 2020, 'A compilation of UAV applications for precision agriculture', *Computer Networks*, vol. 172, May.

Rahimi Eichi, V, Okamato, M, Haefele, SM, Jewell, N, Brien, C, Garnett, T & Langridge, P 2019, 'Understanding the interactions between biomass, grain production and grain protein content in high and low protein wheat genotypes under controlled environments ', *Agronomy*, vol. 9, p. 706.

Rahimi Eichi, V, Okamoto, M, Garnett, T, Eckermann, P, Darrier, B, Riboni, M & Langridge, P 2020, 'Strengths and weaknesses of national variety trial data for multi-environment analysis: A case study on grain yield and protein content', *Agronomy*, vol. 10, no. 753.

Raun, WR & Johnson, GV 1999, 'Improving nitrogen use efficiency for cereal production', *Agronomy Journal*, vol. 91, no. 3.

Raun, WR, Solie, JB, Johnson, GV, Stone, ML, Lukina, EV, Thomason, WE & Schepers, JS 2001, 'In-season prediction of potential grain yield in winter wheat using canopy reflectance', vol. 93, pp. 131-138.

Richards, RA 2000, 'Selectable traits to increase crop photosynthesis and yield of grain crops', *Journal of Experimental Botany*, vol. 51, pp. 447-458.

Rodgers, CO & Barneix, AJ 1988, 'Cultivar differences in the rate of nitrate uptake by intact wheat plants as related to growth rate', *Physiologia Plantarum*, vol. 72, no. 1, pp. 121-126.

Rouse, JW, Haas, RH, Schell, JA & Deering, DW 1974, 'Monitoring vegetation systems in the Great Plains with ERTS', in MD Greenbelt (ed.), *Third Earth Resources Technology Satellite,* vol. 1, pp. 309-317.

Royo, C, Aparicio, N, Blanco, R & Villegas, D 2004, 'Leaf and green area development of durum wheat genotypes grown under Mediterranean conditions', *Leaf and green area development of durum wheat genotypes grown under Mediterranean conditions*, vol. 20, no. 4, pp. 419-430.

Sadras, VO, Hayman, PT, Rodriguez, D, Monjardino, M, Bielich, M, Unkovich, M, Mudge, B & Wang, E 2016, 'Interactions between water and nitrogen in Australian cropping systems: physiological, agronomic, economic, breeding and modelling perspectives', *Crop and Pasture Science*, vol. 67, no. 10, pp. 1019-1053.

Sadras, VO & McDonald, G 2012, *Benchmarking wheat water use efficiency: accounting for climate and nitrogen*, Water use efficiency of grain crops in Australia: principles, benchmarks and managemen, GRDC, Adelaide, Australia.

Sadras, VO & Richards, RA 2014, 'Improvement of crop yield in dry environments: benchmarks, levels of organisation and the role of nitrogen', *Journal of Experimental Botany*, vol. 65, no. 8, May, pp. 1981-1995.

Salmanowicz, BP, Adamski, T, Surma, M, Kaczmarek, Z, Krystkowiak, K, Kuczynska, A, Banaszak, Z, Lugowska, B, Majcher, M & Obuchowski, W 2012, 'The relationship between grain hardness, dough mixing parameters and bread-making quality in winter wheat', *International Journal of Molecular Sciences*, vol. 13, no. 4, Apr, pp. 4186-4201.

Schulthess, AW, Reif, JC, Ling, J, Plieske, J, Kollers, S, Ebmeyer, E, Korzun, V, Argillier, O, Stiewe, G, Ganal, MW, Roder, MS & Jiang, Y 2017, 'The roles of pleiotropy and close linkage as revealed by association mapping of yield and correlated traits of wheat (*Triticum aestivum* L.)', *Journal of Experimental Botany*, vol. 68, no. 15, Jul, pp. 4089-4101.

Sellers, PJ 1985, 'Canopy reflectance, photosynthesis and transpiration', *International Journal of Remote Sensing*, vol. 6, no. 8, 1985, pp. 1335-1372.

Semenov, MA & Halford, NG 2009, 'Identifying target traits and molecular mechanisms for wheat breeding under a changing climate', *Journal of Experimental Botany*, vol. 60, no. 10, pp. 2791-2804.

Sharma, R 1993, 'Selection for biomass yield in wheat', *International Journal of Plant Breeding*, vol. 70, no. 1, pp. 35-42.

Shen, L, He, Y & Guo, X 2013, 'Suitability of the normalized difference vegetation index and the adjusted transformed soil-adjusted vegetation index for spatially characterizing loggerhead shrike habitats in North American mixed prairie', *Journal of Applied Remote Sensing*, vol. 7, Apr 23.

Shewry, PR & Hey, SJ 2015, 'The contribution of wheat to human diet and health', *Food and Energy Security*, vol. 4, no. 3, Oct, pp. 178-202.

Shi, P-J, Men, X-Y, Sandhu, HS, Chakraborty, A, Li, B-L, Ou-Yang, F, Sun, Y-C & Ge, F 2013, 'The "general" ontogenetic growth model is inapplicable to crop growth', *Ecological Modelling*, vol. 266, pp. 1-9.

Simmonds, DH 1989, *Wheat and wheat quality in Australia*, Csiro Publishing.

Simmonds, DH, Barlow, KK & Wrigley, CW 1973, 'Biochemical basis of grain hardness in wheat', *Cereal Chemistry*, vol. 50, no. 5, pp. 553-562.

Simmonds, NW 1995, 'The relation between yield and protein in cereal grain', *Journal of the Science of Food and Agriculture*, vol. 67, no. 3, pp. 309-315.

Sinclair, TR & Rufty, TW 2012, 'Nitrogen and water resources commonly limit crop yield increases, not necessarily plant genetics', *Global Food Security*, vol. 1, no. 2, Dec, pp. 94-98.

Spragg, J 2008, *Benefit to australian grain growers in the feed grain market*, Grains Research and Development Corporation, Victoria, Australia.

Stephens, RC, Saville, DJ & Lindley, TN 1989, 'Grain yield and milling and bread making quality response to fertiliser nitrogen in wheat sown in late autunm', *New Zealand Journal of Crop and Horticultural Science*, vol. 17, pp. 67-75.

Stoddard, FL & Marshall, DR 1990, 'Variability in grain protein in australian hexaploid wheats', *Australian Journal of Agricultural Research*, vol. 41, no. 2, pp. 277-288.

Stone, PJ & Nicolas, ME 1995, 'A survey of the effects of high-temperature during grain filling on yield and quality of 75 wheat cultivars', *Australian Journal of Agricultural Research*, vol. 46, no. 3, pp. 475-492.

Sylvester-Bradley, R, Berry, P, Blake, J, Kindred, D, Spink, J, Bingham, I, McVittie, J & Foulkes, J 2008, *The wheat growth guide*, Second edn, eds C Edwards & G Dodgson, London.

Sylvester-Bradley, R & Kindred, DR 2009, 'Analysing nitrogen responses of cereals to prioritize routes to the improvement of nitrogen use efficiency', *Journal of Experimental Botany*, vol. 60, no. 7, May, pp. 1939-1951.

Sylvester, G 2018, *E-Agriculture in action: drones for agriculture*, Food and Agriculture Organization of the United Nations and International Telecommunication Union, Bangkok.

Symes, KJ 1965, 'The inheritance of grain hardness in wheat as measured by the particle size index', *Crop and Pasture Science*, vol. 16, no. 2, pp. 113-123.

Tanksley, SD & McCouch, SR 1997, 'Seed banks and molecular maps: Unlocking genetic potential from the wild', *Science*, vol. 277, no. 5329, Aug, pp. 1063-1066.

Tardieu, F & Tuberosa, R 2010, 'Dissection and modelling of abiotic stress tolerance in plants', *Current Opinion in Plant Biology*, vol. 13, no. 2, pp. 206-212.

Tauger, MB 2011, 'Bread, Beer and the Seeds of Change: Agriculture's Imprint on World History', *Agricultural History*, vol. 85, no. 4, Fal, pp. 561-562.

Thorwarth, P, Piepho, HP, Zhao, Y, Ebmeyer, E, Schacht, J, Schachschneider, R, Kazman, E, Reif, JC, Würschum, T & Longin, CFH 2018, 'Higher grain yield and higher grain protein deviation underline the potential of hybrid wheat for a sustainable agriculture', *Plant Breeding*, vol. 137, no. 3, pp. 326-337.

Triboi, E, Abad, A, Michelena, A, Lloveras, J, Ollier, JL & Daniel, C 2000, 'Environmental effects on the quality of two wheat genotypes: 1. quantitative and qualitative variation of storage proteins', *European Journal of Agronomy*, vol. 13, no. 1, Jul, pp. 47-64.

Tucker, CJ 1979, 'Red and photographic infrared linear combinations for monitoring vegetation', *Remote Sensing of Environment*, vol. 8, no. 2, 1979, pp. 127-150.

Turner, NC 2004, 'Agronomic options for improving rainfall-use efficiency of crops in dryland farming systems', *Journal of Experimental Botany*, vol. 55, no. 407, pp. 2413–2425.

van Herwaarden, AF, Farquhar, GD, Angus, JF, Richards, RA & Howe, GN 1998, ''Haying-off', the negative grain yield response of dryland wheat to nitrogen fertiliser - I. Biomass, grain yield, and water use', *Australian Journal of Agricultural Research*, vol. 49, no. 7, pp. 1067-1081.

Walsh, OS, Shafian, S & Christiaens, RJ 2018, 'Nitrogen Fertilizer Management in Dryland Wheat Cropping Systems', *Plants-Basel*, vol. 7, no. 1, Mar.

Wang, E, Robertson, MJ, Hammer, GL, Carberry, PS, Holzworth, D, Meinke, H, Chapman, SC, Hargreaves, JNG, Huth, NI & McLean, G 2002, 'Development of a generic crop model

template in the cropping system model APSIM', *European Journal of Agronomy*, vol. 18, no. 1-2, Dec, pp. 121-140.

Watanabe, K, Guo, W, Arai, K, Takanashi, H, Kajiya-Kanegae, H, Kobayashi, M, Yano, K, Tokunaga, T, Fujiwara, T, Tsutsumi, N & Iwata, H 2017, 'High-Throughput Phenotyping of Sorghum Plant Height Using an Unmanned Aerial Vehicle and Its Application to Genomic Prediction Modeling', *Frontiers in Plant Science*, vol. 8, Mar.

West, JS, Bravo, C, Oberti, R, Lemaire, D, Moshou, D & McCartney, HA 2003, 'The potential of optical canopy measurement for targeted control of field crop diseases', *Annual Review of Phytopathology*, vol. 41, 2003, pp. 593-614.

White, JW, Andrade-Sanchez, P, Gore, MA, Bronson, KF, Coffelt, TA, Conley, MM, Feldmann, KA, French, AN, Heun, JT, Hunsaker, DJ, Jenks, MA, Kimball, BA, Roth, RL, Strand, RJ, Thorp, KR, Wall, GW & Wang, G 2012, 'Field-based phenomics for plant genetics research', *Field Crops Research*, vol. 133, Jul 11, pp. 101-112.

Whitehead, K & Hugenholtz, CH 2014, 'Remote sensing of the environment with small unmanned aircraft systems (UASs), part 1: a review of progress and challenges ', *Journal of Unmanned Vehicle Systems*, vol. 2, no. 3, pp. 69-85.

Wilson, B 2007, ''Good bread is back' - A contemporary history of French bread, the way it is made, and the people who make it', *Tls-the Times Literary Supplement*, no. 5436, Jun, pp. 3-4.

Zarco-Tejada, PJ, Catalina, A, Gonzalez, MR & Martin, P 2013, 'Relationships between net photosynthesis and steady-state chlorophyll fluorescence retrieved from airborne hyperspectral imagery', *Remote Sensing of Environment*, vol. 136, Sep, pp. 247-258.

Appendix 1: Estimation of vegetation indices for high-throughput phenotyping of wheat using aerial imaging

Zohaib Khan [1,*], Vahid Rahimi-Eichi [2], Stephan Haefele [2], Trevor Garnett [2] and Stanley J. Miklavcic [1]

[1]Phenomics and Bioinformatics Research Center, University of South Australia, Mawson Lakes Boulevard, Adelaide 5095, Australia.
[2]School of Agriculture, Food and Wine, University of Adelaide, Adelaide 5064, Australia.

*Correspondence: zohaib.khan@unisa.edu.au

CrossMark

Estimation of vegetation indices for high-throughput phenotyping of wheat using aerial imaging

Zohaib Khan[1]* , Vahid Rahimi-Eichi[2], Stephan Haefele[2], Trevor Garnett[2] and Stanley J. Miklavcic[1]

Abstract

Background: Unmanned aerial vehicles offer the opportunity for precision agriculture to efficiently monitor agricultural land. A vegetation index (VI) derived from an aerially observed multispectral image (MSI) can quantify crop health, moisture and nutrient content. However, due to the high cost of multispectral sensors, alternate, low-cost solutions have lately received great interest. We present a novel method for model-based estimation of a VI using RGB color images. The non-linear spatio-spectral relationship between the RGB image of vegetation and the index computed by its corresponding MSI is learned through deep neural networks. The learned models can be used to estimate VI of a crop segment.

Results: Analysis of images obtained in wheat breeding trials show that the aerially observed VI was highly correlated with ground-measured VI. In addition, VI estimates based on RGB images were highly correlated with VI deduced from MSIs. Spatial, spectral and temporal information of images contributed to estimation of VI. Both intra-variety and inter-variety differences were preserved by estimated VI. However, VI estimates were reliable until just before significant appearance of senescence.

Conclusion: The proposed approach validates that it is reasonable to accurately estimate VI using deep neural networks. The results prove that RGB images contain sufficient information for VI estimation. It demonstrates that low-cost VI measurement is possible with standard RGB cameras.

Keywords: Wheat, Phenotyping, Deep learning, Precision agriculture

Background

Satellite multispectral imaging has demonstrated the ability to efficiently map Earth's resources (vegetation, water, minerals etc.) from remote locations [1, 2]. Recent technological advances in imaging methods are moving agricultural practice from traditional farming to precision farming. The unmanned aerial vehicle (UAV) platform is becoming an important tool for field-based precision agriculture [3–5]. Lightweight, high-resolution imaging sensors have been developed and can be used with most UAVs [6, 7]. Aerial platforms can be used to support computerized ground-based vehicles in the management of extensive agricultural lands. Precise spatial application maps can then be developed to direct ground based remedial measures to increase production efficiency. The result is a site specific agricultural management solution based on aerial observations.

A UAV equipped with a multispectral camera can be used to monitor spatial and temporal variations in vegetation characteristics. A vegetation index (VI) is a spectral transformation metric for measuring the presence and state of vegetation [8]. Its basis is the characteristic photosynthetic response of green vegetation to incident light. Healthy plants exhibit high infrared reflectance and low red reflectance due to absorption of red light by chlorophyll, resulting in a high index value. Conversely, unhealthy, stressed or dead vegetation, a manifestation of reduced chlorophyll pigment, displays a low index value.

*Correspondence: zohaib.khan@unisa.edu.au
[1] Phenomics and Bioinformatics Research Center, University of South Australia, Mawson Lakes Boulevard, Adelaide 5095, Australia
Full list of author information is available at the end of the article

Khan *et al. Plant Methods* (2018) 14:20

Page 2 of 11

Therefore, VI measures can be used to facilitate corrective measures in crop management.

Various uses of VI for the detection of biotic and abiotic stresses have been demonstrated. Vegetation indices were correlated with soil moisture measurements to assess the sensitivity of tallgrass prairie grasslands to drought [9]. The indices allowed remote identification of drought affected regions and could potentially be used to quantify the effects of drought on vegetation. Vegetation indices also have the potential to differentiate healthy from diseased plants [10]. Targeted application of insecticides and herbicides which is of immense value to agricultural economics can be automatically carried out by a UAV capable of both observation and treatment application. Apart from stress, VI were shown to be sensitive to phenological changes (e.g. senescence) with age [11]. As a result it was possible to predict the age of plant leaves in forest to assess the state of ecosystem. Gracia-Romero et al. [12] evaluated several aerially assessed and ground based VI and found them to be highly correlated with Maize performance with fertilization. In addition, vegetation indices have demonstrated correlation with several performance characteristics of crops including biomass, yield potential and nutrient concentration [13, 14].

Vegetation indices are generally computed as the ratio of difference to sum of the sensor measurements in two bands. One of the most widely known is the Normalized Difference Vegetation Index (NDVI) [15], extensively used since the introduction of LANDSAT-1 satellite multispectral data. NDVI is based on measurement in Red and Near Infrared (NIR) channels to identify regions of vegetation cover and their condition. Other empirically derived indices based on the same principle make use of different bands in the photosynthetically active spectral range in combination with NIR [16]. The main idea is to maximize sensitivity to vegetation and minimize the noise. The RedEdge Normalized Difference Vegetation Index (RENDVI) is most sensitive to leaf area and less prone to index saturation [17]. The Soil Adjusted Vegetation Index (SAVI) aims to minimize the influence of soil reflectance in computation of VI by adding a background adjustment factor [18]. The Enhanced Vegetation Index (EVI) further corrects for atmospheric noise by introducing aerosol resistance factors [19]. Although important for remote satellites, atmospheric noise is an insignificant factor for UAV imaging. Table 1 lists the common multispectral VIs found in literature.

It is clear from the above definitions that the NIR reflectance is a critical requirement, common to most VI. However, the NIR channel is not available in standard RGB cameras. UAVs equipped with RGB cameras are therefore incapable of providing a direct VI measure. A straightforward solution is a 4-channel camera with the

Table 1 A list of commonly used VIs in literature

Vegetation index	Formula
Normalized Difference Vegetation Index [15]	$NDVI = \frac{NIR - Red}{NIR + Red}$
Green Normalized Difference Vegetation Index [16]	$GNDVI = \frac{NIR - Green}{NIR + Green}$
RedEdge Normalized Difference Vegetation Index [17]	$RENDVI = \frac{NIR - RedEdge}{NIR + RedEdge}$
Soil Adjusted Vegetation Index [18]	$SAVI = \frac{(1+L) \times (NIR - Red)}{NIR + Red + L}$
Enhanced Vegetation Index [19]	$EVI = \frac{G \times (NIR - Red)}{NIR + c_1 Red - c_2 Blue + L}$

additional NIR channel, usually known as a multispectral camera. However, multispectral cameras compatible with UAVs come with a very limited spatial resolution (< 5 million pixels), compared to most RGB cameras (up to 20 million pixels). Although high resolution may not be crucial for accurate NDVI measurement, it is desirable for many image phenotyping tasks such as flower detection, plant height [20] and leaf coverage estimation. Multispectral cameras have relatively low spatial resolution for such tasks. This compels the end-user to either trade-off spatial resolution for spectral resolution, or conduct multiple flights with each sensor separately, to achieve both targets. Some UAVs allow for simultaneously carrying multiple sensors (owing to payload limitations). Such a system would require accurate synchronization, alignment and integration of the sensors. This is a challenging task in dynamic scenarios where vegetation movement is inevitable due to environmental factors.

To circumvent costs, the NIR filter present inside a standard RGB camera can be removed. The implication of such a modification is a camera with blue, green and NIR channels. Then, the tradeoff is to use the blue channel to simulate the absorption in red channel. However, the blue channel in most camera sensors is prone to low signal to noise ratio. In addition, the equivalence of absorption in two different channels may not be necessarily true. An improvement over this design is to remove the NIR filter from an RGB camera and introduce an additional high-pass filter, which theoretically results in NIR, green and red channels [21]. The optimal filter parameters for a specific camera are set to minimize the difference between reference and target spectral values. However, this requires careful customization of camera and measurement of the camera sensitivity function. Yet another approach is to remove the NIR filter and introduce a dual band-pass filter to enhance NDVI measurement [22]. A major drawback as a consequence of modification of an RGB camera is the unavailability of an original RGB image. Apart from retrofit modifications, commercial dual CCD sensors, each with a different

Khan *et al. Plant Methods* (2018) 14:20

Page 3 of 11

color filter to target desired channels have been compared with single CCD sensor with multiple color filters for VI measurement [23]. However, the modifications add to the design and production costs limiting their use to specialized applications.

Although a number of methods for the modification of camera hardware have been proposed, each with its own benefits, this paper proposes a model-based approach to estimating VI from RGB images. The main idea is to learn the spatio-spectral relationships between information in RGB images of vegetation and their corresponding VI values (sourced from MSI). This is achieved by leveraging a deep neural network (DNN) to model the non-linear relationship between an RGB image and its vegetation index. Deep learning is classified as a machine learning method for learning multi-level representations of data [24]. It has performed well on a wide range of plant phenotyping tasks like organ counting [25–27], age estimation [28], feature detection [29, 30], species and disease detection [31, 32]. Our motivation to use DNN was to formulate a regression problem such that the multilayered convolutional features learned by the model relate RGB image data to NDVI. The rationale of our proposed approach is simple but effective, i.e. the spatial density and spectral signature (color) of vegetation reflects its VI.

Limmer and Lensch investigated a contrasting problem of colorizing infrared images [33]. They used DNN to synthesize RGB image of a scene from its infrared counterpart with reasonable visual quality. Our approach to estimating VI is distantly similar to the band simulation approach proposed by Rabetal et al. [21]. The major difference that distinguishes our work is that it does not rely on camera hardware modification and extensive camera sensitivity measurements. Moreover, the use of an unmodified camera allows for retaining the high-resolution RGB image for useful purposes while simultaneously achieving a VI estimate. There are no additional costs associated for the purpose of such application. To the best of our knowledge, this is the first attempt on modeling vegetational indices from color images using deep learning.
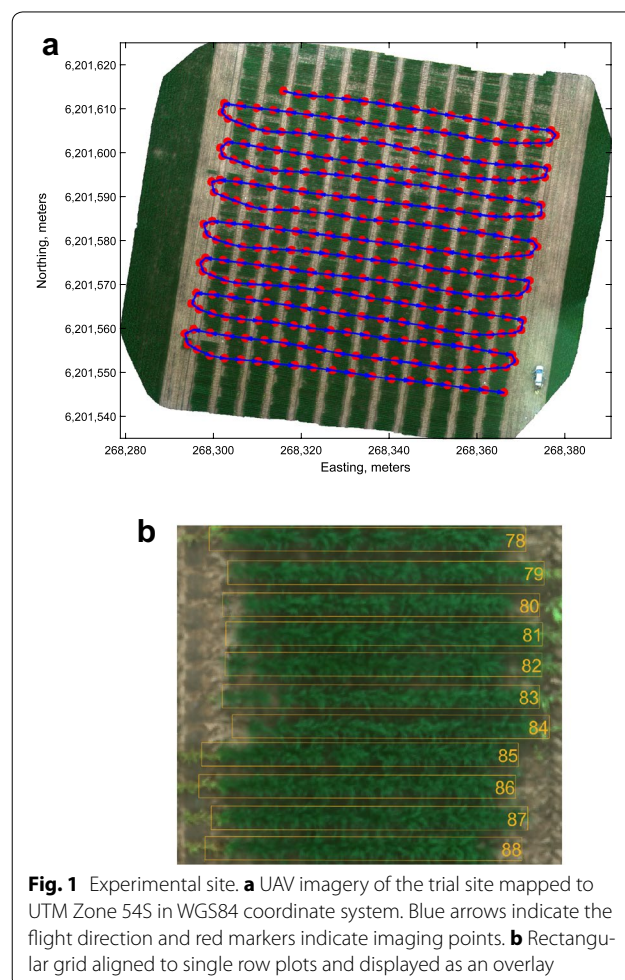
Methods

Breeding experiment

The trial site used for this study was in a farmers' field between Mallala and Balaklava, South Australia (Lat:34°18′4.29012″:S Long:138°28′57.05255″:E). A wheat breeding trial was conducted on site in collaboration with a wheat breeding company (LongReach Plant Breeders). The experiment was sown on 25th May, 2016, and harvested at 214 days after sowing (DaS). A total of 1728 single row wheat plots on the site were considered at 7 growth stages, resulting in 12096 observations.

The three 'bays' monitored on the site were part of a much larger trial which was almost 1400 m long and 72 m wide. Each bay was 19.2 m long and had 12 ranges (12 × 6 m) Germplasm entries were planted in double rows, perpendicular to the ranges, with a row spacing of 0.4 m, such that 24 entries were planted in each range making a total of 288 entries in a bay (see Fig. 1a). The initial length of planted rows was 5 m which was later sprayed back to 4 m. Therefore, each individual entry had two rows of 4 m and an area of 3.2 m². It was noted after emergence that some rows were shorter due to insufficient seed at the time of sowing.

The first bay (coded R40) was planted with double haploid (DH) lines of an EGA Gregory/Spitfire population targeted at studying the genetic control of grain N concentration. In this experiment, the DH entries were replicated twice and a total of 94 DH lines were tested. Along with the DH lines, 19 soft wheat check varieties, 02 hard wheat check varieties, and both hard wheat parents were planted in a fully randomized layout. The

Fig. 1 Experimental site. **a** UAV imagery of the trial site mapped to UTM Zone 54S in WGS84 coordinate system. Blue arrows indicate the flight direction and red markers indicate imaging points. **b** Rectangular grid aligned to single row plots and displayed as an overlay

Khan *et al. Plant Methods* (2018) 14:20

Page 4 of 11

remaining plots in this bay were filled with germplasm not related to the trial. The next two bays (coded R41 and R42) were planted with DH lines of 6 different crosses of soft wheat (3 in each bay), which were part of the soft wheat breeding program. For each cross, 80 different DH lines were grown unreplicated, together with 24 twice replicated check varieties of soft and hard wheat. In addition, a highly disease susceptible line (Morocco) was regularly repeated in each range to increase the disease pressure. All DH lines of each cross were grown in a block (4 ranges within a bay) and check varieties were randomized within this setup.

Ground reference

Ground based NDVI was estimated using a handheld crop sensor, 'GreenSeeker' (Trimble, USA). The measurements were conducted by making a continuous sweep from the start to the end of a plot. A constant height and position over the center of an entry (i.e. the middle of two rows) was ensured by adjusting a thin line with a small weight on the sensor. Two lines in each bay were selected, and the 12 plots behind them were measured, so a total of 24 plots were measured in each bay. The measurements were conducted on the following DaS: 93, 117, 141, 156, 170, and 182.

UAV image acquisition

A 3DR Solo (3D Robotics Inc., USA) drone was used with a custom platform to attach a RedEdge™ MultiSpectral camera (MicaSense Inc., USA). The camera was capable of simultaneously capturing five spectral bands at a resolution of 1.2 megapixels. For flight planning and automatic mission control an open source autopilot software Mission Planner (ArduPilot) was utilized. The multispectral camera was set to auto-capture mode with one image every two seconds. Image overlap was always $\geq 80\%$ at a constant speed of $\leq 3 \text{ ms}^{-1}$, but the actual speed could vary depending on the selected flight altitude, image capture rate and requested overlap. Initially, images were only acquired from 30 m height, but from the fifth session onwards, images were also taken from a lower 20 m height for increased ground resolution.

A total of seven imaging sessions were conducted at intervals ranging from 1 to 3 weeks between August and November of 2016. A trial imaging session was conducted on DaS: 72, and regular imaging sessions were planned thereafter. However, the actual dates were adjusted according to suitable weather conditions (bright and not too windy). Subsequent imaging sessions were conducted at DaS: 93, 113, 135, 141, 156, 170, and 182.

In order to geographically register images captured in multiple sessions, 12 square panels were placed at fixed positions in the surveying area to serve as ground control points (GCP). The GCPs were repeatedly placed at the same position before commencement of an imaging session, throughout the season. An image of a calibrated reflectance panel (MicaSense Inc., USA) was also captured from directly overhead the panel before and after each flight for radiometric calibration. All raw images were stored in a 16-bit TIFF file format.

UAV image processing

The acquired images were imported into Pix4D mapper v3.2 (Pix4D Inc., Switzerland) for offline processing. Camera correction and calibration was applied to remove geometric distortions from images. Finally, a stitched orthomosaic image was generated with a Ground Sampling Distance (GSD) ranging between 2.0 cm (30 m altitude) to 1.3 cm (20 m altitude). The orthomosaic image was radiometrically calibrated with the image of the standard white reflectance panel. Coordinates of the GCPs were used to compute geometric image transformation required to geographically register orthomosaics of successive imaging sessions. The calibrated orthomosaics were imported into MATLAB R2017a (Mathworks Inc., USA) for sampling of the reflectance data of plots. A uniform rectangular grid of fixed dimensions was laid out and aligned with the ground plot locations (see Fig. 1b). The geographic coordinates of rectangles were converted to intrinsic image coordinates to automatically crop the individual plot images. A few sampled plots were missing image data due to being outside the mapped range of UAV on DaS 135. These 18 images were excluded from the analysis. Since the orthomosaic images of different dates varied in resolution, the sampled images were scaled to a uniform size of 208×15 pixels.
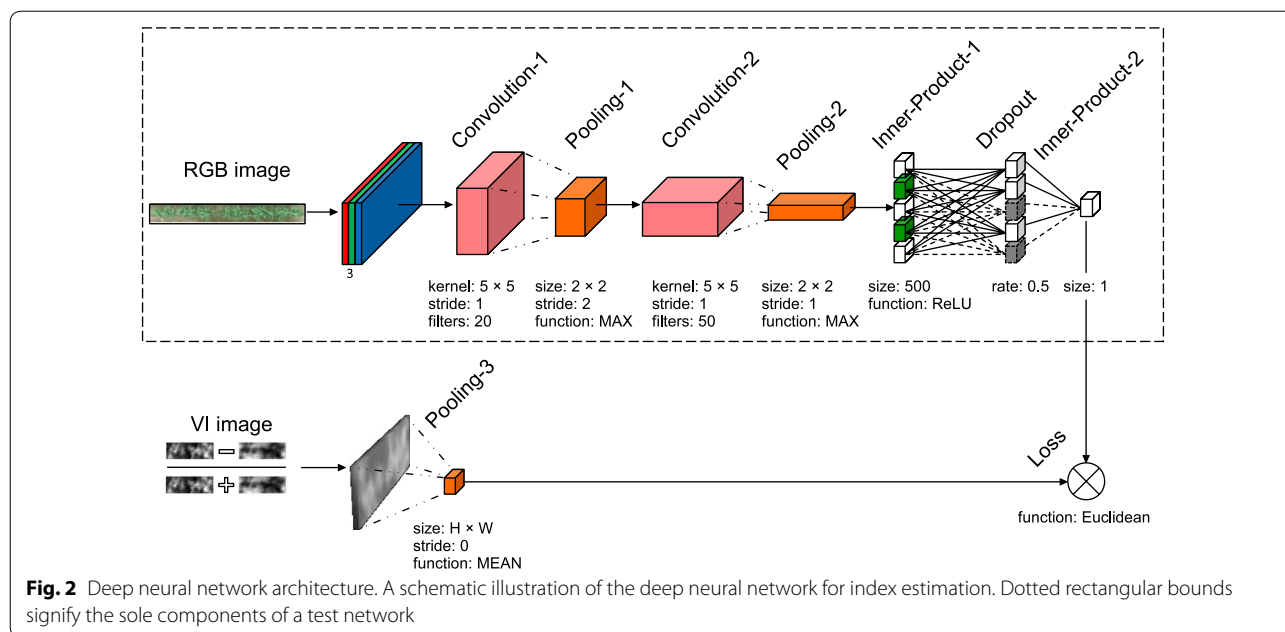
Deep neural network

Our aim was to utilize deep learning to represent an RGB image as a VI, or in other words to estimate the VI from an RGB image.

Architecture

The architecture is a modification of the AlexNet deep convolutional neural network [34]. Deeper networks like ResNet [35] and GoogleNet [36] allow for more complex feature learning in diverse classes but also require much higher resolution input images to propagate through the net. Our choice of a DNN with a few hidden layers was suitable for content and resolution of input images.

The DNN maps a color image to a scalar VI as shown in Fig. 2. The training network is comprised of two convolution layers, two max-pooling layers, one mean-pooling layer, a dropout layer for regularization, and a fully connected layer. The input to the net is a three channel RGB color image of vegetation plot of $H \times W$ pixels. The

Khan *et al. Plant Methods* (2018) 14:20

Page 5 of 11

Fig. 2 Deep neural network architecture. A schematic illustration of the deep neural network for index estimation. Dotted rectangular bounds signify the sole components of a test network

input image passes through the first convolutional layer which extracts 20 feature maps with a 5×5 kernel. The resulting feature maps down-sample by max-pooling of non-overlapping 2×2 regions. The second convolutional layer extracts 50 feature maps with a 5 kernel, followed by another max pooling operation of non-overlapping 2×2 pixels. The feature maps resulting from the second pooling layer connect to two inner product layers (fully connected) with an intermediate rectified linear unit layer and a dropout layer. The inner product layers successively reduce the dimensions of the feature maps down to a scalar. The output of the network is the activation of the (single neuron) final layer. The error was defined by a real-valued Euclidean loss function which computed the difference between the actual VI value and that estimated by the model.

We used the *Caffe Deep Learning Framework* (BVLC, UC Berkeley) [37] for implementation of the design, training and validation of model. The experiments were performed on an Intel Xeon PC with 128GB RAM and a GeForce GTX TITAN X (NVIDIA, USA) graphics processing unit with CUDA enabled for faster computations.

Training

For training the network, RGB image data of vegetation plots was sampled from the multispectral image. The mean VI values were computed from the NIR and Red channels of the corresponding vegetation plots. Then, the network was trained with RGB images as the input source and the VI values as the target output. The Stochastic Gradient Descent algorithm was used to optimize the network weights by minimizing back-propagation error. The weights were iteratively updated so as to minimize the scalar distance (loss) between the output of the mean pooling layer and the final inner inner product layer. A mini-batch of 72 images was randomly sampled from the training set in each iteration. Moreover, the training data was augmented by randomly flipping the images. Training was conducted for the same number of epochs in each fold of validation. A fixed set of values for hyper-parameters was chosen for training across the folds. The base learning rate was initialized as $\alpha = 0.01$ with a momentum $\gamma = 0.9$ for quick convergence. The weight decay parameter was fixed as 0.0005. An inverse decay function defined the learning rate policy which reduced the learning rate with each iteration according to $\alpha \times (1 + \gamma \times \text{iter})^{-\text{power}}$, where power = 0.75.

Testing

A test RGB image was forward propagated through the trained network to get the estimated index value from the final fully connected layer. Note that the dropout layer was excluded from the test network as its only purpose was to provide regularization for training.
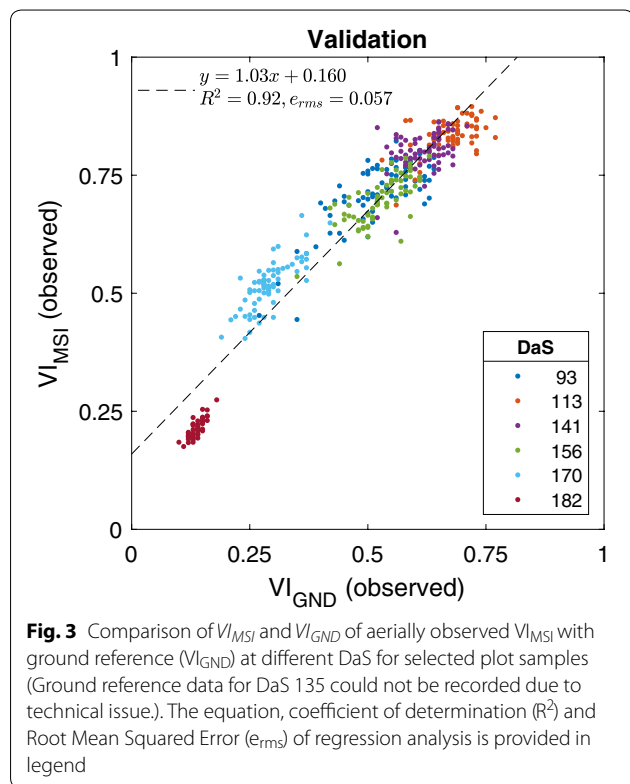
Results

All data was split into training and test sets for experiments. Robust Least Squares Regression was utilized to compare model accuracies. Root Mean Squared Error (RMSE) and coefficient of determination (R^2) were used as the criterion for model evaluation. Pearson's correlation coefficient (r) were also considered to assess the

Khan *et al. Plant Methods* (2018) 14:20

Page 6 of 11

linear correlation between the observations and their estimates.

Validation

We first validate the aerially observed VI by comparison with manually recorded ground measurements for 72 selected reference plots. Figure 3 provides a scatter plot of VI observed by UAV using multispectral imaging (VI$_{MSI}$) and VI measured by ground reference (VI$_{GND}$) at different growth stages (DaS). Note that the term growth stage here refers to imaging time points, and should not be confused with the phenological growth stage. It can be seen that both measurements are highly correlated (R^2, RMSE = 0.057) across all growth stages.

It should be noted that the measurements are prone to methodological differences. The ground sensor's field of view and region of interest chosen, result in measurements of different proportions of vegetation/soil regions. Moreover, the ground based sensor has an an active illumination source, whereas the aerial measurement utilizes solar illumination. A uniform lighting condition is assumed for the duration of the survey which may not always be valid on a particular day. Despite all differentiating factors, the validation model parameters suggest a significant correlation between the aerial and ground based measurements.

Fig. 3 Comparison of *VI$_{MSI}$* and *VI$_{GND}$* of aerially observed VI$_{MSI}$ with ground reference (VI$_{GND}$) at different DaS for selected plot samples (Ground reference data for DaS 135 could not be recorded due to technical issue.). The equation, coefficient of determination (R^2) and Root Mean Squared Error (e$_{rms}$) of regression analysis is provided in legend

Estimation of vegetation index

For index estimation, a DNN model was trained with RGB images of all growth stages. Models were trained in three fold cross validation, where in each fold, two spatially different bays were used for training and the held-out bay for testing. Therefore, the training set comprised 8064 samples (576 plots × 2 bays × 7 growth stages), whereas the test set constituted 4032 (576 plots × 1 bay × 7 growth stages) samples. We term it as DNN-RGB model which attempts to learn the relationship between RGB image and VI. The index observed from multispectral images (VI$_{MS}$) against the index estimated by a trained model using RGB image (VI$_{RGB}$) are presented in Fig. 4a. Regression analysis suggested that the RGB image estimated VI values had a good agreement with the observed VI values ($R^2 = 0.99$, $e_{rms} = 0.019$). The contribution of spatial, spectral and temporal information of images to VI estimation can be validated as follows.

Spectral information

The extent to which RGB color information contributed to vegetation index of a plot was quantified by the method of elimination. For this purpose, color information was removed from all RGB images by conversion to grayscale. Then a DNN was trained with the grayscale images as input and vegetation index as output. The trained model (DNN-GRAY) was utilized to estimate VI of plots given test grayscale images. The results were compared to that of a DNN trained on color images and the differential loss was examined to quantify the advantage of color information. The grayscale estimated index (VI$_{GRAY}$) is plotted against the multispectral observed index (VI$_{MS}$) in Fig. 4c. The root mean square error using grayscale image based VI estimation model was found to be more than twice ($e_{rms} = 0.045$) in comparison to that of RGB image based model. It demonstrates that RGB does contribute useful information for estimation of VI.

Spatial information

The contribution of spatial information in images of vegetation to estimated VI was quantified by purging the spatial dimension. To achieve this objective, spatial information was reduced from all RGB images (by taking the average of pixels in each channel) to a single pixel ($1 \times 1 \times 3$) image. Then a linear regression model was learned with the spatially diminished images as predictor variable and vegetation index as the response variable. The trained regression model (LR-RGB) was used to estimate VI of test plots given single pixel images. The results were compared to that of DNN trained on original RGB images and the differential loss was evaluated to quantify the advantage of spatial information.
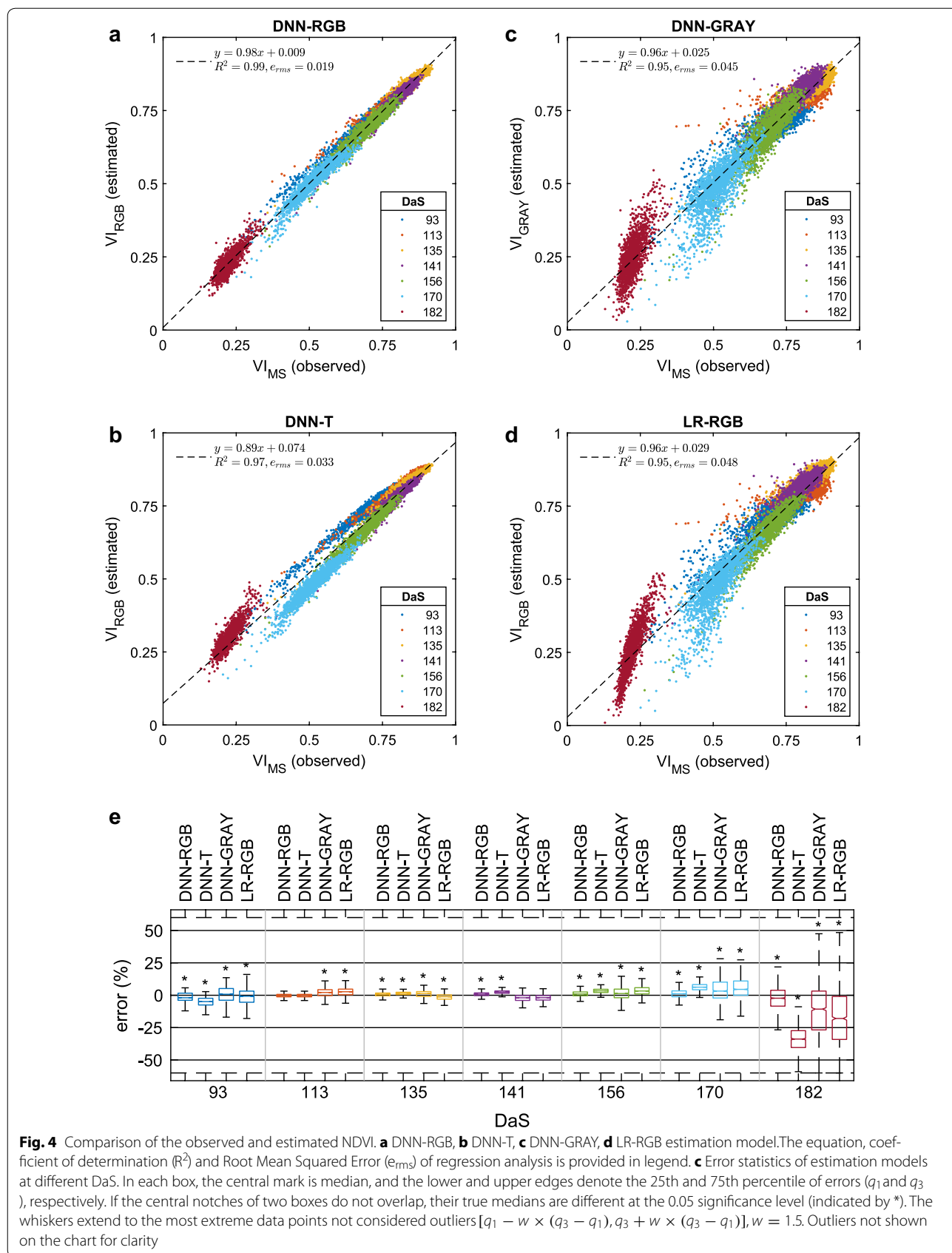
Khan *et al. Plant Methods* (2018) 14:20

Page 7 of 11

Fig. 4 Comparison of the observed and estimated NDVI. **a** DNN-RGB, **b** DNN-T, **c** DNN-GRAY, **d** LR-RGB estimation model. The equation, coefficient of determination (R^2) and Root Mean Squared Error (e_{rms}) of regression analysis is provided in legend. **c** Error statistics of estimation models at different DaS. In each box, the central mark is median, and the lower and upper edges denote the 25th and 75th percentile of errors (q_1 and q_3), respectively. If the central notches of two boxes do not overlap, their true medians are different at the 0.05 significance level (indicated by *). The whiskers extend to the most extreme data points not considered outliers $[q_1 - w \times (q_3 - q_1), q_3 + w \times (q_3 - q_1)]$, $w = 1.5$. Outliers not shown on the chart for clarity

Khan *et al. Plant Methods* (2018) 14:20

Page 8 of 11

Temporal information

The effect of temporal information of VI at different growth stages on estimated vegetation index was evaluated. To this end, RGB images of one growth stage were withheld for training. In this manner, a learned DNN model was made temporally blind to images of one growth stage. For obtaining results, training was done on 10368 images (576 plots × 3 bays × 6 growth stages). The trained model (DNN-T) was tested on 1728 images of the left-out growth stage (576 plots × 3 bays × 1 growth stage). The process was repeated in a similar manner for all growth stages. It is encouraging to see that the DNN predicted VI at unseen growth stages by making use of information in nearby growth stages. It should be noted that a considerably different distribution of VI of the training data from the test data likely resulted in increased estimation error (e.g. DaS 182).

Table 2 summarizes the error statistics and correlation at each growth stage for DNN-RGB, DNN-GRAY,

Table 2 Percentage estimation error statistics, mean (μ), standard deviation (σ), and the correlation coefficient (r) of the observed and estimated VI of each model

DaS	Model	$\mu \pm \sigma$	r
93	DNN-RGB	-1.78 ± 4.03	0.97
	DNN-GRAY	0.00 ± 7.40	0.86
	DNN-T	-5.34 ± 4.30	0.98
	LR-RGB	-1.68 ± 6.92	0.89
113	DNN-RGB	-0.61 ± 2.38	0.98
	DNN-GRAY	1.41 ± 5.67	0.68
	DNN-T	-0.56 ± 2.32	0.99
	LR-RGB	1.91 ± 5.66	0.70
135	DNN-RGB	0.50 ± 1.73	0.96
	DNN-GRAY	0.70 ± 3.22	0.84
	DNN-T	1.27 ± 1.62	0.97
	LR-RGB	-1.57 ± 2.90	0.89
141	DNN-RGB	0.87 ± 1.82	0.97
	DNN-GRAY	-2.07 ± 3.14	0.90
	DNN-T	2.53 ± 1.74	0.97
	LR-RGB	-1.97 ± 2.98	0.91
156	DNN-RGB	1.09 ± 2.51	0.96
	DNN-GRAY	2.08 ± 6.89	0.88
	DNN-T	3.46 ± 2.18	0.97
	LR-RGB	4.07 ± 5.91	0.93
170	DNN-RGB	1.45 ± 4.42	0.95
	DNN-GRAY	6.78 ± 14.78	0.80
	DNN-T	6.62 ± 4.02	0.96
	LR-RGB	9.14 ± 17.84	0.81
182	DNN-RGB	-1.81 ± 9.56	0.83
	DNN-GRAY	-8.13 ± 23.21	0.73
	DNN-T	-28.83 ± 7.13	0.86
	LR-RGB	-11.46 ± 26.03	0.87

DNN-T and LR-RGB models. The errors were calculated as a relative difference of the observed and estimated VI using,

$$\text{error (\%)} = \frac{\text{VI}_{\text{obs}} - \text{VI}_{\text{est}}}{\text{VI}_{\text{obs}}} \times 100 \quad (1)$$
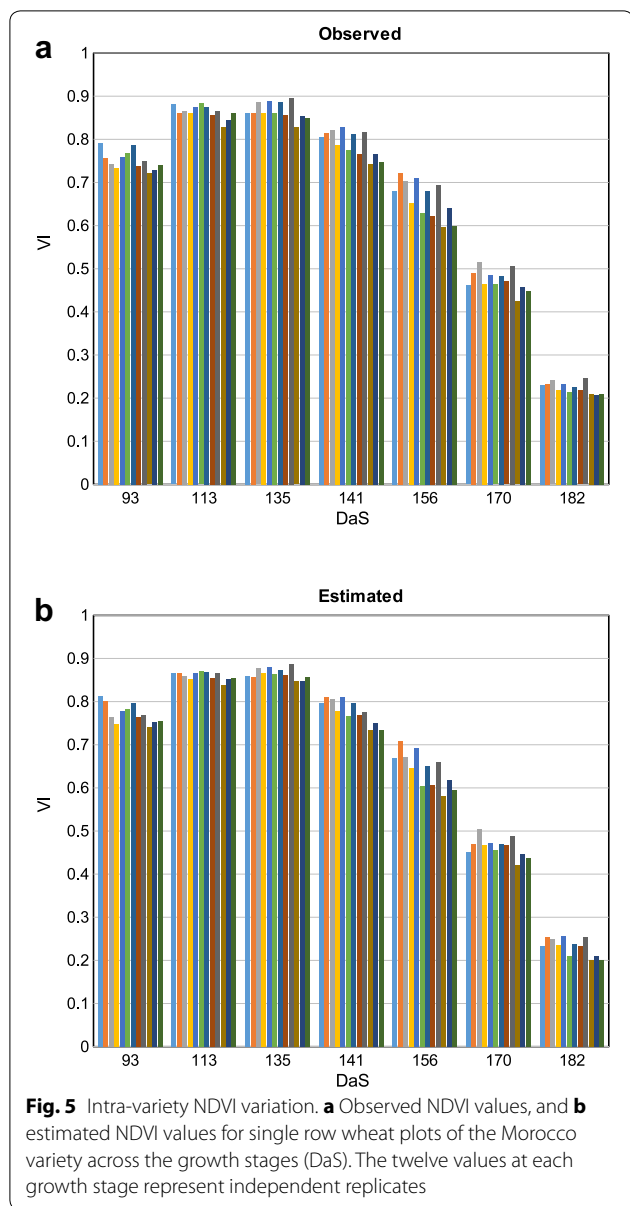
Figure 4e graphically illustrates the statistics of the errors. It can be observed that DNN-RGB consistently outperforms all other methods. The estimation errors were considerably larger for the DNN-T model compared to DNN-RGB model. This is not surprising since the DNN-T model does not recognize spatio-spectral variations at all temporal stages. Similarly, DNN-GRAY model is unable to sufficiently distinguish vegetation and background since it is not familiar with vegetation color resulting in unreliable VI estimates. In contrast, as the scope of a DNN-RGB model is complete, so it is familiar with all the spatial, spectral and temporal variations in VI. In future work, a more complex DNN model could be designed to account for causal relationships of the data by using recurrent neural networks [38].

A significantly higher error was observed by all methods upon senescence (DaS 170, 182). It showed difficulty in accurately modeling relationship of mature plant RGB images and their unique range of VI. Larger errors for LR-RGB model suggested a highly non-linear relationship of RGB images and VI after maturity. It also explained the likely reason for the failure of DNN-T model in mature growth stage, since it was blind to images of that stage. The DNN-T model estimates had high correlation with observed VI, albeit the estimates were biased and resulted in higher average error. In contrast, the DNN-RGB model demonstrated relatively lower errors and its average error consistently remained within $\pm 2\%$ at all growth stages.

A multispectral camera was used for the study to directly compare the RGB image estimated NDVI with a multispectral image observed NDVI. Thus, training was performed on low resolution RGB images sourced from the multispectral sensor. However, the proposed methodology can be extended to high-resolution RGB cameras. A common approach to adapt to a DNN where the input image size differs from the network input is to resize the input image. Therefore, DNN models trained on low resolution RGB images can be extended to an RGB camera by resizing the images.
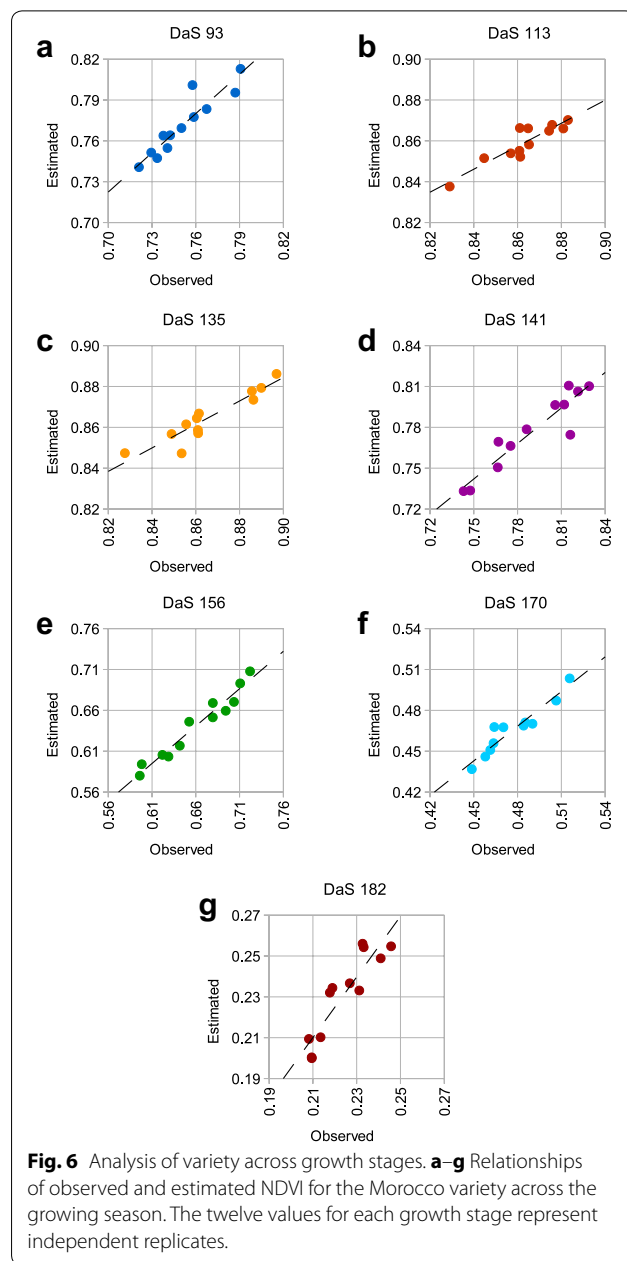
Phenotyping with VI estimation

In order to evaluate the utility of the proposed approach for phenotyping in breeding experiments, we observed if the intra-variety and inter-variety differences were preserved in VI estimation. For this purpose, we selected the Morocco variety as a check-line in the trials and had
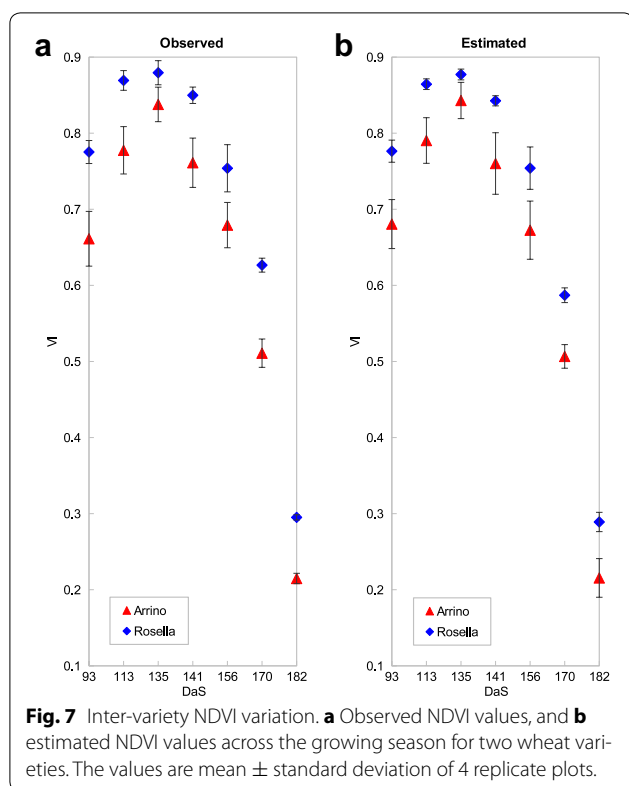
Khan *et al. Plant Methods* (2018) 14:20

Page 9 of 11

Fig. 5 Intra-variety NDVI variation. **a** Observed NDVI values, and **b** estimated NDVI values for single row wheat plots of the Morocco variety across the growth stages (DaS). The twelve values at each growth stage represent independent replicates

Fig. 6 Analysis of variety across growth stages. **a**–**g** Relationships of observed and estimated NDVI for the Morocco variety across the growing season. The twelve values for each growth stage represent independent replicates.

12 replicates allowing comparisons throughout the season. As shown in Fig. 5, the variation in estimated NDVI across the season was consistent with the observed NDVI. Specifically, the trend of observed NDVI within replicates at each growth stage was largely preserved in estimated NDVI values as well.

Using Morocco again as an example, the relationship between the observed and estimated NDVI values was much clearer when plotted individually at each growth stage as shown in Fig. 6. Despite the large changes in NDVI across the season, and the relatively small variability in NDVI of replicates at each growth stage, there was a strong relationship between the observed and estimated values.

In terms of comparison of observed and estimated NDVI across varieties, we selected Arrino and Rosella variety, each with 4 replicates. Relatively subtle differences in observed NDVI between the varieties were also preserved in the estimated NDVI values as shown in Fig. 7. Moreover, the VI variability within a variety was found to be preserved relative to the variability between varieties.

Khan *et al. Plant Methods* (2018) 14:20

Page 10 of 11

Fig. 7 Inter-variety NDVI variation. **a** Observed NDVI values, and **b** estimated NDVI values across the growing season for two wheat varieties. The values are mean ± standard deviation of 4 replicate plots.

Author details
[1] Phenomics and Bioinformatics Research Center, University of South Australia, Mawson Lakes Boulevard, Adelaide 5095, Australia. [2] School of Agriculture, Food and Wine, University of Adelaide, Adelaide 5064, Australia.

Publisher's Note
Springer Nature remains neutral with regard to jurisdictional claims in published maps and institutional affiliations.

An important consideration is the fact that no genotype-specific information was considered in learning of the estimation models. This helps show the robustness of the modeling approach as genotypic variation in growth characteristics would be a source of error in the observed and estimated NDVI relationships.

Conclusion

The use of RGB cameras and UAVs provide a ubiquitous solution for calculating VI for high throughput precision agriculture. This comes at a cost of an estimate of VI rather than actual VI. However, as demonstrated by our experiments, the tradeoff minimally affects the reliability of measurement. The current study was based on single row wheat plants and further analysis will be required to evaluate the feasibility of the proposed approach in broad acre crops. This could include estimation of the VI image of a paddock (instead of the VI of a plot) using an RGB image. In addition, the generalization of this approach by application to other crops of interest will be of significant value.

Authors' contributions
ZK conceived, designed and validated method. VR and SH collected image data. ZK performed experiments. ZK, SJM and TG analyzed and interpreted results. ZK, SH and TG drafted the manuscript. ZK and SJM revised the manuscript. All authors read and approved the final manuscript.

References
1. Mulla DJ. Twenty five years of remote sensing in precision agriculture: key advances and remaining knowledge gaps. Biosyst Eng. 2013;114(4):358–71.
2. Rao M, Silber-Coats Z, Powers S, Fox L III, Ghulam A. Mapping drought-impacted vegetation stress in california using remote sensing. GIsci Remote Sens. 2017;54(2):185–201.
3. Zhang C, Kovacs JM. The application of small unmanned aerial systems for precision agriculture: a review. Precis Agric. 2012;13(6):693–712.
4. Shi Y, Thomasson JA, Murray SC, Pugh NA, Rooney WL, Shafian S, Rajan N, Rouze G, Morgan CLS, Neely HL, Rana A, Bagavathiannan MV, Henrickson J, Bowden E, Valasek J, Olsenholler J, Bishop MP, Sheridan R, Putman EB, Popescu S, Burks T, Cope D, Ibrahim A, McCutchen BF, Baltensperger DD, Avant RV Jr, Vidrine M, Yang C. Unmanned aerial vehicles for high-throughput phenotyping and agronomic research. PloS ONE. 2016;11(7):0159781.
5. Gago J, Douthe C, Coopman RE, Gallego PP, Ribas-Carbo M, Flexas J, Escalona J, Medrano H. UAVs challenge to assess water stress for sustainable agriculture. Agric Water Manag. 2015;153:9–19.
6. Haghighattalab A, Pérez LG, Mondal S, Singh D, Schinstock D, Rutkoski J, Ortiz-Monasterio I, Singh RP, Goodin D, Poland J. Application of unmanned aerial systems for high throughput phenotyping of large wheat breeding nurseries. Plant Methods. 2016;12(1):35.
7. Zaman-Allah M, Vergara O, Araus JL, Tarekegne A, Magorokosho C, Zarco-Tejada PJ, Hornero A, Albà AH, Das B, Craufurd P, Prasanna BM, Cairns J. Unmanned aerial platform-based multi-spectral imaging for field phenotyping of maize. Plant Methods. 2015;11(35):1.
8. Bannari A, Morin D, Bonn F, Huete AR. A review of vegetation indices. Remote Sens Rev. 1995;13(1–2):95–120.
9. Bajgain R, Xiao X, Wagle P, Basara J, Zhou Y. Sensitivity analysis of vegetation indices to drought over two tallgrass prairie sites. ISPRS J Photogramm Remote Sens. 2015;108:151–60.

Khan *et al. Plant Methods* (2018) 14:20

Page 11 of 11

10. Gröll K, Graeff S, Claupein W. Use of vegetation indices to detect plant diseases. In: GIL Jahrestagung. 2007. p. 95–8. https://subs.emis.de/LNI/Proceedings/Proceedings101/article1354.html.
11. Chavana-Bryant C, Malhi Y, Wu J, Asner GP, Anastasiou A, Enquist BJ, Caravasi C, Eric G, Doughty CE, Saleska SR, Martin RE, Gerard FF. Leaf aging of Amazonian canopy trees as revealed by spectral and physiochemical measurements. New Phytol. 2016;214(3):1049–63.
12. Gracia-Romero A, Kefauver SC, Vergara-Diaz O, Zaman-Allah MA, Prasanna BM, Cairns JE, Araus JL. Comparative performance of ground versus aerially assessed rgb and multispectral indices for early-growth evaluation of maize performance under phosphorus fertilization. Front Plant Sci. 2017;8:2004.
13. Islam MR, Garcia SCY, Henry D. Use of normalised difference vegetation index, nitrogen concentration, and total nitrogen content of whole maize plant and plant fractions to estimate yield and nutritive value of hybrid forage maize. Crop Pasture Sci. 2011;62(5):374–82.
14. Panda SS, Ames DP, Panigrahi S. Application of vegetation indices for agricultural crop yield prediction using neural network techniques. Remote Sens. 2010;2(3):673–96.
15. Rouse Jr J, Haas RH, Schell JA, Deering DW. Monitoring vegetation systems in the great plains with ERTS. In: Third earth resources technology satellite-1 symposium, vol. 1; 1974. p. 309–17
16. Gitelson AA, Kaufman YJ, Merzlyak MN. Use of a green channel in remote sensing of global vegetation from EOS-MODIS. Remote Sens Environ. 1996;58(3):289–98.
17. Delegido J, Verrelst J, Meza CM, Rivera JP, Alonso L, Moreno J. A red-edge spectral index for remote sensing estimation of green lai over agroecosystems. Eur J Agron. 2013;46:42–52.
18. Huete AR. A soil-adjusted vegetation index (SAVI). Remote Sens Environ. 1988;25(3):295–309.
19. Huete A, Didan K, Miura T, Rodriguez EP, Gao X, Ferreira LG. Overview of the radiometric and biophysical performance of the modis vegetation indices. Remote Sens Environ. 2002;83(1–2):195–213.
20. Madec S, Baret F, De Solan B, Thomas S, Dutartre D, Jezequel S, Hemmerlé M, Colombeau G, Comar A. High-throughput phenotyping of plant height: comparing unmanned aerial vehicles and ground LiDAR estimates. Front Plant Sci. 2017;8:2002.
21. Rabatel G, Gorretta N, Labbé S. Getting NDVI spectral bands from a single standard RGB digital camera: a methodological approach. In: Conference of the Spanish association for artificial intelligence. Berlin: Springer; 2011. p. 333–342
22. Dworak V, Selbeck J, Dammer K-H, Hoffmann M, Zarezadeh AA, Bobda C. Strategy for the development of a smart NDVI camera system for outdoor plant detection and agricultural embedded systems. Sensors. 2013;13(2):1523–38.
23. Muda MA, Foulonneau A, Bigue L, Sudibyo H, Sudiana D. Small format optical sensors for measuring vegetation indices in remote sensing applications: a comparative approach. In: TENCON region 10 conference. IEEE; 2012. p. 1–6.
24. Schmidhuber J. Deep learning in neural networks: an overview. Neural Netw. 2015;61:85–117.
25. Ubbens J, Cieslak M, Prusinkiewicz P, Stavness I. The use of plant models in deep learning: an application to leaf counting in rosette plants. Plant Methods. 2018;14(1):6.
26. Lu H, Cao Z, Xiao Y, Zhuang B, Shen C. TasselNet: counting maize tassels in the wild via local counts regression network. Plant Methods. 2017;13(1):79.
27. Xu R, Li C, Paterson A, Jiang Y, Sun S, Robertson J. Cotton bloom detection using aerial images and convolutional neural network. Front Plant Sci. 2017;8:2235.
28. Ubbens JR, Stavness I. Deep plant phenomics: a deep learning platform for complex plant phenotyping tasks. Front Plant Sci. 2017;8:1190.
29. Pound MP, Burgess AJ, Wilson MH, Atkinson JA, Griffiths M, Jackson AS, Bulat A, Tzimiropoulos G, Wells DM, Murchie EH, Pridmore TP, French AP. Deep machine learning provides state-of-the-art performance in image-based plant phenotyping. GigaScience. 2017;6(10):1–10.
30. Xiong X, Duan L, Liu L, Tu H, Yang P, Wu D, Chen G, Xiong L, Yang W, Liu Q. Panicle-SEG: a robust image segmentation method for rice panicles in the field based on deep learning and superpixel optimization. Plant Methods. 2017;13(1):104.
31. Šulc M, Matas J. Fine-grained recognition of plants from images. Plant Methods. 2017;13(1):115.
32. Mohanty SP, Hughes DP, Salathé M. Using deep learning for image-based plant disease detection. Front Plant Sci. 2016;7:1419.
33. Limmer M, Lensch HPA. Infrared colorization using deep convolutional neural networks. In: International conference on machine learning and applications (ICMLA); 2016. p. 61–68.
34. Krizhevsky A, Sutskever I, Hinton GE. ImageNet classification with deep convolutional neural networks. In: Advance in neural information processing systems; 2012. p. 1097–1105.
35. He K, Zhang X, Ren S, Sun J. Deep residual learning for image recognition. In: Conference on computer vision and pattern recognition (CVPR). IEEE; 2016. p. 770–778.
36. Szegedy C, Liu W, Jia Y, Sermanet P, Reed S, Anguelov D, Erhan D, Vanhoucke V, Rabinovich A. Going deeper with convolutions. In: Conference on computer vision and pattern recognition (CVPR). IEEE; 2015. p. 1–9.
37. Jia Y, Shelhamer E, Donahue J, Karayev S, Long J, Girshick R, Guadarrama S, Darrell T. Caffe: convolutional architecture for fast feature embedding. 2014. arXiv:abs/1408.5093.
38. Mikolov T, Karafiát M, Burget L, Cernockỳ J, Khudanpur S. Recurrent neural network based language model. Interspeech. 2010;2:1045–8.

Appendix 2: Quantitative Estimation of Wheat Phenotyping Traits Using Ground and Aerial Imagery

Zohaib Khan [1], Joshua Chopin [1], Jinhai Cai [1], Vahid-Rahimi Eichi [2], Stephan Haefele [2] and Stanley J. Miklavcic [1,*]

[1]Phenomics and Bioinformatics Research Centre, University of South Australia, Adelaide 5095, Australia; zohaib.khan@unisa.edu.au (Z.K.); josh.chopin@unisa.edu.au (J.Ch.); jinhai.cai@unisa.edu.au (J.Ca.)
[2]School of Agriculture, Food and Wine, University of Adelaide, Adelaide 5064, Australia; vahid.rahimi-eichi@adelaide.edu.au (V.-R.E.); stephan.haefele@adelaide.edu.au (S.H.)

* Correspondence: stan.miklavcic@unisa.edu.au

Quantitative Estimation of Wheat Phenotyping Traits Using Ground and Aerial Imagery

Zohaib Khan [1] [iD] **, Joshua Chopin** [1] **, Jinhai Cai** [1] [iD] **, Vahid-Rahimi Eichi** [2] **and Stephan Haefele** [2] **and Stanley J. Miklavcic** [1,*]

1   Phenomics and Bioinformatics Research Centre, University of South Australia, Adelaide 5095, Australia;
    zohaib.khan@unisa.edu.au (Z.K.); josh.chopin@unisa.edu.au (J.Ch.); jinhai.cai@unisa.edu.au (J.Ca.)
2   School of Agriculture, Food and Wine, University of Adelaide, Adelaide 5064, Australia;
    vahid.rahimi-eichi@adelaide.edu.au (V.-R.E.); stephan.haefele@adelaide.edu.au (S.H.)
*   Correspondence: stan.miklavcic@unisa.edu.au; Tel.: +61-8-8302-3788

Abstract: This study evaluates an aerial and ground imaging platform for assessment of canopy development in a wheat field. The dependence of two canopy traits, height and vigour, on fertilizer treatment was observed in a field trial comprised of ten varieties of spring wheat. A custom-built mobile ground platform (MGP) and an unmanned aerial vehicle (UAV) were deployed at the experimental site for standard red, green and blue (RGB) image collection on five occasions. Meanwhile, reference field measurements of canopy height and vigour were manually recorded during the growing season. Canopy level estimates of height and vigour for each variety and treatment were computed by image analysis. The agreement between estimates from each platform and reference measurements was statistically analysed. Estimates of canopy height derived from MGP imagery were more accurate (RMSE = 3.95 cm, R^2 = 0.94) than estimates derived from UAV imagery (RMSE = 6.64 cm, R^2 = 0.85). In contrast, vigour was better estimated using the UAV imagery (RMSE = 0.057, R^2 = 0.57), compared to MGP imagery (RMSE = 0.063, R^2 = 0.42), albeit with a significant fixed and proportional bias. The ability of the platforms to capture differential development of traits as a function of fertilizer treatment was also investigated. Both imaging methodologies observed a higher median canopy height of treated plots compared with untreated plots throughout the season, and a greater median vigour of treated plots compared with untreated plots exhibited in the early growth stages. While the UAV imaging provides a high-throughput method for canopy-level trait determination, the MGP imaging captures subtle canopy structures, potentially useful for fine-grained analyses of plants.

Keywords: unmanned aerial vehicle; mobile ground platform; canopy traits; canopy imaging; field phenotyping; wheat; height; vigour

1. Introduction

Plant development is observable as changes in a plant's morphological features, which occur at specific growth stages. For example, plant development may result in the appearance of new features such as reproductive organs (i.e., flowers) or a change in the pigmentation of the plant foliage. Plant growth is not only characterized by an increase in the size of existing plant organs (elongation and thickness of stems and area of leaves), but also by the emergence of new shoots of a similar morphological feature (new leaves, new stems), which contribute to the overall increase in plant vegetative volume [1]. The underlying ability of a plant to grow and develop, steered by the environment, results in a phenotype that can be traced back to its genotype. One aim of a plant

phenotyping exercise is to characterize and quantify the relationship between the genotype and the phenotype as a function of environmental conditions.

Classical phenotyping relies on manual sampling and trait analysis of developing plants to characterize a plant's growth and development. This process requires a significant amount of time and resources. While demanding, manual inspection of plants is feasible on a small scale and under controlled conditions. However, sampling of plants in a field setting, which usually involves an enormous number of plant varieties and is subject to significant variations in environmental conditions (as arise in practical circumstances such as in plant breeding trials), represents an overwhelming prospect.

Novel image analysis systems are now being designed and implemented to automatically capture the ensuing morphometric changes in plant traits in the field [2]. State of the art imaging hardware and image analysis methods have attracted considerable interest from the plant phenotyping community. This is not only due to their potential of relieving the burden of manual phenotyping, but also the possibility of objectively quantifying trait characteristics [3]. Land-based phenotyping platforms, such as the mobile ground platform (MGP) used in this study, are able to capture high resolution images of plant canopies at close range. The corresponding image analysis software is rapidly becoming available and reliable [4–6]. In comparison, aerial imaging platforms such as an unmanned aerial vehicle (UAV), have recently found application in field phenotyping [7,8]. The main advantage of a UAV is that it can cover larger areas, thus offering high-throughput field capture, albeit with a trade-off of resolution. Consequently, these platforms are utilized for the assessment of nurseries and breeder plots [9]. The plot-wise characteristics that are usually targeted for capture are canopy vigour [10,11], canopy height [12], biomass [13], leaf area [14] or ground cover [15].

Canopy height, defined as the distance between the base of a plant and the highest photosynthetic tissue, is a gross, but important indicator of a plant's physical development. Measurement of plant height using a ruler has long been the traditional approach [12,16,17]. Assessment of plant height from images is a far more complex process as it necessitates the estimation of depth in physical units; in discipline terms, a so-called depth map is reconstructed from multiple images of a canopy taken from slightly different viewpoints. Relevant work in this area has shown that accurate estimates are possible and indeed preferable given their objectivity and accuracy, compared with manual measurements, which can be subjective, as well as incomplete [5]. An alternative method, light detection and ranging (LiDAR), uses an active laser sensor to non-destructively measure canopy height with high accuracy [17].

The second readily-identifiable trait that communicates plant status at a given stage of development is canopy vigour. Typically, the physicochemical state of leaf and stem pigmentation and the density of foliage are major factors that contribute to canopy vigour [10,18]. Indirectly, vigour can be quantified in terms of a vegetation index (VI), which involves a plant's calibrated reflectance at different wavelengths. A vegetation index can be used as a non-destructive substitute of vigour, assuming it is proportionally related. Although there are some exceptions [19], vegetation indices are most commonly defined as ratios of differences to sums of reflectance in two or more bands. For example, the commonly-used normalized difference vegetation index (NDVI) is a ratio of the difference between the plant's reflectance in the near-infrared and red bands to the sum of the reflectance [20–22]. While manual hand-held sensors with infrared capabilities have been used to measure the reflectance and compute indices on a small scale, high-throughput imaging techniques are preferable for large-scale studies.

Vegetation indices that can be derived from RGB images [23] include the excess green index (ExG) [24], the modified hue index [25], which applies the inverse cosine function to a combination of the red, green and blue (RGB) values, and the green-red vegetation index (GRVI) [26], defined as the ratio of the difference to the sum of plant reflectance in the green and red channels. Kipp et al. found the relative amount of green pixels (RAGP) index to be proportional to plant vigour [10]. A recent study showed that a number of VIs, including ExG and NDVI, did not significantly differ in the ability to

assess plant vigour [27]. In this study, GRVI has been used to represent and proportionally quantify plant vigour. The index normalizes for variations in light intensities, has been a tested indicator of chlorophyll content in several crops and is shown to be positively correlated with traits such as biomass [28] and leaf area index [29], a quantity related to plant vigour. In this study, images of plant canopies are captured in the RGB channels, making an RGB-derived index suitable to represent vigour by both MGP and UAV. While acknowledging that several different indices can be derived from an RGB image, the rationale for choosing a single index is to compare the attributes of MGP and UAV image-based estimates of vigour on the same scale.

Close-range images of the field are captured with sensors attached to ground vehicles [6,30–33] or mobile platforms [5,34,35] for trait estimation. On the other hand, remote images of the field are captured with sensors attached to aerial platforms [36–39] for trait estimation. Recent studies to quantify plant canopy development from images either report trait comparisons with reference to a different sensor technology such as LiDAR [16,40] or compare image-based estimation techniques with manual methods [5,41]. A comparison of the performance of two imaging methods on the same field study has hitherto not been reported previously. In this paper, we provide such analysis for quantitative estimation of phenotyping traits of wheat in a field trial. Our comparative analysis is both relative and absolute since we have also employed the results of traditional manual methods of measurement as a benchmark for the MGP and UAV imaging. The analysis is focused on canopy height and vigour, which are two important plant phenotyping measures.

2. Materials and Methods

2.1. Experimental Design

A field trial to observe the differential growth of wheat with fertilizer treatment was conducted at Mallala, South Australia (latitude = $-34.457062°$, longitude = $138.481487°$). A set of ten contrasting varieties (*Drysdale, Excalibur, Gladius, Gregory, Kukri, Mace, Magenta, RAC875, Scout, Spitfire*) of spring wheat (*Triticum aestivum* L.) were selected for the experiment to cover a diverse range of growth characteristics. Six replicates of each variety were laid out in a 5×12 randomized split-block design of 60 plots, as shown in Table 1. Additional plots, not included in the trial, were added to either end of the rows to attenuate edge effects on the border plots.

Table 1. Randomized split-block design layout of thrice replicated wheat varieties, Vn, $n \in \{1, \ldots, 10\}$. Shaded blocks were treated with fertilizer.

Col \ Row	1	2	3	4	5	Rep
1	V3	V6	V10	V4	V7	
2	V8	V2	V5	V1	V9	1
3	V2	V5	V1	V9	V8	
4	V7	V4	V6	V3	V10	
5	V9	V1	V10	V6	V8	
6	V7	V3	V4	V5	V2	2
7	V3	V7	V5	V4	V6	
8	V9	V10	V2	V8	V1	
9	V2	V3	V1	V10	V5	
10	V6	V8	V7	V4	V9	3
11	V8	V7	V10	V1	V4	
12	V6	V5	V3	V9	V2	

The trial was sown on 8 July 2016 at a seeding rate of 45 g per plot. The plot dimensions were 1.2 m $\times$ 4 m, containing 6 rows of wheat with an inter-row spacing of 0.2 m. Three replicates of each variety were selected for fertilizer application. A top dressing of a standard mix of 16:8:16 N-P_2O_5-K_2O was applied 35 days after sowing at a rate of 37.5 g m^{-2}. A following top dressing of urea was applied

62 days after sowing at a rate of 4.3 g m^{-2}. The remaining three replicates of each variety served as controls and received no fertilizer treatment.

2.2. Image Data Collection and Analysis

Comparative data collection was performed five times between August and November of 2016 (see Table 2). MGP imaging was conducted following manual measurement of plant heights, whereas UAV imaging was conducted following manual measurement of canopy vigour. For practical reasons (e.g., adverse weather conditions), MGP and UAV could not always be deployed for image collection on the same day. However, imaging sessions differed by at most four days, in most cases fewer (see Table 2). The difference resulted in the unavailability of height reference measurements on some days of UAV imaging and vigour reference measurements on some days of MGP imaging. This limitation was addressed by linearly interpolating reference data taken on days immediately prior to and subsequent to the days of missing data. Such an approach was considered appropriate for the analysis since reference measurements were always available within a range of less than four days.

Table 2. The phenological development stage (BBCH-scale) of wheat and the respective days on which images and reference data were collected. I: interpolated, A: actual, N: not available.

t	Stage	(BBCH-Code)	MGP Date (Height, Vigour)	UAV Date (Height, Vigour)
1	stem elongation	(34)	23/09/16 (A, I)	19/09/16 (I, A)
2		(37)	07/10/16 (A, A)	07/10/16 (A, A)
3	anthesis	(63)	28/10/16 (A, I)	26/10/16 (I, A)
4	grain development	(77)	08/11/16 (A, I)	09/11/16 (I, A)
5	senescence	(92)	18/11/16 (A, N)	18/11/16 (A, N)

2.2.1. MGP Imaging and Canopy Trait Estimation

Our MGP imaging system consisted of two identical EOS 60D digital SLR cameras (Canon Inc., Tokyo, Japan) with a resolution of 18.1 megapixels, synchronized to capture images within 1 ms of each other by means of an electronic trigger. The cameras were mounted on a custom-built wagon, 20 cm apart on a central overhead rail, 1.90 m above ground level. The platform was manually driven to a stop at three equidistant positions in each plot to capture images of its entire area. By fixing the camera positions relative to a plot, subsequently captured images of the same plot automatically fell into coarse alignment. Cameras were adjusted to focus at a depth of 2 m in the early growth stages and 1.5 m at later stages to capture sharp images of canopies with growth. The remaining camera settings were as follows: focal length: 18 mm; aperture: f/9.0; ISO: automatic; and exposure: 1/500 s. The arrangement of MGP imaging system is shown in Figure 1a.

A ColorChecker Passport Photo (X-Rite Inc., Grand Rapids, MI, USA) calibration target was used as a basis for colour correction. The calibration target was attached to the base of the platform such that it was always visible from the perspective of one camera as described in Appendix C. Colour calibration was performed on all images according to the method proposed in [41]. Field imaging was carried out between 23 September 2016 and 18 November 2016 inclusive (see Table 2).

The acquired stereo image pairs were processed to reconstruct the depth of the plot canopy. Firstly, the lens distortion was corrected by taking advantage of the calibration images from the locally flat ground (i.e., no additional calibration was applied or indeed needed). A given stereo pair of cameras was positioned with optical axes aligned in one plane. If the lenses of the stereo cameras were undistorted and the plane of the camera sensors was parallel to the ground plane, the distance between any two key points on the flat ground (plane) would be the same in the stereo pair of two images. By taking advantage of this, we can estimate the lens distortion parameters. Then, a pixel-wise matching technique was used to estimate the distance between corresponding points in the image pair [42]. In this approach, the estimation of a depth image relied on reference data in the form of the camera focal length and the physical distance between the two cameras. An approximate ground

sampling distance (GSD) of 0.04 cm per pixel was achieved in the processed images. A detailed description of the procedure is provided in [5].

The height distribution of plant tissues within a plot, i.e., the frequency of occurrence of plant material at a given height above ground level was computed from the depth images that were derived using the above-mentioned procedure. A sample graph of the height distribution is provided in Figure A3. Overall canopy height, as presented in the analysis to follow, was defined as the 98th percentile of the canopy height distribution of a plot (refer to Appendix B for details on percentile selection).

Vigour per plant pixel, computed separately from the colour-calibrated images, is defined as the ratio of the difference in plant reflectance in green and red channels to the sum of the reflectance,

$$\text{vigour} \sim GRVI = \frac{\text{Green} - \text{Red}}{\text{Green} + \text{Red}} \tag{1}$$

The value of this quantity, averaged over the three RGB images per plot, was used as a representative measure of plot canopy vigour.

2.2.2. UAV Imaging and Canopy Trait Estimation

Our UAV imaging system was a 3DR Solo quadcopter (3D Robotics Inc., Berkeley, CA, USA) with a RX100 III Compact Digital Camera (Sony Corp., Japan) as the payload giving an effective image resolution of 20.1 megapixels. Flights were planned using the open source ground control station software, Mission Planner (ArduPilot), which directed the UAV to follow a preprogrammed path based on the geographical coordinates of the site as shown in Figure 1c. The camera was set to automatically capture snapshots every 2 s during flight at an altitude of 30 m, which resulted in an image-overlap of more than 80%. Five imaging sessions were conducted from 19 September 2016–18 November 2016, inclusive (see Table 2). A standard reflectance panel (MicaSense Inc., Seattle, WA, USA) was photographed before each flight for radiometric calibration of the images. Colour images were stored as compressed JPEG files.

Inaccuracies in location estimates provided by the GPS receiver onboard the UAV contributed to an uncertainty in the global alignment of orthomosaics captured at different times. To overcome this deficiency, square panels, termed ground control points (GCPs), were used to provide a location reference. A total of four such GCPs were consistently placed at fixed field locations before each imaging session. This facilitated alignment and scaling of the orthomosaics over the whole season.

UAV images acquired in a given session were processed offline using the professional photogrammetry software Pix4Dmapper v4.0 (Pix4D, Lausanne, Switzerland). The processing comprised three main steps for 3D canopy reconstruction using the structure from motion (SfM) technique [43]. Initially, 'keypoints' were automatically computed from original images. Keypoints refer to visual features of interest that can be detected reliably in images taken from different perspectives. These points were matched across all the images to estimate camera position, orientation and internal camera parameters. The original images were corrected for any lens distortion using a camera calibration model [44]. In the second step, matched keypoints were triangulated to create a dense three-dimensional point cloud. In the final step, the following raster images were output as TIFF files:

- Height map (also known as a digital surface model): Elevation (in cm) of the mapped surface generated by interpolating the point cloud.
- Terrain map (also known as a digital terrain model): Elevation (in cm) of the mapped terrain excluding any above-ground features (e.g., plants). This output was visually assessed and confirmed to have filtered out the plants within each plot.
- Reflectance map: A colour-calibrated image generated by projecting ortho-rectified images onto the height map. This output is colour calibrated using pixel values of the radiometric calibration target.
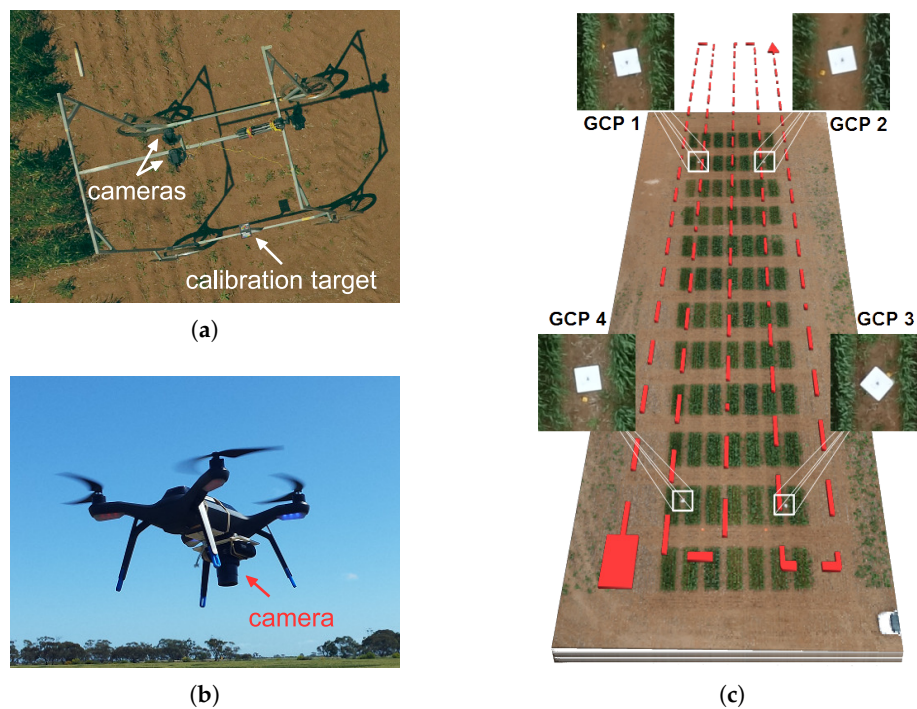
Figure 1. (**a**) The MGP with stereo imaging cameras and calibration target. (**b**) The UAV with the camera payload. (**c**) A perspective view of the trial site with ground control points magnified as insets. The red broken line shows the aerial path taken by the UAV.

The output images resulted in an average GSD of 0.8 cm. The software uses manually-marked locations of each GCP in six to eight images in order to register (position and scale) the output images at different times. Spatial analysis of the trial was performed by importing the reflectance, height and terrain images into MATLAB R2017b (Mathworks Inc., Natick, MA, USA). A rectangular lattice, sized and spaced according to the plot dimensions, was interactively overlaid on the reflectance image to establish the region of interest. The height distribution within the bounds of the region of interest of a plot relative to the ground, was computed by subtracting the terrain map from the height map. The canopy height was designated as the 98th percentile of a plot's height distribution. Vigour, defined by Equation (1), was computed per pixel within the region of interest from the reflectance map. The average of this quantity taken over all plot pixels was used as a representative of plot canopy vigour.

2.2.3. Ground Reference of Canopy Traits

A total of 300 height observations were recorded for the 60 plots on five occasions during the growing season concurrent with the MGP imaging days (see Table 2). Canopy height was manually measured using a meter rule with markings every cm. A measurement was taken by placing the ruler vertically inside a plot and reading the ruler at the top of the canopy. Multiple locations within each plot were sampled and averaged to get a single representative measure of the canopy height of a plot. During the early stages of plant growth, when spikes were not present, canopy height measurement related to the leaves only. Later, when flag leaves and spikes appeared, these features were also included in the measurements. That is, plant height was defined (and recorded) to be at the top of the level of the spike layer; awns, if any were present, were excluded from the measurements.

A total of 240 vigour observations were recorded for the 60 plots on four occasions during the growing season concurrent with the UAV imaging days (Table 2). A GreenSeeker hand-held crop sensor (Trimble Inc., Sunnyvale, CA, USA) was used to record the reference measure of canopy

vigour. GreenSeeker is an active optical sensor that quantifies plant vigour using the NDVI ratio, (NIR − red)/(NIR + red). A continuous longitudinal sweep of the sensor at a constant height above a plot gave a representative measure of canopy vigour. The theoretical range of sensor measurement was (0.00–0.99); a higher value indicated greater vigour, and a lower value indicated less vigour. The observed range of reference canopy vigour of wheat plants in this trial was found to be (0.30–0.80). Although we have shown elsewhere that NDVI can be closely estimated by RGB images [45], it is inherently different from the GRVI derived from RGB images reported in this study. This difference must be borne in mind in the comparison that follows.

2.3. Statistical Analysis

All statistical analyses were performed using the Statistics and Machine Learning Toolbox of MATLAB R2017b (Mathworks Inc., Natick, MA, USA). Canopy traits estimated from the UAV and MGP imagery were compared to the reference manual measurements using the ordinary least squares regression model with a linear and constant term. The *p*-value of the estimated model coefficients was derived from the *t*-statistics and tested against a significance level of 0.05. The goodness of fit was assessed in terms of the coefficient of determination (R^2) and root mean squared error (RMSE). A significant fixed bias was found if the 95% confidence bounds of the estimated coefficient (intercept) did not contain 0. A significant proportional bias was found if the 95% confidence bounds of the estimated coefficient (the slope) did not contain 1. All errors were assumed to follow a normal distribution.

Descriptive statistics of the estimated canopy traits were summarized using box and whisker plots. The central line of a box corresponds to the median, and the lower and upper edges correspond to the first and third quartile, respectively. The whiskers extend to the extreme inlier points, and the outliers are plotted as '+'. The medians are significantly different at $\alpha = 0.05$, if their notches do not overlap.

3. Results

3.1. Comparison of MGP and UAV Estimated Canopy Height

The canopy height estimates of all plots derived from UAV and MGP images are compared against reference ruler measurements in Figure 2a,b. Canopy height estimates from MGP imagery had a better overall fit (RMSE = 3.95 cm, R^2 = 0.94) with manual measurements, compared with estimates derived from UAV imagery (RMSE = 6.64 cm, R^2 = 0.85). The 95% confidence bounds of the regression coefficients confirmed a 12.8-cm fixed bias in heights estimated by MGP imaging and a 4.6-cm fixed bias in heights estimated by UAV imaging. Both MGP and UAV imaging methodologies contained a significant proportional bias, which resulted in an underestimation of canopy height.

Height estimates relevant to different time points (growth stages) were also analysed in order to assess if there was a significant variation in estimation accuracy over time. Figure 2c shows that MGP imaging resulted in median errors closer to zero in the early growth stages t_1 and t_2. UAV imaging, however, consistently underestimated canopy heights at all time points.

With regard to the effect of fertilizer treatment, we demonstrate in Figure 3a,b that the median of canopy heights of plots in the group of treated plots was significantly higher than the heights of plots in the control group, across all five time points. This effect has been captured by both the MGP and UAV imaging system. Thus, although UAV imaging generally gave rise to greater errors (relative to the reference manual measurements), the relative difference in canopy heights between treated and untreated plots was reliably captured.

The results shown in Figure 3a,b distinguish treated plots from control plots, but otherwise collate results for the different varieties. A more detailed picture, as captured by the MGP imaging system, is shown in Figure 3c, which depicts the progressive growth difference due to fertilizer treatment for individual varieties. For each variety, the graph was drawn from the average canopy height over

three replicates of treated plots minus the average canopy height over three replicates of control plots. As expected, there was a positive margin in the heights of fertilized and unfertilized plots, for most varieties. Note that a steep descent in growth difference of the Magenta variety from t_3–t_4 could be traced back to an erroneous estimate of height by MGP imagery.
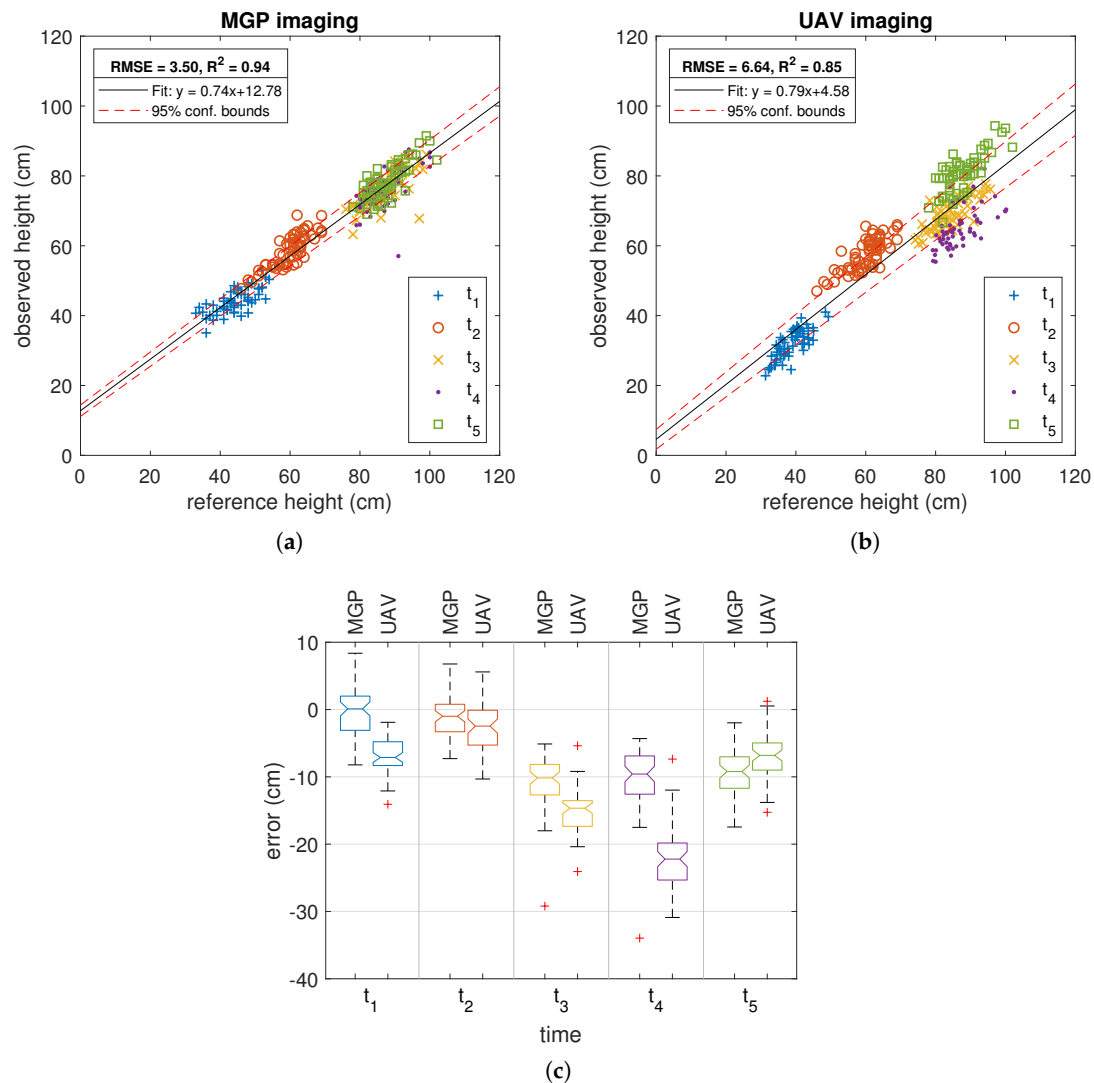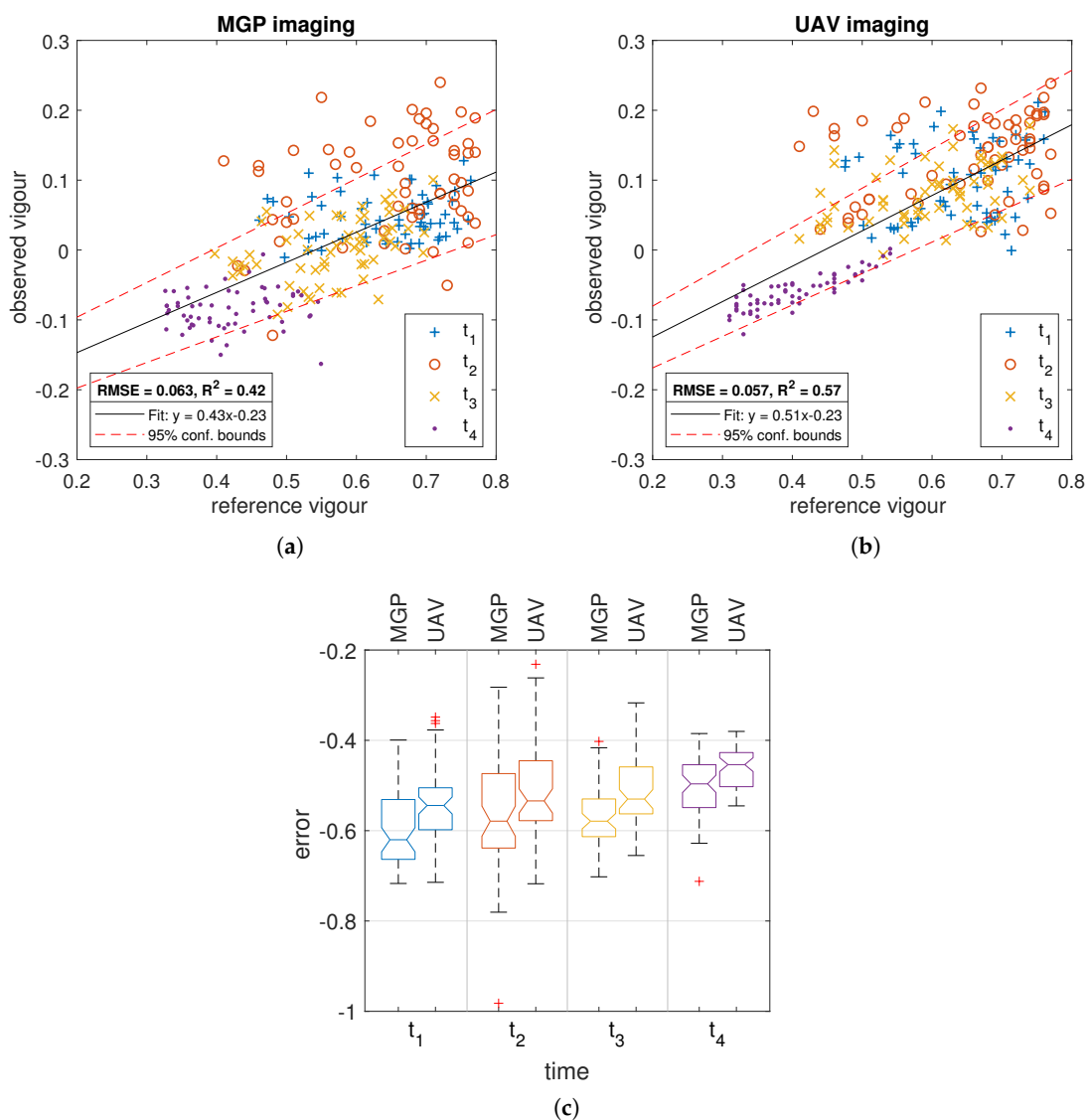

Figure 2. Regression analysis of canopy height estimates for (**a**) MGP imaging and (**b**) UAV imaging, relative to reference heights. (**c**) Distribution of height estimation errors with time, t_n.

We note the characteristic shape of most growth difference curves, which plateau around t_3, the post-anthesis stage of development. Thereafter, there is a minimal difference in plant height for most varieties except for Gregory, Drysdale and Kukri, which maintain a differential height until maturity. The differences between like-treated varieties are subtle and may require a more detailed examination than can be discussed here. Of particular relevance to these observations is the fact that the MGP-based methodology is able to quantitatively capture the temporal change, as well as the differences between the heights of the treated and untreated plots of the same variety.
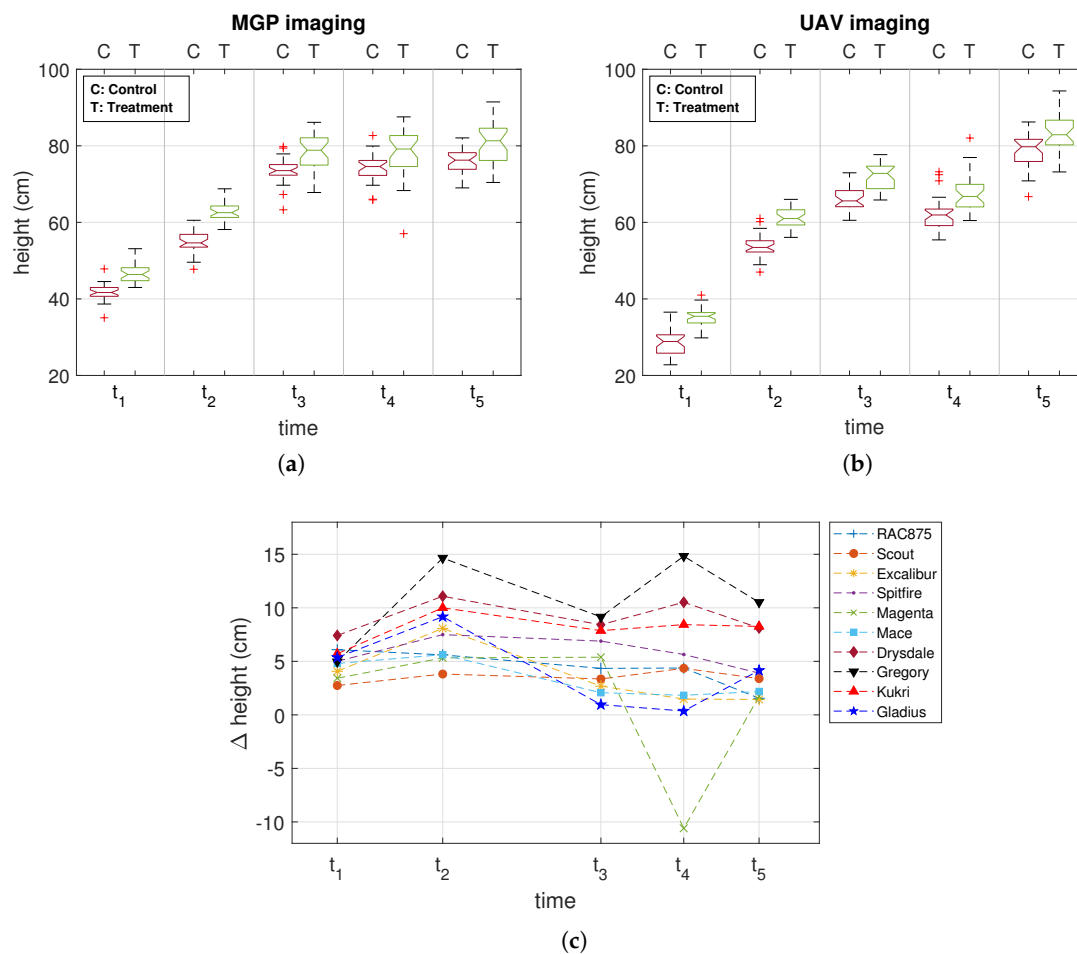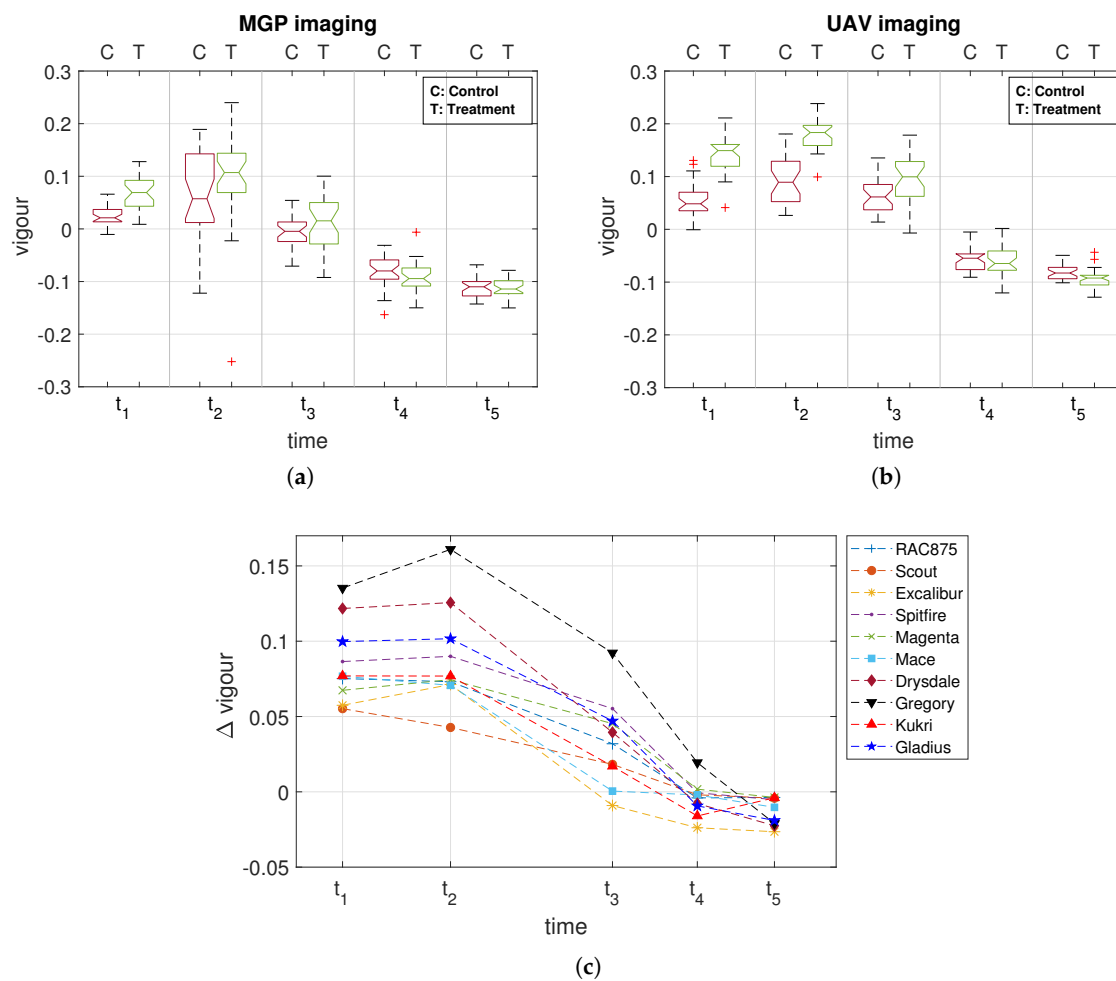
Figure 3. Canopy heights of treated and control plots at time point t_n as derived from (**a**) MGP imaging and (**b**) UAV imaging. The data shown summarize the results over the 60 plots: 10 varieties and three replicates for each treatment. (**c**) Difference between average canopy height of treated and untreated plots of each variety derived from MGP imagery (time axis scaled to actual duration).

3.2. Comparison of MGP and UAV Estimated Canopy Vigour

Canopy vigour of all plots derived from MGP and UAV imagery is compared to reference hand-held sensor measurements in Figure 4a,b. In contrast to the situation with height estimates, the linear regression models associated with canopy vigour estimates by UAV imaging had slightly better agreement with reference measurements (RMSE = 0.057, R^2 = 0.57) than did estimates based on MGP imaging (RMSE = 0.063, R^2 = 0.42). The 95% confidence limits of regression coefficients suggested a statistically-significant fixed and proportional bias in both MGP- and UAV-derived vigour estimates.

Vigour estimation analysed at different time points (Figure 4c) revealed a significant difference between the median error of estimates provided by MGP imaging and UAV imaging, except at t_2. The median errors appear to be relatively lower using UAV imaging, which is consistent with the above finding, and particularly so at the later time points (t_3 and t_4).

Figure 4. Regression analysis of canopy vigour estimates for (**a**) MGP imaging and (**b**) UAV imaging, relative to reference vigour. (**c**) Distribution of vigour estimation errors with time, t_n.

An analysis of the effect of fertilizer application (Figure 5a,b) suggested significantly higher median canopy vigour in the treated plots at the first two time points (t_1 and t_2). The margin of median vigour between treated and control plots was higher as captured by UAV imaging in comparison to MGP imaging. Moreover, the variance within each group was lower in the case of UAV imaging compared with MGP imaging. The difference between median vigour values of the treated and control plots diminished with time and all but disappeared by the mature time points (t_4 and t_5), at which point a significant degree of senescence appears and becomes a dominant feature of the canopies.

Figure 5. Canopy vigour of treated and control plots at time point t_n as derived from (**a**) MGP imaging and (**b**) UAV imaging. The data shown summarize the results over the 60 plots: 10 varieties and three replicates for each treatment. (**c**) Difference between average canopy vigour of treated and untreated plots of each variety derived from UAV imagery (time axis scaled to actual duration).

To complement the analysis summarized in Figure 5a,b, we show the differential development of vigour in different treatments of individual varieties as captured by the UAV imaging system in Figure 5c. For each variety, the graph was drawn from the average canopy vigour over three replicates of treated plots minus the average canopy vigour over three replicates of control plots. We note the characteristic shape of the differential vigour growth curves, which decayed after t_2, the elongation stage of development. As in the case of canopy height, canopy vigour of varieties demonstrated different degrees of margin between treatments, with the differences becoming negligible (or negative) as the canopies degrade with increased senescence (t_4 and t_5). The greatest difference in canopy vigour between fertilized and unfertilized plots was observed at time point (t_2), which approximately concluded the major rainfall period of the season. Provided the canopy vigour estimates were not reliable after t_3, a Δvigour < 0 may have been attributed to a delayed senescence of untreated plots of some varieties than treated plots. For example, Kukri had Δvigour < 0 at t_4, but close to zero at t_5. It is possible that other varieties also reached Δvigour $= 0$ at a later point when both treated and control plots were fully senesced. Overall, UAV imaging was able to quantitatively capture the temporal changes in vigour significantly up to t_3 at the least, as well as the differences between the vigour of the treated and untreated plots of the same variety.

It is important to visually highlight the key differences in the quality of MGP and UAV images, and their derived height and vigour maps, respectively, for trait estimation. Figure 6 shows sample RGB, height and vigour images of a plot as derived from MGP and UAV imaging at two contrasting times of growth, t_2 and t_4. Note the clarity of plant leaves in the MGP image, and its corresponding height and vigour are accurately captured over time. Conversely, the RGB image captured by UAV at t_4 is of relatively poor quality compared to the same at t_2, which also translated into poor quality trait images. In general, the UAV-derived trait images barely contain as detailed information as the MGP-derived trait images. However, they are still able to provide reasonable overall estimate of traits from the noisy, but complete information of a plot. Similar results were obtained with reduced resolution MGP images, details of which can be found in Appendix A.
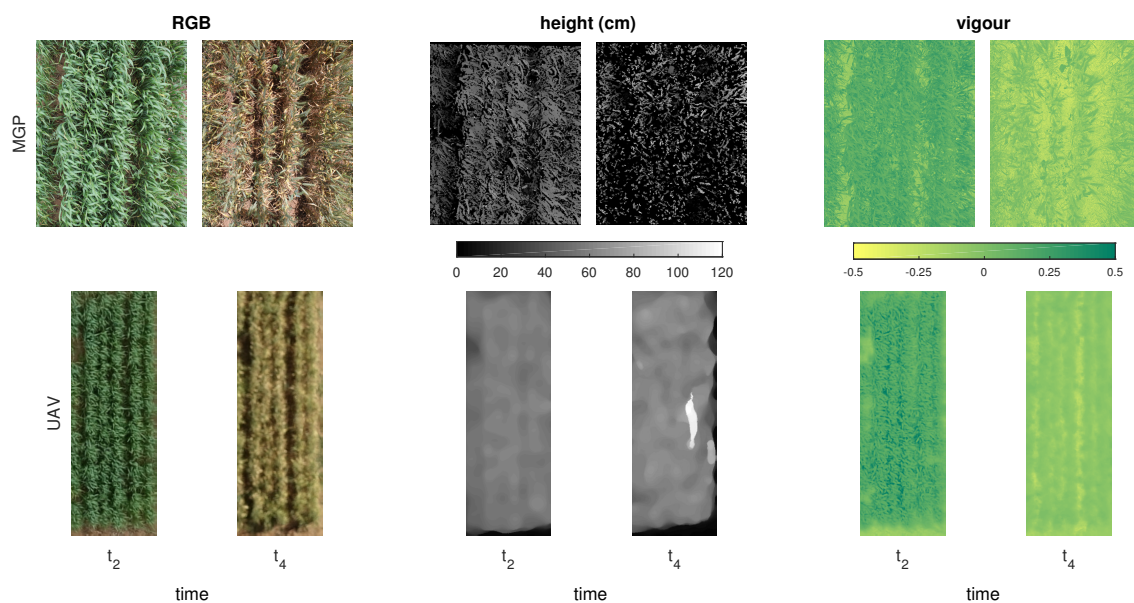
Figure 6. RGB, height and vigour of a wheat plot at time t_2 and t_4 derived from MGP imaging (top) and UAV imaging (bottom). For the purpose of visualization, the illustrated MGP images are a result of stitching the three partial images per plot using Image Composite Editor (Microsoft) software.

4. Discussion

Holman et al. [16] presented a study that addressed questions similar to those posed here, despite in comparison to a different land-based platform. In combination, the two studies are useful in establishing comparative benchmarks for field phenotyping with UAV and MGP technologies and methodologies. The scope covered by the two works not only includes a diverse set of wheat varieties (25 in [16] and 10 in this study), but also a greater range of climates, weather and (sun) lighting conditions. Consequently, the findings of these studies, in terms of the correlation between UAV imaging estimates of height and vigour, add support to the common conclusion of the two. From a broader perspective, our findings are consistent with those of [16] in terms of a favourable comparison of heights derived from UAV images with rule measurements, as well as the correlation with treatment.

A distinct advantage of the MGP imaging system is its ability to provide high resolution images of plots. Indeed, the high resolution not only allows for a greater degree of accuracy for the overall analysis of plots, it also offers the possibility of characterizing structure within the canopy. Plant leaves as a function of height can be distinguished from the terrain allowing for a detailed description of leaf density distribution and related leaf vigour distribution, as well as an accurate estimation of canopy height and overall canopy vigour that have been featured here. On the former note, leaf height and vigour distributions can be used to the advantage of more accurate estimation of canopy coverage.

Moreover, a colour analysis with leaf depth distribution can facilitate assessment of the onset and progression of senescence through a canopy. Furthermore, the accuracy of plant segmentation can be improved by utilizing the combination of pixel height and colour information as a determinant to distinguish desired plant objects from surrounding mosses and weeds. The major disadvantage of MGP phenotyping is the limited spatial domain that can be covered within a reasonable period of time and with a reasonable demand on labour. In contrast, the main advantage of UAV-based phenotyping is its high-throughput capability. Excluding setup time, on average, it took 3 min for UAV imaging of the trial (~20 plots per min) compared to 30 min for MGP imaging (~2 plots per min). A major limitation though is its lower spatial resolution, which may need consideration by the end-user depending on any further information sought from the images. Here, we focused on canopy height and canopy vigour, which can be captured by the UAV system with a reasonable accuracy.

The technical differences between the image processing methodologies also affect the accuracy of trait estimates. Multi-view stereo was used to reconstruct the three-dimensional structure from synchronously-captured field images taken with the MGP. In contrast, the SfM technique was used to reconstruct three-dimensional information from time-lapse UAV images. The SfM technique assumes a stationary scene relative to the camera position. In practice, however, a completely stationary scene is rarely possible to achieve in the field as plants are susceptible to deformation (bending and twisting) through the action of wind. Since height estimates were obtained from depth maps, a few examples revealed that anomalies could be traced back to poor surface reconstruction of the plot canopy. The percentile rank of elevation in affected plots was much different than the reference elevation. Hence, the accuracy of height estimates based on UAV images was inferior to that of the MGP system, which demonstrated a greater reliability in noisy conditions (see also the discussion on structure from motion in [16]). Another differentiating feature is that aerial images are orthorectified, i.e., geometrically corrected to present a uniform scale, and mosaicked, i.e., multiple aerial images are joined together to form one large image. Canopy vigour, however, was relatively less affected by the surface reconstruction errors since it was dependent on average VI reflectance per plot.

It would be fair to say that the results of this study have substantiated canopy height and canopy vigour as relevant quantitative traits to capture and assess plot growth and health and their respective dependencies on treatment, as well as genotype. For instance, the median canopy heights of all treated plots increased at a higher rate than did those of the control plots up until maturity. Similarly, the treated canopies exhibited greater vigour compared to the control plots, although predominantly in the early stages of growth; the significant differences in vigour diminished with the onset of senescence as plants grew into maturity. At the level of individual varieties, the MGP imaging system accurately captured the different growth rates of the ten varieties, both treated and untreated, using canopy height as a quantitative measure, while the UAV imaging system best captured the differing degrees to which the varieties exhibited vigour. The slightly better agreement of manually-measured canopy heights with the MGP-based estimates can be attributed to two issues: the higher resolution of MGP imagery and its superior 3D reconstruction methodology and, conversely, the lower resolution of UAV imagery and its inferior 3D reconstruction by SfM due to the non-stationarity of plants.

Given the brevity of time between manual height measurements and UAV imaging of the field, it is unlikely that significant errors in the comparison were introduced by the interpolation of measurements. On the other hand, the interpolation of manually-conducted GreenSeeker measurements is more likely to be a contributing factor to the less accurate agreement of MGP-based estimates of vigour compared with UAV-based estimates. It is arguably the case that a plant's GreenSeeker values can exhibit a greater variation over a shorter period of time in response to a locally changing environment. Finally, it should be remembered that while correlated, our definition of vigour is fundamentally different from the definition of the NDVI detected by the GreenSeeker sensor. This difference may also be a contributing factor to its lower correlation with image-based vigour measurement by both MGP and UAV imaging systems [29].

Continuous monitoring of crop growth using imaging systems with geospatial information is key to many applications in precision agriculture [46,47]. Of particular significance is the monitoring of canopy height and canopy vigour, which are two good indicators of crop growth. The results presented here not only confirm that these traits can be used to analyse crop responses to changes in treatment, but also prove that these indicators can be reliably obtained either by MGP or UAV imaging. Analysis of the crop growth as a function of interactions with soil and environmental conditions can subsequently provide customized management plans for farmers to maximize yield [48].

5. Conclusions

In this study, we employed UAV and MGP imaging to quantify two canopy traits, height and vigour, for a wheat field trial featuring ten wheat varieties and two treatments. The estimates derived from UAV images and MGP images were validated through a comparison with corresponding manual reference measurements of the traits taken over the course of the season. MGP imaging was found to provide better estimates of height using high resolution images of plot canopy. UAV imaging was found to provide better estimates of canopy vigour. Canopies treated with fertilizer were observed to grow taller, throughout the season, compared to untreated canopies. Treated canopies were observed to exhibit greater vigour than untreated canopies in the early stages of growth, whereas no significant difference could be detected at later stages. Both UAV and MGP imaging and analysis methods were sufficiently accurate to quantify these features.

Field phenotyping is challenging from a number of perspectives. Determining the most appropriate system depends on the application. UAV imaging is a fast and efficient means of covering a large area of land in a short time and is sufficiently accurate for canopy-wide trait estimation. MGP imaging is potentially low-throughput (depending on the platform used) and more labour intensive. However, it can capture detailed canopy structure with high fidelity, which offers the potential for trait analysis at the plant level.

Abbreviations

The following abbreviations are used in this manuscript:

UAV	Unmanned aerial vehicle
MGP	Mobile ground platform
RGB	Red, green and blue
VI	Vegetation index
NDVI	Normalized difference vegetation index
GRVI	Green-red vegetation index
ExG	Excess green index
LiDAR	Light detection and ranging
GSD	Ground sampling distance
SfM	Structure from motion
RMSE	Root mean squared error

Appendix A

A major difference in resolution of MGP and UAV systems is expected to affect the accuracy of trait estimates. For a comparison and determination of scale-related effects, we downscale the MGP images to the same resolution (GSD) as the UAV images. We then re-estimated the traits using these low resolution MGP images. The results of regression analyses of canopy height and vigour from reduced resolution MGP images relative to manual reference observations are presented in Figure A1. As could be expected, the results show that the estimates of the height are less accurate.

As evident from Figure A2, a significant amount of detail in the canopy is missing in reduced resolution MGP images, which are comparable to the resolution of UAV images. However, due to the advantage of multi-view stereo reconstruction, canopy structure is still more detailed in MGP images compared to those deduced from the corresponding UAV images.
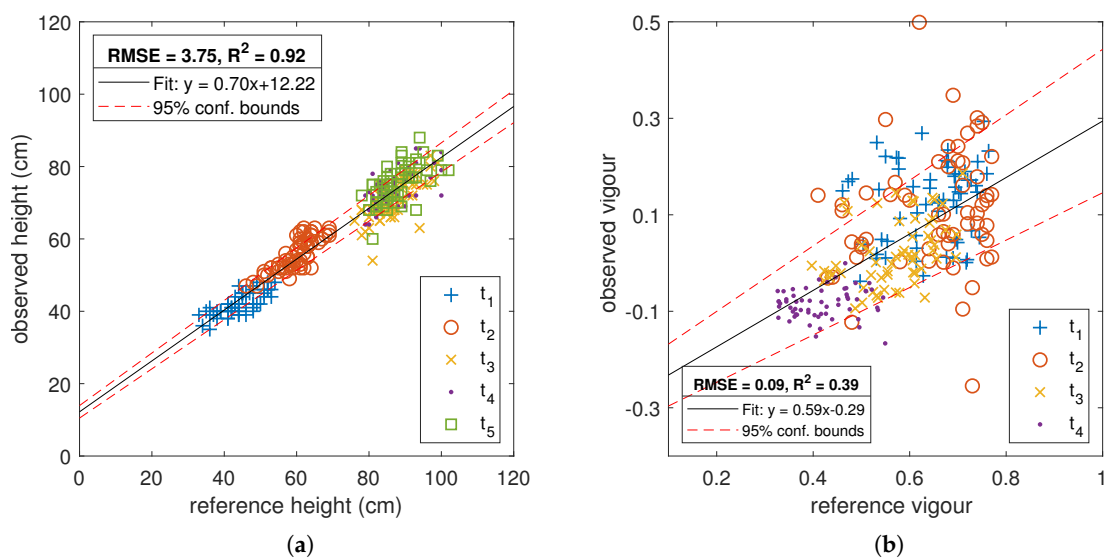

(**a**)   (**b**)

Figure A1. Regression analysis of the canopy trait estimates using reduced resolution MGP images for (**a**) height and (**b**) vigour, relative to reference traits.
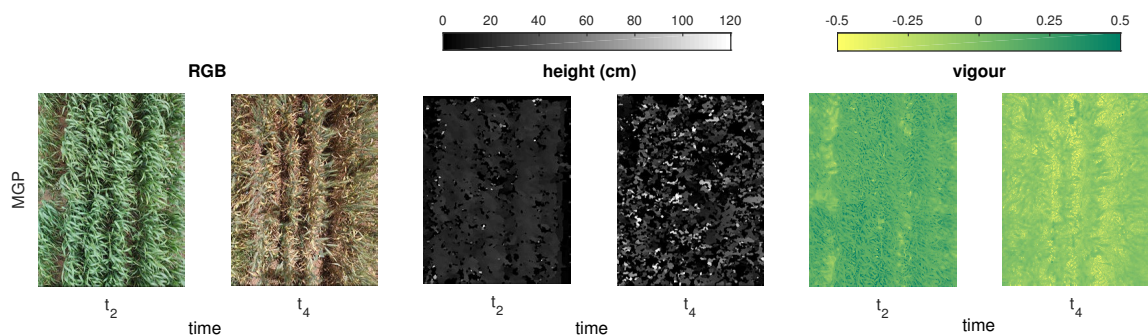

Figure A2. Reduced resolution RGB, height and vigour of the wheat plot in Figure 6 derived from MGP imaging. For the purpose of visualization, the illustrated MGP images are a result of stitching the three partial images per plot using Image Composite Editor (Microsoft) software.

Appendix B

We analyse the height distribution histograms obtained from the MGP and UAV images of the same sample plot on the same day (t_2) in Figure A3. Observe how the MGP image-derived histogram

depicts a detailed height variation from the ground to the top of the canopy. The UAV image-derived histogram conveys less detail, but still captures useful information of the canopy top, which allows for a reasonable estimation of height.
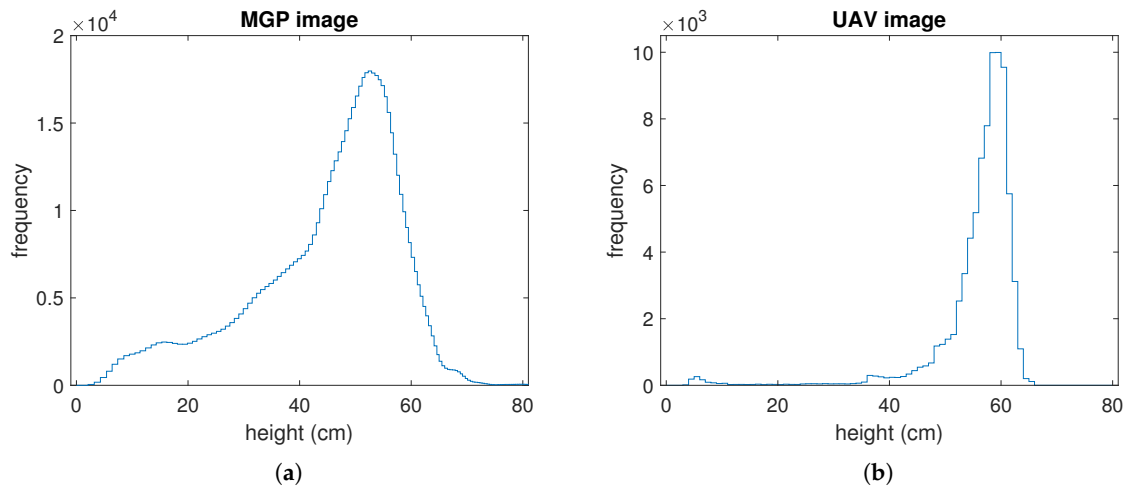

Figure A3. Height distribution histogram of plants of a single plot derived from (**a**) an MGP image and (**b**) a UAV image.

A percentile rank must be selected for the determination of a representative value of canopy height from the height distribution histograms. For this purpose, we sought a range of percentiles from 95–99.5 and found the minimum error between reference and observed heights of MGP images at t_1. Figure A4 shows the error, i.e., the mean absolute difference between the reference and observed heights at each percentile.
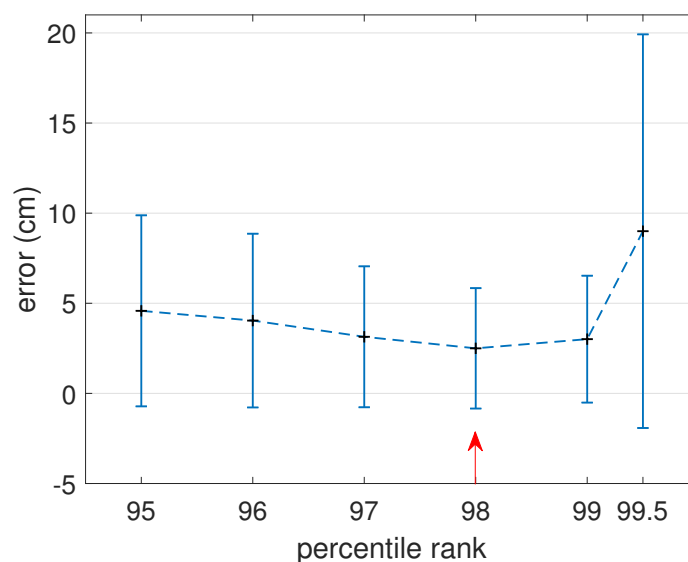

Figure A4. Error between the reference and observed heights from MGP imaging. Data points are the mean $\pm$ standard deviation of all plots at t_1.

The error was found to be minimum at 98%, and the same percentile was used for canopy height estimation from the histograms obtained from UAV images.
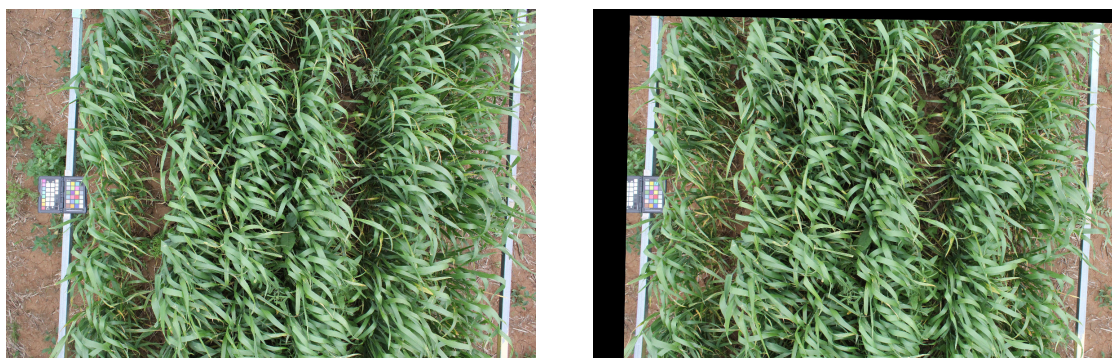
Appendix C

Figure A5. A sample rectified stereo image pair captured by the MGP system.

References

1. Salisbury, F.B.; Ross, C.W. *Plant Physiology*, 4th ed.; Wadsworth Publishing: Belmont, CA, USA, 1992.
2. Patrick, A.; Li, C. High throughput phenotyping of blueberry bush morphological traits using unmanned aerial systems. *Remote Sens.* **2017**, *9*, 1250, doi:10.3390/rs9121250. [CrossRef]
3. Gnädinger, F.; Schmidhalter, U. Digital counts of maize plants by unmanned aerial vehicles (UAVs). *Remote Sens.* **2017**, *9*, doi:10.3390/rs9060544. [CrossRef]
4. Virlet, N.; Sabermanesh, K.; Sadeghi-Tehran, P.; Hawkesford, M.J. Field Scanalyzer: An automated robotic field phenotyping platform for detailed crop monitoring. *Funct. Plant Biol.* **2017**, *44*, 143–153, doi:10.1071/FP16163. [CrossRef]
5. Cai, J.; Kumar, P.; Chopin, J.; Miklavcic, S.J. Land-based crop phenotyping by image analysis: Accurate estimation of canopy height distributions using stereo images. *PLoS ONE* **2018**, *13*, e0196671, doi:10.1371/journal.pone.0196671. [CrossRef] [PubMed]
6. Deery, D.; Jimenez-Berni, J.; Jones, H.; Sirault, X.; Furbank, R. Proximal remote sensing buggies and potential applications for field-based phenotyping. *Agronomy* **2014**, *4*, 349–379, doi:10.3390/agronomy4030349. [CrossRef]
7. Schirrmann, M.; Giebel, A.; Gleiniger, F.; Pflanz, M.; Lentschke, J.; Dammer, K.H. Monitoring agronomic parameters of winter wheat crops with low-cost UAV imagery. *Remote Sens.* **2016**, *8*, 706. [CrossRef]
8. de Castro, A.I.; Torres-Sánchez, J.; Peña, J.M.; Jiménez-Brenes, F.M.; Csillik, O.; López-Granados, F. An automatic Random Forest-OBIA algorithm for early weed mapping between and within crop rows using UAV imagery. *Remote Sens.* **2018**, *10*, 285. doi:10.3390/rs10020285. [CrossRef]
9. Haghighattalab, A.; Pérez, L.G.; Mondal, S.; Singh, D.; Schinstock, D.; Rutkoski, J.; Ortiz-Monasterio, I.; Singh, R.P.; Goodin, D.; Poland, J. Application of unmanned aerial systems for high throughput phenotyping of large wheat breeding nurseries. *Plant Methods* **2016**, *12*, 35. doi:10.1186/s13007-016-0134-6. [CrossRef] [PubMed]
10. Kipp, S.; Mistele, B.; Baresel, P.; Schmidhalter, U. High-throughput phenotyping early plant vigour of winter wheat. *Eur. J. Agron.* **2014**, *52*, 271–278, doi:10.1016/j.eja.2013.08.009. [CrossRef]
11. Di Gennaro, S.F.; Rizza, F.; Badeck, F.W.; Berton, A.; Delbono, S.; Gioli, B.; Toscano, P.; Zaldei, A.; Matese, A. UAV-based high-throughput phenotyping to discriminate barley vigour with visible and near-infrared vegetation indices. *Int. J. Remote Sens.* **2017**, doi:10.1080/01431161.2017.1395974. [CrossRef]
12. Watanabe, K.; Guo, W.; Arai, K.; Takanashi, H.; Kajiya-Kanegae, H.; Kobayashi, M.; Yano, K.; Tokunaga, T.; Fujiwara, T.; Tsutsumi, N.; et al. High-throughput phenotyping of sorghum plant height using an unmanned aerial vehicle and its application to genomic prediction modeling. *Front. Plant. Sci.* **2017**, *8*, 421. doi:10.3389/fpls.2017.00421. [CrossRef] [PubMed]
13. Chen, D.; Shi, R.; Pape, J.M.; Neumann, K.; Arend, D.; Graner, A.; Chen, M.; Klukas, C. Predicting plant biomass accumulation from image-derived parameters. *GigaScience* **2018**, *7*, giy001, doi:10.1093/gigascience/giy001. [CrossRef] [PubMed]

14. Kirk, K.; Andersen, H.J.; Thomsen, A.G.; Jørgensen, J.R.; Jørgensen, R.N. Estimation of leaf area index in cereal crops using red–green images. *Biosyst. Eng.* **2009**, *104*, 308–317, doi:10.1016/j.biosystemseng.2009.07.001. [CrossRef]

15. Makanza, R.; Zaman-Allah, M.; Cairns, J.E.; Magorokosho, C.; Tarekegne, A.; Olsen, M.; Prasanna, B.M. High-Throughput Phenotyping of Canopy Cover and Senescence in Maize Field Trials Using Aerial Digital Canopy Imaging. *Remote Sens.* **2018**, *10*, 330, doi:10.3390/rs10020330. [CrossRef]

16. Holman, F.H.; Riche, A.B.; Michalski, A.; Castle, M.; Wooster, M.J.; Hawkesford, M.J. High throughput field phenotyping of wheat plant height and growth rate in field plot trials using UAV based remote sensing. *Remote Sens.* **2016**, *8*, 1031, doi:10.3390/rs8121031. [CrossRef]

17. Jimenez-Berni, J.A.; Deery, D.M.; Rozas-Larraondo, P.; Condon, A.T.G.; Rebetzke, G.J.; James, R.A.; Bovill, W.D.; Furbank, R.T.; Sirault, X.R. High throughput determination of plant height, ground cover, and above-ground biomass in wheat with LiDAR. *Front. Plant. Sci.* **2018**, *9*, 237, doi:10.3389/fpls.2018.00237. [CrossRef] [PubMed]

18. Benedetti, R.; Rossini, P. On the use of NDVI profiles as a tool for agricultural statistics: The case study of wheat yield estimate and forecast in Emilia Romagna. *Remote Sens. Environ.* **1993**, *45*, 311–326, doi:10.1016/0034-4257(93)90113-C. [CrossRef]

19. Panda, S.S.; Ames, D.P.; Panigrahi, S. Application of vegetation indices for agricultural crop yield prediction using neural network techniques. *Remote Sens.* **2010**, *2*, 673–696, doi:10.3390/rs2030673. [CrossRef]

20. Moriondo, M.; Maselli, F.; Bindi, M. A simple model of regional wheat yield based on NDVI data. *Eur. J. Agron.* **2007**, *26*, 266–274, doi:10.1016/j.eja.2006.10.007. [CrossRef]

21. Raun, W.R.; Solie, J.B.; Johnson, G.V.; Stone, M.L.; Lukina, E.V.; Thomason, W.E.; Schepers, J.S. In-season prediction of potential grain yield in winter wheat using canopy reflectance. *Agron. J.* **2001**, *93*, 131–138, doi:10.2134/agronj2001.931131x. [CrossRef]

22. Magney, T.S.; Eitel, J.U.H.; Huggins, D.R.; Vierling, L.A. Proximal NDVI derived phenology improves in-season predictions of wheat quantity and quality. *Agric. For. Meteorol.* **2016**, *217*, 46–60, doi:10.1016/j.agrformet.2015.11.009. [CrossRef]

23. Hamuda, E.; Glavin, M.; Jones, E. A survey of image processing techniques for plant extraction and segmentation in the field. *Comput. Electron. Agric.* **2016**, *125*, 184–199, doi:10.1016/j.compag.2016.04.024. [CrossRef]

24. Meyer, G.E.; Neto, J.C. Verification of color vegetation indices for automated crop imaging applications. *Comput. Electron. Agric.* **2008**, *63*, 282–293, doi:10.1016/j.compag.2008.03.009. [CrossRef]

25. Mao, W.; Wang, Y.; Wang, Y. Real-time detection of between-row weeds using machine vision. In Proceedings of the ASAE Annual Meeting. American Society of Agricultural and Biological Engineers, Las Vegas, NV, USA, 27–30 July 2003.

26. Motohka, T.; Nasahara, K.N.; Oguma, H.; Tsuchida, S. Applicability of green-red vegetation index for remote sensing of vegetation phenology. *Remote Sens.* **2010**, *2*, 2369–2387, doi:10.3390/rs2102369. [CrossRef]

27. Rasmussen, J.; Ntakos, G.; Nielsen, J.; Svensgaard, J.; Poulsen, R.N.; Christensen, S. Are vegetation indices derived from consumer-grade cameras mounted on UAVs sufficiently reliable for assessing experimental plots? *Eur. J. Agron.* **2016**, *74*, 75–92, doi:10.1016/j.eja.2015.11.026. [CrossRef]

28. Hunt, E.R.; Cavigelli, M.; Daughtry, C.S.; Mcmurtrey, J.E.; Walthall, C.L. Evaluation of digital photography from model aircraft for remote sensing of crop biomass and nitrogen status. *Precis. Agric.* **2005**, *6*, 359–378, doi:10.1007/s11119-005-2324-5. [CrossRef]

29. Hoffmann, H.; Jensen, R.; Thomsen, A.; Nieto, H.; Rasmussen, J.; Friborg, T. Crop water stress maps for an entire growing season from visible and thermal UAV imagery. *Biogeosciences* **2016**, *13*, 6545, doi:10.5194/bg-13-6545-2016. [CrossRef]

30. Montes, J.M.; Technow, F.; Dhillon, B.S.; Mauch, F.; Melchinger, A.E. High-throughput non-destructive biomass determination during early plant development in maize under field conditions. *Field Crops Res.* **2011**, *121*, 268–273, doi:10.1016/j.fcr.2010.12.017. [CrossRef]

31. Mistele, B.; Schmidhalter, U. Spectral measurements of the total aerial N and biomass dry weight in maize using a quadrilateral-view optic. *Field Crops Res.* **2008**, *106*, 94–103, doi:10.1016/j.fcr.2007.11.002. [CrossRef]

32. Mistele, B.; Schmidhalter, U. Tractor-based quadrilateral spectral reflectance measurements to detect biomass and total aerial nitrogen in winter wheat. *Agron. J.* **2010**, *102*, 499–506, doi:10.2134/agronj2009.0282. [CrossRef]

33. Andrade-Sanchez, P.; Gore, M.A.; Heun, J.T.; Thorp, K.R.; Carmo-Silva, A.E.; French, A.N.; Salvucci, M.E.; White, J.W. Development and evaluation of a field-based high-throughput phenotyping platform. *Funct. Plant Biol.* **2014**, *41*, 68–79, doi:10.1071/FP13126. [CrossRef]

34. Freeman, K.W.; Girma, K.; Arnall, D.B.; Mullen, R.W.; Martin, K.L.; Teal, R.K.; Raun, W.R. By-plant prediction of corn forage biomass and nitrogen uptake at various growth stages using remote sensing and plant height. *Agron. J.* **2007**, *99*, 530–536, doi:10.2134/agronj2006.0135. [CrossRef]

35. White, J.W.; Conley, M.M. A flexible, low-cost cart for proximal sensing. *Crop Sci.* **2013**, *53*, 1646–1649, doi:10.2135/cropsci2013.01.0054. [CrossRef]

36. Candiago, S.; Remondino, F.; De Giglio, M.; Dubbini, M.; Gattelli, M. Evaluating multispectral images and vegetation indices for precision farming applications from UAV images. *Remote Sens.* **2015**, *7*, 4026–4047, doi:10.3390/rs70404026. [CrossRef]

37. Gracia-Romero, A.; Kefauver, S.C.; Vergara-Diaz, O.; Zaman-Allah, M.A.; Prasanna, B.M.; Cairns, J.E.; Araus, J.L. Comparative performance of ground versus aerially assessed RGB and multispectral indices for early-growth evaluation of maize performance under phosphorus fertilization. *Front. Plant. Sci.* **2017**, *8*, 2004. doi:10.3389/fpls.2017.02004. [CrossRef] [PubMed]

38. Vergara-Díaz, O.; Zaman-Allah, M.A.; Masuka, B.; Hornero, A.; Zarco-Tejada, P.; Prasanna, B.M.; Cairns, J.E.; Araus, J.L. A Novel Remote Sensing Approach for Prediction of Maize Yield Under Different Conditions of Nitrogen Fertilization. *Front. Plant Sci.* **2016**, *7*, doi:10.3389/fpls.2016.00666. [CrossRef] [PubMed]

39. Liebisch, F.; Kirchgessner, N.; Schneider, D.; Walter, A.; Hund, A. Remote, aerial phenotyping of maize traits with a mobile multi-sensor approach. *Plant Methods* **2015**, *11*, 9. doi:10.1186/s13007-015-0048-8. [CrossRef] [PubMed]

40. Madec, S.; Baret, F.; De Solan, B.; Thomas, S.; Dutartre, D.; Jezequel, S.; Hemmerlé, M.; Colombeau, G.; Comar, A. High-throughput phenotyping of plant height: Comparing unmanned aerial vehicles and ground LiDAR estimates. *Front. Plant Sci.* **2017**, *8*, 2002:1–2002:14, doi:10.3389/fpls.2017.02002. [CrossRef] [PubMed]

41. Chopin, J.; Kumar, P.; Miklavcic, S.J. Land-based crop phenotyping by image analysis: Consistent canopy characterization from inconsistent field illumination. *Plant Methods* **2018**, *14*, 39. doi:10.1186/s13007-018-0308-5. [CrossRef] [PubMed]

42. Hirschmueller, H. Stereo processing by semiglobal matching and mutual information. *Trans. Pattern Anal. Mach. Intell.* **2008**, *30*, 328–341, doi:10.1109/TPAMI.2007.1166. [CrossRef] [PubMed]

43. Koenderink, J.J.; Van Doorn, A.J. Affine structure from motion. *J. Opt. Soc. Am. A* **1991**, *8*, 377–385, doi:10.1364/JOSAA.8.000377. [CrossRef] [PubMed]

44. Heikkila, J.; Silven, O. A four-step camera calibration procedure with implicit image correction. In Proceedings of the Conference on Computer Vision and Pattern Recognition, San Juan, Puerto Rico, USA, 17–19 June 1997; pp. 1106–1112.

45. Khan, Z.; Rahimi-Eichi, V.; Haefele, S.; Garnett, T.; Miklavcic, S.J. Estimation of vegetation indices for high-throughput phenotyping of wheat using aerial imaging. *Plant Methods* **2018**, *14*, 20. doi:10.1186/s13007-018-0287-6. [CrossRef] [PubMed]

46. Zhang, C.; Kovacs, J.M. The application of small unmanned aerial systems for precision agriculture: A review. *Precis. Agric.* **2012**, *13*, 693–712, doi:10.1007/s11119-012-9274-5. [CrossRef]

47. Mulla, D.J. Twenty five years of remote sensing in precision agriculture: Key advances and remaining knowledge gaps. *Biosyst. Eng.* **2013**, *114*, 358–371, doi:10.1016/j.biosystemseng.2012.08.009. [CrossRef]

48. Ni, J.; Yao, L.; Zhang, J.; Cao, W.; Zhu, Y.; Tai, X. Development of an unmanned aerial vehicle-borne crop-growth monitoring system. *Sensors* **2017**, *17*, 502, doi:10.3390/s17030502. [CrossRef] [PubMed]